

# **Investigations into Epoxide-modified Polyurethane-Polyisocyanurate Reaction Systems for Rigid Foam Applications**

Dissertation with the aim of achieving a doctoral degree  
at the Faculty of Mathematics, Informatics and Natural Sciences  
Department of Chemistry  
of Universität Hamburg

Submitted by

**Mengyu Zhang**

2021 in Hamburg



The experimental work in this thesis was conducted in the research group of Prof. Dr. Luinstra, Institute for Technical and Macromolecular Chemistry, Chemistry department, Universität Hamburg from September 2017 to March 2021.

Date of disputation: 06.08.2021

Date of print: 18.08.2021

1st Reviewer: Prof. Dr. Gerrit A. Luinstra

2nd Reviewer: Prof. Dr. Berend Eling



## List of Abbreviations

ATR	attenuated total reflectance
BADGE	bisphenol A diglycidyl ether
BDMAPAP	1-(Bis(3-(dimethylamino) propyl)amino)propan-2-ol
CDCl <sub>3</sub>	deuterated chloroform
CDI	carbodiimide
Comp.	component
DAB	DABCO <sup>®</sup> T ( <i>N,N,N'</i> -trimethylaminoethyl ethanolamine)
DABCO	1,4-diazabicyclo[2.2.2]octane
DBTDL	dibutyltin dilaurate
DMA	dynamic mechanical analysis
DMA	dynamic mechanical analysis
DMAE	2-dimethylaminoethanol
DMAEE	2-(2-(dimethylamino) ethoxy)ethanol
DMAH	6-dimethylamino-1-hexanol
DMSO-d <sub>6</sub>	deuterated dimethyl sulfoxide
EE	ethyl acetate
Ep	epoxide
ESI	electrospray ionization
FA	formic acid
FTIR	Fourier-transform infrared
GC	gas chromatography
GPC	gel permeation chromatography
HPLC	high-performance liquid chromatography
LC	liquid chromatography
LC-MS	liquid chromatography–mass spectrometry
MS	mass spectroscopy
NCO	isocyanate
NMR	nuclear magnetic resonance

Oxa	oxazolidinone
PE	petroleum ether
PEG	polyethylene glycol
PMPT	<i>N,N,N',N'',N''</i> -pentamethyldiethylenetriamine
PUR-PIR	polyurethane-polyisocyanurate
T <sub>cure</sub>	curing temperature
TDHT	tris(3-dimethylaminopropyl)-hexahydro-s-triazine
T <sub>g</sub>	glass transition temperature
T <sub>g0</sub>	glass transition temperature of the reactant mixture prior to reactions
T <sub>g∞</sub>	glass transition temperature of the fully cured polymer system
TGA	thermogravimetric analysis
T <sub>max</sub>	the maximum temperature
TMEDA	<i>N,N,N',N'</i> -Tetramethylethylenediamine
TMS	tetramethylsilane
TOF	time-of-flight
TTT	time-temperature-transformation
UV	ultraviolet

## Table of content

Abstract.....	1
Zusammenfassung.....	3
1. Introduction.....	6
1.1 Polyurethane chemistry in rigid foam applications .....	6
1.2 Resin curing and the time-temperature-transformation (TTT) cure diagram ....	15
1.3 Methods employed to study the chemical reaction pathways.....	19
2. Motivation.....	23
3. Results and Discussion .....	24
3.1 Reaction pathway elucidation in a monofunctional model epoxide-modified PUR/PIR system .....	24
3.1.1 Epoxide_alcohol_isocyanate_catalyst (“Ep_ROH_NCO_catalyst”) system .....	27
3.1.1.1 Formulation and reaction condition .....	27
3.1.1.2 Chemical bond analysis .....	28
3.1.1.3 Reaction pathway discussion .....	40
3.1.1.4 Catalyst selectivity .....	53
3.1.1.5 Effect of solvent.....	62
3.1.2 “Ep_ROH_NCO_DAB” system incorporated with blowing agents and hindered amine.....	64
3.1.3 The effect of disubstituted aryl urea on isocyanurate and carbodiimide selectivity .....	75
3.1.4 Epoxide modified “mono_PUR/PIR” system.....	79

3.1.5 The “Model” system .....	92
Summary and conclusion of the monofunctional reaction systems .....	97
3.2 The study of reactant conversion and chemical bond formation in foam systems .....	98
3.2.1 Foam system at isothermal reaction conditions .....	100
3.2.2 Free foaming reactions .....	109
3.2.3 Post cure of foams .....	116
3.2.4 PUR/PIR foam chemistry and the effect of epoxide modification .....	120
Summary of and conclusions on the foam system .....	127
4. Experimental part .....	129
4.1 Chemicals and reaction setup .....	129
4.2 Analysis methods .....	132
4.3 Monofunctional model reaction systems .....	136
4.3.1 Preparation and characterization of the reference substances used for product identification .....	136
4.3.2 Product assignment in HPLC .....	151
4.3.3 Product assignment in LC-MS .....	153
4.3.4 Product quantification by <sup>1</sup> H NMR .....	161
4.3.5 Carbodiimide quantification by the gas evolution method .....	163
4.3.6 Preparation of DABCO <sup>®</sup> T-urethane .....	164
4.3.7 Molecular weight distribution .....	166
4.3.8 Online FTIR spectroscopy .....	166
4.4 Foam systems .....	168
4.4.1 Determination of isocyanate conversion using FTIR .....	168



4.4.2 Soxhlet extraction .....	170
4.4.3 TGA measurements .....	172
5. Bibliography .....	173
6. Safety Data.....	179
7. Appendix.....	183
Acknowledgements.....	190
Declaration on Oath .....	191

## Abstract

This study was conducted to obtain a fundamental understanding of the chemistry that occurs in epoxide-modified polyurethane-polyisocyanurate rigid foam systems. The study consisted of two parts. In the first part, model reaction systems were investigated using low molecular mass, mono-functional analogs as reactants. The second part dealt with essentially the same chemistry in polymerizing systems where the impact of network growth and vitrification on the course of the reaction was investigated.

In the model systems, analytic techniques comprising HPLC, LC-MS, NMR, FTIR and volumetric gas measurement were utilized for the identification and quantification of the various reaction products that were formed in the system. The effects of reaction temperature, catalyst choice and the combination of the individual reactants on the product formation were studied. A set of reaction pathways was proposed to account for the observations.

At low reaction temperatures (about 80 °C), the urethane and urea forming reactions proceed with high conversions and the excess of isocyanate is mainly converted into isocyanurate. A small portion of the epoxide in conjunction with the employed tertiary amine catalyst forms a co-catalyst, which accelerates isocyanurate formation. The epoxide conversion increases with reaction temperature and reaches more than 90% at 160 °C. It reacts with isocyanurate and urethane to form oxazolidinone. The reaction between epoxide and urethane also results in the formation of a series of urethane-epoxide adducts. Carbodiimide appeared at about 130 °C and its formation becomes more pronounced at 160 °C. It undergoes consecutive addition reactions. The isocyanurate and carbodiimide formation are competing reactions at high reaction temperatures. The carbodiimide formation is promoted by the presence of disubstituted ureas.

Among the selected tertiary amine catalysts, those with a pendent primary hydroxyl group show a higher catalytic activity in both isocyanurate and carbodiimide

formation at 160 °C; catalysts with more than one tertiary amino group and bearing a hydroxyl group show a higher catalytic activity in epoxide opening reactions, leading to a higher epoxide conversion and an improved oxazolidinone formation at 160 °C. *N,N,N'*-trimethyl aminoethyl ethanolamine (DABCO<sup>®</sup> T) shows the highest catalytic activity in both cases and was used as the primary catalyst in the present thesis work.

The reaction kinetics of the polymer generating system was mainly studied using FTIR. The results with respect to bond formation were related to that of the corresponding model systems. The differences between the model reactions and polymerizing foam systems were discussed in terms of chain mobility and diffusion control of the reaction system. Finally, methods to improve chemical conversions in foam systems were proposed and evaluated.

The chain mobility and diffusivity of the reactive groups influence both the reactant conversion and the type and amount of the chemical bond formation in foam building systems. Vitrification occurs when the system's *T<sub>g</sub>* exceeds the curing temperature and drastically imparts the overall reaction conversion. This is especially true for the chemical reactions that occur in the later stages of the reaction, such as the decomposition of isocyanurate by epoxide to form oxazolidinone and the consecutive reactions of carbodiimide. The low reactant conversions are especially obvious in the near surface area of the cup foam, where the reaction temperatures remain lower. Post cure of the foam at 200 °C for a few hours increases the isocyanate and epoxide conversions significantly. The modification of PUR/PIR foam system with epoxide also improves the conversion of isocyanate into isocyanurate in the near surface area of the foam. In the core of the foam where already high reaction temperatures are achieved, the combination of epoxide further increases the temperature resulting in higher isocyanate conversions and the formation of oxazolidinone.

## Zusammenfassung

Diese Studie wurde durchgeführt, um ein grundlegendes Verständnis der Chemie zu erlangen, die in epoxidmodifizierten Polyurethan-Polyisocyanurat Hartschaumsystemen abläuft. Dabei bestand die Studie aus zwei Teilen. In einem ersten Teil wurden Modellreaktionssysteme basierend auf niedermolekularen, monofunktionellen Reaktanten untersucht. Der zweite Teil handelte von polymerisierenden Systemen, in denen der Einfluss von Netzwerkaufbau und Verglasung auf den Reaktionsverlauf analysiert wurde.

Modellsysteme wurden mittels HPLC, LC-MS, NMR, FTIR und volumetrischer Messung der Gasphase charakterisiert, um die verschiedenen im System gebildeten Reaktionsprodukte zu identifizieren und quantifizieren. Der Einfluss der Reaktionstemperatur, des Katalysators und der Kombination der einzelnen Reaktanten auf die Produktbildung wurden untersucht. Eine Reihe von Reaktionswegen wurde vorgeschlagen, um die Beobachtungen zu erklären.

Bei niedrigen Temperaturen (ca. 80 °C) verlaufen die Urethan- und Harnstoffbildungsreaktionen mit hohen Umsätzen, überschüssiges Isocyanat wird hauptsächlich in Isocyanurat umgewandelt. Ein kleiner Teil des Epoxids bildet dabei zusammen mit dem eingesetzten tertiären Aminkatalysator einen Cokatalysator, der die Bildung des Isocyanurats beschleunigt. Mit zunehmender Reaktionstemperatur steigt der Umsatz an Epoxid jedoch an und erreicht bei 160 °C mehr als 90 %. Sowohl dessen Reaktion mit Isocyanurat als auch mit Urethan führt zur Bildung von Oxazolidinon. Die Reaktion mit Urethan führt des Weiteren zur Ausbildung einer Reihe von Urethan-Epoxid-Addukten. Ab 130 °C kann die Ausbildung von Carbodiimid beobachtet werden. Diese nimmt mit zunehmender Temperatur zu, es kommt zudem auch zu Folgereaktionen. Bei hohen Reaktionstemperaturen stehen die Bildung von Isocyanurat und Carbodiimid in direkter Konkurrenz. Dabei wird die Bildung von Carbodiimid durch die Anwesenheit von disubstituierten Harnstoffen gefördert.

Unter den ausgewählten tertiären Aminkatalysatoren zeigen diejenigen mit einer primären Hydroxylgruppe eine höhere katalytische Aktivität sowohl bei der Isocyanurat- als auch bei der Carbodiimidbildung bei 160 °C; Hydroxylmodifizierte Katalysatoren mit mehr als einer tertiären Aminogruppe besitzen eine katalytische Aktivität bei der Öffnung von Epoxiden. Dies führt zu einer höheren Umsetzung des Epoxids und einer verbesserten Oxazolidinonbildung. In beiden Fällen zeigt *N,N,N'*-Trimethylaminoethylethanolamin (DABCO® T) die höchste katalytische Aktivität. Daher wurde dieses in der vorliegenden Arbeit primär als Katalysator verwendet.

Mit Hilfe von FTIR-Untersuchungen wurde die Reaktionskinetik der Polymerisation analysiert. Die Ergebnisse bezüglich der Bindungsbildung wurden mit denen korrespondierender Modellsysteme in Beziehung gesetzt. Die Unterschiede zwischen niedermolekularen Modellreaktionen und makromolekularen Schaumsystemen wurden hinsichtlich Kettenbeweglichkeit und Diffusionskontrolle des Reaktionssystems diskutiert. Es wurden Methoden zur Verbesserung der chemischen Umsetzung in Schaumsystemen abgeleitet und bewertet.

In Schäumen wird durch die Beweglichkeit der makromolekularen Ketten und durch die Diffusion der reaktiven Gruppen sowohl der Umsatz der Edukte als auch die Art und Anzahl der chemischen Bindungen beeinflusst. Es kommt zur Verglasung, sobald die Glasübergangstemperatur des Systems dessen Reaktionstemperatur überschreitet. Dies hat einen starken Einfluss auf den gesamten Reaktionsumsatz. Am stärksten werden Reaktionen beeinflusst, die bevorzugt gegen Ende ablaufen. Dies sind beispielsweise die Umsetzung von Isocyanurat durch Epoxid zu Oxazolidinon und die Folgereaktionen des Carbodiimids. Besonders im Bereich der kühleren Schaumoberfläche kommt es daher zu niedriger Umsetzung der Edukte. Erfolgt jedoch eine mehrstündige Nachhärtung der Schäume bei 200 °C, können die Umsetzungen sowohl des Isocyanats als auch des Epoxids deutlich erhöht werden. Durch die Modifizierung des PUR/PIR-Schaumsystems mit Epoxid wird auch die Umsetzung des Isocyanats zu Isocyanurat im oberflächennahen Bereich des Schaums

verbessert. Die normalerweise bereits hohe Temperatur im Schaumkern wird durch den Einsatz von Epoxid noch weiter erhöht. Dies führt insgesamt zu einem höheren Umsatz des Isocyanats und zur Bildung von Oxazolidinon.

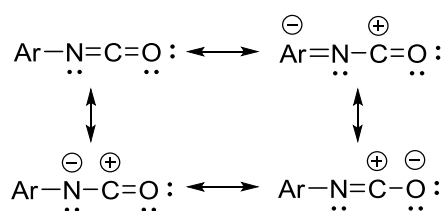
## 1. Introduction

### 1.1 Polyurethane chemistry in rigid foam applications

Polyurethane-polyisocyanurate (PUR/PIR) rigid foams are well known for their thermal insulation<sup>[1,2]</sup> and flame retardant properties<sup>[3,4]</sup> and are therefore widely used in roofing and construction panel applications<sup>[5]</sup>. In addition to good thermal insulation and flame retardant performance, properties such as low friability, high compressive strength and low density are required<sup>[6-10]</sup>. As a reactive system, the production process of PUR/PIR rigid foam is essentially a reaction process along which the desired foam properties are developed. Therefore, the foam performance is basically controlled by the chemical reactions that occur during the foaming process. Hence, a fundamental understanding of the chemistry in PUR/PIR rigid foams will be the basis for further control of the chemical reactions, thereby providing room for making adjustments to the foam performance as required. The study on the chemistry in PUR/PIR rigid foams, particularly those with epoxide modification, will be the focus of this thesis.

The chemistry in PUR/PIR rigid foam formation is highly complex. Chemical reactions involved in the preparation of PUR/PIR rigid foam include the formation of urethane, urea, allophanate, biuret, isocyanurate, carbodiimide and oxazolidinone linkages, and possibly their subsequent addition and decomposition reactions. The various chemical reactions can take place simultaneously or successively in the foaming process. Meanwhile, during the foaming process, the instantaneous concentrations of the reactive groups and the temperature change dynamically with the conversion. This dynamic character further increases the complexity of the reactions in PUR/PIR systems. Current knowledge on the individual chemical reactions and simple reaction systems under various reaction conditions will be presented in the following part. This will start with a general introduction on polyurethane chemistry which then leads into the details of the specific reactions.

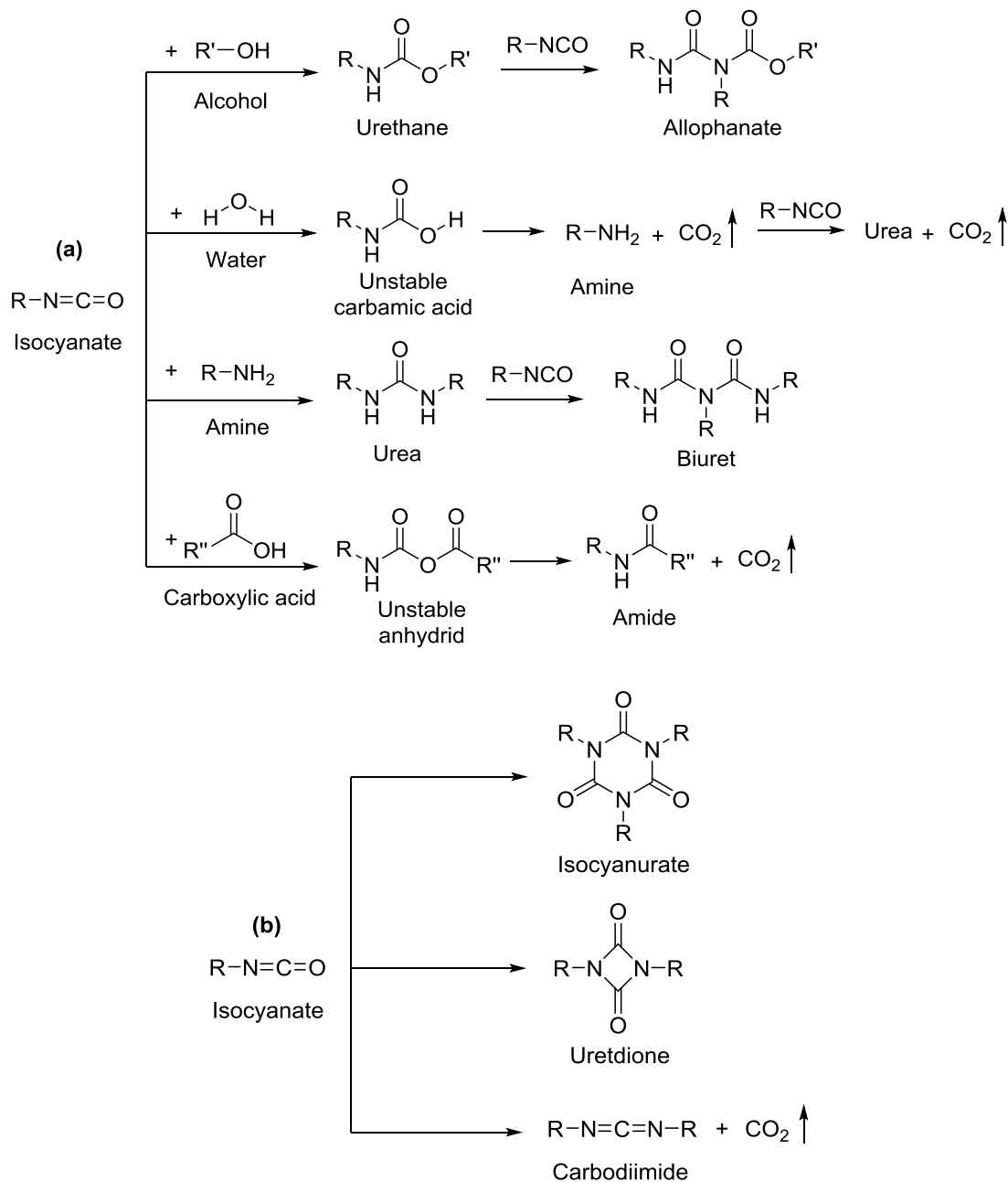
Polyurethane was discovered in 1937 by Otto Bayer. Isocyanate reactions lay the foundations of the polyurethane chemistry. The structure of an aromatic isocyanate can be expressed by the schematic resonance structures (Scheme 1). It exemplifies that the carbon atom in the -N=C=O group is electron deficient, and that the transition state for nucleophilic attack at the carbon atom is stabilized. It indicates a high reactivity of the isocyanate towards nucleophiles.



**Scheme 1.** Schematic resonance structures of aromatic isocyanate

Polyurethanes are a class of materials prepared from isocyanates. They not only contain urethane groups but may also contain other linkages such as urea, biuret, allophanate, amide, isocyanurate, uretdione, carbodiimide, oxazolidinone, ether and ester. The isocyanate reactions can be divided into two main categories. One category is the polyaddition reaction between isocyanate and compounds with or without active hydrogen. Urethane, urea, biuret, allophanate, amide, oxazolidinone forming reactions belong to this category (Scheme 2 (a)). The other category is the reaction of isocyanate with additional isocyanate molecules to produce linkages such as isocyanurate, uretdione and carbodiimide (Scheme 2 (b))<sup>[11-14]</sup>.





**Scheme 2.** (a) Isocyanate reactions with alcohol, water, amine and carboxylic acids,  
 (b) isocyanate-isocyanate reactions

When producing polyurethane materials, the isocyanate generally participates in more than one chemical reaction. Various linkage combinations can provide materials with balanced and, for a certain application, improved properties. During rigid foam manufacturing, several reactions might take place. These are (1) blowing reactions, such as isocyanate reacting with water or carboxylic acid to produce substituted urea

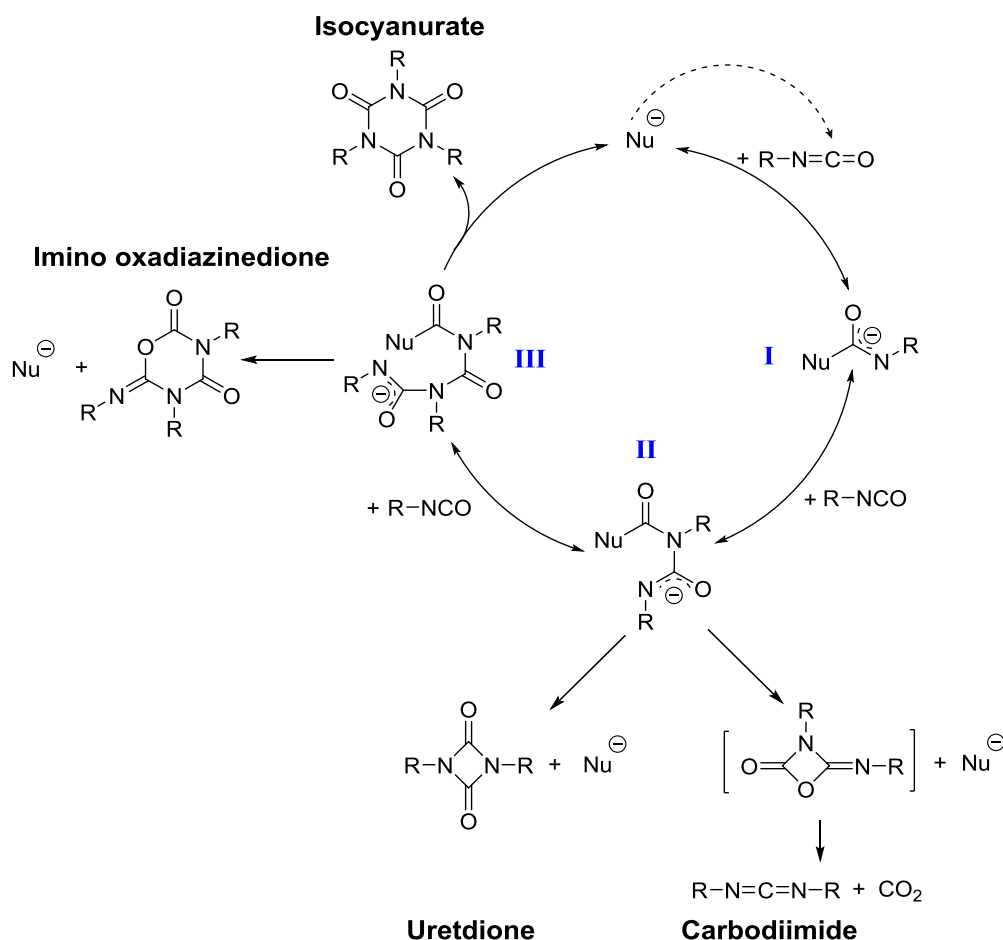
and CO<sub>2</sub>, (2) gelling reactions, in which isocyanate reacts with polyol or polyamine to form urethane and substituted urea, respectively, (3) urethane and urea reacting with isocyanate to generate allophanate and biuret, respectively, (4) isocyanate trimerization to produce isocyanurate, (5) other modification reactions, such as oxazolidinone and carbodiimide formation. Relevant parts of the current knowledge of these reactions will be given in the following parts. Reactions that are closely related in terms of their reaction pathways will be discussed together.

### **Isocyanurate, imino oxadiazinedione, uretdione and carbodiimide formation**

Isocyanurate prepared from aromatic isocyanate exhibits a cyclic structure without reactive hydrogens. Its presence in rigid foams typically improves its fire retardancy properties<sup>[3,4]</sup>. Using an excess of isocyanate in the formulation and a nucleophilic catalyst, isocyanurate is formed in a cyclotrimerization reaction of the isocyanate. Nucleophiles like carboxylates<sup>[15]</sup>, alkoxides<sup>[16]</sup>, epoxide in combination with tertiary amines or halides<sup>[17-19]</sup>, tertiary amines<sup>[20]</sup>, hexahydrotriazines<sup>[21]</sup>, quaternary ammoniums<sup>[22]</sup>, organometallic catalysts<sup>[23]</sup>, urethanes<sup>[24]</sup>, *N*-heterocyclic carbenes<sup>[25]</sup> and phosphines<sup>[26]</sup> have been reported as catalysts for the trimerization reaction. Although a recent study has shown that the trimerization mechanism of aliphatic isocyanate is more complex<sup>[27]</sup>, the widely accepted trimerization mechanism for aromatic isocyanate is relatively simple (**Scheme 3**)<sup>[14,28]</sup>. The carbon atom in the -N=C=O group has the lowest electron density. Upon attack of a nucleophile, intermediate **I** is formed. As the adjacent nitrogen and oxygen atoms are more electronegative than the carbon atom, the negative charge built up is stabilized. The formation of the intermediate **I** was recently observed in a trimerization reaction using *p*-tolyl isocyanate as reactant and potassium acetate<sup>F</sup> as a catalyst<sup>[24]</sup>. In the same manner, the obtained intermediate **I** can further react with another two (or more) isocyanate molecules and upon an intramolecular cyclization, the isocyanurate is produced and a nucleophile is regenerated. Reaction media with high dielectric constant and isocyanates with electron withdrawing substitutes and less steric hindrance were reported to undergo an accelerated isocyanurate formation<sup>[19]</sup>.

Along the isocyanurate formation pathway, several other reactions may occur simultaneously and interfere with isocyanurate formation (Scheme 3). The outcome largely depends on the reactant structure, catalyst species and reaction conditions. For instance, during the trimerization process, instead of further reacting with another isocyanate, the intermediate **II** can undergo a ring closure reaction to produce uretdione. The formation of uretdione is reversible. It has been reported that its formation normally takes place at low temperatures and that it dissociates back to isocyanate at around 80 - 100 °C<sup>[13]</sup>. Besides the formation of uretdione, the structure **II** also has the ability to undergo another cyclization reaction, finally yielding carbodiimide<sup>[29]</sup>. Phospholene oxides, which are thought to form comparable phosphinimide intermediates with isocyanate, are effective catalysts for the carbodiimide formation<sup>[30-32]</sup>. Isocyanates that are sterically hindered have been reported to easily convert into carbodiimide using alkali metal alkoxides and phenoxides catalysts<sup>[33]</sup>. When hindered alkali metal alkoxides or phenoxides catalysts are used in combination with hindered isocyanate, carbodiimide has been reported to be produced in high yields<sup>[34]</sup>.

Except for uretdione and carbodiimide, imino oxadiazinedione can be formed through the cyclization of intermediate **III**. The formation of imino oxadiazinedione, however, was mainly reported for aliphatic isocyanates<sup>[26,35,36]</sup>.



**Scheme 3.** Reaction pathways during isocyanurate formation

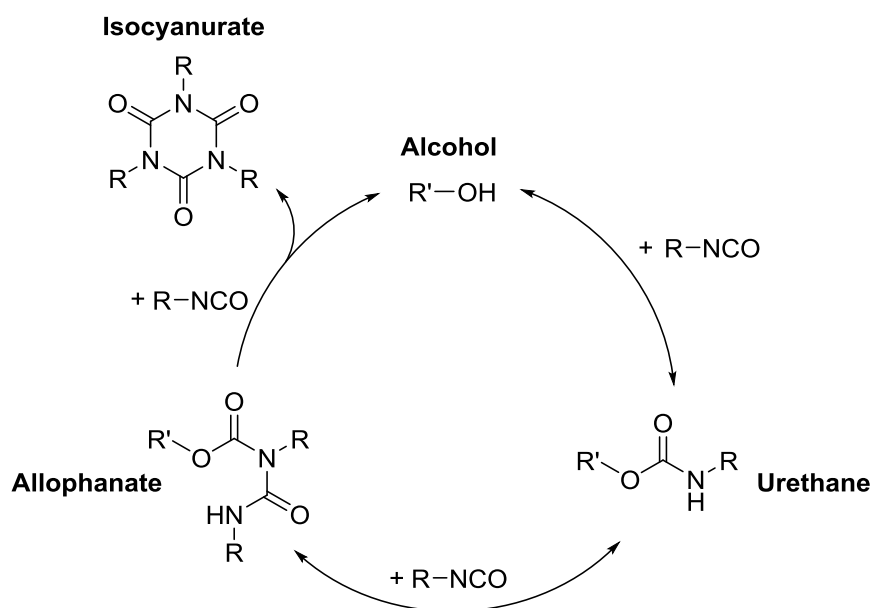
### Urethane, urea, allophanate and biuret formation

Two reactions are of crucial importance in polyurethane foam applications, i.e. isocyanate reacting with polyol to yield urethane and isocyanate reacting with water to yield urea and  $\text{CO}_2$ . The reaction rates of these two reactions can be controlled by catalysis. It has been reported that organometallic catalysts such as tin, mercury, bismuth, zirconium and lead catalysts are effective for urethane formation<sup>[37–40]</sup>. The catalytic action of tertiary amine catalysts is dependent on its structure. For instance, 1,4-diazabicyclo(2.2.2)octane (DABCO) with low steric hindrance on the nitrogen atom has been reported to be a strong urethane promoting catalyst, whereas, bis(2-dimethylaminoethyl) ether, which activates water through multiple hydrogen bonding, is known to be a fast urea forming catalyst<sup>[41,42]</sup>. The urethane or urea formed can further react with another equivalent of isocyanate to produce allophanate

or biuret, respectively (Scheme 2 (a)). The formation of urethane, urea, allophanate and biuret are all reversible and the bonds will be broken above their ceiling temperatures to give back the initial reactants. The sequence of thermal stability has been proposed in a review article to be as follows: allophanate < biuret < urethane < urea < isocyanurate<sup>[43]</sup>. Especially, allophanate and biuret that show low thermal stability readily decompose at high temperatures and regenerate urethane and urea, respectively, along with isocyanate.

The formation of urethane, allophanate and isocyanurate are closely related to each other<sup>[24]</sup>. The reaction of urethane with isocyanate yields allophanate. When the allophanate reacts with another (or more) isocyanate molecules, followed by an intramolecular cyclization reaction, isocyanurate can be formed, finally liberating alcohol (or urethane) (Scheme 4). The reaction temperature, reactant ratios and catalyst all have an effect on the product formation. At high reaction temperatures, isocyanurate would be thermodynamically favored as this product has the highest thermal stability in a series with urethanes, allophanates and isocyanurates. When isocyanate is used in excess over the alcohol, the produced urethane will further react with the remaining isocyanate to produce allophanate or isocyanurate<sup>[44]</sup>. Another factor is the catalyst. Previous studies have shown that catalysts like dibutyltin dilaurate (DBTDL) are highly selective towards urethane formation, whereas 1,4-diazabicyclo[2.2.2]octane (DABCO) catalyzes the urethane reaction but also the allophanate formation, albeit at a much lower rate. Tertiary amine catalysts like *N,N,N',N'',N''*-Pentamethyl diethylenetriamine (PMPT) and tris(3-dimethyl aminopropyl)-hexahydro-s-triazine (TDHT), amino alcohol catalysts like *N,N,N'*-trimethyl aminoethyl ethanolamine (DABCO<sup>®</sup> T), metal carboxylates and alkoxides, however, show a stronger catalytic tendency for isocyanurate formation. When using PMPT, TDHT and potassium carboxylates as catalysts, urethane and isocyanurate reactions take place simultaneously and allophanate is observed transiently in small amounts as an intermediate. With DABCO<sup>®</sup> T as a catalyst, the urethane reaction was followed by the isocyanurate reaction, however, when the

isocyanurate reaction sets in, it became the dominant reaction and allophanate formation was not observed.<sup>[45,46]</sup>



**Scheme 4.** The formation of isocyanurate via alcohol or urethane

Alcohol and urethane can promote isocyanurate formation. The presence of water retards its formation<sup>[47,48]</sup>. In the cited paper, model reactions containing phenyl isocyanate, n-butanol, water and PMPT catalyst were carried out in acetonitrile at 50 °C. Alcohol was reported to catalyze the isocyanurate formation, whereas the addition of water retarded the isocyanurate forming reactions. Biuret was observed as an intermediate during the process but instead of further reacting with isocyanate to produce isocyanurate, it was considered to mainly convert back to urea and isocyanate in the later stage of the reaction.

### Oxazolidinone formation

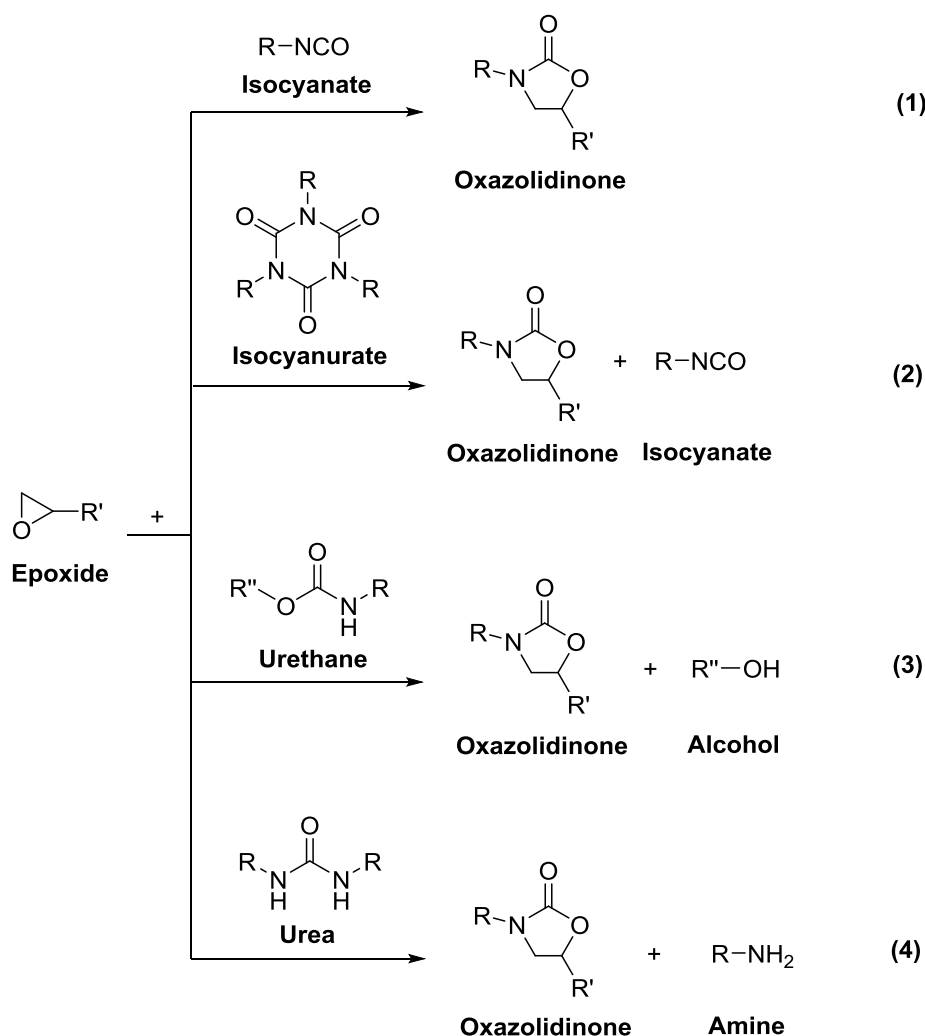
Polyisocyanurate crosslinks lead to rigid foams with good thermal stability and some fire resistance. However, the highly crosslinked nature of polyisocyanurate networks also causes the foam to be brittle and fragile. Oxazolidinones also have a thermally stable cyclic structure. Being more thermally stable than urethane<sup>[49]</sup> it may be considered to be a promising building unit for rigid foam modification<sup>[50]</sup>.

The oxazolidinone linkage can be formed by reacting epoxide with isocyanate. Several ways of oxazolidinone formation have been reported in literature in the context of isocyanate chemistry. There under is the addition of epoxide to isocyanate and a decomposition of isocyanurate upon the attack of an epoxide (Scheme 5 (1) and (2))<sup>[51-53]</sup>. These two pathways both involve epoxide ring opened nucleophiles as intermediates. Lithium halides<sup>[54]</sup>, chromium complexes<sup>[55]</sup>, alkoxides of alkali earth metals<sup>[50]</sup>, tertiary amines<sup>[53]</sup>, 2,4,6-tris-(dimethylamino methyl)-phenol<sup>[56]</sup>, ammonium halides<sup>[17]</sup>, *N*-heterocyclic carbenes - Lewis acids complexes<sup>[57]</sup> and organoantimony - iodide complexes<sup>[58]</sup> have been reported as catalysts.

Along with the oxazolidinone formation, competing reactions like isocyanate trimerization and epoxide homopolymerization may occur. The reaction selectivity is influenced by the type of catalyst, reaction temperature, reactant ratios and the chemical structures of the reagents. When using tertiary amine, 2,4,6-Tris-(dimethyl aminomethyl)-phenol and ammonium halides as catalysts, isocyanurate formation was favored at low temperature, while oxazolidinone formation and epoxide homopolymerization took place at high temperature<sup>[56,59,60]</sup>. Yb(OTf)<sub>3</sub> was reported to catalyze epoxide homopolymerization, but not the oxazolidone or isocyanurate formation at temperatures below 130 °C. With increasing reaction temperature, isocyanurate formation occurs first and followed by oxazolidinone formation<sup>[52]</sup>. With organoantimony iodide as a catalyst, the oxazolidinone formation was proved to be much faster than the trimerization reaction or the epoxide homopolymerization<sup>[58]</sup>. Except for the reaction temperature and catalyst employed, the reactant equivalent ratio also played a role in the reaction product formation. It was found that a higher isocyanate ratio lead to increased isocyanurate formation, while an excess of epoxide promoted oxazolidinone formation<sup>[51,60,61]</sup>. Also the chemical nature of the reactants showed an effect. In epoxide-isocyanate reactions aromatic isocyanates with electron-withdrawing substituents were reported to readily form isocyanurate<sup>[55]</sup>.

Besides the addition of epoxide to isocyanate and the decomposition of isocyanurate upon the attack of an epoxide, studies have shown that oxazolidinone can also be

formed in the reaction between epoxide and urethane or urea (Scheme 5 (3) and (4)). In these reactions, tertiary amines, quaternary ammonium salts and ionic liquids were used as catalysts. There was evidence showing that these reactions proceed via an intermolecular addition process without dissociation of the urethane or urea bond.<sup>[62–65]</sup>



**Scheme 5.** Formation pathways of oxazolidinone

## 1.2 Resin curing and the time-temperature-transformation (TTT) cure diagram

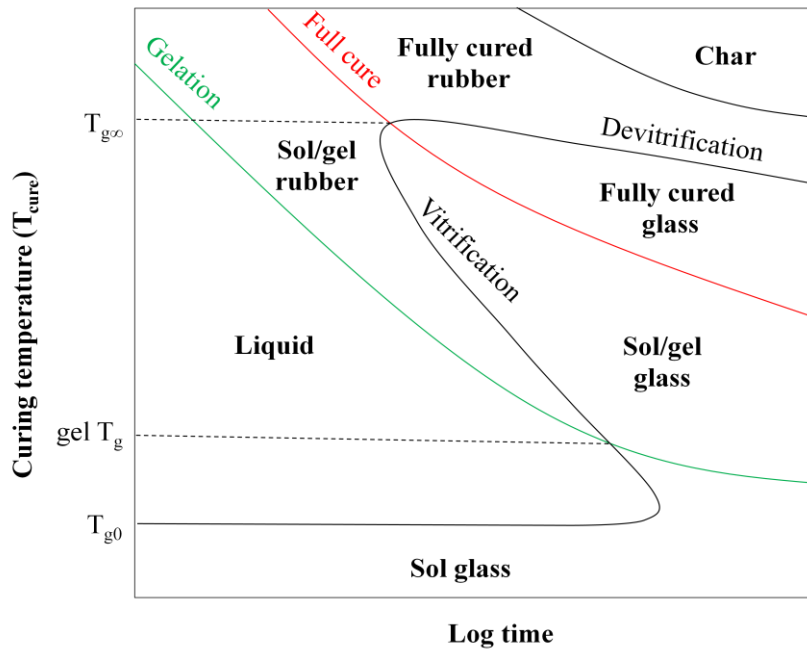
In addition to the chemistry, the physical state of the polymer forming system also plays an important role in the reaction process. The physical state will affect the macroscopic flow, polymer chain mobility and molecular diffusion rates, and will in turn affect the reaction rate and possibly the extent of conversion. During the curing



reaction of a thermosetting system, the polymer chains grow and the crosslink density increases with increasing conversion and the physical state of the system changes from liquid to gel to rubber and then, depending on the temperature, to glass. Among all these transformations, the transition from rubber to glass normally has the highest impact on the reaction conversion. The temperature at which the polymer transforms from a rubber to a glass is known as the glass transition temperature (T<sub>g</sub>) of the polymer. The polymer turns into a glass when the cure temperature is lower than the system T<sub>g</sub>. In the glassy state, the molecular chain segments no longer have sufficient mobility for collisions and any intermolecular reaction essentially stops. Factors affecting the value of the T<sub>g</sub> include (a) chemical structure: polymers with relatively “flexible” chains and little interactions show a low T<sub>g</sub>; (b) chemical composition: in a single-phase copolymer, the T<sub>g</sub> of a copolymer lies in-between the two T<sub>g</sub> values of the corresponding homopolymers; (c) molecular architecture: increased molecular weight and crosslinking density both lead to a higher T<sub>g</sub><sup>[66]</sup>. When these factors are translated to terms of polyurethane rigid foams, they correspond in a first approximation to the hydroxyl value and functionality of employed polyols, weight fraction of aromatic structures and polyisocyanurate content. Studies have shown that as the values of the above fractions increase, the T<sub>g</sub> of the foam matrix material increases as well<sup>[56,67]</sup>. Because of the high crosslink density and high aromatic content, rigid foams usually have relatively high values of T<sub>g</sub>, in general higher than 150 °C. Therefore, a high curing temperature, T<sub>cure</sub>, will be required to maintain chain mobility and achieve full cure.

The curing behavior of a polymer system, including gelation, vitrification, full cure, devitrification and char formation, can be systematically understood by using the time-temperature-transformation (TTT) cure diagram. The TTT cure diagram illustrates the relationship between curing time, curing temperature and the physical transformations of the reaction system. The cure behavior of different systems which include epoxy and styrene curing systems has been mapped into the so-called TTT cure diagram to describe their curing behavior<sup>[68–72]</sup>. The TTT cure diagram is system

specific and can provide a theoretical framework to understand the curing behavior of solvent free thermosetting polymerization systems. Figure 1 shows a typical TTT cure diagram of a thermosetting system<sup>[68,69,71,72]</sup>. The diagram is divided into several zones separated by five contour lines. Each zone represents a different physical state of the reaction system. The five contour lines can be constructed by determining the times to system gelation, vitrification, full cure, devitrification and char formation at different isothermal curing temperatures,  $T_{\text{cure}}$ . Gelation is the point when molecules with infinite molecular weight are formed. Vitrification occurs when the  $T_g$  of the system exceeds the  $T_{\text{cure}}$ . When the system enters the vitrified state, the mobility of the macromolecular chains reduces strongly and the reaction rate slows down substantially. Full cure corresponds to complete conversion of the reactive groups. Devitrification can occur upon thermal decomposition and is commonly associated with a decrease in  $T_g$ . Upon prolonged exposure to high temperatures, the network can further deteriorate and char formation can occur. Three critical temperatures  $T_{g_0}$ , gel  $T_g$  and  $T_{g_\infty}$  are marked on the temperature axis.  $T_{g_0}$  is the glass transition temperature of the reactant mixture prior to the start of the reaction. The gel  $T_g$  is the temperature at which gelation and vitrification occur simultaneously. When  $T_{\text{cure}}$  is below the gel  $T_g$ , the system vitrifies before gelation occurs; when  $T_{\text{cure}}$  is higher than the gel  $T_g$  the system will gel prior to vitrification.  $T_{g_\infty}$  is the glass transition temperature of the fully cured polymer system. When  $T_{\text{cure}}$  is above  $T_{g_\infty}$ , full cure can be achieved. However, when  $T_{\text{cure}}$  is below  $T_{g_\infty}$ , the system will vitrify before full cure is reached. If  $T_{\text{cure}}$  is not too far below  $T_{g_\infty}$ , the reaction may continue in the vitrified state, albeit at a much lower rate and full cure can eventually be obtained with enough reaction time. However, when  $T_{\text{cure}}$  is substantially below  $T_{g_\infty}$  it is not likely that full cure will be achieved. The studies on simple reaction systems, such as epoxide-amine and isocyanate-polyol curing systems have shown that the reaction rate prior to vitrification is largely kinetically controlled but becomes diffusion controlled after vitrification. The reaction after vitrification slows down and the reaction finally grinds to a hold and unreacted reactive groups remain<sup>[73-75]</sup>.



**Figure 1.** Schematic time-temperature-transformation (TTT) cure diagram of a typical thermosetting system

Unlike the isothermal reaction conditions shown in the TTT cure diagram, foaming reactions are generally non-isothermal processes. With increasing conversion, the heat builds up with the exothermal processes and the temperature of the foam increases. The foam starts to cool down when the major reactions in the foam have seized, either because of system vitrification or full conversions of reactive groups. Despite the non-isothermal reaction process, the TTT cure diagram can still be used to understand the curing process of rigid foams in a qualitative manner.

During a rigid foam expansion, four characteristic times can be used to describe the foam expansion characteristics, these are: start time, gel time, end of rise time and the time at which the full hardness has been obtained. Start time is the time when foaming begins after the reactants have been mixed. The moment at which gelation occurs is defined as the gel time. The system  $T_g$  after gelation is still low and the system temperature further increases because the reaction continues. At this stage, the foam expands in the rubbery state until the end of rise time is reached. At the end of rise time, the strength of the polymer matrix is high enough to withstand the gas pressure

in the foam cells and the foam expansion stops. Although the foam stops rising from a macroscopic perspective, the curing reaction can continue as long as the system  $T_g$  is below  $T_{cure}$ . With continuing reaction the polymer network further densifies and at a certain moment the polymer starts to vitrify. The vitrification is associated with hardness development of the foam. Typically after a few minutes, the foam reaches full hardness. Because of the thermal insulation property of rigid foams, high reaction temperatures can be reached in the core of the foam and hence a high or even complete reactant conversion can be obtained. In case of a full curing, the system usually reaches its maximum temperature when all the reactive groups have been converted, then the foam starts to cool down and the polymer vitrifies to a fully cured glass. The reaction temperature at the foam surface can be much lower than that in the foam core because heat is lost to the environment. The system vitrifies when the  $T_g$  of the polymer matrix exceeds the reaction temperature, the polymerization reaction ceases and an incompletely cured glass is obtained. The incomplete cure of the foam polymer matrix material can become an issue and may give rise to some concerns. As reported in previous studies on polyurethane-polyisocyanurate rigid foam, the extent of cure was closely related to the isocyanurate content in the system, hence affecting foam properties like flammability<sup>[76]</sup>, dimensional stability, compression strength<sup>[9]</sup> and surface adhesion. In summary, full cure of the rigid foams could only be achieved when  $T_{cure}$  is either above or just below  $T_{g\infty}$ . The  $T_{g\infty}$  of the foams can experimentally be determined using dynamic mechanical analysis (DMA) on the final foam<sup>[67,77]</sup>. The value of  $T_{g\infty}$  determined can serve as a guide for the selection of  $T_{cure}$ . Of course, potential cure problems can also be alleviated by applying longer cure times.

### **1.3 Methods employed to study the chemical reaction pathways**

Polyurethane rigid foams are thermosetting materials that are insoluble and infusible once formed. The highly crosslinked nature of the polymer strongly hampers the elucidation of the chemistry that takes place during its formation with molecular methods. The reason is that the analytical techniques such as solvent based nuclear magnetic resonance (NMR) spectroscopy, mass spectroscopy (MS), liquid

chromatography (LC) and gas chromatography (GC) can no longer be used. Previous studies on the chemistry of rigid foams mainly relied on data obtained by Fourier transform infrared (FTIR) spectroscopy. For example, in epoxy-isocyanurate foams bearing oxazolidinone and isocyanurate linkages, the influence of reactant ratios and curing temperature on the formation of the chemical linkages was studied using FTIR spectroscopy<sup>[56]</sup>. In PUR/PIR foams, isocyanate conversion and ratio between isocyanurate and urethane linkages were monitored using FTIR spectroscopy<sup>[9]</sup>; Real time FTIR was also used in a qualitative analysis when studying the effect of catalysts on the type of bond formation in flexible and rigid foams<sup>[78,79]</sup>. Although FTIR can easily be applied from an experimental point of view, the analysis shows limitations when applied to complex reaction systems in which a variety of linkages are formed with similar absorbances and a quantification of the chemical entities is desired. As to the quantification, the temperature development obtained under pseudo-adiabatic reaction conditions was used to calculate the polyisocyanurate yield in polyisocyanurate foam<sup>[48,80]</sup>. This adiabatic temperature method was used as an easy to apply *in situ* method in high throughput experimentation. In the calibration, the urethane and urea formation were assumed to go to completion in the first part of the reaction and that the isocyanurate formation occurred thereafter. This method would have limitations when applied to a more complex reaction system, e.g. in which oxazolidinone and carbodiimide forming reactions may occur along with the isocyanurate formation.

Because of the limited availability of analytic methods for foam systems, model reactions with low molecular mass and mono-functional or bi-functional reaction analogs can provide a deeper insight into the fundamental chemistry. Model reactions resembling different reactive foam systems have been studied under various reaction conditions and were reported upon. For example, in catalytic studies on flexible foam systems, mono-functional and bi-functional reactants were used and the product analysis was performed using chemical titration and HPLC<sup>[81,82]</sup>. A urethane-modified isocyanurate foam system was studied by using phenyl isocyanate and n-propanol as

reactants, diglyme as solvent and a hydroxyl alkyl quaternary ammonium carboxylate as catalyst. FTIR spectroscopy was used as analytical method and the reaction mechanism could be elucidated<sup>[22]</sup>. In another study on urethane-modified isocyanurate foams, a model system containing mono-functional isocyanate, alcohol and epoxide was used. Sulfonium zwitterions in combination with alkali metal carboxylates were employed as catalyst. The major products were quantified by HPLC and an insight into the reaction pathways was obtained<sup>[83]</sup>.

These previous studies have provided a basic understanding of the general reactions that occur in polyisocyanurate foam and the analytic methods employed were proven to be effective in the product identification and quantification. Nevertheless, they still have limitations in one or several of the following aspects : (a), less functional groups were incorporated into the model reaction system than in the real foam system for simplification, (b), relatively large amounts of solvents were added and reactions were carried out at low temperatures to study the reaction kinetics, and (c), the temperature gradient from the foam core to the foam surface could not be mimicked adequately which limits a proper investigation of the temperature effects.

The objective of this investigation is to obtain a fundamental understanding of the chemistry that occurs in epoxide-modified polyurethane-polyisocyanurate rigid foam systems. In this study, all the key functional groups that are used in such foams were involved. These comprise isocyanate, epoxide, alcohol, water, formic acid, amine and catalyst. Systems that contain so many different reactive groups show complex reaction profiles and a dedicated program of work was required to elucidate the various reaction pathways. The study began with an investigation of model reaction systems using mono-functional analogs as reactants and HPLC, LC-MS, NMR spectroscopy and FTIR spectroscopy as experimental techniques. The model reactions were carried out in bulk or with small amounts of solvent to mimic the real rigid foam system. The catalyst selectivity and the influence of the addition of each of the individual reactants on the product distribution are discussed. Various reaction temperatures were selected to study the temperature dependency of the reaction

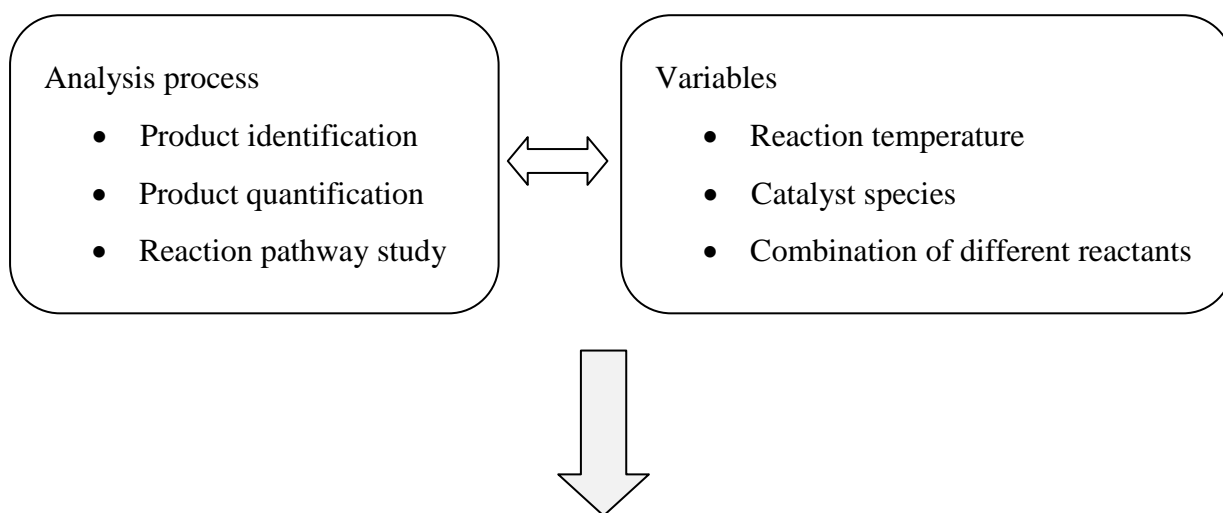
pathways. Thereafter, foam systems were studied and the reaction kinetics and bond formations were compared to that of the corresponding model systems. The differences observed were discussed in terms of diffusion control caused by the vitrification of the foam system. Methods to improve the chemical conversion were proposed and evaluated.

## 2. Motivation

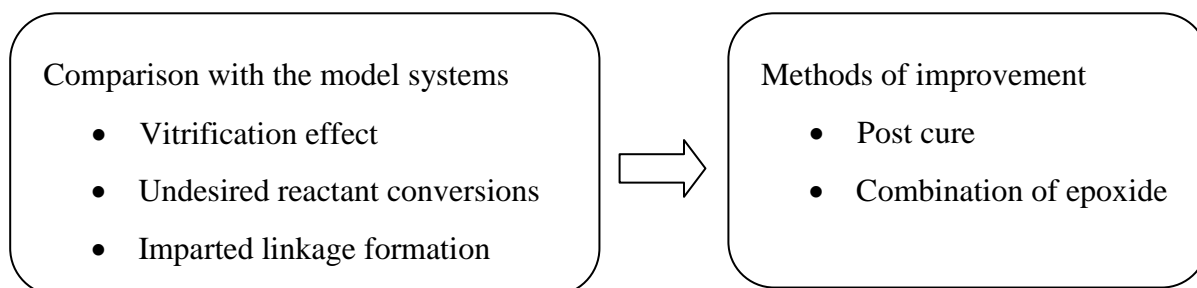
The aim of this study is to obtain a fundamental understanding of the chemistry that occurs in epoxide-modified polyurethane-polyisocyanurate rigid foam systems. The understanding of the reaction profile should provide possibilities to further tailor the various reaction pathways during the foam building reaction, in order to achieve desired chemical linkages balance for the best properties of the final polymer.

**Approach:** The study consists of two parts. It starts with a mono-functional model reaction system to reach an insight into all the reactions that can take place. The study continued to the foam systems in which the effect of network growth and vitrification on the course of reaction was investigated.

### Model reaction systems



### Foam systems





### 3. Results and Discussion

#### 3.1 Reaction pathway elucidation in a monofunctional model epoxide-modified PUR/PIR system

Model reaction systems containing low molecular weight, monofunctional reactants were first studied to understand the type of chemical bond formation and the reaction pathways. The system referred to as the “Model” system was used to study the detailed chemistry of an optimized epoxide-modified polyurethane-polyisocyanurate rigid foam formulation. In the “Model” system, the reactant equivalents are the same as in the foam system (Table 1). 1-Naphthyl isocyanate was used as the isocyanate component because its high boiling point enables the reaction to be carried out at high temperatures. 1-Octanol was used as the analogue of a polyol because its NMR signature has less overlap with the other relevant NMR signals. This allows a more accurate assess of the product concentrations such as urethane. In the foam system, polyethylene glycol with a molecular mass of 600 (PEG 600) was used as polyol. The polar ether groups in the polyether chain provided system compatibility. In the “Model” system, compatibilization was obtained by addition of a non-reactive ethylene glycol dimethyl ether homologue. The amount employed was kept to a lowest level for compatibility also for minimized solvent effects, in this case 29 wt% of the total weight of the reaction mixture. Two terms - “reactant equivalent” and “NCO index” - are used in describing the formulations. The “reactant equivalent” equals to the mass of a substance divided by its equivalent weight (Equation 1). In this formulation, the equivalent weight is the mass of a component which will react with 1 mol of isocyanate functionality. It is worth to mention that the equivalent weights of water and formic acid are 9 and 23, respectively, because they react with two isocyanates to form the final product - urea. “Isocyanate index” (NCO index) is a quantity referring to the excess of isocyanate added to the formulation with respect to reactive entities towards it. The amount of isocyanate added is divided by the theoretical amount required for full conversion of any entity reactive towards it (“component A”), and multiplied by 100 (Equation 2). “NCO index 200” thus means

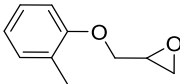
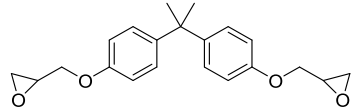
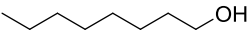
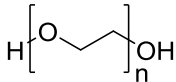
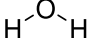
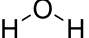
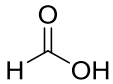
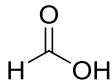
the amount of isocyanate added is 2 times the amount required to have a complete conversion of the component A with isocyanate.

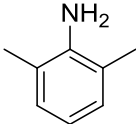
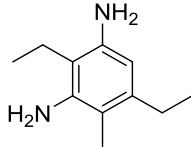
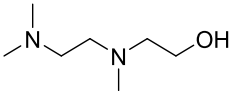
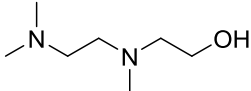
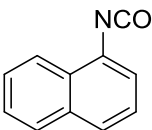
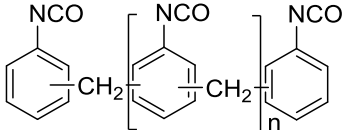
$$\text{Reactant equivalent} = \frac{\text{Mass of a substance}}{\text{Equivalent weight}} \quad \text{Equation 1}$$

$$\text{NCO index} = \frac{\text{Actual amount of isocyanate added}}{\text{Theoretical amount of isocyanate required}} \times 100 \quad \text{Equation 2}$$

The NCO index was kept at 200 in this study. *N,N,N'*-trimethyl aminoethyl ethanolamine (DABCO<sup>®</sup> T) was employed as catalyst and added dissolved in component A. The catalyst amount was 0.025 equivalent per equivalent amount of reactive groups in the component A, not counting the hydroxyl functionality of DABCO<sup>®</sup> T in the index calculation.

**Table 1.** Formulations of the “Model” and foam systems

	<b>Reactant equivalent</b>	<b>Reactants in Model system*</b>	<b>Reactants in Foam system</b>
<b>Comp. A</b>	1.0	 Glycidyl 2-methylphenyl ether	 Bisphenol A diglycidyl ether
	0.5	 1-Octanol	 Polyethylene glycol 600
	1.0	 Water	 Water
	0.5	 Formic acid	 Formic acid

	0.5	 2,6-Dimethyl aniline	 Diethyltoluenediamine
	0.0875	 DABCO <sup>®</sup> T	 DABCO <sup>®</sup> T
<b>Comp. B</b>	7.0	 1-Naphthyl isocyanate	 Lupranat <sup>®</sup> M20R

\* Tetraethylene glycol dimethyl ether or polyethylene glycol dimethyl ether (Mw=1000) was added as solvent to obtain a compatible Component A. Solvent content: 29 wt%

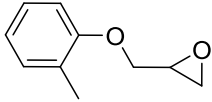
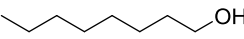
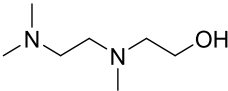
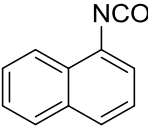
The “Model” system contains many different reactive groups, so complex reaction process can be expected. A dedicated program of experimental work was required to elucidate the various reaction pathways. The investigation started with a series of simplified monofunctional reaction systems. In this process, the effects of reaction temperature, catalyst choice and the combination of the individual reactants on the product formation were discussed. Subsequently, the “Model” system was studied and compared to the foam system in Chapter 3.2. The first monofunctional system investigated is referred to as the “Ep\_ROH\_NCO\_catalyst” system and contains epoxide, alcohol, isocyanate and catalyst.

### 3.1.1 Epoxide\_alcohol\_isocyanate\_catalyst (“Ep\_ROH\_NCO\_catalyst”) system

#### 3.1.1.1 Formulation and reaction condition

The formulation of the “Ep\_ROH\_NCO\_catalyst” system with DABCO<sup>®</sup> T as catalyst (“Ep\_ROH\_NCO\_DAB”) is shown in Table 2.

**Table 2.** Formulations of the “Ep\_ROH\_NCO\_DAB” system

	Reactant	Chemical structure	Reactant equivalent
<b>Component A</b>	Glycidyl 2-methylphenyl ether		1.0
	1-Octanol		0.5
	DABCO <sup>®</sup> T		0.0375
<b>Component B</b>	1-Naphthyl isocyanate		3.0

A temperature gradient exists from the foam surface to the foam core in the real foaming process. The monofunctional “Ep\_ROH\_NCO\_DAB” system was therefore conducted at three temperatures, using an external oil bath set at 80 °C, 130 °C or 160 °C. A reactant amount of 2 g was taken to minimize the temperature difference between the oil bath and the reaction system. The oil bath was pre-heated to the required temperature and the reaction vessel was put at once into the hot oil. This assured a fast heating mimicking the temperature profile as it would occur in a real foaming reaction. The maximum temperature in the reaction system was obtained within 2-3 minutes. The temperature differences between the oil bath and the recorded maximum temperatures of the reactions were equal or less than 5 °C (Table 3). The total reaction time was 10 minutes, which is close to the heat development duration in the real foaming process and is a time frame of interest for this study.

**Table 3.** Temperature difference between the oil bath and the reaction system

<b>Oil bath temperature ( °C)</b>	<b>Maximum temperature of reaction system ( °C)</b>	<b>Deviation ( °C)</b>
80	83	+3
130	135	+5
160	164	+4

### 3.1.1.2 Chemical bond analysis

High performance liquid chromatography (HPLC) equipped with a UV detector and HPLC coupled to an ESI-TOF mass spectrometer (LC-MS) were used for product identification. <sup>1</sup>H NMR spectrometry and gas evolution measurement were used for the product quantification.

HPLC with UV detection and LC-MS were used to complement and verify the result of each individual technique. The reaction products of the “Ep\_ROH\_NCO\_DAB” system were a mixture of different substances. The chromatograms of reaction products obtained at different reaction temperatures are shown in Figure 2 and the product assignments are listed in Table 4. In HPLC, the UV absorption signal was utilized to detect each component. The component identities were assigned by comparing their retention times with that of reference substances. The reference substances include the reactants, products isolated from the product mixture by column chromatography and other potential products indicated by the ESI-MS (+) measurement. The potential reaction products were separately synthesized (c.f. Experimental). The structures of the reference substances were confirmed by one or several of the analytical methods such as <sup>1</sup>H NMR, <sup>13</sup>C NMR, ESI-MS (+) and FTIR.

The risk of using only an UV detector is missing the detection of components with no or only a weak UV absorption. Furthermore, some reference substances were difficult to separate or synthesize, thus a few of the peaks in the HPLC chromatogram remained unassigned. Therefore, LC-MS was used as a complementary method by

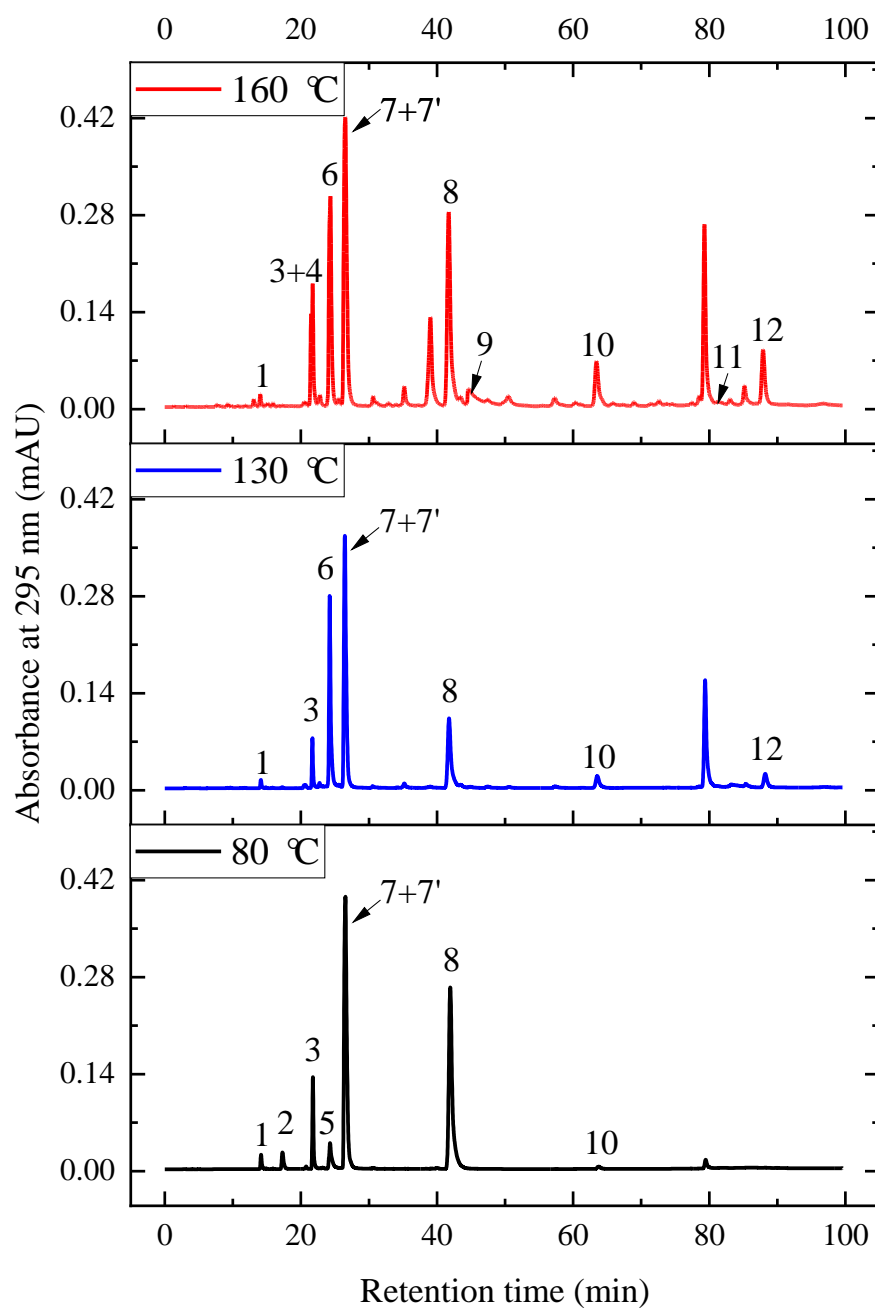
which more components could be identified by mass spectroscopy. The component assignments were performed by comparing the base peak in the mass spectrum with the exact mass of some potential substances, calculated to the first decimal place and most peaks in the LC-MS chromatogram could now be assigned. Although still a few substances remained unidentified, the product quantification showed that they were only present in low amounts. Preparative HPLC, which was not available during this study, could be a useful technique in future studies for an even further refined identification of low amounts of unknown products.

The reaction products can be subdivided into four categories (Table 4). The first category is the isocyanurate conformational isomers. The formation of the conformational isomers is caused by the bulky naphthyl substituent. Steric hindrance causes the naphthyl groups to adopt an out-of-plane structure and restricts rotation over the C-N bond. Thus the three naphthyl groups can either be on one side (*syn*-isocyanurate, peak 7'), or on two sides (*anti*- isocyanurate, peak 7)<sup>[84,85]</sup>. The two conformational isomers were separated by column chromatography and their structures were determined by <sup>1</sup>H NMR, <sup>13</sup>C NMR, ESI-MS (+) and FTIR. An attempt to obtain the absolute conformation of the *anti*- isocyanurate was undertaken using single crystal X-ray diffraction. Despite the relatively poor quality of the single crystal, the evidence from the result indicated that the substance could be an isocyanurate species instead of the imino oxadiazinedione isomer. Because the formation of conformational isomers is a special case when using the bulky 1-naphthyl isocyanate and the molecular conformation is not the focus of this thesis, the *syn*- and *anti*-isocyanurates are most of the time taken together as isocyanurate without any further differentiation.

The second product category includes urethane (peak 8), urea (peak 3), amine (peak 1) and their subsequent reaction products with epoxide (peak 10, 12, 16, 18, 20 and 22). The reaction pathways will be discussed in detail in Chapter - 3.1.1.3. The third category is oxazolidinone and the fourth category is the subsequent reaction products of carbodiimide (CDI) (peak 4, 9, 9', 11, 14, 15, 17, 19 and 21). As carbodiimide

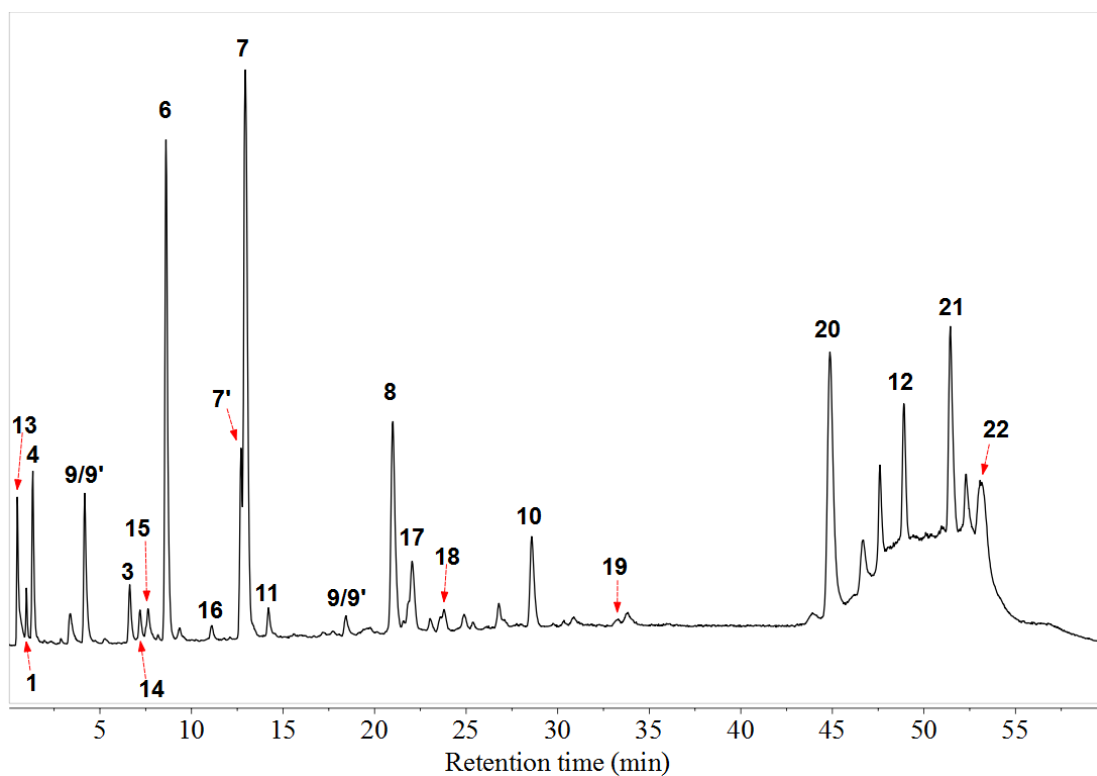
quickly participates in consecutive reactions once formed, the carbodiimide monomer cannot be found in the final product. The uncategorized substances include unreacted epoxide, decomposition products and an internal reference standard that was used in the HPLC tests.

The products from the first and second category are formed and unreacted epoxide is detected in the reaction mixture of 80 °C. <sup>1</sup>H NMR analysis shows that oxazolidinone from the third category is only formed in trace amount and no carbodiimide related products in the fourth category can be detected using ESI-MS (+). The products from the first three categories are formed at 130 °C. Epoxide is still present (<sup>1</sup>H NMR). ESI-MS(+) shows that the carbodiimide consecutive products are present in low abundance. Products of all four categories are present and the epoxide has almost completely reacted when the reaction is performed at 160 °C.



**Figure 2 (a).** Chromatograms of reaction products at different reaction temperatures, detected by HPLC with UV detection





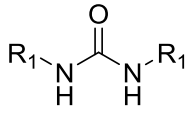
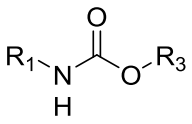
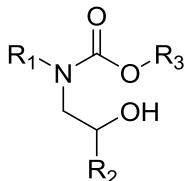
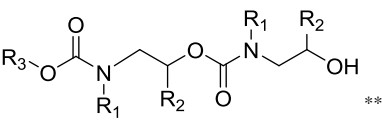
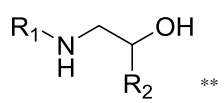
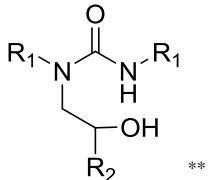
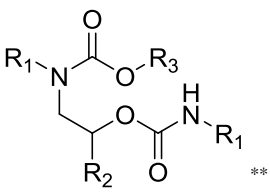
**Figure 2 (b).** Chromatograms of reaction products at 160 °C, detected by LC-MS

**Table 4.** Product assignments of Figure 1.

**Category 1 - isocyanurate**

Peak	Product species	Chemical structure *	Remarks
7	<i>anti</i> -Isocyanurate		Conformational isomer
7'	<i>syn</i> - Isocyanurate		Conformational isomer

Category 2 - urethane, urea, amine and their addition products with epoxide

Peak	Product species	Chemical structure *	Remarks
1	Naphthyl amine	$R_1-NH_2$	$R_1NCO$ reacts with water or decomposition of urea/urethane
3	Urea		
8	Urethane		
10	Alcohol_2		Urethane (peak 8) reacts with epoxide
12	Alcohol_3		Urethane_2 (peak 19) reacts with epoxide
16	Amino alcohol		Amine (peak 1) react with epoxide
18	Alcohol_5		Urea (peak 3) reacts with epoxide
20	Urethane_2		Alcohol_2 (peak 10) reacts with $R_1NCO$

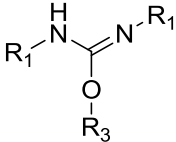
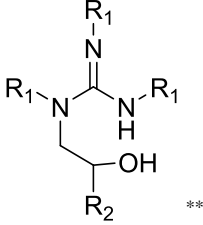
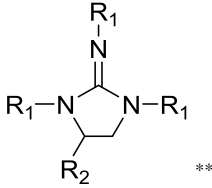
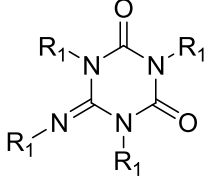

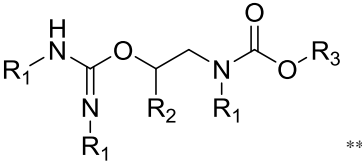
22	Urethane_3		Alcohol_3 (peak 12) reacts with R <sub>1</sub> NCO
----	------------	--	--

### Category 3 - oxazolidinone

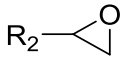
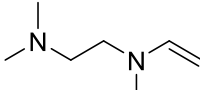
Peak	Product species	Chemical structure *	Remarks
6	Oxazolidinone		

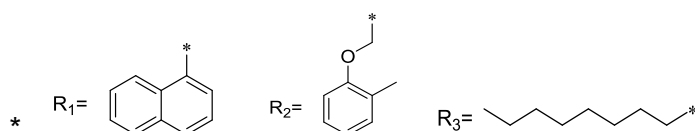
### Category 4 - carbodiimide subsequent products

Peak	Product species	Chemical structure *	Remarks
4	Guanidine		CDI reacts with amine (peak 1)
9	Oxazolidinimine		CDI reacts with epoxide
9'	Imidazolidinone		Isomer of 9

11	Isourea		CDI reacts with octanol
14	Alcohol_4		Guanidine (peak 4) reacts with epoxide
15	Imidazolidinimine		Ring closure product of 14
17	Iminotriazinedione		CDI reacts with R <sub>1</sub> NCO
19	Iminotriazinone		CDI reacts with R <sub>1</sub> NCO
21	Isourea_2		Alcohol_2 (peak 10) reacts with CDI

### Others

Peak	Product species	Chemical structure *	Remarks
2	Epoxide		Unreacted
5	p-Xylene		Internal reference standard
13	Olefin		Decomposition of DABCO® T



\*\* and/or regioisomers

The major products were quantified by  $^1\text{H}$  NMR. The carbodiimide quickly converts into a series of derivatives. The total amount of carbodiimide produced as an intermediate during the reaction was calculated by measuring the  $\text{CO}_2$  evolution. The negative values reported for the carbodiimide formation at  $80^\circ$  and  $130^\circ\text{C}$  must be taken as the experimental error in the gas measurements. In line with this, no carbodiimide based products are detected by ESI-MS in the reaction mixture of  $80^\circ\text{C}$  and only at very low concentration for reaction performed at  $130^\circ\text{C}$ . Therefore, the negative values were taken as 0% when calculating the isocyanate conversion into “Others”.

Both isocyanate and alcohol reaches full conversions at all three reaction temperatures, whereas always some epoxide is left (Table 5). The main reaction products are shown to be isocyanurate (Category 1), urethane (Category 2: peak 8), oxazolidinone (at  $130^\circ\text{C}$  and  $160^\circ\text{C}$ , Category 3) and carbodiimide (at  $160^\circ\text{C}$ , as intermediate, Category 4). The amounts of the products being formed are expressed as the conversion of isocyanate, epoxide and alcohol, respectively. Besides the quantified

products, other products are formed of which the amounts were not quantified individually but taken all together in a class termed “Others”. These products were not identified positively either because the signals overlaps in NMR or because their synthesis as reference is too elaborate.

According to the results of the product identification and the GPC measurement, the reactant conversions into “Others” can mainly be attributed to three kinds of reactions. The first kind is the reaction between urethane and epoxide. Except for the urethane that remains in the final product, some urethane formed during the reaction reacts with epoxide and generated a series of subsequent products (Category 2: peak 10, 12, 19 and 21). The detailed reaction pathways will be discussed in Chapter 3.1.1.3. The second kind concerns the consecutive reactions of carbodiimide. Although the amount of isocyanate which converts into carbodiimide is quantified by gas evolution method, the subsequent reaction of carbodiimide can further consume additional isocyanate, epoxide and alcohol. A further option is the homo-polymerization of the epoxide. Although there is no conclusive evidence that polyether is formed, an indication for polymerization was obtained from a GPC measurement. The GPC result shows that oligomers with molecular weights between 1000 and 1700 are detected in the reaction product obtained at 160 °C (Experimental Part).

**Table 5 (a).** Isocyanate conversion into each product

Isocyanate conversion into	80 °C		130 °C		160 °C	
	Average (%)	Experiment error (%)	Average (%)	Experiment error (%)	Average (%)	Experiment error (%)
Isocyanurates	77	1	65	7	52	1
Oxazolidinone	0	0	4	1	9	1
Urethane	15	1	10	1	9	0
Carbodiimide (as intermediate)	-3 (0)	2 (0)	-1 (0)	1 (0)	4	2
Urea	3	1	2	1	2	
Naphthyl amine	1	0	1	0	1	0
Others	4	3	19	6	24	2
<b>Total isocyanate conversion</b>	100	0	100	0	100	0

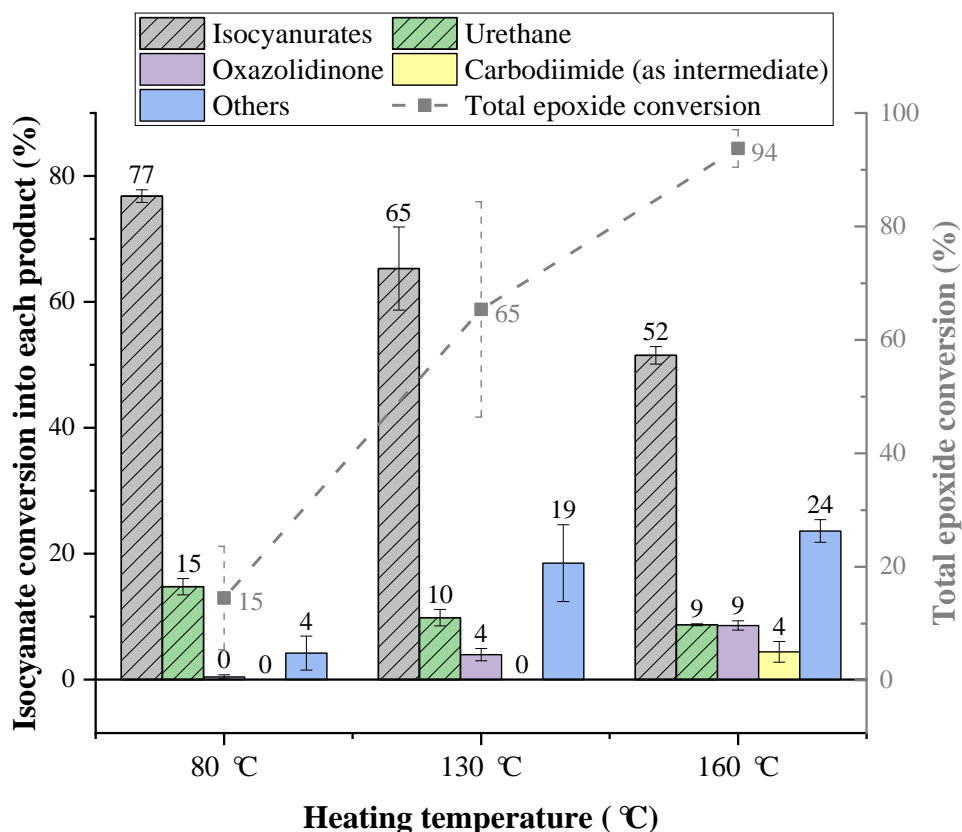
**Table 5 (b).** Epoxide conversion into each product

Epoxide conversion into	80 °C		130 °C		160 °C	
	Average (%)	Experiment error (%)	Average (%)	Experiment error (%)	Average (%)	Experiment error (%)
Oxazolidinone	1	1	12	3	26	2
Others	13	10	54	17	68	4
<b>Total Ep conversion</b>	15	9	65	19	94	3

**Table 5 (c).** Alcohol conversion into each product

Alcohol conversion into	80 °C		130 °C		160 °C	
	Average (%)	Experiment error (%)	Average (%)	Experiment error (%)	Average (%)	Experiment error (%)
Urethane	89	8	59	8	52	1
Others	12	8	41	8	48	1
<b>Total alcohol conversion</b>	100	0	100	0	100	0

The amounts of the main products are expressed in the isocyanate conversion and presented as a bar diagram (Figure 3, numerical values on the left). The total epoxide conversion is shown as a dashed line (numerical values on the right).



**Figure 3.** Main products (numerical values on the left) and epoxide conversion (numerical values on the right) at the three reaction temperatures



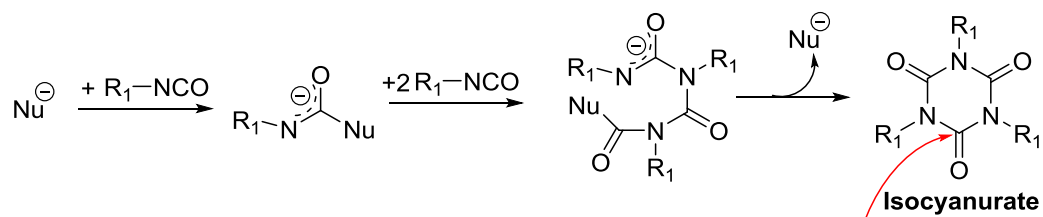
The results of product identification and quantification show that the reaction at 80 °C is relatively simple. Alcohol and isocyanate have full conversions while only 15% of epoxide has reacted. The majority of alcohol reacts with isocyanate and remains as urethane in the product mixture. The conversion of isocyanate into urethane amounts to 15%, which is close to the expected value of 17%. The rest of the isocyanate mainly converts into isocyanurate. These two reactions accounts for nearly 92% of the total isocyanate conversion. Although consecutive products of a reaction between urethane and epoxide are detected by HPLC and ESI-MS (+), these products were are in concentration. The amounts of isocyanurate and urethane decrease while the amounts of oxazolidinone, carbodiimide (as intermediate) and “Others” increase at higher temperatures. The total epoxide conversion also increases with reaction temperature and reaches 94% at 160 °C.

### **3.1.1.3 Reaction pathway discussion;**

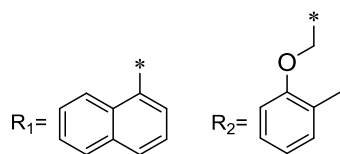
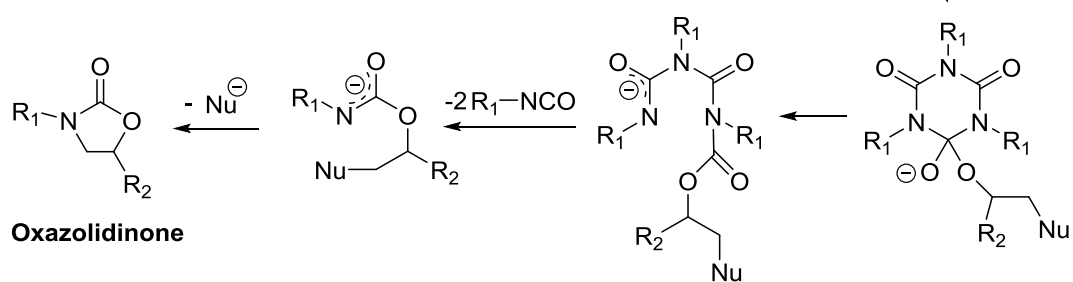
#### **Isocyanurate formation, decomposition and oxazolidinone formation**

Isocyanurate is the predominant product at all reaction temperatures. The most accepted mechanism of aromatic isocyanurate formation is shown in Scheme 6-Isocyanurate formation. The pathway was offered in the introduction<sup>[24,28,60]</sup>. In the “Ep\_ROH\_NCO\_DAB” reaction system, three species - DABCO<sup>®</sup> T (the catalyst), urethane and alkoxide formed by epoxide ring opening reaction- can act as nucleophiles for the isocyanurate formation. Their structures are shown in Table 6. DABCO<sup>®</sup> T is a good catalyst for the isocyanurate formation. In addition, urethane and epoxide were proven to promote the isocyanurate formation (c.f. Chapter 3.1.1.4- Catalyst selectivity).

### Isocyanurate formation

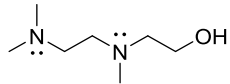
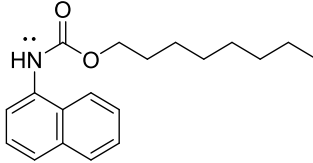
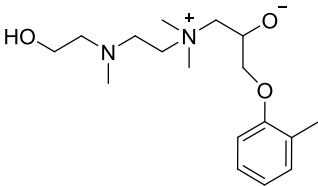


### Isocyanurate decomposition



**Scheme 6.** Isocyanurate formation, decomposition and oxazolidinone formation

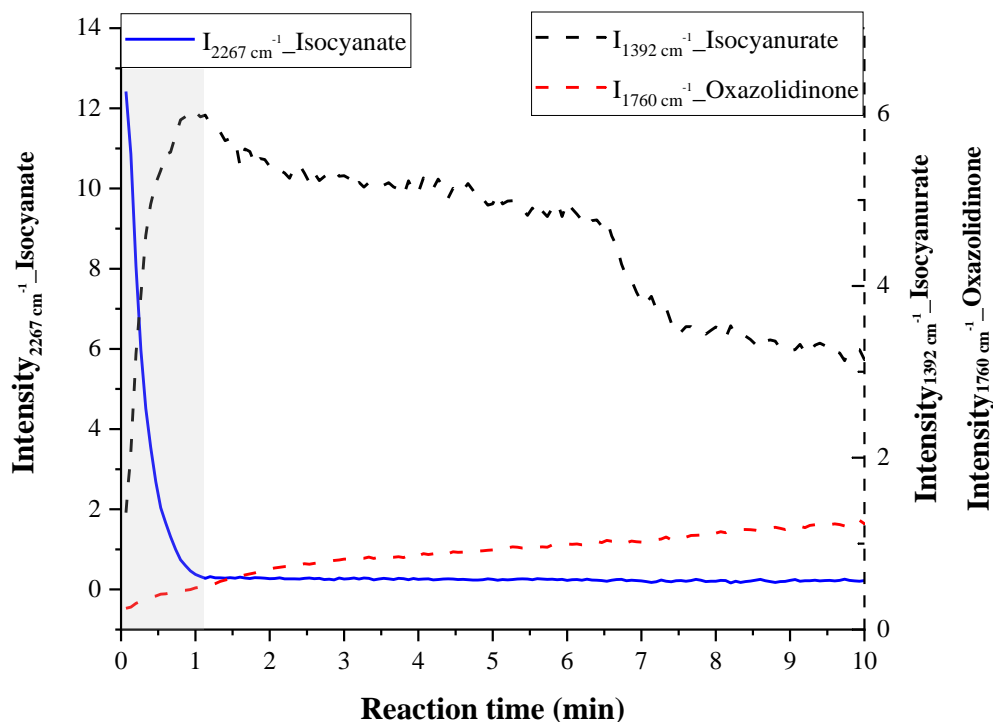
**Table 6.** Nucleophiles for the isocyanurate formation in the “Ep\_ROH\_NCO\_DAB” system

Item	Species	Structure
1	DABCO <sup>®</sup> T	
2	Urethane	
3	Alkoxide	

Product analysis in the “Ep\_ROH\_NCO\_DAB” system shows that the formation of isocyanurate is kinetically controlled whereas oxazolidinone is the thermodynamically favored product. The formation of isocyanurate starts to occur at low reaction temperature and accounts for 77% of the isocyanate conversion at 80 °C. This value decreases to 52% when the reaction temperature is increased to 160 °C. The change of isocyanurate amount at 160 °C was tracked by an online FTIR study in which the reaction was conducted isothermally at 160 °C and FTIR spectra were recorded with reaction time. The FTIR spectra were normalized using the aromatic C-H stretching at 3056 cm<sup>-1</sup>. The intensity of the absorption at 2267 cm<sup>-1</sup> was used to monitor the change of isocyanate whereas the intensity of the absorptions at 1392 cm<sup>-1</sup> was used to track the amount of the isocyanurate. The intensities of the absorptions were plotted against the reaction time (Figure 4). The isocyanurate concentration builds up rapidly in the first minute of reaction when there is free isocyanate in the system (shown in the grey zone). Afterwards, the isocyanate is almost completely consumed and the

amount of isocyanurate begins to decrease. It has been reported that isocyanurate can be decomposed by epoxide at high temperatures as shown in Scheme 6. During this process, oxazolidinone and isocyanate are produced<sup>[52, 53, 86]</sup>.

In the “Ep\_ROH\_NCO\_DAB” system, oxazolidinone can be formed via several reaction pathways. The first is the isocyanurate-epoxide reaction as shown in Scheme 6. The second is the urethane-epoxide addition-elimination reaction which will be discussed in the next section and the last possibility considered here is the isocyanate-epoxide addition reaction. No matter through which pathway the oxazolidinone is formed, it is always thermodynamically controlled. This is inferred from the fact that the oxazolidinone is hardly formed at 80 °C but accounts for 8.6% of the isocyanate conversion at 160 °C. The amount of oxazolidinone formed at 160 °C was also tracked by the online FTIR using the intensity of the absorption at 1760 cm<sup>-1</sup> (Figure 4). The amount of the oxazolidinone increases steadily with reaction time but the increment in the first minute is not as distinct as that of the isocyanurate. The above observations are consistent to the assumption that the formation of isocyanurate is kinetically controlled. It is the predominant reaction product at low reaction temperature and at high reaction temperature it is formed rapidly in the beginning of the reaction but is converted into the thermodynamically favored oxazolidinone at a later stage.

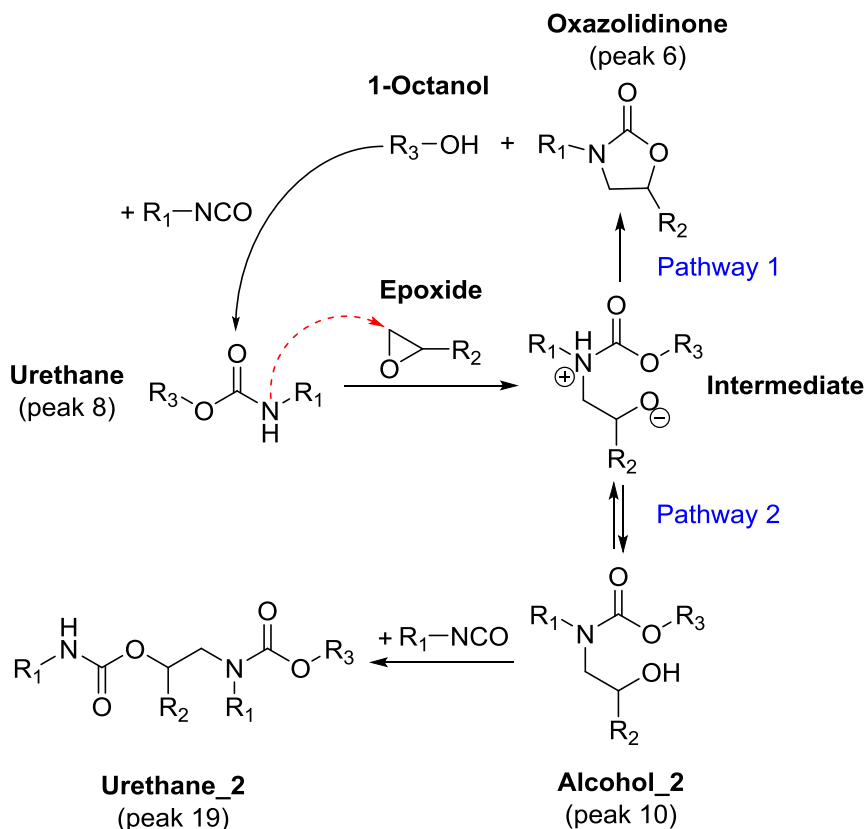


**Figure 4.** The absorption intensity of isocyanate, isocyanurate, oxazolidinone, urethane and carbodiimide by online FTIR at a reaction temperature of 160 °C

### Reactions between urethane and epoxide

In addition to acting as a nucleophile for the isocyanurate formation, the urethane is also shown to act as a nucleophile for the epoxide ring opening reaction. The nucleophilicity of urethane is resulting from the nitrogen atom lone pair in the carbamate group<sup>[62-64]</sup>. The reaction between epoxide and urethane can at least take place via two reaction pathways (Scheme 7). Firstly, an intermediate is considered to be formed in the nucleophilic addition reaction between urethane and epoxide. The intermediate can either undergo cyclization to form oxazolidinone and alcohol as shown in pathway 1 or undergo intramolecular proton transfer through pathway 2 to produce alcohol\_2 (category 2: peak 10). Along pathway 1, the regenerated alcohol can further react with an isocyanate to reproduce the starting urethane. Hence pathway 1 is part of a catalytic cycle and in principal, oxazolidinone can be generated

when isocyanate and epoxide monomers are still present in the reaction system. In pathway 2, the alcohol<sub>2</sub> can further react with an isocyanate to produce urethane<sub>2</sub> (category 2: peak 19). Then the urethane<sub>2</sub> acts as a new starting point to react with another epoxide and forms the subsequent products of alcohol<sub>3</sub> (category 2: peak 12), urethane<sub>3</sub> (category 2: peak 19) and probably oxazolidinone after releasing a molecule of alcohol<sub>2</sub>. Alcohol<sub>2</sub>, urethane<sub>2</sub>, alcohol<sub>3</sub> and urethane<sub>3</sub> which formed along pathway 2 were detected by HPLC with UV detection or by LC-MS, which indicates that pathway 2 does occur in the “Ep\_ROH\_NCO\_DAB” system. When the temperature is increased from 80 °C to 160 °C, the signals of alcohol<sub>2</sub> and alcohol<sub>3</sub> in HPLC chromatograms intensifies, indicating that the reactions in pathway 2 become more significant at higher temperatures. This is also reflected in the decrease of urethane amount in the final reaction product and the increase of reactant conversions into “Others” as reaction temperature increases. As to pathway 1, the oxazolidinone formation via urethane cannot be confirmed, because oxazolidinone can also be formed in the isocyanurate-epoxide reaction. Therefore, the formation of oxazolidinone by urethane and epoxide in the presence of catalyst DABCO<sup>®</sup> T was further studied in a model reaction (Table 7).



**Scheme 7.** Reaction pathways between epoxide and urethane

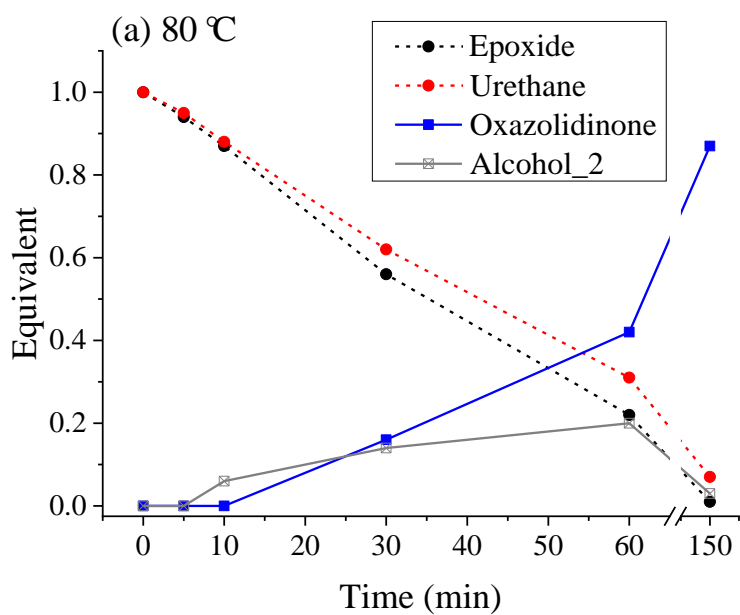
The reaction with the recipe in Table 7 was conducted at two reaction temperatures of 80 °C and 160 °C. Samples were taken during the reaction process. The changes in the concentrations of the reactants (epoxide and urethane) as well as that of the products (oxazolidinone and alcohol\_2) were calculated from <sup>1</sup>H NMR spectra (Table 8; Figure 5). 1-Octanol was formed as a byproduct but its chemical shifts in <sup>1</sup>H NMR were overlapping with other signals, and therefore its content was not quantifiable.

**Table 7.** Recipe of the model reaction between epoxide and urethane

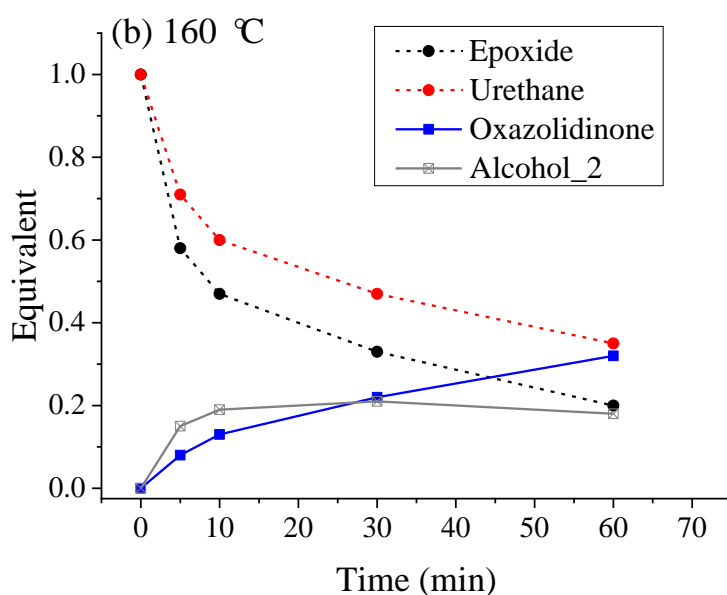
Reactant	Epoxide	Urethane	DABCO <sup>®</sup> T
Equivalent	1.0	1.0	0.025
Structure			

**Table 8.** The equivalent change of reactants and products with reaction time

Temperature	Time (min)	Epoxide	Urethane	Oxazolidinone	Alcohol_2
80 °C	0	1.00	1.00	0	0
	5	0.94	0.95	0	0
	10	0.87	0.88	0	0.06
	30	0.56	0.62	0.16	0.14
	60	0.22	0.31	0.42	0.20
	150	0.01	0.07	0.87	0.03
160 °C	0	1.00	1.00	0	0
	5	0.58	0.71	0.08	0.15
	10	0.47	0.60	0.13	0.19
	30	0.33	0.47	0.22	0.21
	60	0.20	0.35	0.32	0.18







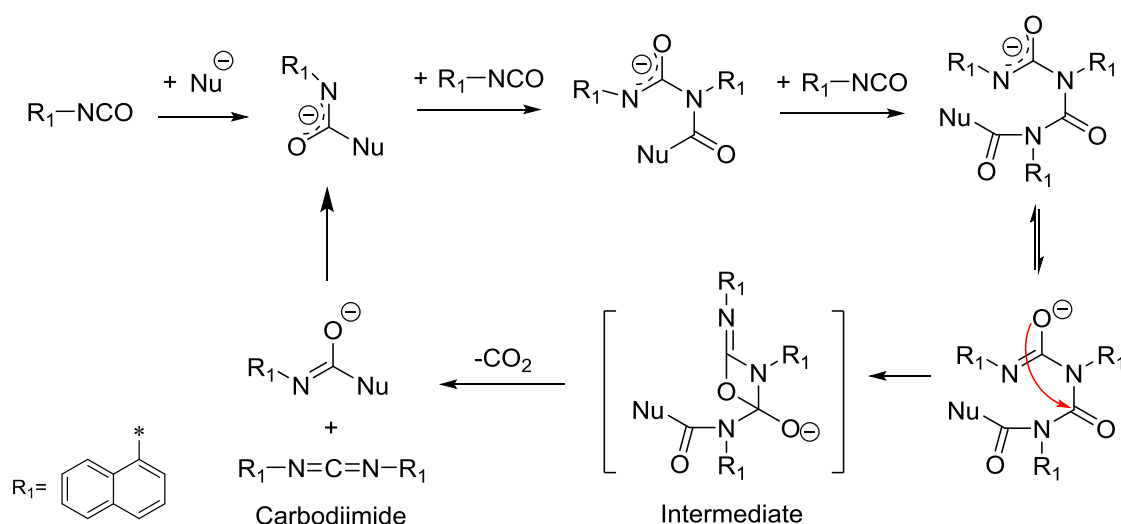
**Figure 5.** The equivalent change of reactants and products with reaction time at reaction temperatures of: (a) 80 °C, (b) 160 °C

The results obtained at 80 °C shows that the oxazolidinone is formed by the reaction of urethane and epoxide with a yield of 87% after 150 minutes. However, the reaction is slow. During the time scale of interest of 10 minutes, with 1 equivalent of epoxide, only 0.06 equivalent of Alcohol\_2 is formed, and no oxazolidinone is detected. This reaction is faster at 160 °C. After 10 minutes of reaction, 0.13 equivalent of oxazolidinone and 0.19 equivalent of Alcohol\_2 are formed. However, the reaction is not yet finished after 60 minutes. During the reactions at both 80 °C and 160 °C, alcohol\_2 is observed first built up in concentration and then decreases. This indicates that alcohol\_2 is an intermediate, its zwitterionic form (Intermediate) is depicted as a common intermediate for pathway 1 and 2 (Scheme 7). Oxazolidinone is considered to be the thermodynamically favored product. In the absence of free isocyanate in the system, which could potentially further react with alcohol\_2 to form urethane\_2, the Intermediate would form the oxazolidinone along pathway 1. In the “Ep\_ROH\_NCO\_DAB” system, however, the reactions are more complex than in the above model reaction because isocyanate is used in excess. In such a situation, the alcohol\_2 formed in pathway 2 and the 1-octanol released in pathway 1 can further

react with isocyanate to form urethane\_2 (category 2: peak 19) and the starting urethane, respectively, as shown in Scheme 7. Furthermore, these two alcohols can also react with carbodiimide at high temperatures to form isourea\_2 (category 4: peak 20) and isourea (category 4: peak 11), respectively. These reactions all have an influence, thus influencing the selectivity between pathway 1 and pathway 2.

### Carbodiimide formation

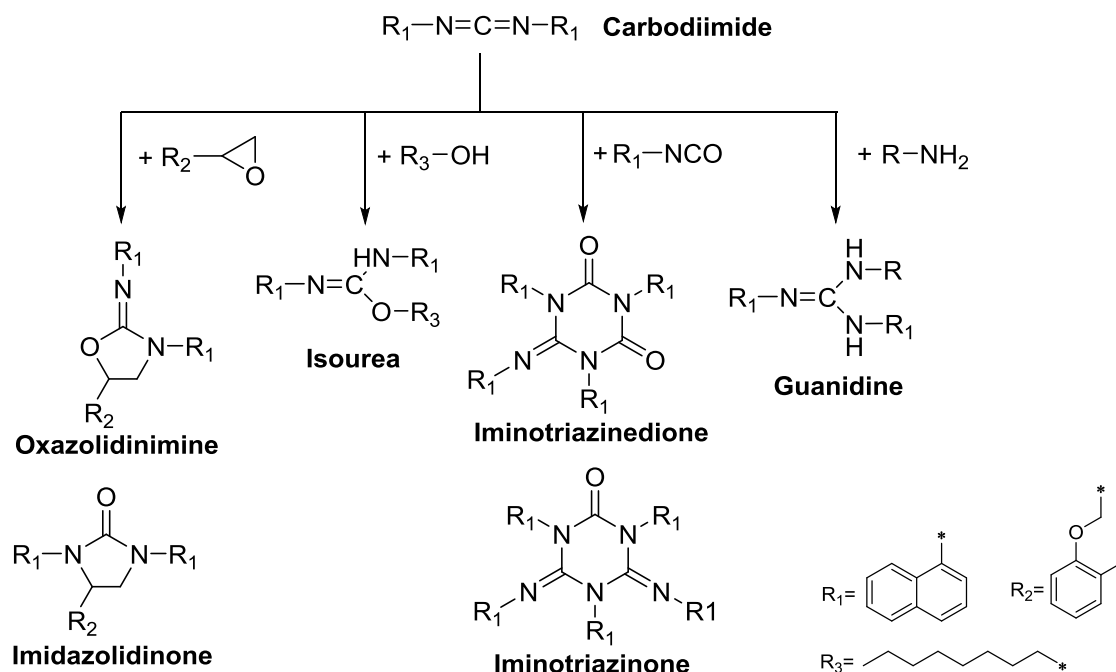
The carbodiimide formation starts from 130 °C onwards and becomes more pronounced at 160 °C. The mechanistic pathway contains a four-ring intermediate for CO<sub>2</sub> elimination and is supported by a DFT calculation by Rebecca Sure from BASF using piperidinium chloride as catalyst (Scheme 8, c.f. Appendix). Upon the attack of a nucleophile, one isocyanate can stepwise react with further isocyanates to form the cyclic and unstable intermediate. The carbodiimide is formed with the elimination of one molecule of CO<sub>2</sub> and the product molecule can further act as a nucleophilic catalyst.



**Scheme 8.** The proposed reaction pathway of carbodiimide formation

The carbodiimide formed is shown to be highly reactive and quickly participates in subsequent reactions (Scheme 9). As a result, no carbodiimide monomer was found in the final product. The carbodiimide reacts with epoxide to form two isomers, oxazolidinimine and imidazolidinone (Category 4: peak 9 and 9'). It also reacts with

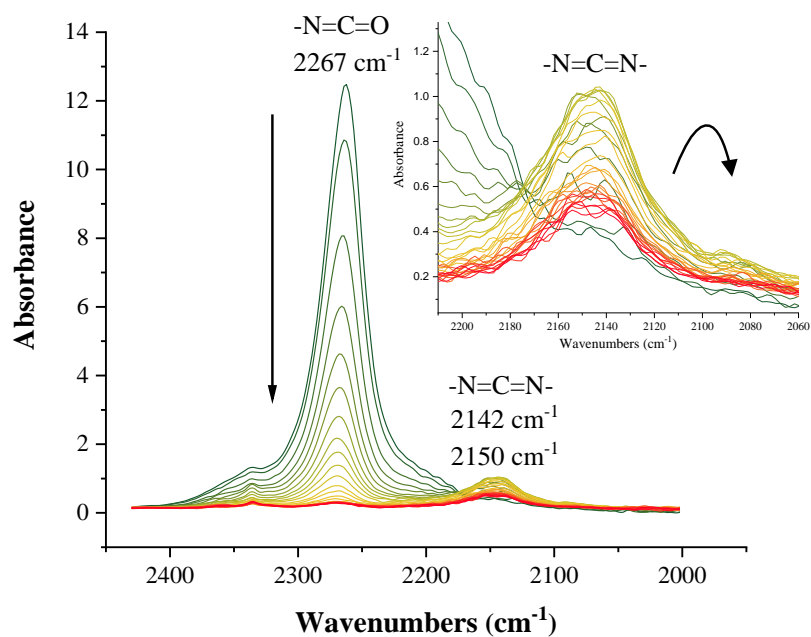
alcohols and formed isourea products (Category 4: peak 11 and 21). Besides, the carbodiimide undergo homocyclization with isocyanate and produces iminotriazinedione and iminotriazinone (Category 4: peak 17 and 19). Moreover, it reacts with amine and generates guanidine (Category 4: peak 4). At 160 °C, these subsequent reactions further contribute to the increase of the reactant conversions into “Others”.



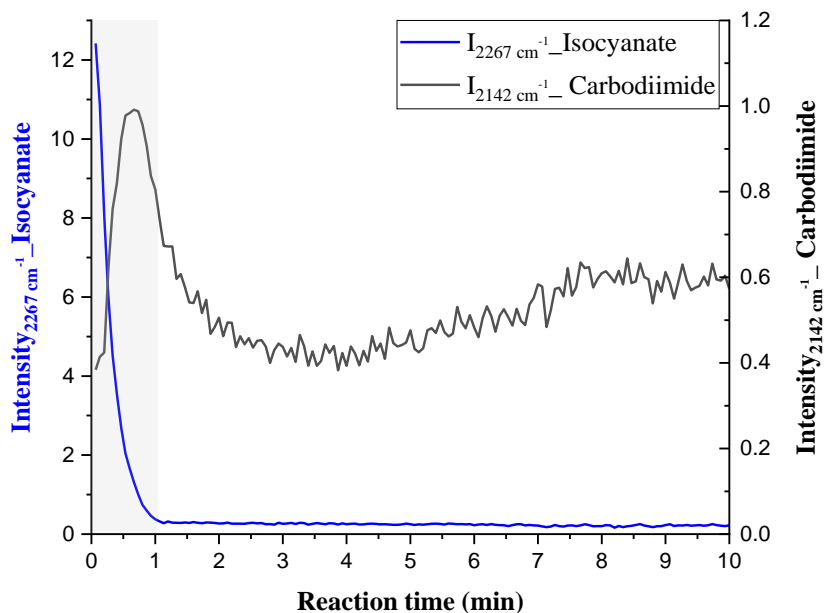
**Scheme 9.** Subsequent reactions of carbodiimide

The carbodiimide formation and subsequent reactions in the “Ep\_ROH\_NCO\_DAB” system at 160 °C were further studied using online FTIR. The FTIR spectra recorded during the first two minutes of reaction are given in Figure 6, showing the frequency range from 2000 to 2430  $\text{cm}^{-1}$ . A spectrum was recorded every 4 seconds. The color gradient from green to red was used to represent the reaction duration. The carbodiimide shows a  $N=C=N$  stretching band at 2142 and 2150  $\text{cm}^{-1}$  and the absorbance at 2267  $\text{cm}^{-1}$  originates from the  $N=C=O$  stretching of the isocyanate group. From the enlarged insert in Figure 6, it can be observed that the carbodiimide

absorbance first increases and then decreases. The carbodiimide absorbance partially overlaps with that of the isocyanate. This makes it hard especially in the first minute of reaction when the isocyanate shows a strong absorption to calculate its intensity. Thus in the spectra recorded in the first minute of reaction, Gaussian-Lorentzian Cross Function was used for peak fitting (Experiment Part). The intensity of the carbodiimide absorbance at  $2142\text{ cm}^{-1}$  was plotted against the reaction time (Figure 7). Meanwhile, the corresponding isocyanate amount in the system is also shown by the intensity of the isocyanate absorption at  $2267\text{ cm}^{-1}$ . The carbodiimide is formed rapidly at the beginning of the reaction when there is a relatively high amount of isocyanate in the system. The amount of carbodiimide quickly declines after reaching a maximum, indicating the rate of consumption exceeds the rate of formation. The slight increase after 5 minutes can be caused by the decomposition of isocyanurate (as shown in Figure 4). The free isocyanate released during the decomposition of isocyanurate can participate in the carbodiimide formation. The rise and fall in the intensity of carbodiimide monomer substantiates that the carbodiimide is indeed formed during the reaction process and that it is readily converted thereafter in the subsequent reactions. Thus, in the final reaction product, only the subsequent reaction products were detected by the HPLC or ESI-MS.



**Figure 6.** The FTIR intensity change of the carbodiimide absorbance with time in the “Ep\_ROH\_NCO\_DAB” system during the first 2 minutes. Spectra were taken every 4 seconds.



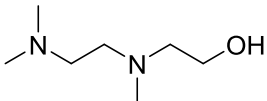
**Figure 7.** Intensity changes of the carbodiimide absorbance at  $2142\text{ cm}^{-1}$  and isocyanate absorbance at  $2267\text{ cm}^{-1}$  with time ( $160\text{ }^{\circ}\text{C}$ , “Ep\_ROH\_NCO\_DAB”)

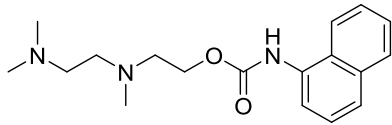
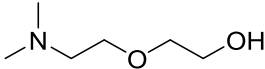
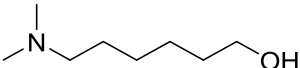
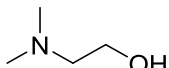
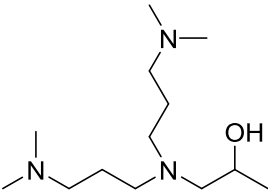
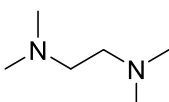
### 3.1.1.4 Catalyst selectivity

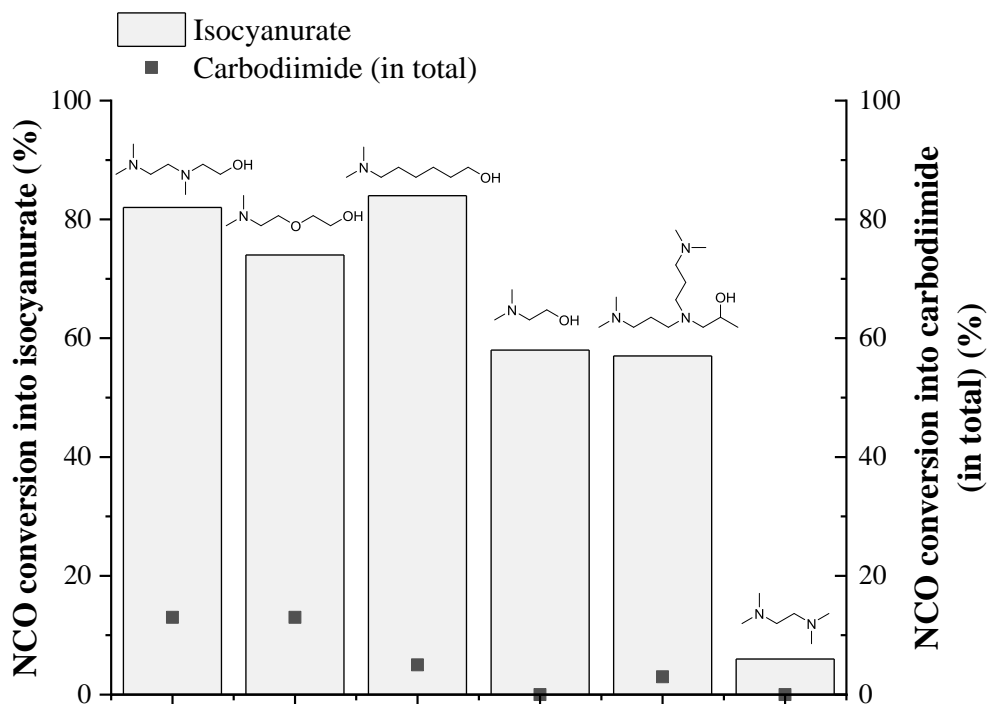
The action of DABCO<sup>®</sup> T as catalyst was reported above and the reaction pathway were proposed. In this chapter, the catalytic activities of some representative tertiary amine catalysts other than DABCO<sup>®</sup> T will be presented (Table 9).

Firstly, their catalytic activities towards isocyanurate and carbodiimide formation were studied using the “NCO\_catalyst” system containing only isocyanate and catalyst. The reaction temperature of 160 °C was selected to possibly involve the carbodiimide reaction. In the “NCO\_catalyst” system, 0.0125 equivalent of catalyst was added to 1 equivalent of 1-naphthyl isocyanate and the mixture was heated at 160 °C for 10 minutes. A reactant amount of 1.4 g was taken to minimize the temperature difference between the oil bath and the reaction system. After reaction, the amount of isocyanurate in the product was quantified using <sup>1</sup>H NMR. The total amount of carbodiimide (including the monomer in the final product and the carbodiimide that further participated in the subsequent reactions with isocyanate or itself to form a variety of dimers and trimers) was calculated using the gas evolution method. Any isocyanate residue was detected to level accessible by using FTIR (Table 9; Figure 8).

**Table 9.** Reaction products of the “NCO\_catalyst” system at 160 °C using different tertiary amine catalysts

No.	Catalyst	Isocyanate conversion (%) into		Unreacted NCO
		Isocyanurate	Carbodiimide (in total)	
1	/	0	0	Y
2	DABCO <sup>®</sup> T 	82	13	N

3	<p>DABCO<sup>®</sup> T -urethane</p> 	85	9	N
4	<p>2-(2-(dimethylamino)ethoxy)ethanol (DMAEE)</p> 	74	13	N
5	<p>6-dimethylamino-1-hexanol (DMAH)</p> 	84	5	N
6	<p>2-dimethylaminoethanol (DMAE)</p> 	58	0	Y
7	<p>1-(Bis(3-(dimethylamino)propyl)amino)propan-2-ol (BDMAPAP)</p> 	57	3	Y
8	<p><i>N,N,N',N'</i>-Tetramethylethylene diamine (TMEDA)</p> 	6	0	Y



**Figure 8.** The amounts of isocyanurate and carbodiimide (in total) in the reaction products of the “NCO\_catalyst” system at 160 °C using different tertiary amine catalysts

No reaction takes place and the isocyanate remains unreacted without the presence of a catalyst. Isocyanurate is the main product for all the catalysts. The catalytic action towards the formation of isocyanurate and carbodiimide almost follow the same trend although the amount of carbodiimide is much smaller than that of isocyanurate. Catalysts with multi-electron donating sites in the molecular structure show a slightly higher activity in catalyzing the carbodiimide formation. Tertiary amines with a primary hydroxyl group show the highest catalytic activity, followed by the catalyst with a secondary hydroxyl group and finally the tertiary amine without a hydroxyl group. According to literature, the hydroxyl group forms a urethane that can promote isocyanurate formation<sup>[24]</sup>. Primary hydroxyl groups with a lower steric hindrance are more nucleophilic than secondary hydroxyl groups. Therefore, it is reasonable that tertiary amines with a primary hydroxyl group show a higher catalytic activity than those with a secondary hydroxyl group, which in terms are more active than those



without a hydroxyl group. The improved catalytic activity through urethane formation is further supported by a comparative experiment (Table 9, experiment No. 3). DABCO<sup>®</sup> T-urethane was prepared in advance by reacting DABCO<sup>®</sup> T with isocyanate. Purification was conducted using column chromatography. When the DABCO<sup>®</sup> T-urethane was used as catalyst, the reaction product showed a similar profile as that obtained with DABCO<sup>®</sup> T.

The chain length between the tertiary amine and the hydroxyl group also plays a role in the catalytic activity. When the chain is too short, as is the case for 2-dimethyl aminoethanol (Table 9, experiment No.6), the catalytic activity is much smaller than for a hydroxyl-amine with a longer chain length like 6-dimethyl amino-1-hexanol (Table 9, experiment No.5). One explanation could be that the short chain length limits the mobility of the tertiary amine moiety after the hydroxyl has reacted with isocyanate, thus reducing its catalytic activity.

The results in Table 9 show that DABCO<sup>®</sup> T exhibits the highest activity for both the isocyanurate and carbodiimide formation and achieves full isocyanate conversion. *N,N,N',N'*-Tetramethylethylenediamine (TMEDA) shows the lowest catalytic activity with only 6% of the isocyanate being converted into isocyanurate while no carbodiimide was formed. The low catalytic activity of TMEDA made it a good reference to further study the catalytic effect of alcohol and epoxide. TMEDA was used instead of DABCO<sup>®</sup> T in the “Ep\_ROH\_NCO\_DAB” system with the same equivalent amounts and the new system was referred to as the “Ep\_ROH\_NCO\_TMEDA”. In order to study the influence of epoxide and alcohol individually epoxide and alcohol were also incorporated separately in the formulation (Table 10).

**Table 10.** Formulations of the “Ep\_ROH\_NCO\_TMEDA”, “Ep\_NCO\_TMEDA”, “ROH\_NCO\_TMEDA” and “NCO\_TMEDA” systems

	Reactant	Reactant equivalent			
		Ep_ROH_NCO _TMEDA	Ep_NCO _TMEDA	ROH_NCO _TMEDA	NCO _TMEDA
<b>Comp. A</b>	Glycidyl 2-methylphenyl ether	1.0	1.0		
	1-Octanol	0.5		0.5	
	TMEDA	0.0375	0.0375	0.0375	0.0375
<b>Comp. B</b>	1-Naphthyl isocyanate	3.0	3.0	3.0	3.0

The above reaction systems were reacted at 80 °C and 160 °C for 10 minutes, respectively, and the product yields (Table 11). It shows that both alcohol and epoxide can promote isocyanurate formation. When comparing the results of “NCO\_TMEDA” with that of “ROH\_NCO\_TMEDA” at 80 °C, it shows that the addition of epoxide increases the isocyanate conversion into isocyanurate from 0 to 93%. The alkoxide formed in the epoxide ring opening reaction upon the attack of a tertiary amine is a strong nucleophile that is very efficient as a catalyst in promoting isocyanurate formation<sup>[18,19]</sup>. The total epoxide conversion during the reaction, however, is only 19%, which indicates that the epoxide only acts as a catalyst activator. The co-catalytic effect of epoxide in accelerating isocyanurate formation will be discussed in detail in Chapter 3.1.4. The addition of alcohol can also increase isocyanurate formation, but when compared to the epoxide to a much lower extent of only 23%. Although the epoxide added was twice the equivalent amount of the alcohol, the low epoxide conversion suggests a stronger catalytic activity of the alkoxide than of the alcohol or urethane towards isocyanurate formation. A similar catalytic effect of alcohol and epoxide is also observed at 160 °C. Although the addition of both alcohol

and epoxide promote isocyanurate formation, their efficiency in accelerating carbodiimide formation is limited. The results of “NCO\_TMEDA”, “ROH\_NCO\_TMEDA” and “Ep\_NCO\_TMEDA” at 160 °C show that there is a small increase in carbodiimide formation when epoxide is incorporated into the formulation, whereas solely with added alcohol, the formation of carbodiimide does not occur.

**Table 11.** Product distribution of “NCO\_TMEDA”, “ROH\_NCO\_TMEDA”, “Ep\_NCO\_TMEDA” and “Ep\_ROH\_NCO\_TMEDA” systems when reacted at (a) 80 °C and (b) 160 °C

(a) 80 °C

<b>Isocyanate conversions (%) into</b>	<b>NCO_TMEDA</b>	<b>ROH_NCO_TMEDA</b>	<b>Ep_NCO_TMEDA</b>	<b>Ep_ROH_NCO_TMEDA</b>
Isocyanurate	0	23	93	77
Carbodiimide (in total)	0	0	0	0
Oxazolidinone	/	/	0	1
Urethane	/	17	/	14
Unreacted NCO	Y	Y	Y	N
<b>Alcohol conversion (%)</b>	/	100	/	100
<b>Ep conversion (%)</b>	/	/	19	21

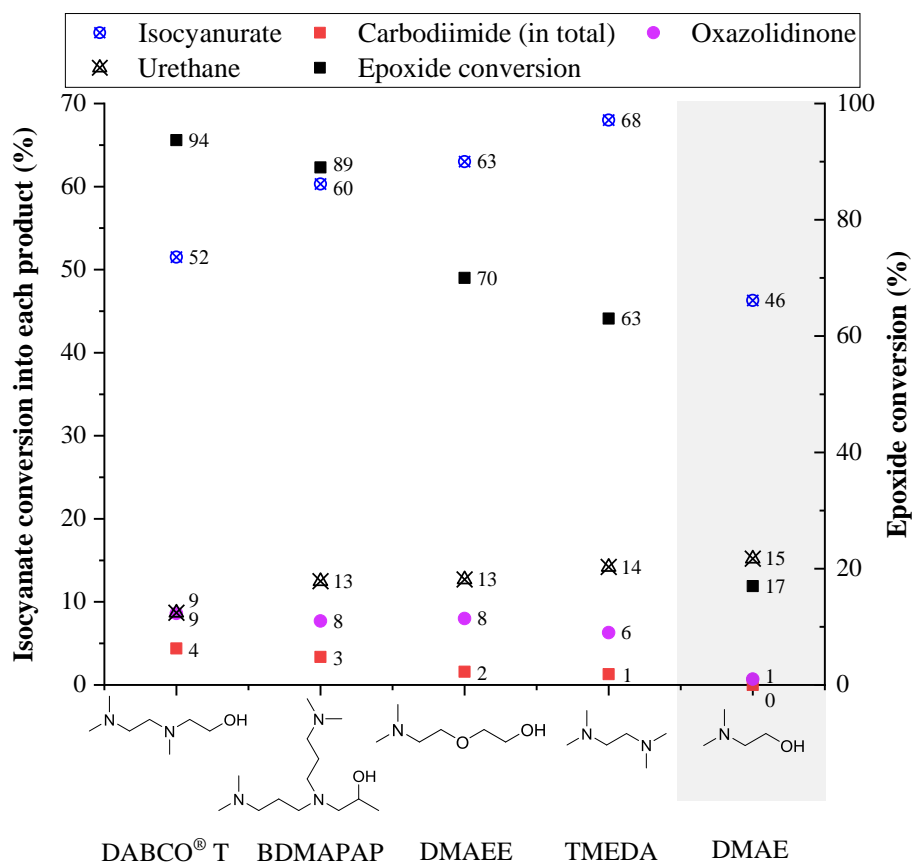
(b) 160 °C

<b>Isocyanate conversions (%) into</b>	<b>NCO _TMEDA</b>	<b>ROH_NCO _TMEDA</b>	<b>Ep_NCO _TMEDA</b>	<b>Ep_ROH_NCO _TMEDA</b>
Isocyanurate	6	35	79	68
Carbodiimide (in total)	0	0	2	1
Oxazolidinone	/	/	10	6
Urethane	/	14	/	14
Unreacted NCO	Y	Y	N	N
<b>Alcohol conversion (%)</b>	/	100	/	100
<b>Ep conversion (%)</b>	/	/	77	63

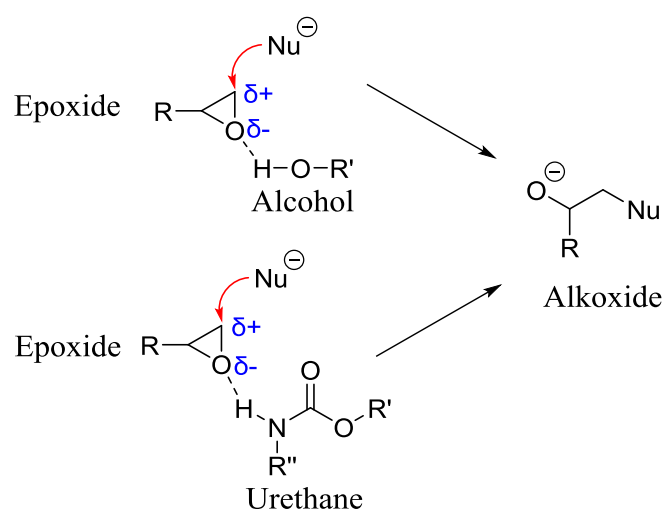
In the next, the reaction selectivity of different catalysts in the “Ep\_ROH\_NCO\_catalyst” system is considered in more detail. The catalysts were added at the same equivalent amount and the reaction products at 160 °C after 10 minutes of reaction were presented (Figure 9). Alcohol has fully reacted in all the reactions and a full conversion of isocyanate is obtained with all the catalysts except DMAE. Different to the results of the “NCO\_catalyst” system, the isocyanate conversion is now also promoted by the addition of alcohol and epoxide. DMAE with a short chain length shows the lowest activity and free isocyanate was still observed after 10 minutes of reaction. Although DMAE has a similar chain length as TMEDA, the reaction of the hydroxyl group in DMAE with isocyanate is considered to constrain the mobility of the tertiary amine moiety.

As to the epoxide conversion, DABCO<sup>®</sup> T exhibits the highest catalytic activity with an overall epoxide conversion of 94%. The catalytic activity towards epoxide conversion follows the sequence of DABCO<sup>®</sup> T > BDMAPAP > DMAEE > TMEDA > DMAE. Except for the special case of DMAE, along with the increase of

epoxide conversion, the amount of oxazolidinone also increases while the amounts of isocyanurate and urethane in the final products decrease, indicating an increase in the extent of both isocyanurate-epoxide and urethane-epoxide reactions. As the epoxide reactions are normally initiated by a ring opening and alkoxide forming process, it can be expected that the ability for the catalyst to open the epoxide ring follows the sequence of DABCO<sup>®</sup> T > BDMAPAP > DMAEE > TMEDA. From this sequence, it can be seen that catalysts bearing a hydroxyl group show a higher activity than those without. The hydroxyl group was reported to promote the cleavage of the C-O bond in the epoxide ring by hydrogen bond formation to the oxygen (Scheme 10)<sup>[87,88]</sup>. The hydrogen bond formed by a primary hydroxyl group is stronger than that of a secondary hydroxyl group. When the hydroxyl group is converted into urethane, the urethane hydrogen may offer the same catalysis in form of a H-bond donor. Besides the influence of the hydroxyl group, the catalytic activity towards epoxide ring opening also depends on the number of tertiary amino groups in the catalyst molecule. DABCO<sup>®</sup> T and BDMAPAP bearing two active tertiary amino groups show higher catalytic activity than DMAEE with only one tertiary amino group. Catalysts that provide a higher epoxide conversion also show more carbodiimide formation, although all together in relatively low amounts. The reason could be, when the epoxide conversion increases the amount of isocyanurate in the final product decreases and thus there is a higher opportunity for the isocyanate to convert into carbodiimide.



**Figure 9.** The product profiles of “Ep\_ROH\_NCO\_catalyst” system with different catalysts, reacted at 160 °C



**Scheme 10.** The mechanism of epoxide ring opening reaction catalyzed by alcohol and urethane

The catalytic activity of some representative tertiary amine catalysts was presented in this Chapter. In reaction systems with only isocyanate and catalyst at 160 °C, the main product is isocyanurate accompanied by some carbodiimide with its subsequent reaction products. Tertiary amines with a pendent primary hydroxyl group show the highest catalytic activity towards both isocyanurate and carbodiimide formation, followed by those with a secondary hydroxyl group. Tertiary amino alcohols with a short chain length between the amine and hydroxyl group show limited catalytic activity whereas straight tertiary amines exhibit the lowest catalytic activity. With epoxide, and to some extent also with alcohol, the formation of isocyanurate is promoted at both low and high reaction temperatures. However, the mediation of carbodiimide formation by alcohol and epoxide at high temperatures is not obvious.

Tertiary amines with more than one tertiary amino groups and bearing a hydroxyl group show high catalytic activity towards epoxide mediated reactions, leading to high epoxide conversion and oxazolidinone formation as well as low isocyanurate and urethane contents in the final reaction products.

Among the examined catalysts, DABCO<sup>®</sup> T shows the highest catalytic activity towards isocyanurate and carbodiimide formation in the “NCO\_catalyst” system and the highest catalytic activity towards epoxide conversion in the “Ep\_ROH\_NCO\_catalyst” system. Consequently, DABCO<sup>®</sup> T was used as the primary catalyst.

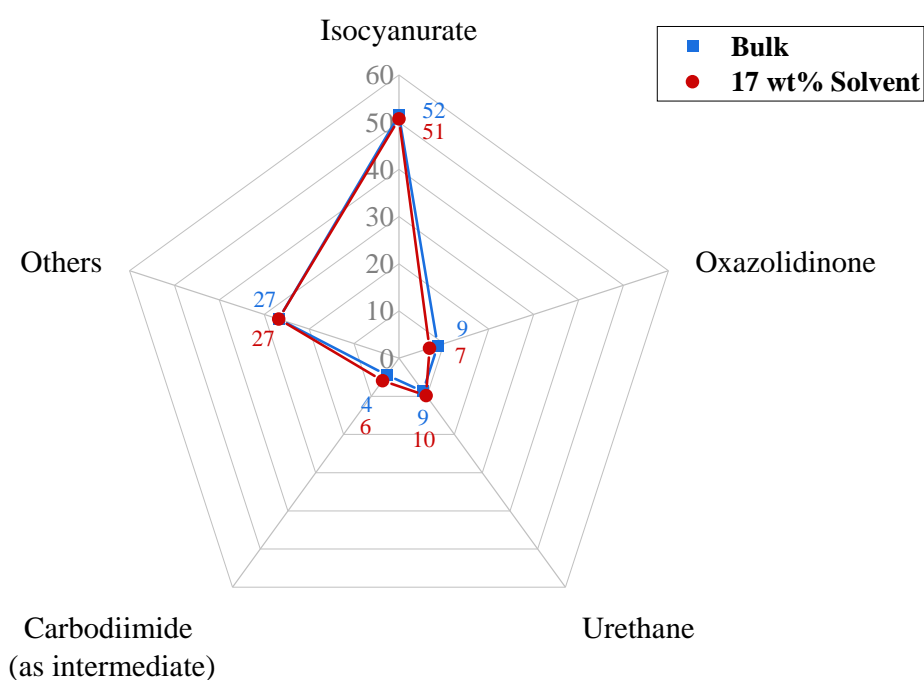
### **3.1.1.5 Effect of solvent**

The non-reactive ethylene glycol dimethyl ether homologue was added in the “Ep\_ROH\_NCO\_DAB” system as a solvent and its influence on the reaction products is discussed in this Chapter.

In the “Model” system and other monofunctional systems containing water and formic acid, ethylene glycol dimethyl ether homologues were added as solvent to obtain a homogeneous Component A. Although the solvent amount was kept to a lowest level, the effect of adding solvent is unknown. Therefore, triethylene glycol

dimethyl ether was added in the “Ep\_ROH\_NCO\_DAB” system to study the influence on the reaction products.

The amount of triethylene glycol dimethyl ether added in the “Ep\_ROH\_NCO\_DAB” system was 17 wt% of the total reaction system. After 10 minutes of reaction at 160 °C, the main products were quantified and compared to that of the “Ep\_ROH\_NCO\_DAB” bulk system. The product amounts were expressed in the isocyanate conversion (Figure 10).



**Figure 10.** Reaction products of the Ep\_ROH\_NCO\_DAB system with and without solvent

It shows that the addition of triethylene glycol dimethyl ether does not have a substantial influence on the course of the reaction except that epoxide related reactions are somewhat slower. The total epoxide conversion decreases by 16% from 94% to 78% by the dilution with solvent. As the amount of epoxide added in the system is only one third equivalent of the isocyanate, the 16% decrease of epoxide conversion does not show a substantial change in the reaction product distribution. The amount of oxazolidinone formed is slightly smaller while the amount of urethane



and carbodiimide (as intermediate) are a little larger. The reduced reaction temperature of the solvent system may account for the slightly reduced oxazolidinone yield and less reaction between the epoxide and urethane. The peak temperature of 164 °C in the bulk system is only 158 °C in the solvent system. The epoxide related reactions including the oxazolidinone formation and the epoxide-urethane addition reaction are favoured at higher reaction temperatures (Chapter 3.1.1.3).

### **3.1.2 “Ep\_ROH\_NCO\_DAB” system incorporated with blowing agents and hindered amine**

The reaction products and reaction pathways of the “epoxide\_alcohol\_isocyanate\_DABCO<sup>®</sup> T (Ep\_ROH\_NCO\_DAB)” system was discussed in the last Chapter. Real foaming systems will contain some chemical blowing agents to expand the foam. The most used chemical blowing agents in rigid foams are water and formic acid. Thus, these were incorporated separately in the “Ep\_ROH\_NCO\_DAB” reaction system and their influence on the reaction was studied.

Sometimes sterically hindered amines are used in the rigid foam formulation to speed up the reaction and to achieve a higher exotherm. The reaction between amine and isocyanate is a fast and highly exothermic reaction. In the model system, monofunctional 2,6-dimethyl aniline was incorporated into the “Ep\_ROH\_NCO\_DAB” system and its effect on the reaction product was evaluated. The systems containing water, formic acid and 2,6-dimethyl aniline, respectively, are referred to as “Ep\_ROH\_NCO\_H<sub>2</sub>O\_DAB”, “Ep\_ROH\_NCO\_FA\_DAB” and “Ep\_ROH\_NCO\_RNH<sub>2</sub>\_DAB” systems. The employed reactant equivalents (Table 12) are based on the “Model” system. In all the recipes, the NCO index was kept at 200 and the catalyst amount was kept at 0.025 equivalents per equivalent amount of reactive groups in the Component A. The hydroxyl functionality of DABCO<sup>®</sup> T was not part of the calculations. Ethylene glycol dimethyl ether homologues were used as solvents to obtain a compatible Component A in the “Ep\_ROH\_NCO\_H<sub>2</sub>O\_DAB”

and “Ep\_ROH\_NCO\_FA\_DAB” systems. The solvent amounts were kept to the lowest levels, resulting in a solvent content of 3 wt% and 9 wt%, respectively.

**Table 12.** Recipes of the “Ep\_ROH\_NCO\_H<sub>2</sub>O\_DAB”, “Ep\_ROH\_NCO\_FA\_DAB” and “Ep\_ROH\_NCO\_RNH<sub>2</sub>\_DAB” systems

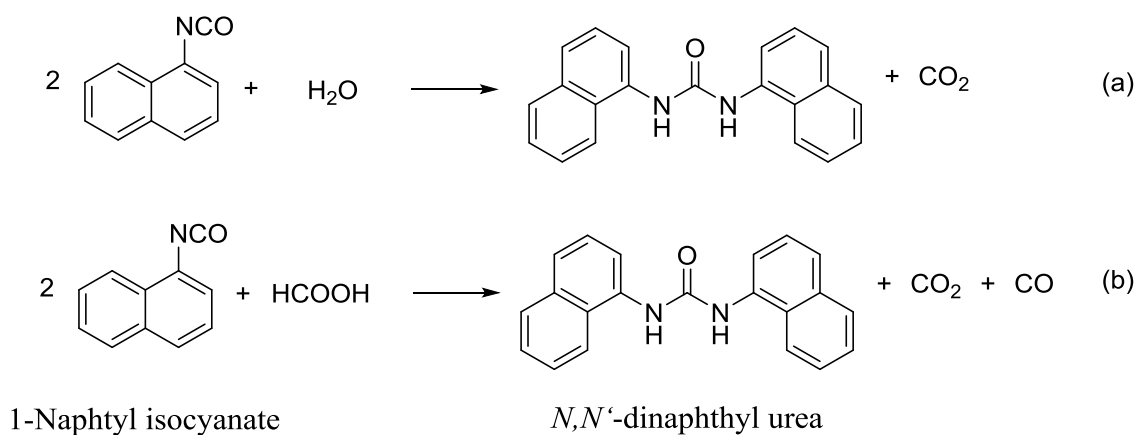
	Reactant	Equivalent		
		Ep_ROH_NCO_H <sub>2</sub> O_DAB*	Ep_ROH_NCO_FA_DAB**	Ep_ROH_NCO_RNH <sub>2</sub> _DAB
<b>Comp. A</b>	Glycidyl 2-methylphenyl ether	1.0	1.0	1.0
	1-Octanol	0.5	0.5	0.5
	Water	1.0		
	Formic acid		0.5	
	2,6-Dimethyl aniline			0.5
	DABCO® T	0.0625	0.0500	0.0500
<b>Comp. B</b>	1-Naphthyl isocyanate	5.0	4.0	4.0

Triethylene glycol dimethyl ether or polyethylene glycol dimethyl ether (Mw=1000) was added as solvent. Solvent content: \* 3 wt% and \*\* 9 wt %

Two temperatures, 80 °C and 160 °C, were selected to evaluate the reactions at low resp. high temperatures. ESI-MS and LC-MS were used for the product identification, while <sup>1</sup>H NMR or the gas evolution method were used for the product quantification.

When reacted at 80 °C, product identification shows the product species in the “Ep\_ROH\_NCO\_H<sub>2</sub>O\_DAB” and “Ep\_ROH\_NCO\_FA\_DAB” systems are the same as those in the “Ep\_ROH\_NCO\_DAB” system. Water or formic acid reacts with

some of the 1-naphthyl isocyanate and form *N,N'*-dinaphthyl urea, carbon dioxide and carbon monoxide (Scheme 11).

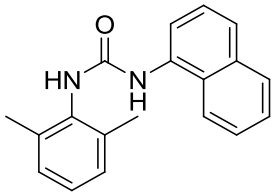
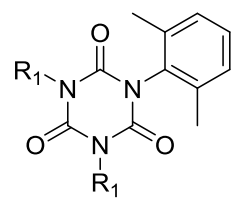


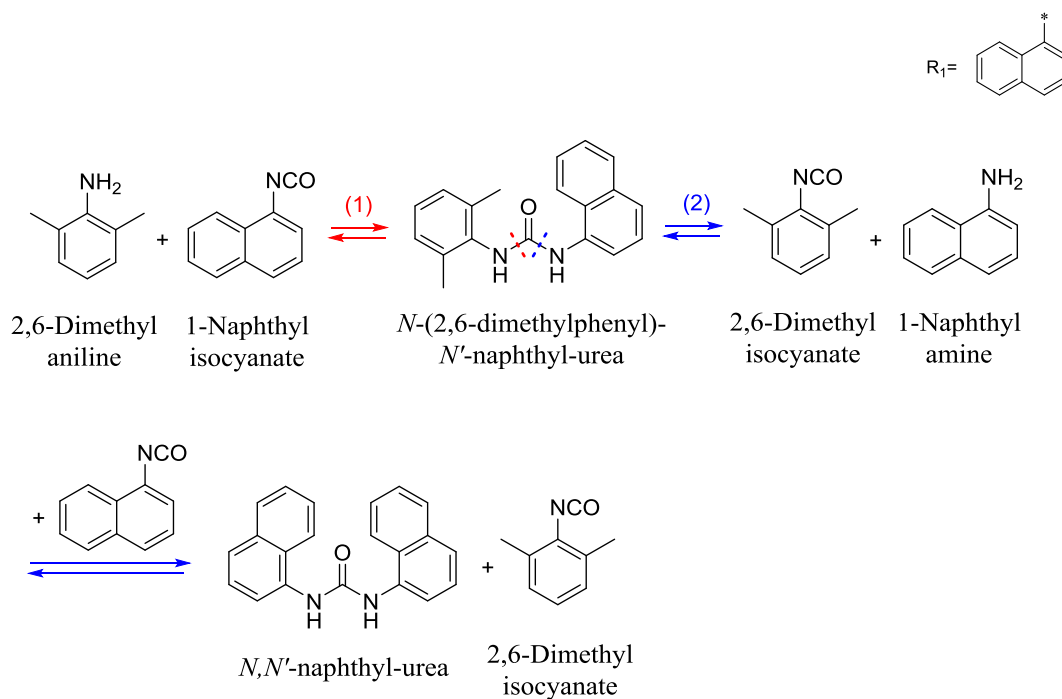
**Scheme 11.** The reactions between isocyanate and (a) water (b) formic acid

In the “Ep\_ROH\_NCO\_RNH<sub>2</sub>\_DAB” system, two additional products (Table 13) were detected using ESI-MS (+). One of them is the anticipated *N*-(2,6-dimethylphenyl)-*N'*-naphthyl urea. The other one is assigned to the 1-(2,6-dimethylphenyl)-3,5-di(1-naphthyl)-isocyanurate, which is formed from two 1-naphthyl isocyanate molecules and one 2,6-dimethyl phenyl isocyanate molecule. The 2,6-dimethyl phenyl isocyanate is considered to be generated by the equilibrium reactions of urea (Scheme 12). The 2,6-dimethyl aniline added in the system first reacts with 1-naphthyl isocyanate forming *N*-(2,6-dimethylphenyl)-*N'*-naphthyl urea. This urea compound can then participate in two equilibrium reactions - equilibrium (1) and (2). In equilibrium (2), the generated 1-naphthyl amine can further react with 1-naphthyl isocyanate to form *N,N'*-dinaphthyl urea. The predicted pK<sub>a</sub> values of 1-naphthyl amine and 2,6-dimethyl aniline amount to 4.21±0.10 and 4.31±0.10, respectively (Temp: 25 °C. Data cited from SciFinder (predicted values calculated using Advanced Chemistry Development (ACD/Labs) Software V11.02)). The similar pK<sub>a</sub> values suggest that the two amine anions will have similar leaving group abilities. However, the large excess of 1-naphthyl isocyanate in the reaction system can shift the equilibrium to the formation of *N,N'*-naphthyl urea and 2,6-dimethyl isocyanate.

This equilibrium reaction is further supported by the result of the product quantification.

**Table 13.** Additional product species detected in the ESI-MS (+) spectrum of the “Ep\_ROH\_NCO\_RNH<sub>2</sub>\_DAB” system

Exact mass	m/z detected	Molecular structure
290.142	291.150	 <i>N</i> -(2,6-dimethylphenyl)- <i>N'</i> -naphthyl urea
486.169	486.183	 1-(2,6-dimethylphenyl)-3,5-di(1-naphthyl)-isocyanurate



**Scheme 12.** The reaction between 1-naphthyl isocyanate and 2,6-dimethyl aniline

The reactants reach high conversions except that epoxide remains largely unreacted in 10 minutes at 80 °C (Table 14). The amounts of urethane formed in the four reaction systems are all close to their anticipated values, however, some discrepancies are also found (Table 15). The anticipated values were calculated by assuming complete reactions of water, formic acid, 2,6-dimethyl aniline or 1-octanol with 1-naphthyl isocyanate to form the corresponding urea or urethane. The majority of 1-octanol ranging from 89% to 93% depending on the reaction system reacts with isocyanate and remains as urethane in the final product. When water, formic acid or amine is incorporated in the formulation, more urea is detected in the reaction products as expected. In the “Ep\_ROH\_NCO\_H<sub>2</sub>O\_DAB” and “Ep\_ROH\_NCO\_FA\_DAB” systems, the amounts of *N,N'*-dinaphthyl urea are even a little bit higher than their anticipated values, indicating that all of the water and formic acid should have reacted with 1-naphthyl isocyanate to form *N,N'*-dinaphthyl urea. Although water and formic acid have the potentials to react with epoxide and form diol or β-hydroxy ester, respectively<sup>[88]</sup>, the high urea amounts suggest their reactions with isocyanate are much faster.

Similarly, in the “Ep\_ROH\_NCO\_RNH<sub>2</sub>\_DAB” system, the low epoxide conversion of only 7% indicates that 2,6-dimethyl aniline is consumed rapidly by isocyanate to form urea, leaving little room for the ring-opening addition reaction between epoxide and 2,6-dimethyl aniline. Because of the equilibrium reactions of the various urea groups, the amount of *N*-2,6-dimethylphenyl-*N'*-phenyl urea in the final product is much lower than its anticipated value. <sup>1</sup>H NMR shows the overall conversion of 2,6-dimethyl aniline is 98%. Therefore, 12% of the isocyanate could have theoretically reacted with 2,6-dimethyl aniline to form *N*-2,6-dimethylphenyl-*N'*-phenyl urea. The equilibrium exchange reactions results in the value being only 3%. Thus, 12% of the isocyanate is converted into *N,N'*-dinaphthyl urea. This indicates the excess of 1-naphthyl isocyanate in the system largely shifts the equilibrium to the direction of *N,N'*-dinaphthyl urea and 2,6-dimethyl isocyanate formation.

Alike in the four reaction systems, the remainder of the isocyanate is predominantly converted into isocyanurate. The slightly lower conversion of 1-naphthyl isocyanate into trinaphthyl-isocyanurate in the Ep\_ROH\_NCO\_RNH<sub>2</sub>\_DAB system may have been caused either by the additional consumption of 1-naphthyl isocyanate in the urea equilibrium reactions and/or by the formation of the hybrid isocyanurate (Table 13). As the reference compound of this hybrid isocyanurate was not obtained, its amount is not quantifiable and the amount of 1-naphthyl isocyanate consumed in this trimerization reaction is combined into “Others”.

**Table 14.** Reactant conversions in “Ep\_ROH\_NCO\_DAB”, “Ep\_ROH\_NCO\_H<sub>2</sub>O\_DAB”, “Ep\_ROH\_NCO\_FA\_DAB” and Ep\_ROH\_NCO\_RNH<sub>2</sub>\_DAB at 80 °C

<b>Reactant conversions (%)</b>	Ep_ROH_NCO_DAB	Ep_ROH_NCO_H <sub>2</sub> O_DAB	Ep_ROH_NCO_FA_DAB	Ep_ROH_NCO_RNH <sub>2</sub> _DAB
<b>Isocyanate</b>	100	100	100	100
<b>Epoxide</b>	15	7	6	7
<b>Alcohol</b>	100	100	100	100

**Table 15.** Product distributions expressed in isocyanate conversions in “Ep\_ROH\_NCO\_DAB”, “Ep\_ROH\_NCO\_H<sub>2</sub>O\_DAB”, “Ep\_ROH\_NCO\_FA\_DAB” and “Ep\_ROH\_NCO\_RNH<sub>2</sub>\_DAB” at 80 °C (anticipated values shown in brackets below)

<b>Isocyanate conversion into (%)</b>	Ep_ROH_NCO_DAB	Ep_ROH_NCO_H <sub>2</sub> O_DAB	Ep_ROH_NCO_FA_DAB	Ep_ROH_NCO_RNH <sub>2</sub> _DAB
Trinaphthyl-isocyanurate	77	63	63	54
Naphthyl-urethane	15 (17)	9 (10)	12 (13)	11 (13)
<i>N,N'</i> -dinaphthyl urea	3 (0)	20 (20)	14 (13)	<b>12</b> <b>(0)</b>
<i>N</i> -(2,6-dimethyl-- <i>p</i> henyl)- <i>N'</i> -naphthyl urea	/	/	/	<b>3</b> <b>(13)</b>
1-naphthyl amine	1	3	4	4
Others	7	5	8	16

The reactant conversion and product formation in the “Ep\_ROH\_NCO\_H<sub>2</sub>O\_DAB”, “Ep\_ROH\_NCO\_FA\_DAB” and “Ep\_ROH\_NCO\_RNH<sub>2</sub>\_DAB” systems at high temperature of 160 °C was also studied and compared to that of the “Ep\_ROH\_NCO\_DAB” system (Table 16 and 17). The reactants reach high conversions in all systems. The epoxide now also has high conversions of above 90% at 160 °C. Similar to the results obtained at 80 °C, more urea is formed when either water, formic acid or 2,6-dimethyl aniline is incorporated in the formulation. 90% of water, 96% of formic acid and 94% of 2,6-dimethyl aniline have reacted with

1-naphthyl isocyanate to produce the corresponding urea. These high conversions indicate faster reactions of water, formic acid and 2,6-dimethyl aniline with isocyanate than with epoxide. Next to the increase in urea, when there is water, formic acid or 2,6-dimethyl aniline in the formulation, the total amounts of carbodiimide formed during the reaction also increase. Concomitantly, the amounts of isocyanurate decrease. Similar to the “Ep\_ROH\_NCO\_DAB” system, the formed carbodiimide quickly participates in the consecutive reactions and no carbodiimide monomer is detected in the final product. Because the NCO index is kept at 200 in all the reaction systems, the total conversions of isocyanate into isocyanurate and carbodiimide (as intermediate) are around 55% in the “Ep\_ROH\_NCO\_DAB”, “Ep\_ROH\_NCO\_H<sub>2</sub>O\_DAB” and “Ep\_ROH\_NCO\_FA\_DAB” systems. The slightly lower value of 52% in the “Ep\_ROH\_NCO\_RNH<sub>2</sub>\_DAB” is caused by the equilibration reactions between the different urea groups as explained above. Although the total conversions of isocyanate into isocyanurate and carbodiimide had no substantial difference in systems, the ratio between the “isocyanate conversion into carbodiimide (as intermediate)” and the “isocyanate conversion into isocyanurate” (Table 17: B divided by A) increases from 0.09 to 0.66-0.68 when water resp. formic acid was added. The higher ratio of 1.33 in the “Ep\_ROH\_NCO\_RNH<sub>2</sub>\_DAB” system originates from two reasons. One aspect is that smaller amounts of trinaphthyl-isocyanurate were formed in the “Ep\_ROH\_NCO\_RNH<sub>2</sub>\_DAB” system by the equilibration reactions between different urea groups. The hybrid isocyanurate is generated but is not quantifiable, and thus is not accounted for. The other aspect is a larger amount of carbodiimide (as intermediate) is formed in the “Ep\_ROH\_NCO\_RNH<sub>2</sub>\_DAB” system. This may be caused by the higher peak temperature (172 °C) in the reaction system. It has shown above that carbodiimide formation is favored at high reaction temperature. Hindered amines are usually added in the formulation to achieve such a high exotherm.

The isocyanate conversion into oxazolidinone or urethane does not show substantial difference among the four systems: 25%-29% of epoxide is converted into



oxazolidinone and 48%-56% of alcohol is converted into urethane (Table 17). Some additional reaction products were detected using LC-MS. These products are hard to identify and quantify and therefore their amounts are taken together in a class termed “Others”. In the “Ep\_ROH\_NCO\_H<sub>2</sub>O\_DAB” and “Ep\_ROH\_NCO\_FA\_DAB” systems, the product species in the class “Others” are almost the same as those detected in the “Ep\_ROH\_NCO\_DAB” system. However, in the “Ep\_ROH\_NCO\_RNH<sub>2</sub>\_DAB” system, additional products species were detected. These 2,6 dimethyl aniline derived products were detected by LC-MS (Table 18).

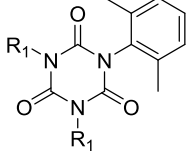
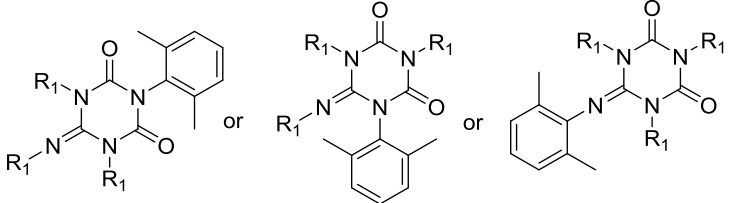
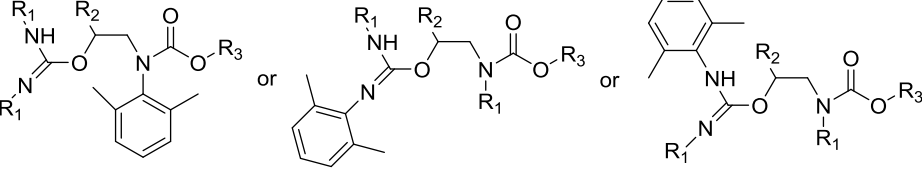
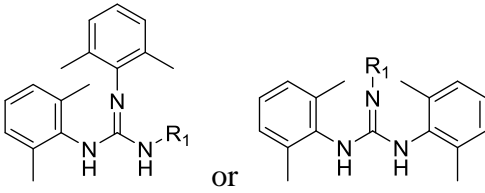
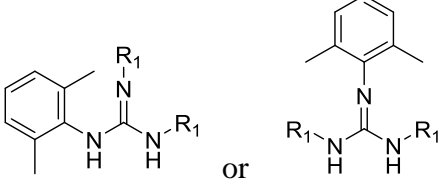
**Table 16.** Reactant conversions in “Ep\_ROH\_NCO\_DAB”, “Ep\_ROH\_NCO\_H<sub>2</sub>O\_DAB”, “Ep\_ROH\_NCO\_FA\_DAB” and “Ep\_ROH\_NCO\_RNH<sub>2</sub>\_DAB” at 160 °C

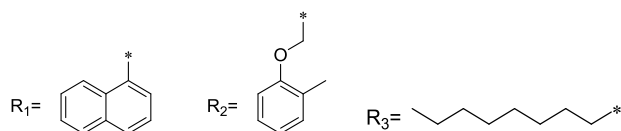
<b>Reactant conversions (%)</b>	Ep_ROH_NCO_DAB	Ep_ROH_NCO_H <sub>2</sub> O_DAB	Ep_ROH_NCO_FA_DAB	Ep_ROH_NCO_RNH <sub>2</sub> _DAB
<b>Isocyanate</b>	100	100	100	100
<b>Epoxide</b>	94	99	91	100
<b>Alcohol</b>	100	100	100	100

**Table 17.** Product distributions expressed in isocyanate conversions in “Ep\_ROH\_NCO\_DAB”, “Ep\_ROH\_NCO\_H<sub>2</sub>O\_DAB”, “Ep\_ROH\_NCO\_FA\_DAB” and “Ep\_ROH\_NCO\_RNH<sub>2</sub>\_DAB” at 160 °C (anticipated values shown in the brackets below)

<b>Isocyanate conversions into (%)</b>		Ep_ROH_NCO_ DAB	Ep_ROH_NCO_ H <sub>2</sub> O_DAB	Ep_ROH_NCO_ FA_DAB	Ep_ROH_NCO_ RNH <sub>2</sub> _DAB
<b>A</b>	Trinaphthyl- isocyanurate	<b>52</b>	<b>34</b>	<b>33</b>	<b>22</b>
<b>B</b>	Carbodiimide (as intermediate)	<b>4</b>	<b>22</b>	<b>22</b>	<b>30</b>
Naphthyl oxazolidinone		9 (33)	6 (20)	6 (25)	8 (25)
Naphthyl urethane		9 (17)	5 (10)	7 (13)	6 (13)
N,N'-dinaphthyl urea		2 (0)	18 (20)	12 (13)	<b>22</b> <b>(0)</b>
N-(2,6-dimethylphenyl)- N'-naphthyl urea		/	/	/	<b>1</b> <b>(13)</b>
1-Naphthyl amine		1	1	0	0
Others		23	14	20	12
<b>B divided by A</b>		<b>0.09</b>	<b>0.66</b>	<b>0.68</b>	<b>1.33</b>
<b>System peak temp.</b>		164 °C	169 °C	168 °C	172 °C

**Table 18.** Structures corresponding to the three new mass peaks detected in the ESI-MS (+) spectra of the “Ep\_ROH\_NCO\_RNH<sub>2</sub>\_DAB” system

Exact mass	m/z detected	Possible molecular structures
485.174	486.169	 <p>Isocyanurate</p>
610.237	611.235	 <p>Iminotriazinedione</p>
735.300	736.401	 <p>Isourea</p>
393.221	394.223	 <p>Guanidine</p>
415.205	416.215	 <p>Guanidine</p>



In summary, when water, formic acid or 2,6-dimethyl aniline is incorporated into the “Ep\_ROH\_NCO\_DAB” system, more urea is formed at both low and high reaction temperatures. Water, formic acid and 2,6-dimethyl aniline react rapidly with isocyanate with high conversions, which leaves little chance for their potential ring-opening addition reactions with epoxide. When 2,6-dimethyl aniline is added in the reaction system, equilibrium reactions between different urea groups exist. *N,N'*-dinaphthyl urea and 2,6-dimethyl isocyanate are generated by an equilibration. Unlike urethane which further reacted with epoxide to generate oxazolidinone and a series of urethane-epoxide adducts, the disubstituted aryl urea shows a low tendency to react with epoxide. When water, formic acid or 2,6-dimethyl aniline is incorporated in the “Ep\_ROH\_NCO\_DAB” system individually and reacted at 160 °C, the total amounts of carbodiimide formed during the reaction all increase at the expense of the isocyanurate formation. They share in common that disubstituted aryl urea is readily formed. Therefore, efforts were undertaken to gain an insight into the possible relationship between disubstituted aryl urea and carbodiimide formation.

### **3.1.3 The effect of disubstituted aryl urea on isocyanurate and carbodiimide selectivity**

The influence of disubstituted aryl urea on isocyanurate and carbodiimide selectivity was studied using a simplified reaction system which contains only isocyanate and DABCO<sup>®</sup> T catalyst. Disubstituted aryl urea was added to the system and the outcome was studied. Note that carbodiimide is produced at high temperatures such as 160 °C and when there is an excess of isocyanate, the formation of isocyanurate and carbodiimide are competing reactions. The result presented in this chapter shows that the presence of disubstituted aryl urea can influence the reaction selectivity towards carbodiimide formation.

In the “Reference” system, DABCO<sup>®</sup>T was added to 1-naphthyl isocyanate at a molar ratio of 0.013:1 and the system was heated to 160 °C. In the “Urea on top” system, 0.034 mol *N,N'*-dinaphthyl urea was added additionally (Table 19). The products

present at 10 minutes of reaction were analyzed by ESI-MS (+) and  $^1\text{H}$  NMR. In these two systems, the products are the same in terms of species. The main products are isocyanurate and carbodiimide derived products. The carbodiimide related products include the carbodiimide monomer and its subsequent reaction products to iminodiazetidione, carbodiimide dimer, iminotriazinedione, iminotriazinone, carbodiimide trimer and guanidine. The total amount of carbodiimide formed during the process comprising the carbodiimide remaining in the final product and the part as intermediate involved in the consecutive reactions was calculated from the  $\text{CO}_2$  evolution. The amounts of the isocyanurate were determined by  $^1\text{H}$  NMR. The product amounts were expressed in the isocyanate conversion (Table 20).

**Table 19.** Recipes in the study of the influence of disubstituted aryl urea

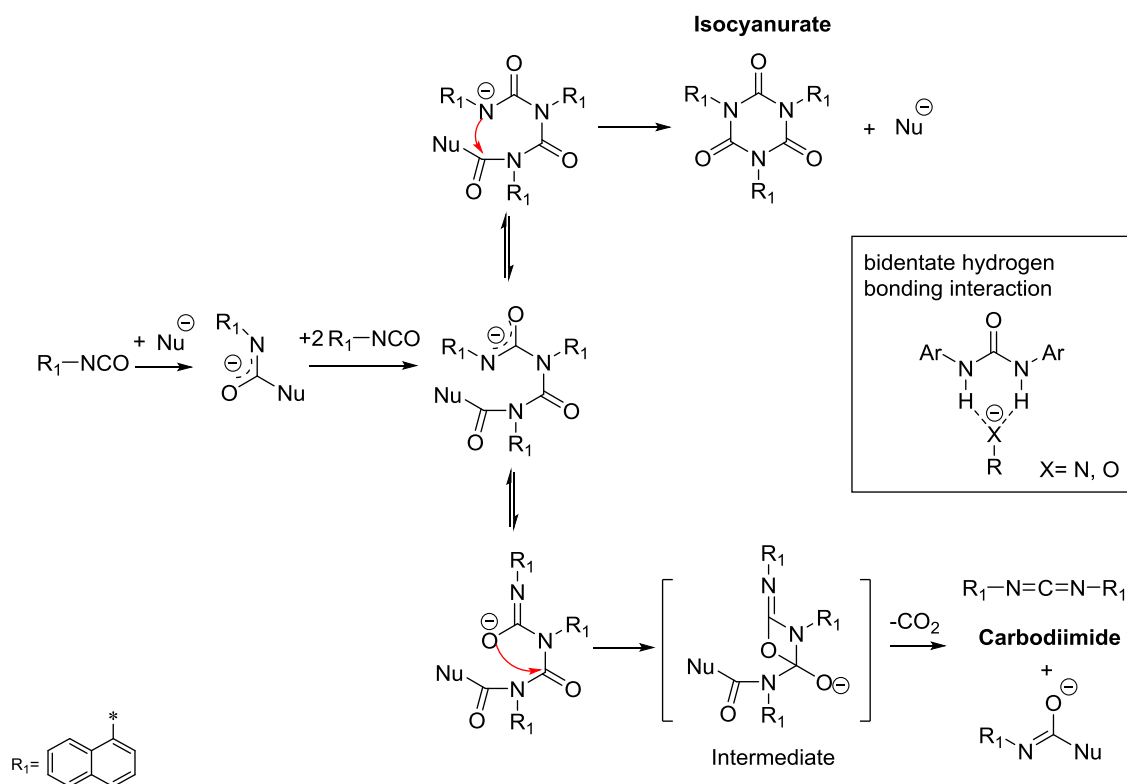
<b>Reaction system</b>	1-Naphthyl isocyanate (molar ratio)	DABCO <sup>®</sup> T (Catalyst) (molar ratio)	<i>N,N'</i> -dinaphthyl urea (molar ratio)
<b>Reference</b>	1	0.013	
<b>Urea on top</b>	1	0.013	0.034

**Table 20.** Reaction product quantification

<b>Reaction system</b>		<b>Reference</b>	<b>Urea on top</b>
Isocyanate conversion (%) into	Isocyanurate	82	69
	Carbodiimide (in total)	16	28
“Isocyanate conversion into total carbodiimide” divided by “Isocyanate conversion into Isocyanurate”		0.20	0.41
<i>N,N'</i> -dinaphthyl urea in the final product (mol% relative to isocyanate fed)		0.014	0.035
Peak temperature of reaction system		181 °C	164 °C

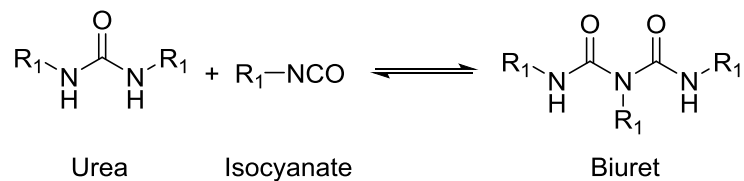
The presence of *N,N'*-dinaphthyl urea leads to larger formation of carbodiimide. When *N,N'*-dinaphthyl urea is added to the reference system, the isocyanate conversion into isocyanurate decreases from 82% to 69% while the isocyanate conversion into total carbodiimide increases from 16% to 28%. The ratio between “isocyanate conversion into total carbodiimide” and “isocyanate conversion into isocyanurate” increases from 0.20 to 0.41. The promotion of carbodiimide formation is also supported by the peak reaction temperature difference of the two reaction systems. Although the reaction systems were both heated in an oil bath of 160 °C, the peak temperature of the “Reference” was 17 °C higher than that of the “Urea on top”. According to literature, the isocyanurate formation is an exothermic reaction whereas the carbodiimide formation is endothermic<sup>[29,59]</sup>. In the “Reference” system, a small amount of urea (0.014 mol % relative to the initial isocyanate amount) is formed presumably by a reaction of water from the air with isocyanate. In the gas evolution method used for the determination of carbodiimide content, a completely water-free environment cannot be secured. Nevertheless, the urea amount in the “Urea on top” system is 2.5 times higher than that of the “Reference” system. The higher urea amount drives the reaction towards carbodiimide formation.

In the “Urea on top” system, the amount of urea in the final product does not show significant changes relative to the amount added, hence the urea acts only as a catalyst. There are two plausible explanations for the catalytic action. One is, when the carbon atom of the isocyanate moiety is nucleophilically attacked, the negative charge build up is stabilized by adjacent nitrogen and oxygen atoms (Scheme 13). It could be that the *N,N'*-dinaphthyl urea is more efficient in stabilizing the intermediates that are formed during the carbodiimide formation. Such a stabilization may be a double hydrogen bonding interaction.



**Scheme 13.** Possible mechanism for *N,N'*-dinaphthyl urea in promoting carbodiimide formation

Another plausible catalytic pathway is the intermediate formation of a biuret, by urea reacting with isocyanate. The biuret formed at low temperatures can convert back to urea and isocyanate at high temperatures after the reaction system is fully heated (Scheme 14). The regenerated isocyanate at high temperature will have a higher chance to convert to carbodiimide. Although biuret is not detected in the final product of the “Urea on top” system, the possibility of its formation as an intermediate cannot be ruled out. The biuret has been reported to be formed as an intermediate when using *N,N,N',N'',N'''*-Pentamethyl diethylenetriamine as catalyst. Instead of further reacting with isocyanate to produce isocyanurate, the biuret formed in that system was considered to mainly convert back to urea and isocyanate in the later stage of the reaction<sup>[47]</sup>.



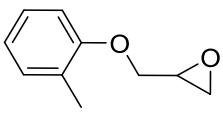
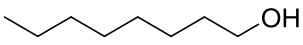
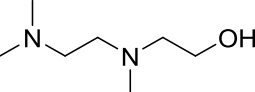
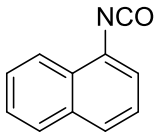
**Scheme 14.** the reversible reaction of biuret

### 3.1.4 Epoxide modified “mono\_PUR/PIR” system

The modification of polyurethane-co-polyisocyanurate (PUR/PIR) foams by the addition of epoxide was reported useful for obtaining rigid foams with improved properties<sup>[50,89]</sup>. The influence of epoxide on the reaction chemistry will be discussed based on a model system characteristic for the PUR/PIR rigid foams (Table 21). In the “mono\_PUR/PIR” system, 1-octanol and water were selected to simulate the gelling and blowing reaction, respectively. The NCO index was set at 200 to include the isocyanurate and carbodiimide reactions. DABCO<sup>®</sup> T was used as catalyst and poly(ethylene glycol) dimethyl ether (Mn =1,000) was added as solvent to obtain a homogeneous A component. The reactant equivalents of the “mono-add. Ep” system, were the same as in the “mono\_PUR/PIR” system, except that 0.5 equivalent of glycidyl 2-methylphenyl ether was added additionally as epoxide. The reactions were conducted at 80 °C and 160 °C.



**Table 21.** Recipe of the “mono\_PUR/PIR” and the “mono-add. Ep”

	Reactant	Structure	Equivalent mono_PUR/PIR*	Equivalent mono-add. Ep**
<b>Comp. A</b>	Glycidyl 2-methylphenyl ether			0.5
	1-Octanol		0.5	0.5
	Water	H <sub>2</sub> O	1.0	1.0
	DABCO® T		0.0375	0.0375
<b>Comp. B</b>	1-Naphthyl isocyanate		3.0	3.0

Poly (ethylene glycol) dimethyl ether (Mn ~1,000) was used as solvent to obtain a homogeneous A component, solvent content: \* 29 %, \*\* 26 %

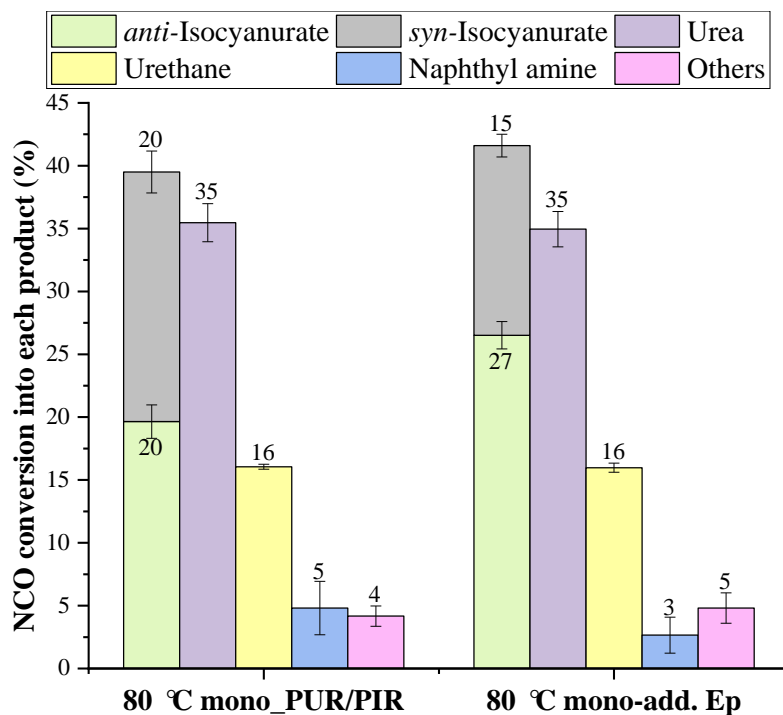
The product amounts after 10 minutes at 80 °C were determined by the <sup>1</sup>H NMR and expressed in the isocyanate conversion (Table 22, 23; Figure 11). The main products are isocyanurate, urea and urethane, which account for over 90% of the isocyanate conversion, irrespective of the presence of epoxide. The amounts of urethane in the two systems are similar and both close to the anticipated values. The same holds true for urea. Nearly all the alcohol and water in the system have reacted with isocyanate to form urethane and urea, respectively. The remainder of the isocyanate is mainly converted into isocyanurate. The total amounts of isocyanurate are also similar in the two systems but in the “mono-add. Ep” system, a higher portion of anti-isocyanurate (orange bar in Figure 11) is formed. In the “mono-add. Ep” system, the total epoxide conversion is low at 80 °C and only amounts to 6%.

**Table 22.** Reactant conversions of “mono\_PUR/PIR” and “mono-add. Ep” reacted at 80 °C for 10 minutes

Reactant conversion	mono_PUR/PIR		mono-add. Ep	
	Average (%)	Experimental error (%)	Average (%)	Experimental error (%)
Isocyanate	100	0	100	0
Epoxide	/	/	6	6
Alcohol	100	0	100	0

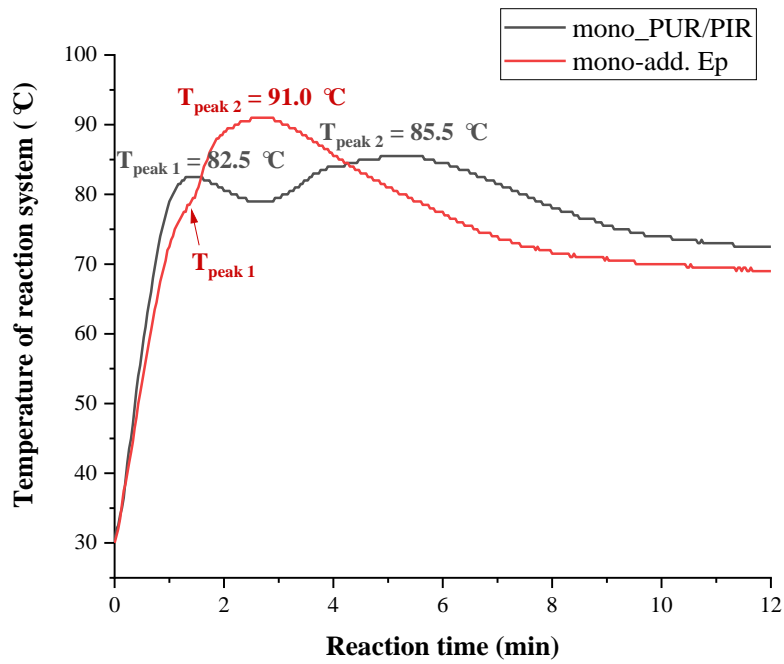
**Table 23.** Product distribution expressed in isocyanate conversions of “mono\_PUR/PIR” and “mono-add. Ep” reacted at 80 °C for 10 minutes (anticipated values shown in the brackets below)

Isocyanate conversion into	mono_PUR/PIR		mono-add. Ep	
	Average (%)	Experimental error (%)	Average (%)	Experimental error (%)
<i>anti</i> - Isocyanurate	20	1	27	1
<i>syn</i> - Isocyanurate	20	2	15	1
Isocyanurate ( <i>anti</i> - + <i>syn</i> -)	40	3	42	2
Urethane	16 (17)	0	16 (17)	0
Urea	35 (33)	2	35 (33)	1
Naphthyl amine	5	2	3	1
Others	4	1	5	1

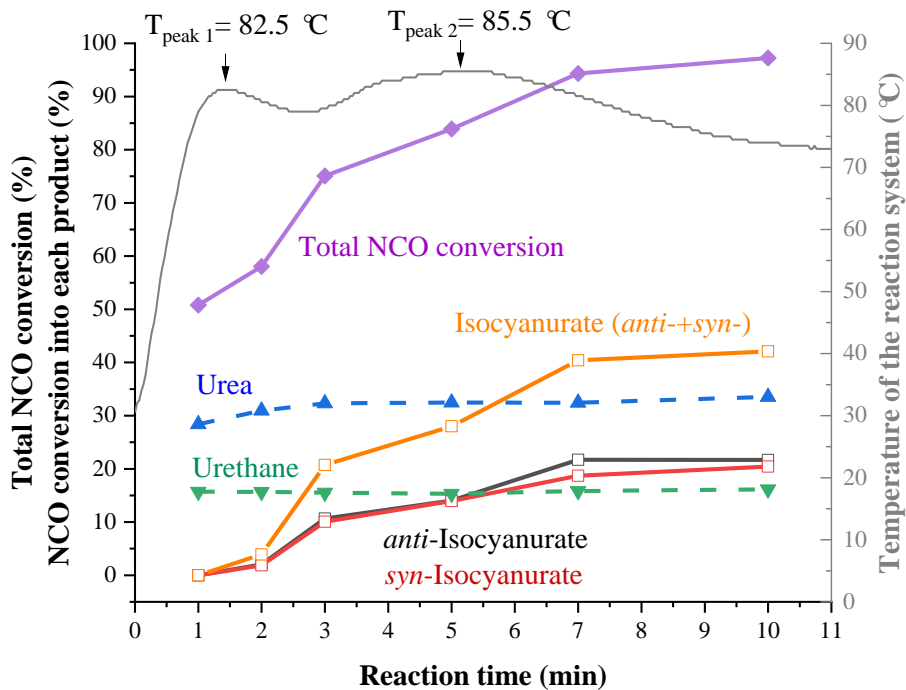


**Figure 11.** Product distribution (expressed as isocyanate conversion) of “mono\_PUR/PIR” and “mono-add. Ep” when heated at 80 °C for 10 minutes

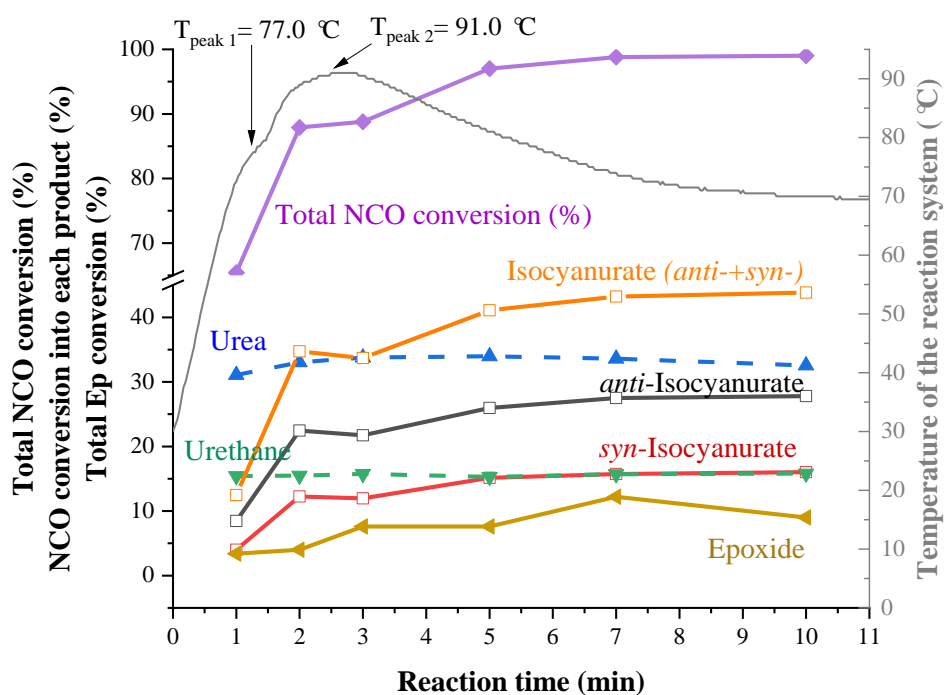
Although the final products after 10 minutes of reaction time are similar in the two systems, their exotherms develop in a different manner. A thermocouple was inserted into the reaction mixture and the temperature development of the two reaction systems was recorded as a function of time (Figure 12.). Both systems show two temperature maxima. The two maxima of the “mono\_PUR/PIR” system are at 82.5 °C after 1.5 minutes (Peak 1) and at 85.5 °C after 5 minutes (Peak 2). In the “mono-add. Ep” system the first peak shows up as a shoulder after about 1.5 minutes and then the temperature development accelerates, reaching a second maxima after 2.5 minutes with a temperature of 91.0 °C. The product mixture changes with reaction time (Figure 13). The amount of free isocyanate was determined by reacting the product with diethyl amine and calculated the amount of urea formed by diethyl amine and isocyanate using  $^1\text{H}$  NMR. The total isocyanate conversion was calculated based on the amount of free isocyanate in the product



**Figure 12.** Temperature developments of the “mono\_PUR/PIR” and “mono-add. Ep” systems when heated at 80 °C



**Figure 13 (a).** Product development (left Y axis) and system temperature (right Y axis) with time in the “mono\_PUR/PIR” system, reaction temperature: 80 °C

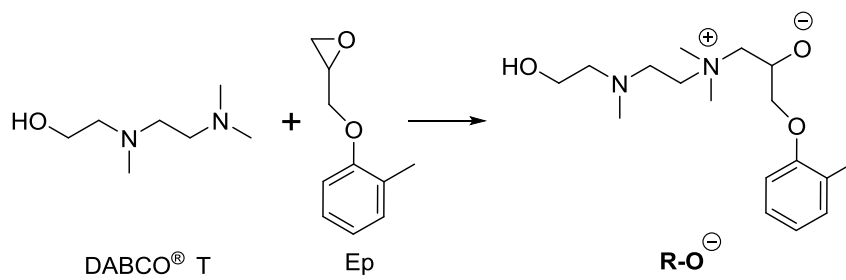


**Figure 13 (b).** Product development (left Y axis) and system temperature (right Y axis) with time in the “mono-add. Ep” system, reaction temperature: 80 °C

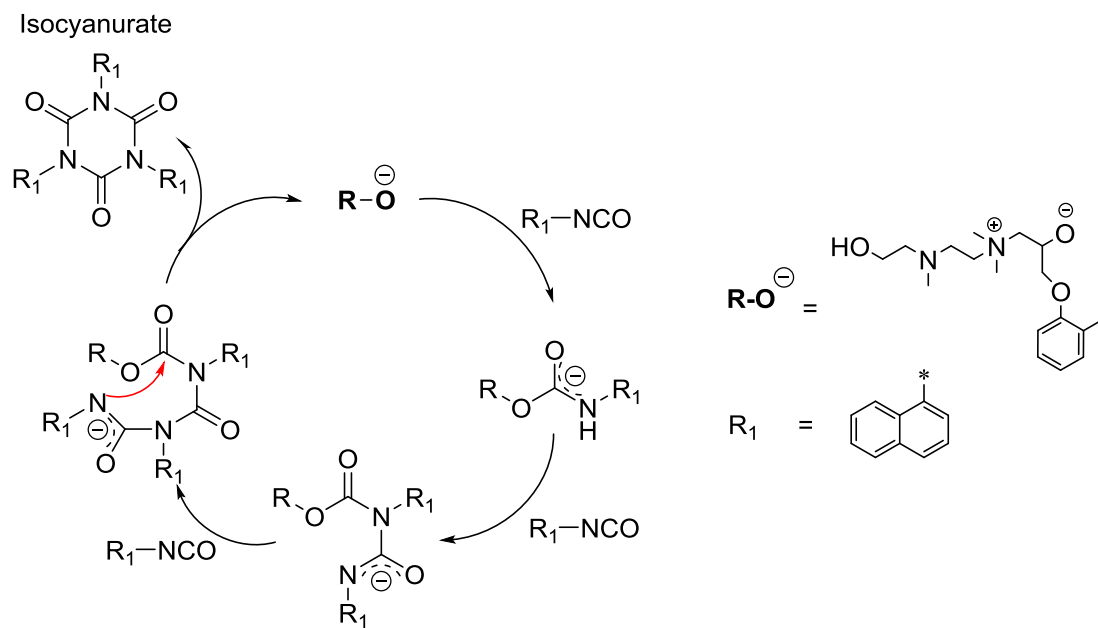
The product development curves in Figure 13 visualize that the system with additional epoxide has a faster isocyanate conversion and isocyanurate formation. In the “mono\_PUR/PIR” system (Figure 13 (a)), urea and urethane are formed in the very beginning of the reaction. The amounts formed in the first minute are already close to their expected values whereas no isocyanurate formed. This is a strong indication that the urethane and urea forming reactions are faster than the isocyanurate formation. The first exothermal peak is thus caused by the formation of urea and urethane alone. Subsequently isocyanurate is produced leading to the second exothermal peak after about 5 minutes. In the “mono-add. Ep” system (Figure 13 (b)), the urea and urethane forming reactions also proceed fast, but here the isocyanurate formation kicks in much earlier and faster than in the “mono\_PUR/PIR” system. This leads to a faster NCO conversion and a larger heat buildup. The reaction is practically finished after 5 minutes.

The faster NCO conversion and isocyanurate formation are caused by the addition of the epoxide. It is proposed that the epoxide acts as a co-catalyst for the isocyanurate formation. A possible reaction pathway involves an epoxide ring opening by the tertiary amine catalyst- DABCO<sup>®</sup> T producing an alkoxide (Scheme 15). The alkoxide is more nucleophilic than the tertiary amine and can attack the central carbon atom of the NCO group. After successive reactions of the first anionic intermediate with two more isocyanates followed by a ring closure step, isocyanurate is formed. Although DABCO<sup>®</sup> T can also catalyze the isocyanurate formation by this route, the stronger alkoxide nucleophile is more effective. As the amount of DABCO<sup>®</sup> T in the system is relatively small, only a minor portion of epoxide acts as a co-catalyst.

The co-catalyst hypothesis is also supported by the ratio between *anti*- and *syn*-isocyanurate when epoxide is added. In the “mono-add. Ep” system, the ratio between *anti*- and *syn*-isocyanurate amounts to 1.7 while in the “mono\_PUR/PIR” system, this is only 1.1. From DFT calculations, the *anti*-isomer was reported to be thermodynamically more stable than the *syn*-isomer by approximately 2.3 kJ/mol<sup>[85]</sup>. In the “mono-add. Ep” system, after 1 minute of reaction time when the system temperature only is 72.5 °C, a significantly higher portion of *anti*- isocyanurate is formed (Figure 14). However, in the “mono-PUR/PIR” system, after 5 minutes of reaction when the system temperature already have achieved a temperature of 85.5 °C, the *anti*- and *syn*- isocyanurate amounts are still about the same. Therefore, the higher portion of *anti*-isocyanurate in the “mono-PUR/PIR” system is not caused by the reaction temperature and would possibly lie in the fundamental nature of the two nucleophiles, the tertiary amine of DABCO<sup>®</sup> T and the alkoxide of the DABCO<sup>®</sup> T-epoxy adduct: When the more bulky alkoxide acts as the nucleophile, then during the ring closure step to form the isocyanurate, the formation of less crowded *anti*-isocyanurate is favored .

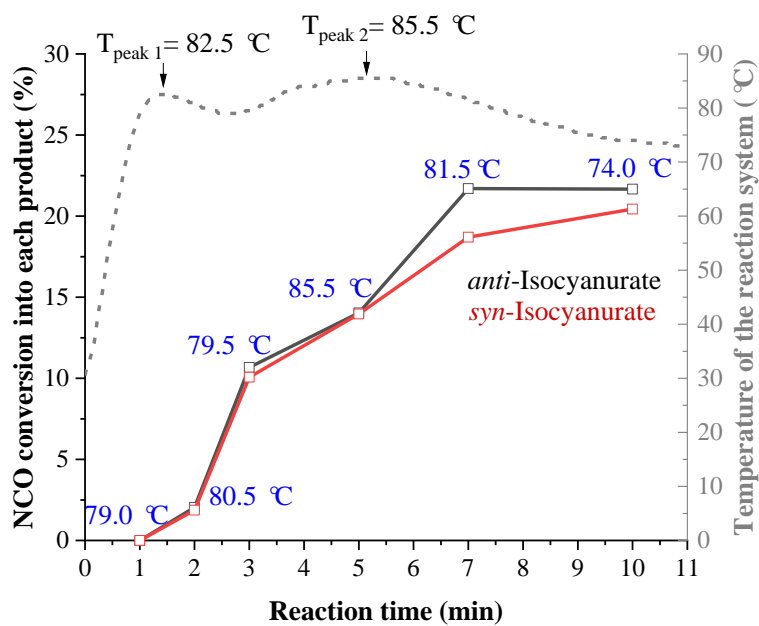


Alkoxide formation

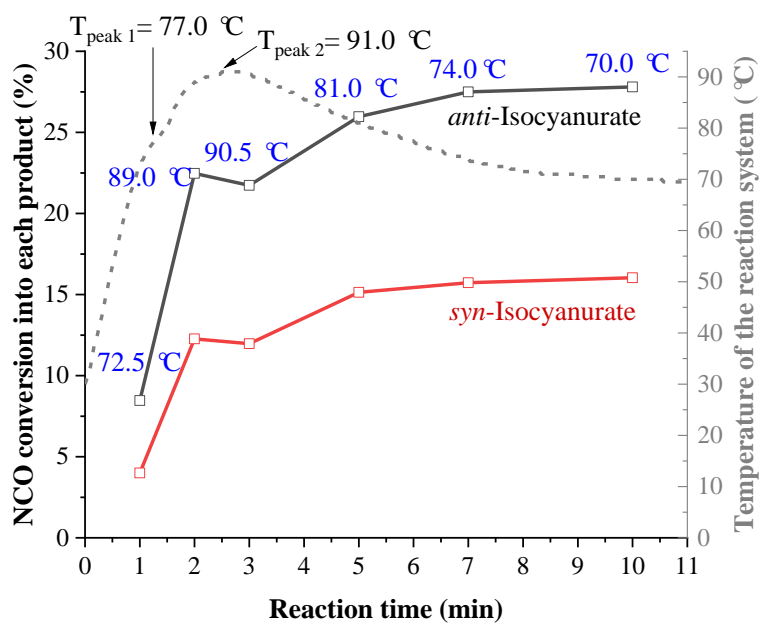


Alkoxide catalyzes isocyanurate formation

**Scheme 15.** The proposed mechanism of epoxide as a co-catalyst in promoting isocyanurate



(a) "mono\_PUR/PIR" system



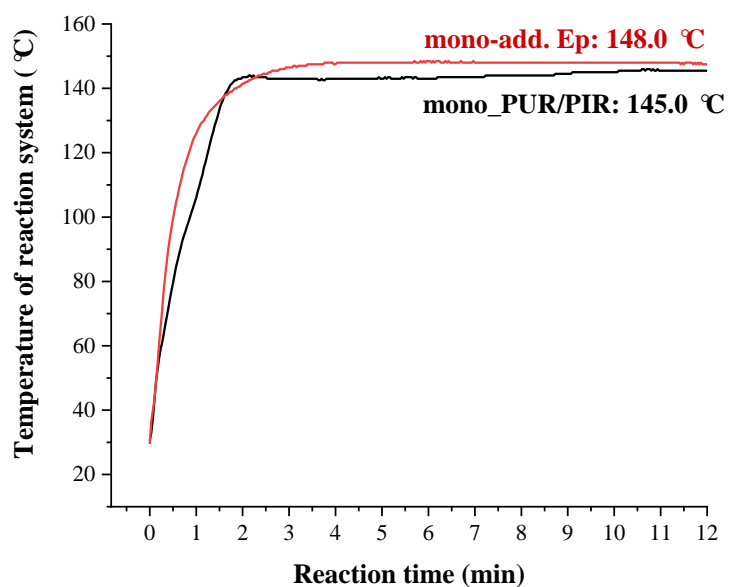
(b) "mono-add. Ep" system

**Figure 14.** System temperature and the amounts of anti- and syn- isocyanurate at each sampling point

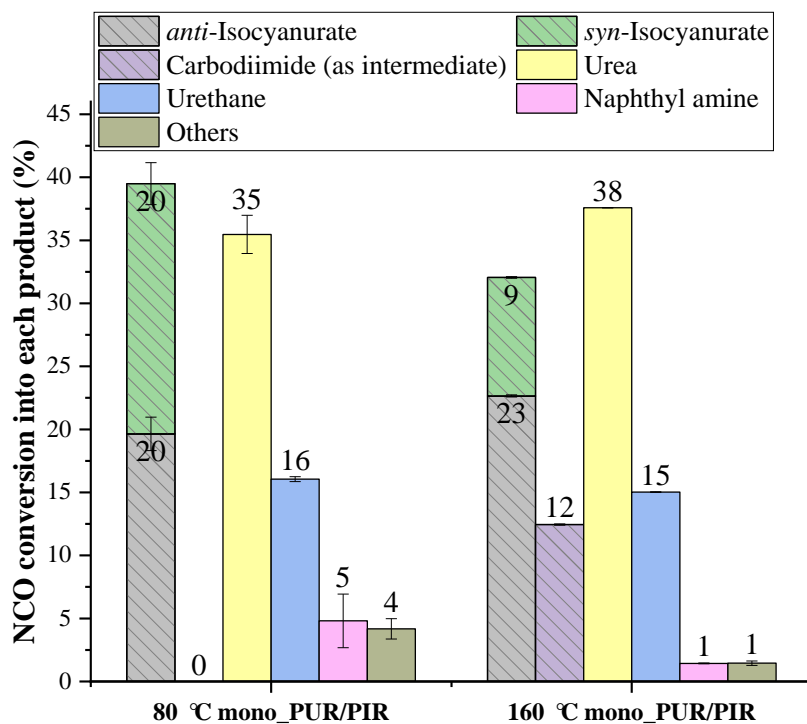


In summary, at a temperature of 80 °C, urea and urethane are formed in the beginning of the reaction, followed by isocyanurate formation in the second phase. When additional epoxide is present, most of the epoxide remains unreacted but a small amount will react with DABCO<sup>®</sup> T and act as the dominant catalyst for the isocyanurate formation.

The same reactions were also conducted at a higher heating temperature of 160 °C (Figure 15). In the “mono-add. Ep” system, the heat buildup in the first 40 seconds is faster than in the “mono\_PUR/PIR” system, but in the second stage of the reaction, the temperature developments of both systems are very similar, although the final reaction temperature that is reached in the “mono-add. Ep” is 3 °C higher than of the “mono\_PUR/PIR”. Both systems are strongly fast and complete within 2 to 3 minutes. In such fast reacting systems, the potential acceleration by the epoxide becomes insignificant. The high reactivity prohibited sampling and therefore only the final reaction products after 10 minutes of reaction were analyzed. The reaction products of the “mono\_PUR/PIR” system when heated at 160 °C were compared to those at 80 °C. The yields in urea and urethane are not affected by the temperature (Figure 16). The main difference is that carbodiimide reactions take place at 160 °C. These reactions compete with the isocyanurate forming reaction and less isocyanurate is formed. Meanwhile, the amount of the relatively unstable *syn*-isocyanurate decreases with increasing reaction temperature.



**Figure 15.** Temperature development of “mono\_PUR/PIR” and “mono-add. Ep” systems when heated at 160 °C



**Figure 16.** Product distribution of “mono\_PUR/PIR” system at 80 °C and 160 °C at 10 minutes of reaction time

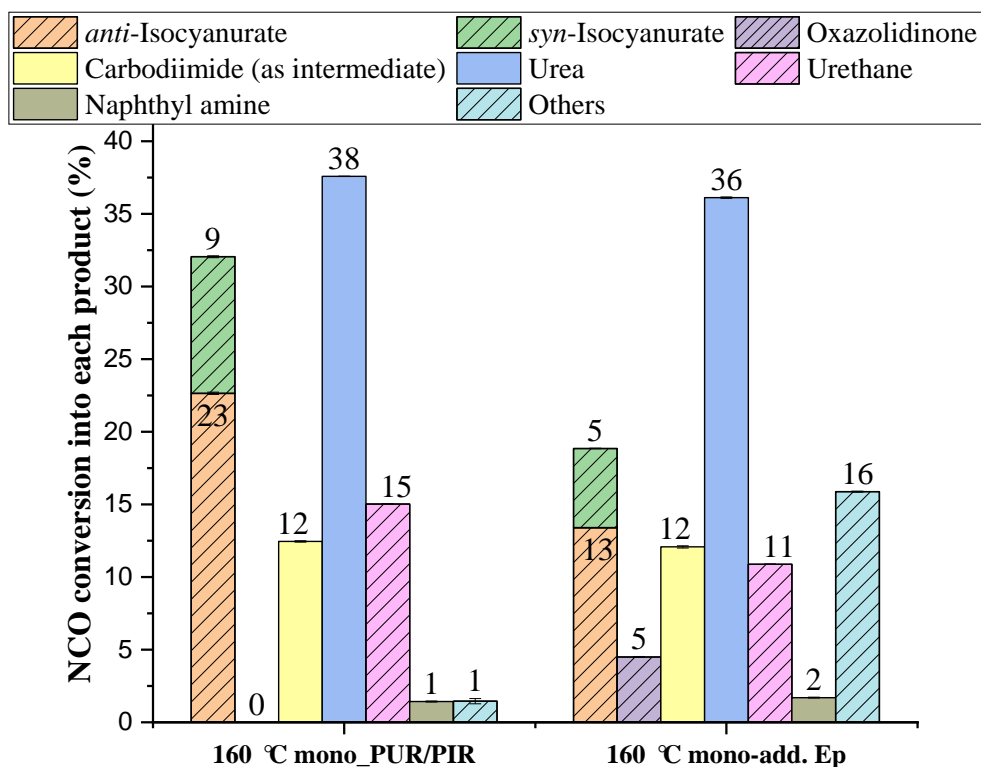
The reactant conversions and reaction products of the “mono-add. Ep” system when heated at 160 °C after 10 minutes were compared to that of the “mono\_PUR/PIR” system. The amounts of urea and carbodiimide (as intermediate) formed in the two systems are similar (Table 24, 25; Figure 17). When additional epoxide is present, the amounts of isocyanurate and urethane decrease while the amounts of oxazolidinone and “Others” increase. ESI-MS (+) shows that the isocyanate conversion into “Others” can be attributed by two classes of reactions. One class is the addition reaction between epoxide and the formed urethane. The other class is the subsequent reactions of carbodiimide. The total epoxide conversion in the “mono-add. Ep” system amounts to 96%, indicating that at higher temperatures, most of the epoxide have reacted with isocyanurate and urethane. Oxazolidinone and a series of urethane-epoxide adducts are formed as discussed in Chapter 3.1.1.

**Table 24.** Reactant conversions of “mono\_PUR/PIR” and “mono-add. Ep” when heated at 160 °C for 10 minutes

<b>Reactant conversion (%)</b>	<b>mono_PUR/PIR</b>	<b>mono-add. Ep</b>
<b>Isocyanate</b>	100	100
<b>Epoxide</b>	/	96
<b>Alcohol</b>	100	100

**Table 25.** Product distribution expressed in isocyanate conversions of “mono\_PUR/PIR” and “mono-add. Ep” when heated at 160 °C for 10 minutes (anticipated values shown in the brackets below)

<b>Isocyanate conversion into (%)</b>	<b>mono_PUR/PIR</b>	<b>mono-add. Ep</b>
<b><i>anti</i>- isocyanurate</b>	23	13
<b><i>syn</i>- isocyanurate</b>	9	5
<b>Isocyanurate (<i>anti</i>- + <i>syn</i>-)</b>	32	19
<b>Urethane</b>	15 (17)	11 (17)
<b>Urea</b>	38 (33)	36 (33)
<b>Carbodiimide (as intermediate)</b>	12	12
<b>Naphthyl amine</b>	1	2
<b>Oxazolidinone</b>	/	5
<b>Others</b>	1	16



**Figure 17.** The product distribution of “mono\_PUR/PIR” and “mono-add. Ep” systems when heated at 160 °C for 10 minutes

In summary, at 80 °C, 94% epoxide stays unreacted but acts as a co-catalyst for the isocyanurate formation and accelerates the isocyanate conversion, while at 160 °C, the reaction is so fast that acceleration by catalysis originating from the epoxide becomes insignificant. Epoxide reacts with isocyanurate and urethane at high conversion to form oxazolidinone and a series of epoxide-urethane adducts.

### 3.1.5 The “Model” system

This chapter reports on the “Model” reaction system which contains all the reactants of the epoxide-PUR/PIR (Table 26).

**Table 26.** Reactant equivalents of the “Model” system

	<b>Reactant</b>	<b>Equivalent “Model” system*</b>
<b>Component A</b>	Glycidyl 2-methylphenyl ether	1.0
	1-Octanol	0.5
	Water	1.0
	Formic acid	0.5
	2,6-Dimethyl aniline	0.5
	DABCO <sup>®</sup> T	0.0875
<b>Component B</b>	1-Naphthyl isocyanate	7.0

\* Tetraethylene glycol dimethyl ether or polyethylene glycol dimethyl ether (Mw=1000) was added to obtain a compatible Component A. Solvent content: 29 wt%

Reactions were conducted at three temperatures of 80 °C, 130 °C and 160 °C. The products were identified by LC-MS and quantified by <sup>1</sup>H NMR and the gas evolution method at 10 minutes of reaction time. The product species show a high similarity to that of the “Ep\_ROH\_NCO\_RNH<sub>2</sub>\_DAB” system. A detailed product assignment is given in the Experimental Part. The following two points must be considered regarding the quantification (Table 27). Firstly, the amount of the total isocyanurate formed is higher than the amount of trinaphthyl isocyanurate. Because 2,6-dimethyl phenyl isocyanate is formed in the urea equilibration reactions, it can subsequently react with two 1-naphthyl isocyanates to form a hybrid isocyanurate. The mass peak of the hybrid isocyanurate was detected by LC-MS, but the lack of a reference compound, prohibited its quantification. Secondly, the amount of the carbodiimide (as intermediate) can only be determined approximately by assuming that both water and formic acid were fully converted into CO<sub>2</sub> or CO. This assumption is safe to take because no water and formic acid signals were detected in <sup>1</sup>H NMR spectra after the

completion of the reaction. In the model reaction systems, gases can be produced by three reactions, that is, the reaction of isocyanate with water, the reaction of isocyanate with formic acid and the carbodiimide formation. In the previous discussed “Ep\_ROH\_NCO\_H<sub>2</sub>O\_DAB” and “Ep\_ROH\_NCO\_FA\_DAB” systems, the gas volume generated by the isocyanate-water or the isocyanate-formic acid reactions can be determined by the amount of urea formed in the system. However, in the “Model” system, urea is generated by three individual pathways, namely, the reaction of isocyanate with water, formic acid and amine. Consequently, an assumption has to be made for the amount of the carbodiimide formed (as intermediate), the one calculated by the CO<sub>2</sub> evolution method can only be an approximate value (Table 27).

*N,N'*-dinaphthyl urea (Figure 18, green bar) is formed in relatively high amounts, the amount being independent on the reaction temperature. When the temperature is 160 °C, the amounts of trinaphthyl isocyanurate and urethane decrease, while the amount of oxazolidinone and carbodiimide (as intermediate) increase. The total epoxide conversion is only 5% at 80 °C but reached 98% at 160 °C. The observations for the “Model” system are largely in line with that of the “Ep\_ROH\_NCO\_DAB” system. The underlying reaction pathways were discussed in Chapter 3.1.1.3. The “Model” system gives a larger amount of urea and there is also a higher tendency to produce carbodiimide at high temperatures. The presence of urea promoted the carbodiimide formation and the possible pathways were already discussed in Chapter 3.1.3.

**Table 27(a).** Isocyanate conversion into different reaction products

Isocyanate conversion into	80 °C		130 °C		160 °C	
	Average (%)	Experimental error (%)	Average (%)	Experimental error (%)	Average (%)	Experimental error (%)
Trinaphthyl-isocyanurate	40	1	38	1	18	4
Naphthyl oxazolidinone	0	0	1	0	4	1
Naphthyl urethane	7	0	5	0	4	0
<i>N,N'</i> -dinaphthyl urea	32	2	33	0	35	2
<i>N</i> -(2,6-dimethylphenyl)- <i>N'</i> -naphthyl urea	2	1	1	0	1	0
Carbodiimide (as intermediate)	0	0	5	1	29	-
Naphthyl amine	8	3	1	0	0	0
Others	12	1	15	0	9	4
<b>Total isocyanate conversion</b>	100	0	100	0	100	0

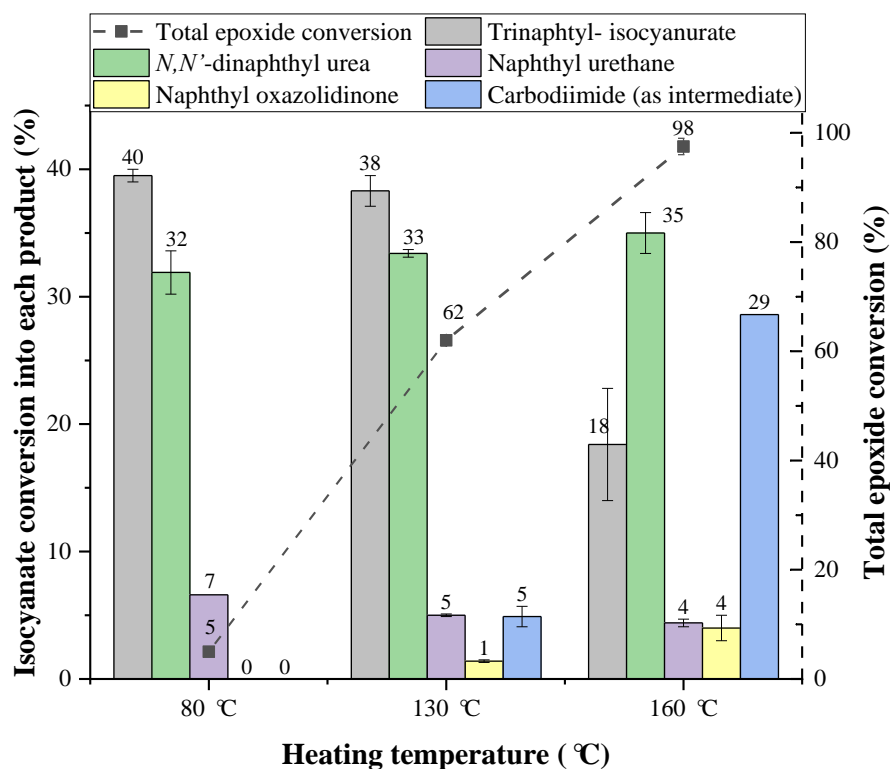
**Table 27 (b).** Epoxide conversion into different reaction products

Epoxide conversion into	80 °C		130 °C		160 °C	
	Average (%)	Experimental error (%)	Average (%)	Experimental error (%)	Average (%)	Experimental error (%)
Naphthyl oxazolidinone	0	0	10	1	28	5
Others	5	0	52	1	70	4
<b>Total Ep conversion</b>	5	0	62	1	98	2



**Table 27(c).** Alcohol conversion into different reaction products

Alcohol conversion into	80 °C		130 °C		160 °C	
	Average (%)	Experimental error (%)	Average (%)	Experimental error (%)	Average (%)	Experimental error (%)
Naphthyl urethane	92	0	70	1	62	3
Others	8	0	30	1	39	3
<b>Total alcohol conversion</b>	100	0	100	0	100	0



**Figure 18.** The yield of the main reaction products expressed in the 1-naphthyl isocyanate conversion (left Y axis) and the total epoxide conversion (right Y axis) formed at the three reaction temperatures in the “Model” system

## Summary and conclusion of the monofunctional reaction systems

Low molecular mass model reaction systems with monofunctional reactants were studied to obtain a basic understanding of the chemistry. The reaction products were identified by means of HPLC equipped with a UV detector and LC-MS. The products were quantified by using  $^1\text{H}$  NMR and a gas evolution method. Reaction systems were studied by varying the reaction temperature, catalyst species and combination of each individual reactant. The effect of these variables on the chemical bond formation was investigated. The underlying reaction mechanisms were discussed and further substantiated with additional dedicated model reactions where required.

DABCO<sup>®</sup> T which is a tertiary amine bearing two tertiary amino groups and a pendent primary hydroxyl group, shows the highest catalytic activity towards both the isocyanurate and carbodiimide formation as well as the epoxide mediated reactions. Consequently, it was used as the primary catalyst in this thesis work.

In the monofunctional model reaction system using DABCO<sup>®</sup> T as a catalyst, urethane and urea formation start already at reaction temperatures as low as 80 °C. Urethane is formed by the reaction between 1-naphthyl isocyanate and 1-octanol; urea is formed by the reaction between 1-naphthyl isocyanate and water, formic acid or 2,6-dimethyl aniline. Urea equilibration reactions with isocyanates exist. The urethane and urea forming reactions proceed fast achieving high reactant conversions in the early stages of the reaction. At low reaction temperatures, the remaining isocyanate mainly converts into isocyanurate. Carbodiimide formation and its subsequent reactions are observable at about 130 °C and become more pronounced at 160 °C. The isocyanurate and carbodiimide formation are competing reactions, where the presence of disubstituted urea promotes carbodiimide formation. Bidentate hydrogen bonding interaction and the reversible biuret reaction are proposed to be the two possible reasons that could steer the reaction towards carbodiimide formation. When epoxide is added to modify the PUR/PIR system, over 85% of the epoxide remains unreacted at 80 °C. A small portion of the epoxide performs as a co-catalyst in conjunction with catalyst DABCO<sup>®</sup> T and accelerates isocyanurate formation as well as isocyanate

conversion at low temperatures. The co-catalytic effect is ascribed to the formation of an alkoxide. This alkoxide originates from the ring opening reaction of epoxide upon the attack of the tertiary amine group of DABCO<sup>®</sup> T. At 160 °C, the overall conversion of epoxide reaches more than 90%. The epoxide is found to react with isocyanurate and urethane to form oxazolidinone and a series of urethane-epoxide adducts.

### **3.2 The study of reactant conversion and chemical bond formation in foam systems**

After having obtained an insight into the chemistry from the study on monofunctional model reaction system, the study was extended to foams. The fundamental difference between the two systems is that a polymer network is formed that possesses a glass transition temperature. The glass transition temperature depends on the crosslink density of the polymer matrix material and can reach values higher than 200 °C. The results show that the chemistry in the foam systems shares the same principles as that of the monofunctional systems. However, the chain segments in the polymer have low mobilities after vitrification. The limited mobilities have a strong impact on the reaction rate and hence on the final conversion of the reactive groups and the formation of the chemical bonds. Post curing at high temperatures and incorporation of epoxide into the PUR/PIR foam system were proven to improve the overall conversion of the system.

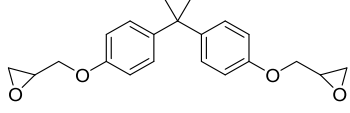
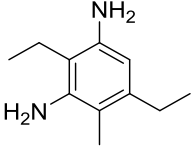
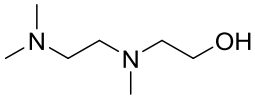
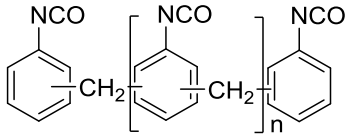
In the foam system, the reactant equivalents are the same as that of the monofunctional “Model” system, but the starting materials are polyfunctional, i.e. either bi- or higher-functional (Table 28).

The system was either cured isothermally on a temperature-controlled sample cell or cured pseudo-adiabatically in a paper cup without external heating. The isothermal cure was used to study the effects of time and temperature on the conversion of the reaction and the type of linkages that are formed. The cup foam experiments should

provide a good insight in the chemistry for the next step, which would be the production of the foam under relevant industrial production conditions.

ATR-IR spectroscopy, Soxhlet extraction and DMA were used to study the foam systems. Because of the highly crosslinked nature of the polymeric matrix material, the chain mobility is insufficient to allow solid-state NMR analysis. Some preliminary solid-state NMR work showed that the spectra obtained exhibited broad line shapes and provided limited information. Thus, the isocyanate conversion was calculated by using ATR-IR spectroscopy and that of the epoxide was determined by quantitative extractions using the Soxhlet extraction. The product amounts of isocyanurate, oxazolidinone and carbodiimide were assessed semi-quantitatively by using normalized intensities of the corresponding IR absorptions. The determination of the conversion of reactants like polyol, amine, formic acid and water as well as the formation of chemical bonds such as urethane and urea were not possible. The N-H stretch vibration of the amine and O-H stretch vibrations of water, formic acid and polyol overlap in the frequency range between  $3150\text{ cm}^{-1}$  and  $3460\text{ cm}^{-1}$ . The same was found for the carbonyl stretch vibrations of urethane and urea, which overlap in the range between  $1730\text{ cm}^{-1}$  and  $1640\text{ cm}^{-1}$  and therefore the formation of urethane and urea were not tracked during the reaction. For the “Model” system discussed in Chapter 3.1.5, it is shown that at  $80\text{ }^{\circ}\text{C}$ , isocyanate reacts readily with alcohol and water to form urethane and urea, respectively, and that these reactions are largely completed before isocyanurate formation become dominant. When the isocyanurate reaction sets in, the crosslink density increases rapidly and the chain mobility decreases as a result of vitrification. Because the urethane and urea reactions take place first, it is expected that these reactions will not significantly be affected by the vitrification process. The conversions of isocyanate and epoxide as well as the formation of isocyanurate, oxazolidinone and carbodiimide, however, will be affected by vitrification. The extent to which these reactions are influenced by vitrification will be discussed.

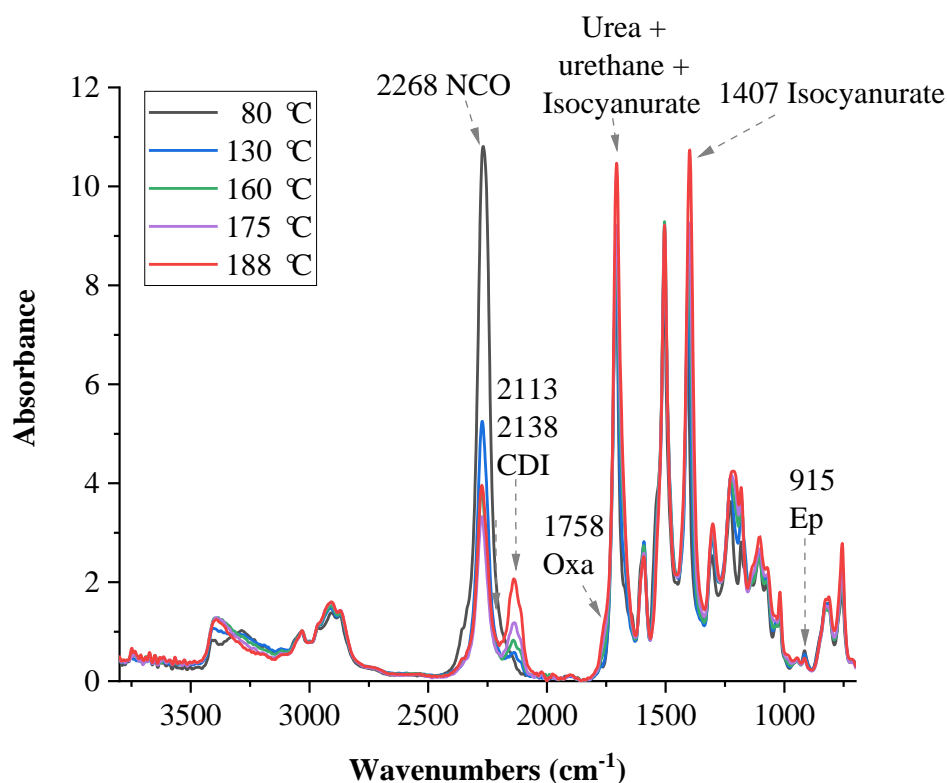
**Table 28.** Foam system used for the study

	<b>Reactant</b>	<b>Structure</b>	<b>Equivalent</b>
<b>Component A</b>	Bisphenol A diglycidyl ether		1.0
	Polyethylene glycol 600	$\text{H} \left[ \text{O} \text{---} \text{CH}_2 \text{---} \text{CH}_2 \right]_n \text{OH}$	0.5
	Water	$\text{H} \text{---} \text{O} \text{---} \text{H}$	1.0
	Formic acid	$\text{H} \text{---} \text{C}(=\text{O}) \text{---} \text{OH}$	0.5
	Diethyl toluenediamine		0.5
	DABCO <sup>®</sup> T		0.0875
<b>Component B</b>	Lupranat <sup>®</sup> M20R		7.0

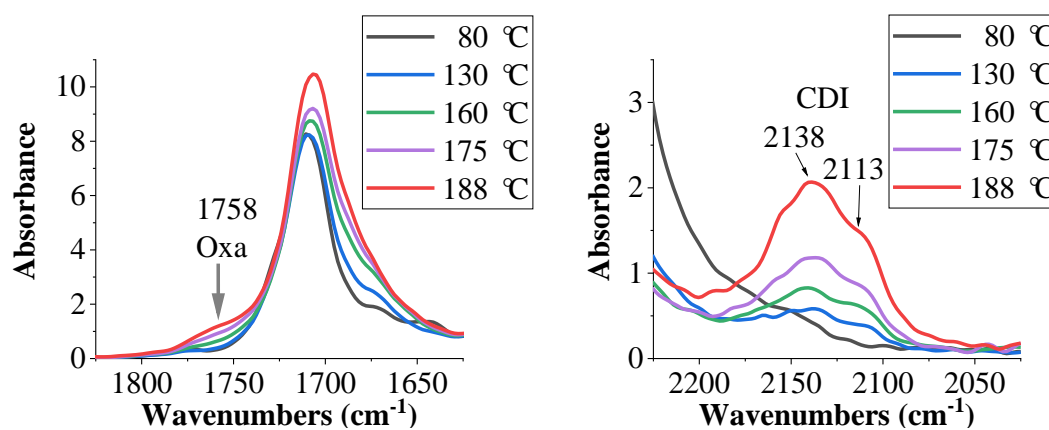
### 3.2.1 Foam system at isothermal reaction conditions

Initially, isothermal reactions were conducted to obtain an understanding of how the temperature and time affect the various reactions that occur during foam formation. Five different temperatures, viz. 80 °C, 130 °C, 160 °C, 175 °C and 188 °C were selected to study the relevant temperature range during the preparation of the foam. The isothermal reactions were monitored by using an ATR-FTIR instrument equipped with a temperature-controlled sample cell. The reaction system from Table 28 was

mixed at room temperature in a cup and a small amount of the resin was quickly transferred onto the preheated sample cell upon which the recording of the IR spectra was started. The FTIR spectra were normalized using the aromatic C-H stretching vibration at  $3035\text{ cm}^{-1}$ . The spectra obtained after 10 minutes of reaction at the different isothermal reaction temperatures are shown in Figure 19(a). The signal at  $2268\text{ cm}^{-1}$  is the NC=O stretching vibration and its absorption intensity was used to calculate the isocyanate conversion using the Lambert–Beer law (as described in the Experimental Part). The epoxide conversion was estimated from the intensity of the oxirane absorption at  $915\text{ cm}^{-1}$ . The product formation of isocyanurate, oxazolidinone and carbodiimide were taken from the intensities of their specific absorptions. As already mentioned in the previous chapter, the carbonyl stretch vibration of urea, urethane and isocyanurate strongly overlap in the region between  $1730\text{ cm}^{-1}$  and  $1640\text{ cm}^{-1}$ . Peak fitting is giving large intervals of error which made a meaningful quantification of urea and urethane formation impossible. Other entities can be semi-quantified by considering their respective absorptions. Isocyanurate shows a second characteristic absorption around  $1407\text{ cm}^{-1}$ ; the carbonyl stretching vibration of oxazolidinone is located at  $1758\text{ cm}^{-1}$  and shows only a minor overlap with the urethane carbonyl band (Figure 19 (b)). The carbodiimide has two absorptions at  $2113\text{ cm}^{-1}$  and  $2138\text{ cm}^{-1}$ . The absorption at  $2113\text{ cm}^{-1}$  shows less overlap with the isocyanate band at  $2268\text{ cm}^{-1}$ (Figure 19 (c)). The absorption intensities at  $1407\text{ cm}^{-1}$ ,  $1758\text{ cm}^{-1}$  and  $2113\text{ cm}^{-1}$  were used to track the amounts of isocyanurate, oxazolidinone and carbodiimide, respectively. It shows that a complete isocyanate conversion cannot be achieved after 10 minutes of reaction, not even at temperatures as high as  $188\text{ }^{\circ}\text{C}$  (Figure 19); Isocyanurate is generated at all reaction temperatures; carbodiimide is detected in reaction mixture hotter than  $130\text{ }^{\circ}\text{C}$  and oxazolidinone formation only become significant above  $160\text{ }^{\circ}\text{C}$ .



(a)



(b)

(c)

**Figure 19.** ATR-IR spectra of foam system taken after 10 minutes of reaction (a) full spectra, enlargement of the (b) oxazolidinone and (c) the carbodiimide area

The absorption intensities of isocyanate, epoxide, isocyanurate, carbodiimide, and oxazolidinone were plotted *versus* reaction time to explore how the reaction temperature and time affect the conversions of the reactants and to detect the

formation of linkages (Figure 20-1(a)-20-5(a)). The colors from black to red were used to represent data collected at the different reaction temperatures that were varied between 80 °C and 188 °C.

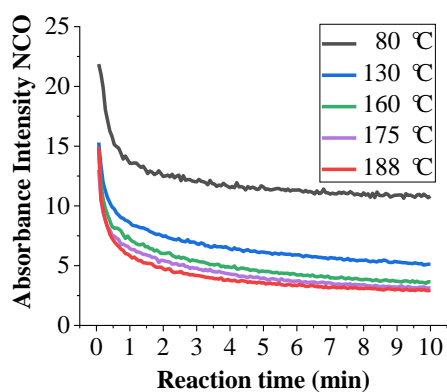
A complete cure is not achieved as is indicated by the isocyanate conversion, not even at 188 °C, which is the highest temperature the equipment could reach. This indicates that the prospective fully cured polymer may exhibit a glass transition temperature ( $T_{g\infty}$ ) above 188 °C. According to Gilham's time-temperature-transformation theory, complete cure is not likely to be obtained when the maximum reaction temperature is below  $T_{g\infty}$  because the reaction system vitrifies before completion of the reaction<sup>[69]</sup>. Vitrification retards the rate of reaction and results in only minor intensity changes of the various chemical functionalities at the later stages of the reaction.

The intensity changes are obvious within the first 1 to 2 minutes of reaction at all curing temperatures, suggesting relatively high reaction rates in the early stages of the reaction. Thereafter, the changes start to slow down, which marks the vitrification of the system. Once the vitrification sets in, the reactions can proceed but the reaction rate is much lower. The reaction can proceed to higher conversions at higher cure temperatures. This is supported by the observation that at a higher temperature, higher isocyanate and epoxide conversions are achieved and higher amounts of isocyanurate, carbodiimide and oxazolidinone are obtained. The underlying reason is that as the reaction proceeds, the molecular weight and the system  $T_g$  increase and if the reaction is carried out below  $T_{g\infty}$ , the polymer  $T_g$  will eventually reach the reaction temperature  $T_{cure}$ . Hence, when the reaction is carried out at a higher  $T_{cure}$ , a higher polymer  $T_g$  will be achieved and higher conversions obtained.

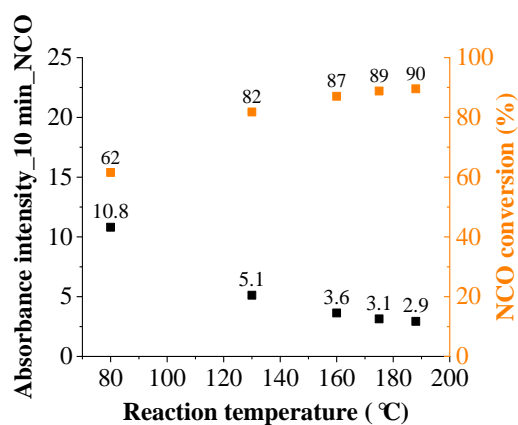
The isocyanate conversion after 10 minutes of reaction increases from 62% to 82% when increasing the reaction temperature from 80 °C to 130 °C (Figure 20-1(b)). A further increase in reaction temperature to 188 °C only increases the conversion to 90%. The intensity of isocyanurate absorption increases from 7.0 to 9.8 when the temperature is increased from 80 °C to 188 °C (Figure 20-2(b)), suggesting that already at 80 °C significant amounts of polyisocyanurate are formed. The formation



of polyisocyanurate increases the crosslink density and contributes strongly to the build-up of the polymer Tg. The carbodiimide reaction takes place above 130 °C and its apparent amount increases with temperature (Figure 20-3 (b)). The decrease at the starting point of 80 °C is just caused by the partial overlap with the strong isocyanate absorption nearby. The carbodiimide intensity builds up in the first minute of reaction till vitrification sets in. Subsequently, the intensity slightly decreases, suggesting that the carbodiimide in the vitrified state is faster consumed than new linkage is generated, but the changes are small (Figure 20-3(a)). Oxazolidinone formation is obvious at temperatures over 160 °C and its amount increases with temperature (Figure 20-4 (a)). The weak oxirane absorption makes it hard to obtain significant data for the epoxide conversion, however, the trend provides some information as to how epoxide reacts, No obvious change is observed in the epoxide intensity at 80 °C (Figure 20-5 (a)). This is in line with the observations made in the monofunctional “Model” system that over 95% of the epoxide stays unreacted at 80 °C. The epoxide intensity decreases slightly with time at 130 °C. The epoxide absorption signal shows a clear decrease at 160 °C and higher temperatures. It coincides with the onset of oxazolidinone formation.

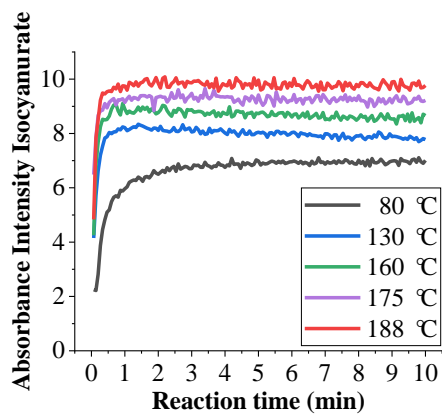


20-1(a)

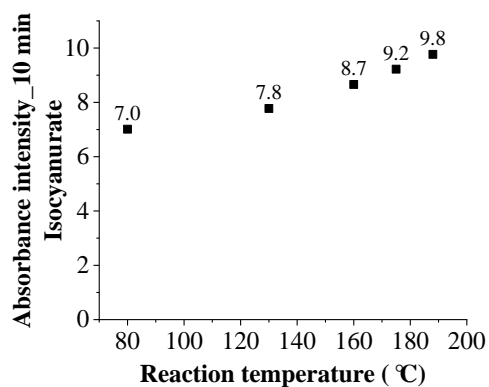


20-1(b)

Isocyanate absorption at 2268 cm<sup>-1</sup>

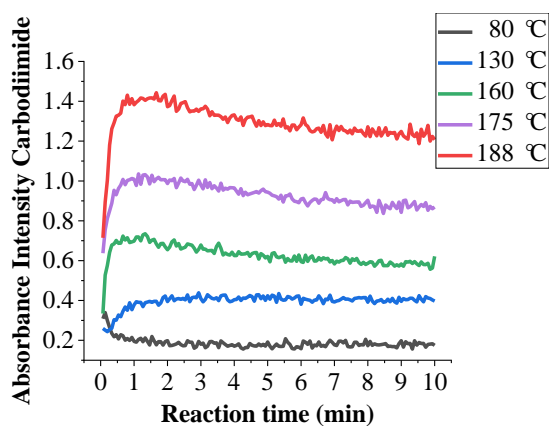


20-2(a)

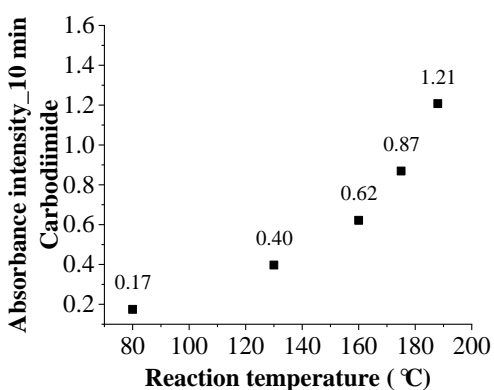


20-2(b)

Isocyanurate absorption at  $1407\text{ cm}^{-1}$

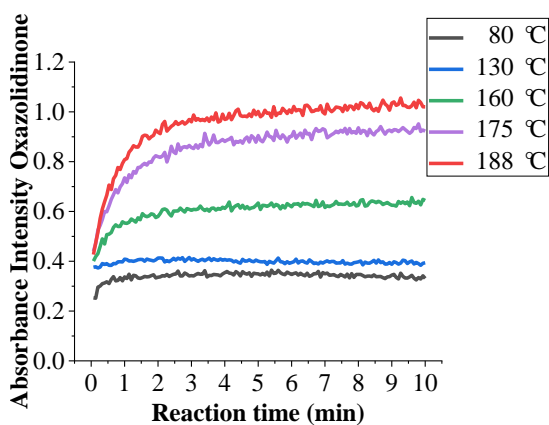


20-3(a)

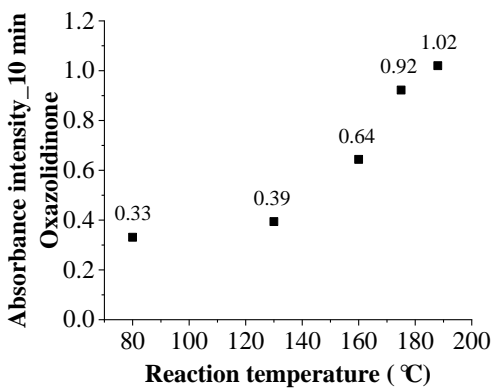


20-3(b)

Carbodiimide absorption at  $2113\text{ cm}^{-1}$

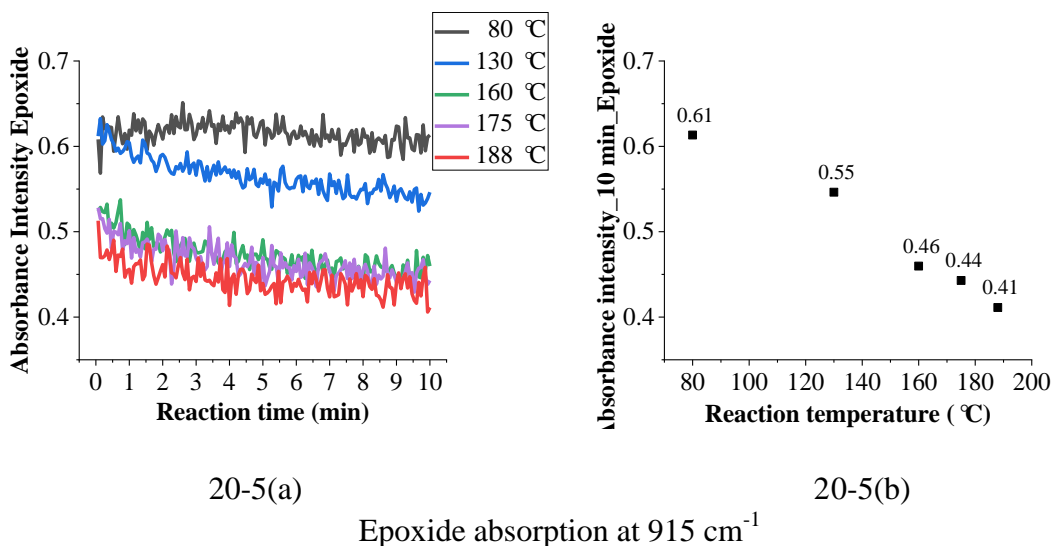


20-4(a)



20-4(b)

Oxazolidinone absorption at  $1758\text{ cm}^{-1}$



**Figure 20.** (a) Absorption intensity change with reaction time and temperature; (b) Absorption intensities after 10 minutes isothermal reaction at different temperatures

On one hand, the chemistry in the foam system thus shares some common features with the monofunctional system. These are:

- Isocyanurate formation starts at relatively low reaction temperatures of about 80 °C
- Carbodiimide and oxazolidinone formation is detected at temperatures over 130 °C and 160 °C, respectively, and their amounts increases with increasing reaction temperatures
- Most of the epoxide remains unreacted at 80 °C and shows high conversions at 160 °C.

On the other hand, the chemistry in the foam system exhibits some differences to the monofunctional system, especially in the isocyanurate decomposition reaction, oxazolidinone formation and the occurrence of carbodiimide based reactions. To further substantiate the differences, the corresponding monofunctional “Model” system was isothermally reacted under the same reaction conditions as the foam system and tracked with online FTIR. FTIR spectra were normalized using the

aromatic C-H stretching at  $3056\text{ cm}^{-1}$ . Two temperatures,  $80\text{ }^{\circ}\text{C}$  and  $160\text{ }^{\circ}\text{C}$ , were selected to monitor the reaction progress (Figure 21).

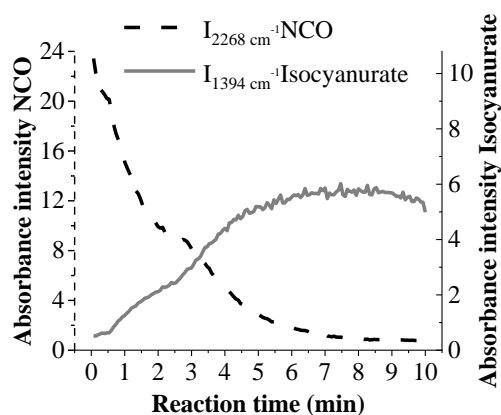
The amount of isocyanate in the “Model” system decreases steadily and is virtually zero after about 8 minutes at  $80\text{ }^{\circ}\text{C}$ . In the foam system, however, the isocyanate conversion starts to slow down after about 2 minutes because of vitrification. The isocyanate conversion only amounts to 62% after 10 minutes.

The isocyanate in the “Model” system is fully consumed after 1.5 minutes at  $160\text{ }^{\circ}\text{C}$ . At the same time, the isocyanurate concentration shows a maximum. The isocyanurate intensity then decreases with time and reaches a plateau value after about 5 minutes. The final isocyanurate intensity at  $160\text{ }^{\circ}\text{C}$  is lower than that at  $80\text{ }^{\circ}\text{C}$ , indicating that less isocyanurate is present in the final product at higher temperatures. This is consistent with the results of the  $^1\text{H}$  NMR study discussed in Chapter 3.1.5: Isocyanurate generated in the monofunctional system can be decomposed by epoxide at high temperatures yielding oxazolidinone. The oxazolidinone intensity in the monofunctional system keeps increasing with reaction time and reaches a maximum after 5 minutes. The isocyanate is fully consumed after 1.5 minutes of reaction, thus the oxazolidinone must be mainly formed in the reaction between isocyanurate and epoxide and/or the reaction between urethane and epoxide. This further indicates that isocyanurate is formed at a higher rate than oxazolidinone. The isocyanurate concentration builds up within the first minute in the foam system at  $160\text{ }^{\circ}\text{C}$ , after which it about stays constant. The higher absorption intensity at  $160\text{ }^{\circ}\text{C}$  (over a reaction at  $80\text{ }^{\circ}\text{C}$ ) suggests that isocyanurate had less chance to react with epoxide once generated. The early polyisocyanurate formation in the foam increases the crosslink density of the thermoset and with that the  $T_g$  increases to supersede the  $T_{\text{cure}}$  and the reaction grinds to a hold.

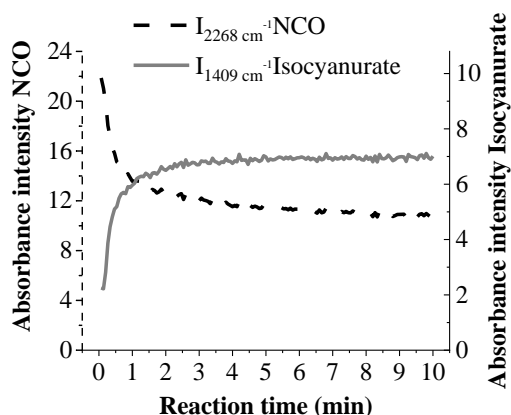
Oxazolidinone entities are formed within the first 2 minutes of reaction and then remains at a constant level. As there is still free isocyanate left when oxazolidinone formation is over, the oxazolidinone can originate from either of three reactions, i.e. be generated in the reaction between isocyanurate with epoxide, urethane with

epoxide or directly in the reaction between isocyanate and epoxide. In principle these reactions can proceed till vitrification sets in.

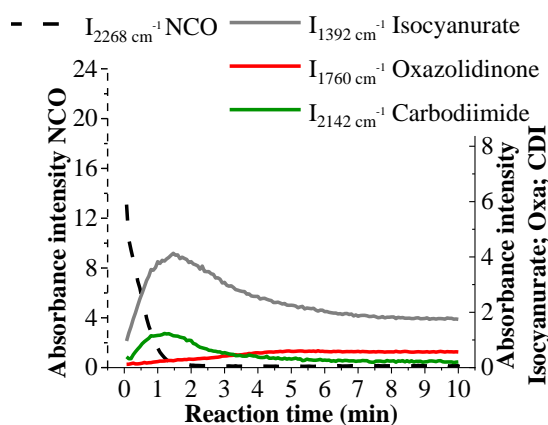
The vitrification in foam system has an impact on the carbodiimide reactions as well. In the monofunctional system, carbodiimide concentration first increases and later it is consumed. No carbodiimide is detected in the final products. However, the carbodiimide formed in the foam system has less chance to participate in consecutive reactions. After vitrification, the intensity only slightly decreases in the later stage of the reaction.



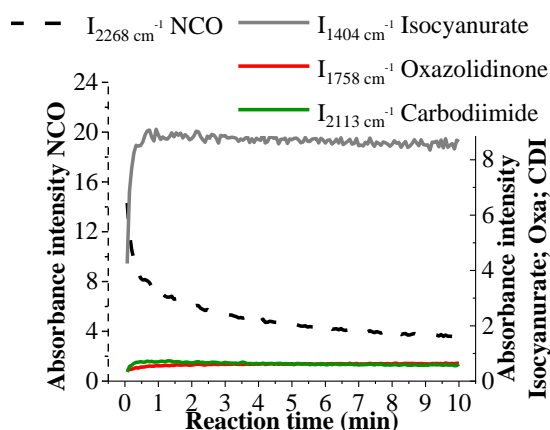
21-1 (a) “Model” system at 80 °C



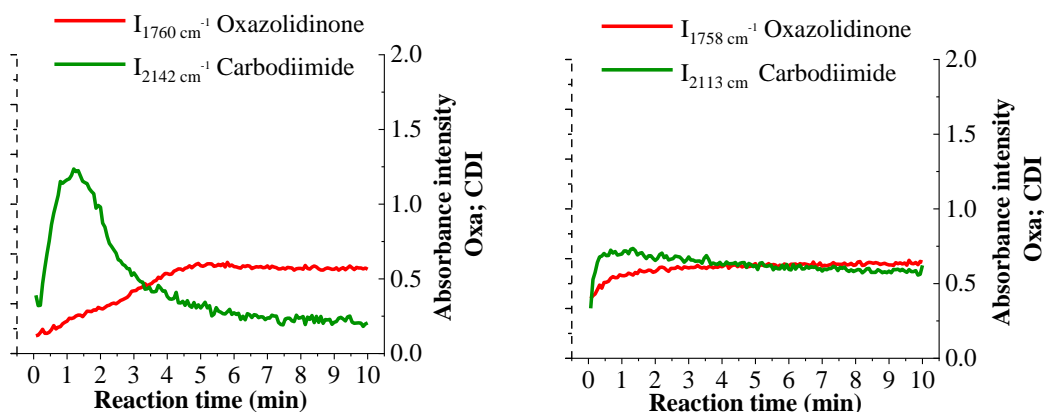
21-1(b) Foam system at 80 °C



21-2 (a) “Model” system at 160 °C



21-2 (b) Foam system at 160 °C



21-3 (a) “Model” system at 160 °C

21-3 (b) Foam system at 160 °C

(Enlargement of the oxazolidinone and carbodiimide intensity)

**Figure 21.** Absorption intensity changes with time in the “Model” and Foam systems

The present study at isothermal reaction conditions reveals relationships between the reaction temperature and time and the extent of conversion of the reactive groups in the foam and monofunctional systems. The work provides a basis to understand the curing process during foam production and post-cure treatment, which will be discussed in the next chapters.

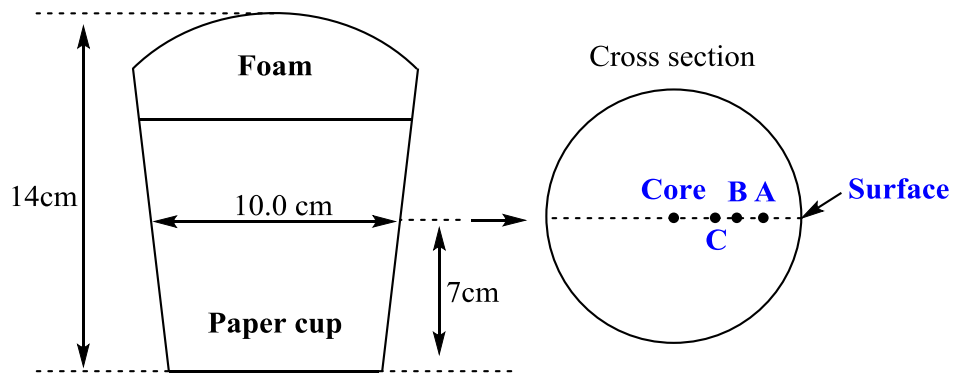
### 3.2.2 Free foaming reactions

Rigid foams were prepared in paper cups to simulate the open mold foaming process of industrial production. For the preparation of a cup foam, 50g of reactants were mixed in a 720 mL paper cup using an overhead stirrer. The foaming reaction starts as soon as the reactants are mixed. The average gelling time is 18 seconds and the foam shows a free rise density of  $28.5 \pm 0.22$  g/L. The reactions are self-accelerating by the temperature increase of the reactants, which is caused by the exothermic reaction. No external heating was applied.

The temperature development in the foam is a dynamic process which increases to a maximum temperature and then decreases again. Because rigid foams have thermal

insulating properties, a temperature gradient develops from the foam core to the foam surface. The foam material in the foam core is cured under pseudo-adiabatic conditions whereas the foam material at the surface will exchange heat with the environment. Consequently, the maximum temperature ( $T_{\max}$ ) measured in the core of the foam is higher than that at the surface.

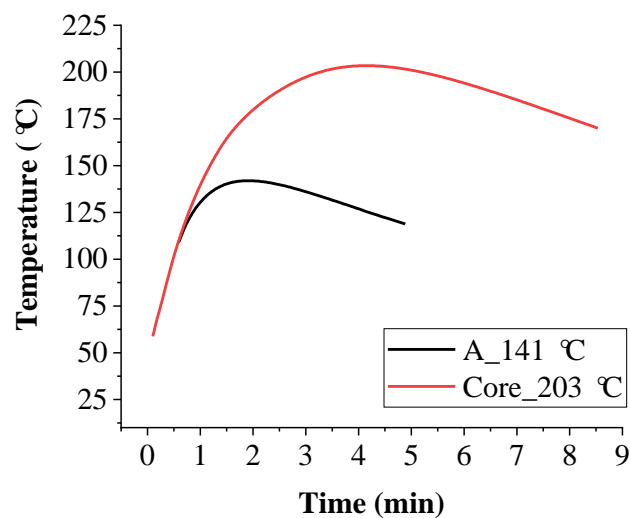
The temperature profiles were recorded at different depths along the radial axis of the cross section at the half-height of the final foam using a K type thermocouple (Figure 22; Table 29). The higher maximum temperature in the core of the foam is also accompanied by a longer residence time at high temperatures before the foam finally cools down (Figure 23).



**Figure 22.** Dimensions of cup foams and measuring positions of temperature profiles

**Table 29.** Measuring positions and corresponding maximum temperatures

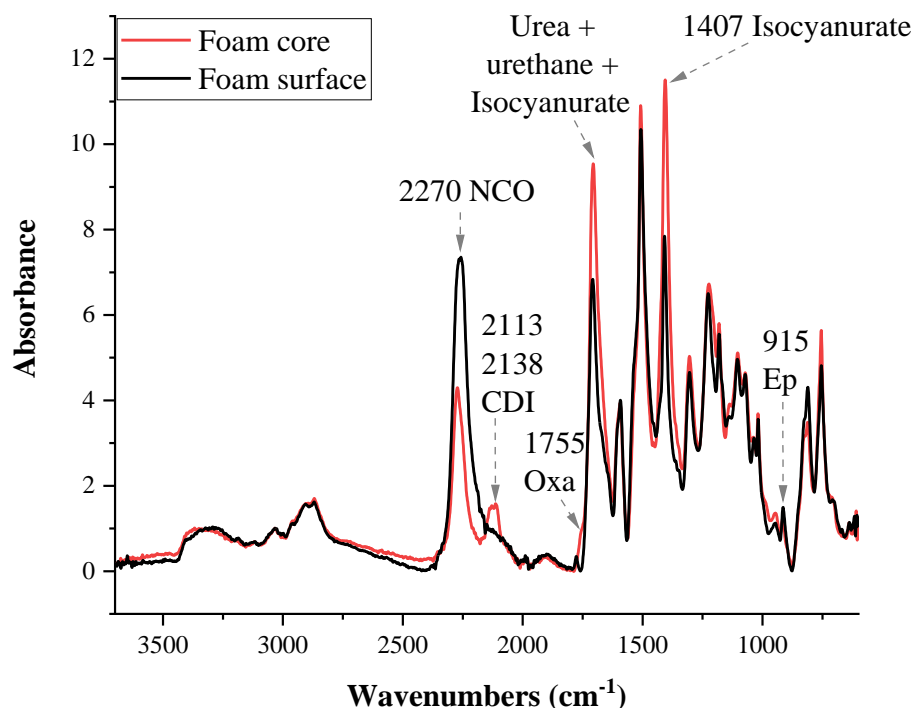
Mark in Figure 22	Position (radial depth from surface, in the middle cross section, cm )	$T_{\max}$ ( °C )
A	1.8	141
B	2.5	159
C	3.6	182
Core	5.0	203



**Figure 23.** Temperature developments in position A (black) and foam core (red)

Samples from the above positions together with a sample from the surface were measured by offline ATR-IR after the foam had cooled down to room temperature. FTIR spectra were normalized on the aromatic C-H stretch at  $3035\text{ cm}^{-1}$ . The absorbance of the N=C=O stretching frequency at  $2270\text{ cm}^{-1}$  was used to calculate the isocyanate conversion, the method being described in Experimental part. The intensities of the carbodiimide absorption at  $2113\text{ cm}^{-1}$ , isocyanurate absorption at  $1407\text{ cm}^{-1}$ , oxazolidinone absorption at  $1755\text{ cm}^{-1}$  and epoxide absorption at  $915\text{ cm}^{-1}$  were used to study the changes in the respective chemical bonds in a semi-quantitative manner. The relative amounts of urea and urethane again were not quantified.





**Figure 24.** ATR-IR spectra taken from the foam surface and the foam core

FTIR data show that full isocyanate conversion is not achieved, not even in the foam core. No carbodiimide or oxazolidinone is detected in the foam surface (Figure 24). The intensity changes at the various maximum temperatures show a similar trend as in the isothermal reactions discussed in Chapter 3.2.1. The intensities of isocyanate and epoxide decrease while the intensities of isocyanurate, carbodiimide and oxazolidinone increase from the foam surface to the foam core and hence with increasing values of  $T_{\max}$  (Figure 25). The strongest changes occur in the foam layer from the surface to 1.8 cm beneath it (position A). This region will be referred to as the “near surface region” in this chapter. The maximum temperature at position A is 141 °C. Carbodiimide and oxazolidinone formation starts at about position A and further intensifies when approaching the foam core.  $T_{\max}$  increases from 141 °C to 203 °C from position A to the foam core, however, the corresponding intensity changes are not as distinct as in the “near surface region”. The results clearly show that the “near surface region” exhibits a much lower extent of reaction than the inner

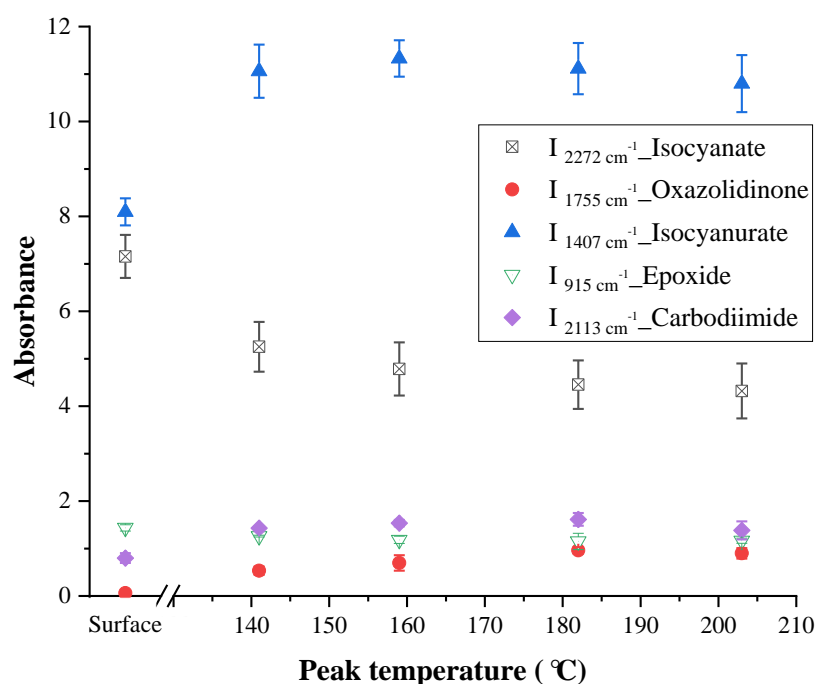
core of the foam. The poor conversion near the surface may cause the formation of a layer with poor mechanical properties such as increased friability, low compressive and adhesive strengths.

The isocyanate conversions at the different positions in the foam were calculated from IR spectroscopic data (Table 30). A DMA trace taken from the foam core (Figure 26) shows that the  $\tan \delta$  starts to increase whereas  $G'$  decreases at about 230 °C. This indicates that the system  $T_g$  is about 230 °C. As full curing is not achieved in the foam core, the  $T_{g \infty}$  of the fully cured system is expected to be even higher than 230 °C. The reaction temperature in the foam surface is far below this temperature and hence the system vitrifies early and only an isocyanate conversion of 66% is obtained. The isocyanate conversion increases to 75% at position A (1.8 cm below the surface) where  $T_{max}$  reached 141 °C. From position A to the foam core the increase in conversion is only modest (to 80%) although a significantly higher  $T_{max}$  (203 °C) has been reached. The same trend is observed for the isocyanurate formation. This indicates that the polyisocyanurate amount at 1.8cm beneath the surface already leads to a system  $T_g$  that is high enough to cause a limited chain mobility.

The epoxide conversion was measured by extracting the unreacted epoxide using a Soxhlet extractor. The sample size was about 10 grams. Because a relatively large amount of sample is needed to allow accurate weighing of the extract, the epoxide conversion cannot be determined at the various positions in the foam. Instead, the average epoxide conversion of the entire foam was determined. Bifunctional epoxide was used in the foam formulation. If one of the two epoxide functional groups reacts, the entire molecule is immobilized and will not be extracted anymore. A conversion of the epoxy functional group is then difficult to derive. This problem was circumvented by preparing foams using equivalent amounts of a mono-functional epoxide (glycidyl 2-methylphenyl ether). Note that the incorporation of mono-functional epoxide changes the polymer network topology and the  $T_{g \infty}$  of the polymer may be reduced.

The extractions show that a large portion of epoxide remains unreacted (Table 30).

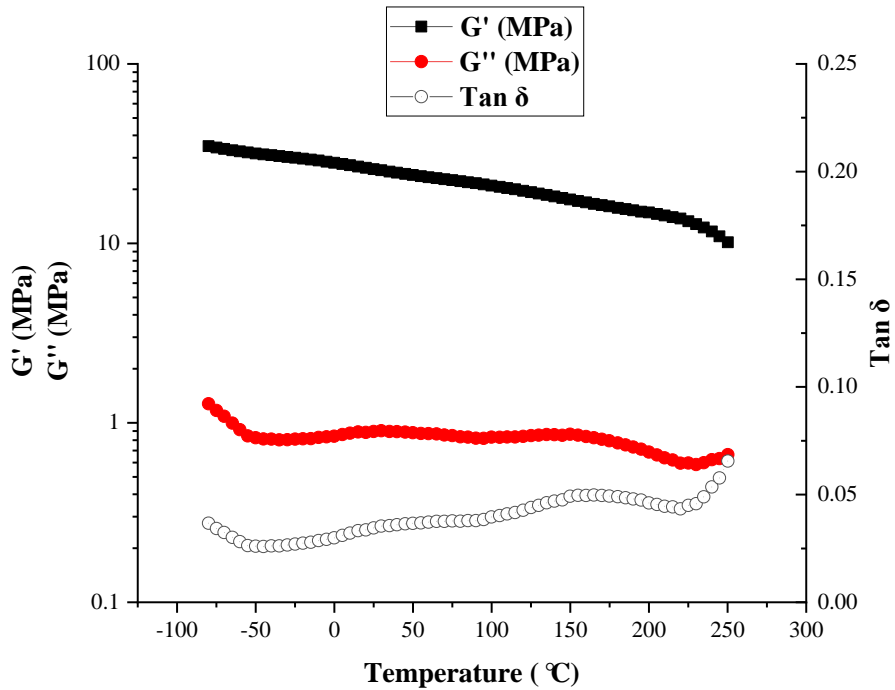
When monofunctional epoxide was used, 81 % of the epoxide could be extracted indicating the highest epoxide conversion that can be achieved in the small cup foam amounts to only 19%. The result of the isothermal cure in Chapter 3.2.1 suggests that the epoxide has a low tendency to react at low temperatures, hence it can be expected that the amount of unreacted epoxide is high in the near surface area where the temperature is lower.



**Figure 25.** Change in absorption intensities as a function of  $T_{\max}$

**Table 30.** Isocyanate conversions at different foam positions

Mark in Figure 22	Position (radial depth from surface, cm )	$T_{\max}$ ( $^{\circ}\text{C}$ )	NCO conversion (%)	Epoxy extracted (%)	
				mono Ep	bi Ep
Surface	0	-	$66 \pm 2$	81	59
A	1.8	141 $^{\circ}\text{C}$	$75 \pm 3$		
B	2.5	159 $^{\circ}\text{C}$	$77 \pm 3$		
C	3.6	182 $^{\circ}\text{C}$	$79 \pm 2$		
Core	5.0	203 $^{\circ}\text{C}$	$80 \pm 3$		



**Figure 26.** DMA of a sample taken from the foam core

The rate of cooling during the preparation of a cup foam is relatively high because of the high surface to volume ratio. The  $T_{\max}$  achieved in the core of the foam may not have reached the full potential of the industrial process. The time the foam remains at

high temperatures is also relatively short. Furthermore, the foam exhibits a high system  $T_g$ , higher than the achieved  $T_{max}$ . The combination of these factors might have contributed to the relatively poor conversion of the foam matrix material.

The time-temperature- $T_g$  issues will be further amplified in the foam layer near the surface, resulting in yet lower conversions. External heat supply can alleviate the cure deficiencies. The most convenient way to supply heat into the system is to put the cup in an oven. The temperature for effective post cure should ideally be above the  $T_{g\infty}$  of the polymer. However, in a high  $T_{g\infty}$  system like the present foam, tempering of the foam above  $T_{g\infty}$  may lead to polymer decomposition. DMA analysis reveals that the prospective fully cured foam system exhibits a  $T_{g\infty}$  above 230 °C, while a TGA measurement recorded at a heating rate of 10 °C/min under  $N_2$  atmosphere shows that the polymer decomposition starts at about 250 °C (TGA trace shown in the Experimental Part). A heat treatment of the foam at a temperature above  $T_{g\infty}$  would result in foam degradation and therefore tempering was carried out at temperatures below  $T_{g\infty}$ .

### **3.2.3 Post cure of foams**

The isothermal foam reactions discussed in Chapter 3.2.1 gives evidence that the reactions proceeds slowly in the vitrified state. The influence of a post cure temperature and duration on the overall conversion and formation of chemical bonds will be discussed in this chapter. The cup foams, prepared as described in Chapter 3.2.2, were used for the present post cure study. Two temperatures, viz. 100 °C and 200 °C, were selected to study the post cure behavior. Freshly prepared cup foams were transferred into a preheated oven immediately after their preparation, i.e. after about 5 minutes of reaction. The changes in the amount of isocyanate, epoxide, isocyanurate, carbodiimide and oxazolidinone with post-cure time were tracked by taking the foams out of oven at set times. Small sample amounts from both the foam surface and the foam core were taken and submitted to ATR-FTIR analysis. Peak intensity normalization and determination of the isocyanate conversion were carried

out as before.

Increased post-cure temperatures lead to higher reactant conversions (Figure 27). The system reactions proceed with time whereby the most significant changes happen within the first 2 hours of tempering at both curing temperatures. The isocyanate conversion increases from 65% to 93% at the foam surface and from 80% to 89% in the foam core after a post cure of 2 hours at 200 °C. Strong oxidative degradation of the foam surface occurred after 24 hours at that temperature. These data were not considered in the curing analysis. Isocyanate conversion reaches 96% in the foam surface after 6 hours and the same conversion is reached in the foam core after 24 hours. A better heat transfer on the surface and a possible reaction with water from the atmosphere could explain these results. The isocyanate conversion also increases when post-curing is carried out at 100 °C, but the final conversion remains lower than at 200 °C. The isocyanate conversion in the foam core reaches 85% after 2 hours at 100 °C and then stays a constant, while the isocyanate conversion at the foam surface reaches 86% after 24 hours.

The epoxide conversion shows a similar temperature and time dependency as the isocyanate conversion. The epoxide intensity decreases readily within the first 2 hours at a post-cure temperature of 200 °C. No epoxide could be extracted from the foam surface material after 6 hours of tempering and the same was found for the foam core after 24 hours, indicating that the epoxide had fully reacted. Extended heating at 100 °C proves to be too low a temperature for the epoxide reaction and full epoxide conversion is not achieved after 24 hours. The epoxide reaction in the present post cure studies shows a similar behavior to that observed for the monofunctional systems and the isothermal foaming reactions.

Isocyanurate formation is different at the core and the surface when post-curing at 200 °C. The isocyanurate concentration at the surface first increases corresponding to the increase in isocyanate conversion, and then decreases again. It is shown in the previously studied monofunctional system that the isocyanurate can be decomposed by epoxide to form oxazolidinone. The isocyanurate transformation rate appears faster

than its formation rate in the foam core where the isocyanate conversion is already high. Post-curing at 100 °C shows the same trend as at 200 °C but the changes are smaller.

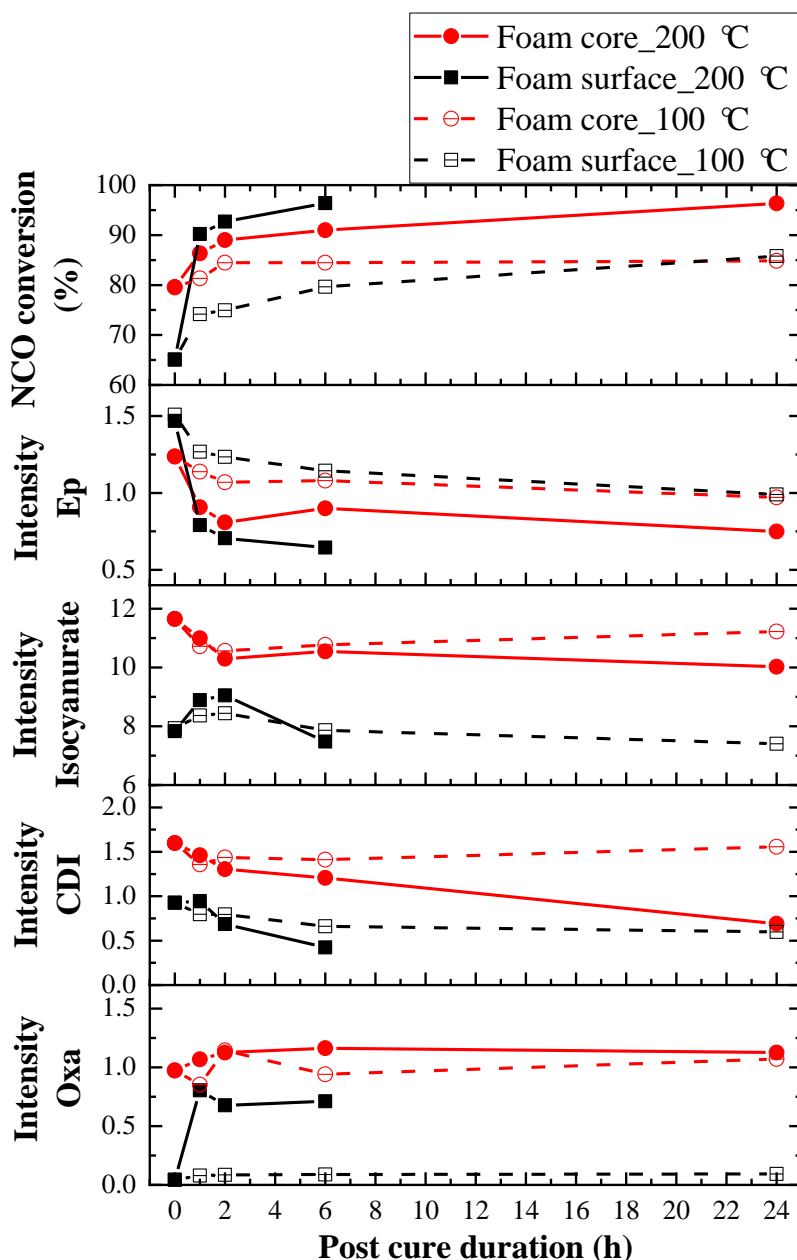
The oxazolidinone amount increases both in the surface layer and in the foam core at 200 °C. The oxazolidinone intensity shows a stronger increase at the surface than in the foam core as there is more unreacted epoxide in the near surface area. The isocyanurate amount decreases while oxazolidinone increases, suggesting that during post cure, the reaction of isocyanurate with epoxide is one of the possible pathways to form oxazolidinone. Note that its formation by reactions between urethane or isocyanate with epoxide cannot be ruled out. As discussed above, the epoxide is fully reacted at the foam surface after 6 hours at 200 °C and in the foam core after 24 hours of tempering. However, the oxazolidinone intensity at the foam surface is unexpectedly lower than that in the foam core. This could indicate that some of the epoxide participates in other reactions like the ring open reaction by urethane or a homopolymerization reaction whereby polyether linkages would be formed. The formation of polyether from the epoxide could not be secured as the IR signal is too similar to other compounds in the system; in particular, the polyether glycol also has the ether related vibration at 1100 cm<sup>-1</sup>. The post cure temperature of 100 °C is too low for oxazolidinone formation - the oxazolidinone content only shows a minor increase in the foam core and on the foam surface after prolonged heating. This corresponds with a minimal change in the epoxide intensity.

Tracking the carbodiimide peak is not so straightforward as the intensity of its signal is partially overlapping with the adsorption of the isocyanate peak at 2270 cm<sup>-1</sup>. This is especially true when the intensity of the isocyanate peak is strong. The higher intensity on the foam surface at the starting point of the post cure is caused by the strong isocyanate absorption. The characteristic double peak stretching of the carbodiimide is not present. The carbodiimide forming rate in the foam core appears to be lower than its consumption rate. In the foam core, a higher amount of carbodiimide and a lower amount of free isocyanate already exists prior to post cure.

A decrease in carbodiimide intensity is observed. A post-curing temperature of 100 °C is too low a temperature for the carbodiimide reactions to take place and only minimal intensity changes are observed.

The results of the post-curing experiments show that when the post curing temperature is sufficiently below  $T_{g\infty}$  of the polymer system, like in the present case at 100 °C, reactions proceeds slowly and full conversion of the reactive groups cannot be obtained within 24h. Besides this, a certain temperature is required for the oxazolidinone and carbodiimide reactions to take place. These reactions do not occur at 100 °C. Temperatures of at least 130 °C are required for an observable rate. When the post cure is carried out somewhat below  $T_{g\infty}$  - in the present study 200 °C - nearly full reactant conversions and a high extent of chemical bond formation could be obtained with prolonged heating times. Most of the post-curing already proceeds within the first few hours. It should be mentioned that high post-curing temperatures cause polymer degradation. High temperatures and long heating times should be avoided.





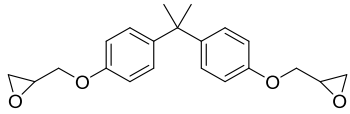
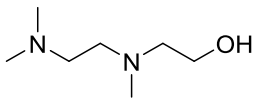
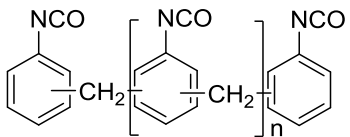
**Figure 27.** Isocyanate conversion and FTIR intensity changes of epoxide, isocyanurate, carbodiimide and oxazolidinone during post cure

### 3.2.4 PUR/PIR foam chemistry and the effect of epoxide modification

In this thesis, epoxide was incorporated into a conventional PUR/PIR foam recipe for system modification. The monofunctional systems have been discussed in Chapter 3.1.4, whereas in this chapter the two model systems of Table 31 were used to further study the influence of epoxide in the foam chemistry. In these two model systems, the same equivalent amounts of reactants were used except that in the “Add Ep” system,

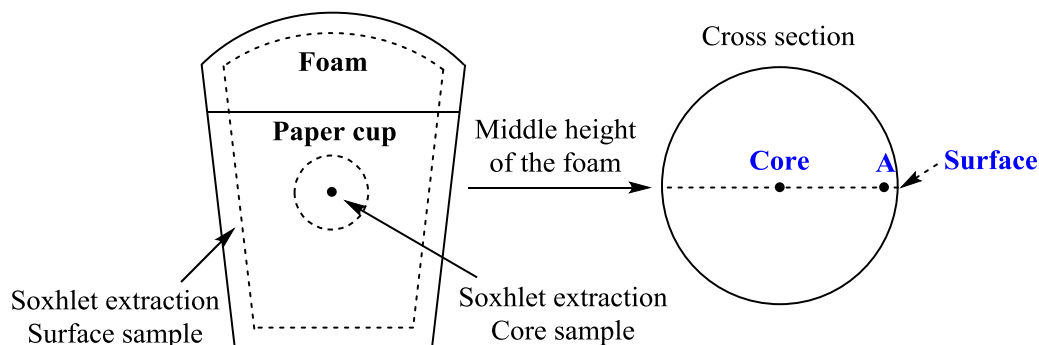
0.5 equivalent of bisphenol A diglycidyl ether was added (“on top”).

**Table 31.** Formulations of “PUR/PIR” and “Add Ep” systems

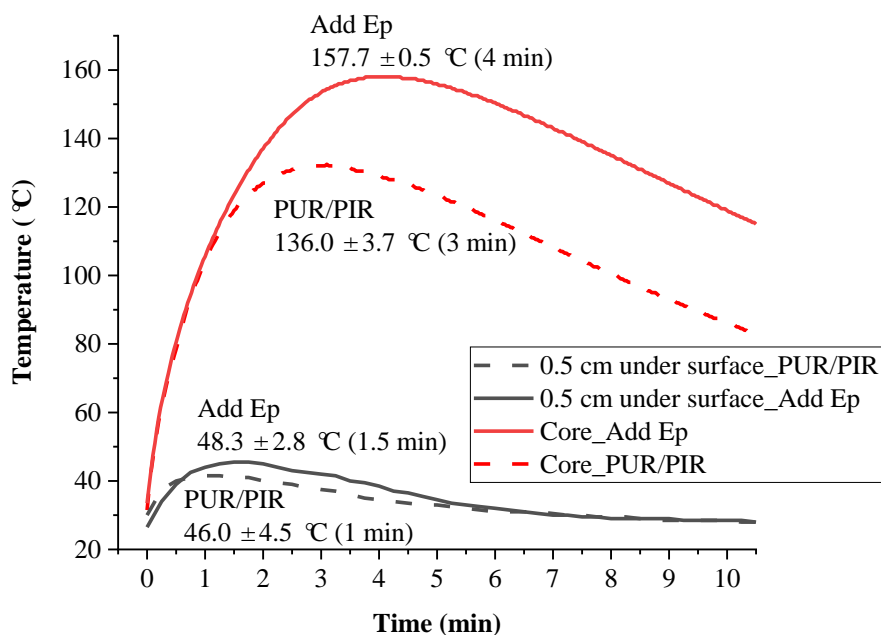
	Reactant	Structure	Equivalent PUR/PIR	Equivalent Add Ep
<b>Component A</b>	Bisphenol A diglycidyl ether		-	<b>0.5</b>
	PEG 600	$\text{H} \left[ \text{O} \text{---} \text{CH}_2 \text{---} \text{CH}_2 \right]_n \text{OH}$	0.5	0.5
	Water	$\text{H} \text{---} \text{O} \text{---} \text{H}$	1.0	1.0
	DABCO <sup>®</sup> T		0.0375	0.0375
<b>Component B</b>	Lupranat <sup>®</sup> M20R		3.0	3.0

Foams of 50g were prepared in paper cups as described in Chapter 3.2.2. The temperature development during foaming was recorded in the foam core and at 0.5 cm beneath the foam surface (core and position A in Figure 28) using a Type K thermocouple. When epoxide is added “on top”, the maximum temperature of the foam core is about 20 °C higher than in the “PUR/PIR” system (Figure 29). The higher maximum temperature also results in a longer cooling time and the foam stays at high temperatures for a longer period. One of the conclusions previously drawn from the studies on the monofunctional system is that the epoxide promotes isocyanurate formation. This reaction is known to be strongly exothermic and increases the system reaction temperature. The temperature difference measured in these two systems at 0.5 cm beneath the foam surface, however, only amounts to 2 °C. This is ascribed to cooling effects of the foam surface by the surrounding air that quenches further

reactions, notably those that take place at higher temperatures.



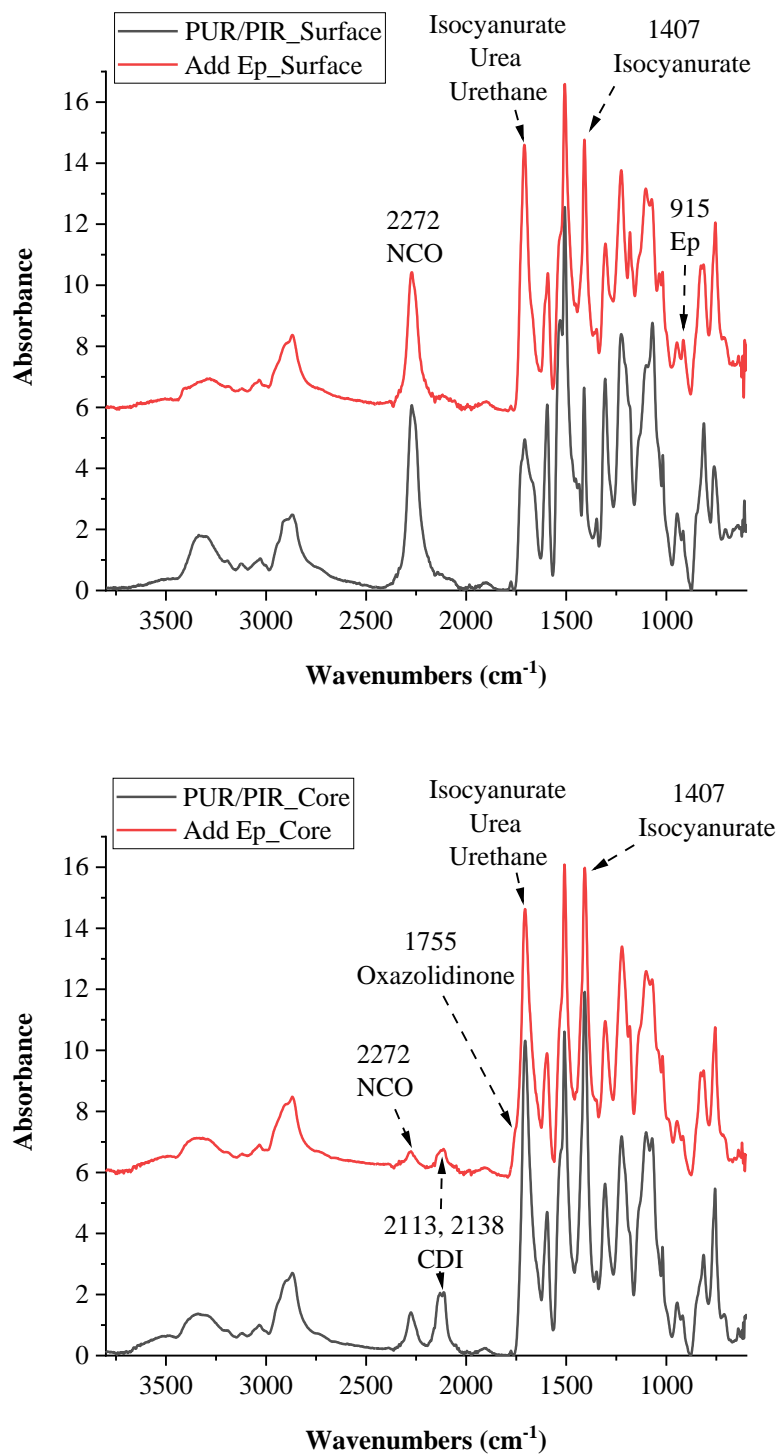
**Figure 28.** Positions for the temperature profile measurements and samples cut for the soxhlet extraction



**Figure 29.** Temperature profiles of the “PUR/PIR” and “Add Ep” systems, determined in the Core and at 0.5 cm beneath the surface (position A in Figure 28)

The epoxide conversion was determined by Soxhlet extraction using dichloromethane as solvent. The sample size was about 10 g. Samples for Soxhlet extraction were taken from the foam surface layer with a thickness of about 1 cm and from the core of the foam (Figure 28). Changes in chemical entities were again by ATR-FTIR spectroscopy; spectra were normalized like before (Figure 30). Samples were taken

from the core and 0.5 cm beneath the foam surface. To compare the formation of the various linkages in two different recipes, the measured absorption intensities were divided by the initial NCO intensity of the corresponding recipe (Table 32).



**Figure 30.** FTIR spectra of “PUR/PIR” and “Add Ep” systems; up: 0.5 cm beneath the surface; below: foam core

**Table 32.** Reactant conversions and amounts of chemical linkages formation in “PUR/PIR” and “Add Ep” systems

	Foam surface		Foam core	
	PUR/PIR	Add Ep	PUR/PIR	Add Ep
<b>NCO conversion</b>	81 ± 2 %	86 ± 1 %	95 ± 1 %	97 ± 0 %
<b>Reacted Ep (Soxhlet extraction)</b>	/	20 %	/	99 %
<b>Isocyanurate intensity / Initial NCO intensity</b>	0.21 ± 0.01	0.28 ± 0.03	0.37 ± 0.01	0.32 ± 0.01
<b>Carbodiimide intensity / Initial NCO intensity</b>	0	0	0.063 ± 0.004	0.027 ± 0.003
<b>Oxazolidinone intensity</b>	/	0	/	0.042 ± 0.003

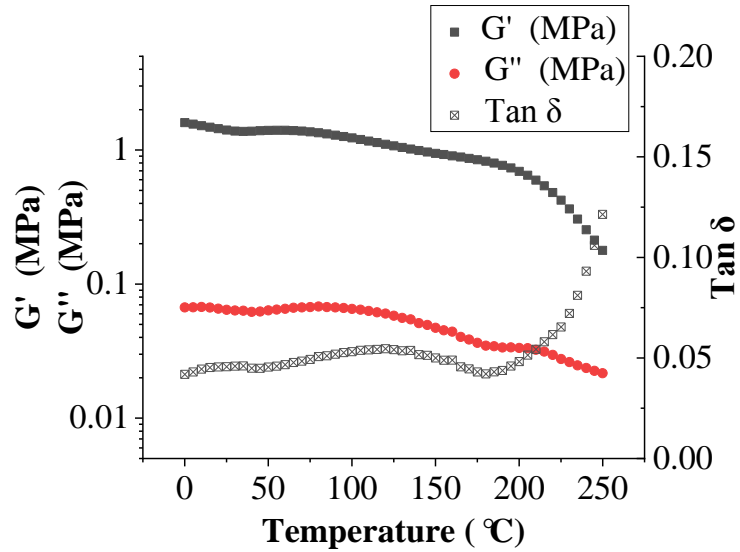
The IR spectra indicate that samples from the near surface area of “PUR/PIR” and “Add Ep” foams show the same absorptions except for the epoxide stretch vibration that shows up at 915 cm<sup>-1</sup> in the “Add Ep” system (Figure 30(a)). This indicates a similar chemical composition in two systems in the near surface area. The isocyanate stretching vibration is clearly observable in both systems. It indicates an incomplete isocyanate conversion. Isocyanurate is detected at 1407 cm<sup>-1</sup> and no carbodiimide or oxazolidinone is formed. The absorption intensities of isocyanate and isocyanurate in the near surface area are different in two systems. The isocyanate conversion increases from 81% to 86% in the presence of epoxide and the value of “Isocyanurate intensity / Initial NCO intensity” increases from 0.21 to 0.28, suggesting a higher isocyanurate concentration. A temperature effect is unlikely to be the cause of the differences, as the temperature profiles of the two systems are quite similar in the near surface area. The presence of the epoxide must be the prime reason. Soxhlet extraction shows, however, that 80 % of the epoxide in the near surface area does not

react in the “Add Ep” system. This agrees with the results obtained for the monofunctional system as discussed in Chapter 3.1.4. Evidence was found in the monofunctional system that a small portion of epoxide reacts with the tertiary amine catalyst DABCO<sup>®</sup> T to generate an alkoxide, which is more effective catalyst for isocyanurate formation

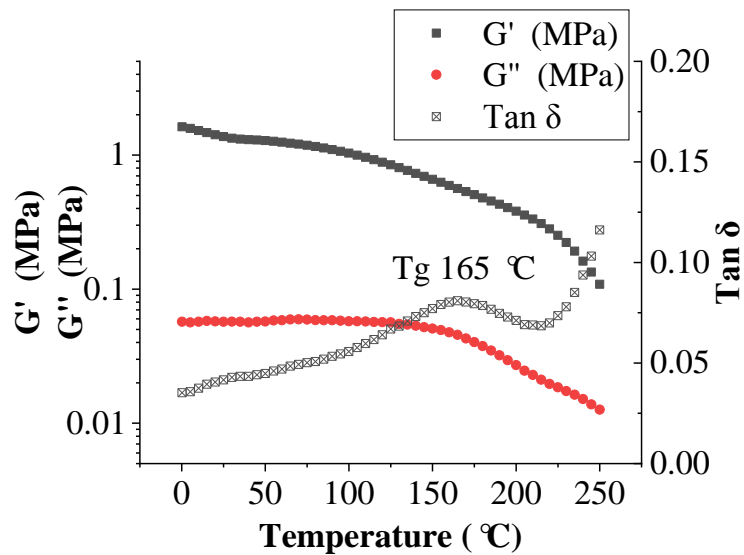
Isocyanate and carbodiimide are detected in the foam of both systems (Figure 30(b)). The high reaction temperatures in the foam core allow the isocyanate conversion to reach 95% even without the addition of epoxide. The higher peak temperature in the “Add Ep” system further promotes the isocyanate and carbodiimide reactions and oxazolidinone is formed. Most of the epoxide has reacted. The epoxide stretch at  $915\text{ cm}^{-1}$  almost disappears from the spectra and only 1% of epoxide can be extracted from the foam. Less isocyanurate is found in the foam core of “Add Ep” than “PUR/PIR”. The value of “Isocyanurate intensity / Initial NCO intensity” decreases from 0.37 to 0.32 when epoxide is present. It must be concluded that this decrease is caused by epoxide related reactions. These reactions include oxazolidinone formation and potential epoxide ring opening reactions, i.e., urethane-epoxide addition reactions and epoxide homopolymerization reactions. The hydroxyl groups generated by epoxide ring opening reactions can react with isocyanate and compete with the isocyanurate formation reaction. The formation of oxazolidinone is evident from the presence of the IR vibration at  $1755\text{ cm}^{-1}$ . Urethane-epoxide addition reactions as observed in the monofunctional model reactions can also occur in the foam system. Besides, the formation of epoxide homopolymerization products cannot be excluded. A lower system Tg is expected as less isocyanurate is detected in the foam core of the “Add Ep” system.

Additional experiments with surfactant were carried out with both systems. 2 wt% Niax Silicone L-6900, a silicone copolymer surfactant was added to obtain foams with a fine and uniform cell structure. The homogeneous polymer foams so obtained allowed the cutting and preparation of testing bars for DMA (Figure 31). Samples were taken from the foam core. No obvious Tg is observed until  $225\text{ }^{\circ}\text{C}$  in the

“PUR/PIR” system, however, in the “Add Ep” system, a secondary transition associated with a polymer softening is observed at about 165 °C. The secondary transition is presumed to go along with a higher chain mobility in this temperature region. Thus, the addition of epoxide not only changes the chemical reaction pathways, its presence also increases the chain mobility of the growing polymer network leading to higher conversions.



(a)



(b)

**Figure 31.** DMA traces of samples taken from the core of the foam: (a) “PUR/PIR” system and (b) “Add Ep” system

In summary, the results of the “PUR/PIR” and “Add Ep” foam systems are much in line with the conclusions obtained on the corresponding monofunctional systems described in Chapter 3.1.4. In the foam surface, over 80% of epoxide remains unreacted but some of the reacted epoxide acts as a co-catalyst promoting the isocyanate conversion and isocyanurate formation. In the foam core where temperature is sufficient to have high isocyanate conversions even without epoxide, oxazolidinone is formed when epoxide is present. The epoxide improves the chain mobility of the polymer matrix material in the foam core, which might have assisted in achieving higher conversions.

### **Summary of and conclusions on the foam system**

The results show that the chemistry in the foam systems reminiscent of the corresponding monofunctional systems. The isocyanurate formation starts already at relatively low reaction temperatures while oxazolidinone and carbodiimide formation only can take place above 130 °C. The majority of epoxide remains unreacted at low temperatures such as 80 °C and approaches nearly full conversion at temperatures above 160 °C. The low chain mobility in the foams after system vitrification has a major impact on the reactant conversion. When the system T<sub>g</sub> exceeds the curing temperature, complete conversion cannot be achieved as the reaction seizes upon vitrification. Reactions that take place at the later stages in the monofunctional reaction system, like the reaction of isocyanurate with epoxide to form oxazolidinone and carbodiimide consecutive reactions, are less obvious in the foam system because of vitrification and short time exposure to high temperatures.

The low reactant conversions in the foam, especially in the near surface area will reduce material strength. Post-curing at temperatures of about 200 °C effectively increases the isocyanate and epoxide conversions. The most significant changes happen within the first few hours of post cure. System modification with epoxide also improves the conversion of isocyanate into isocyanurate. This is especially beneficial for the near surface area of the foam where the reaction temperature is relatively low and poor isocyanate conversions are obtained. In the core of the foam where already



high reaction temperatures are achieved, the addition of epoxide further increases the temperature resulting in higher isocyanate conversions and formation of oxazolidinone.

## 4. Experimental part

### 4.1 Chemicals and reaction setup

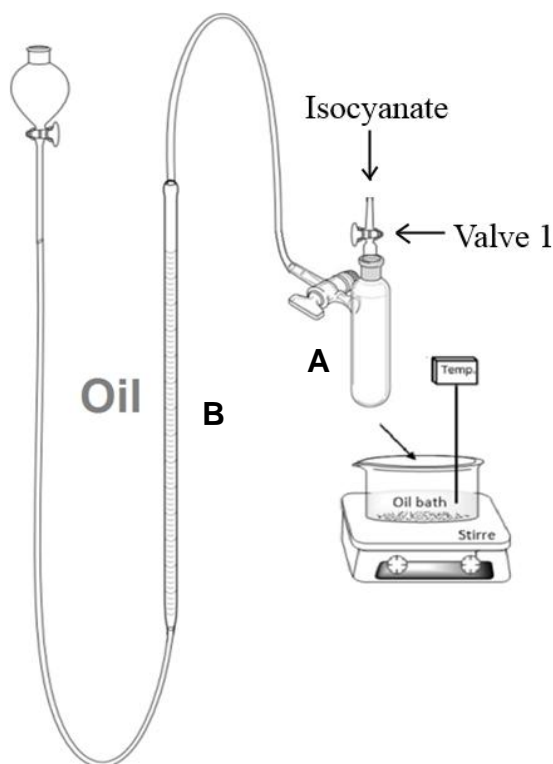
#### Chemicals

Glycidyl 2-methylphenyl ether (Grilonit<sup>®</sup> RV 1805, EMS-GRILTECH) was distilled under reduced pressure and dried over activated 4Å molecular sieves. 1-Octanol (99%, Grüssing GmbH), 2,6-dimethylaniline (99%, Sigma Aldrich), *N,N,N'*-trimethylaminoethyl ethanolamine (DABCO<sup>®</sup> T, Evonic), 2-(2-(dimethylamino) ethoxy)ethanol (provided by BASF Polyurethanes GmbH), 6-dimethylamino-1-hexanol (97%, TCI), 2-dimethylaminoethanol (provided by BASF Polyurethanes GmbH), 1-(Bis(3-(dimethylamino)propyl)amino)propan-2-ol (provided by BASF Polyurethanes GmbH), *N,N,N',N'*-Tetramethylethylenediamine (99%, SIAL), tetraethylene glycol dimethyl ether (99%, Sigma Aldrich) and triethylene glycol dimethyl ether (for synthesis, Merck) were dried over activated 4Å molecular sieves prior to use. Polyethylene glycol dimethyl ether (Mn=1000, Sigma Aldrich) was dried at 80 °C using vacuum and stored under nitrogen protection. 1-Naphthyl isocyanate (99%, Acros Organics) was stored at 4 °C under argon protection and warmed up to room temperature before the experiment. Other reagents were used as received, which includes 1-Naphthyl amine (99%, Merck), formic acid (98%, VWR), diethyl amine (99.5%, Sigma Aldrich), 3-methyl-1-phenyl-2-phospholene 1-oxide (provided by BASF Polyurethanes GmbH), Lupranat<sup>®</sup> M 20 R (PMDI, average functionality 2.7, BASF Polyurethanes GmbH), polyethylene glycol 600 (potassium free, provided by BASF Polyurethanes GmbH), diethyl methyl benzene diamine (provided by BASF Polyurethanes GmbH), bisphenol A diglycidyl ether (epoxide equivalent weight 172-176, Sigma Aldrich), Niax Silicone L-6900 (Momentive Performance Materials), dichloromethane (technical grade, Grüssing GmbH), ethyl acetate (technical grade, VWR), petroleum ether 50-70 (technical grade, VWR), acetonitrile (HPLC grade, VWR), acetone (technical grade, VWR), Kieselgel 60 (silica gel 60, Merck) and Aluminum oxide (Merck). Deionized water was used for

the reactions, while ultrapure water was used for the HPLC analysis.

### **Reaction setup**

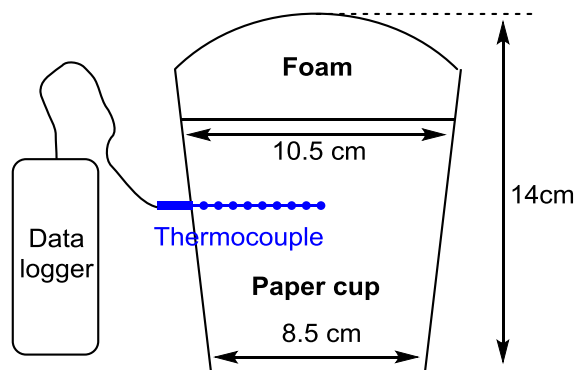
Monofunctional reaction systems: the setup for the monofunctional reaction systems is shown in Figure 32. A 25 mL Schlenk tube (A) with magnetic stirrer was used as the reaction vessel. A gas burette (B) filled with oil was connected to the Schlenk tube. The volume of gas generated during the reaction was measured with the gas burette and the total amount of carbodiimide produced was calculated. Prior to conducting the reaction, the Schlenk tube was purged with nitrogen before getting connected to the gas burette and the oil bath was pre-heated to the desired temperature. The reactions were carried out with a reactant amount of 2 grams to minimize the temperature difference between the heating oil and the reaction system. The Component A which contained all the reagents except the isocyanate was premixed and the required amount was injected in the Schlenk tube through Valve 1. The injections were performed with syringes and the “weighing by difference” method was applied. The A-component was stirred at room temperature and the pre-weighed Component B, viz. 1-naphthyl isocyanate, was quickly injected into the Schlenk tube. In order to add the isocyanate quickly and accurately, the syringe was first flushed with the isocyanate and then the theoretical required amount was taken up into the syringe. It was demonstrated that the flushing could compensate for the weight loss caused by the residue left in the syringe and in this manner the isocyanate could be added within a few seconds with a weight deviation of less than 1%. After the isocyanate injection, Valve 1 was closed and the Schlenk tube was put immediately into the pre-heated oil bath. After 10 minutes of reaction, the Schlenk tube was cooled to room temperature. The volume of gas generated during the reaction was determined after having adjusted the internal pressure in the vessel to atmospheric pressure. Subsequently the reaction product was analyzed. In the reactions where the system temperature was recorded, the reaction procedure in principle remained the same with the difference that the gas burette was removed and a type K thermocouple inserted.



**Figure 32.** Reaction setup for the monofunctional reaction systems

Foam systems: The foams were prepared in 720 mL paper cups with a reactant amount of 50 grams. Component A containing all the reagents except the isocyanate was premixed shortly before the foaming reaction. The paper cup was placed on a balance and the corresponding amount of Component A was weighed into the cup. Subsequently, the pre-weighed amount of isocyanate was added. Then the reactants were mixed using an IKA mechanical overhead stirrer equipped with a dispersing disc. For the isothermal reactions monitored with online ATR-IR, the reactants were mixed for 5 seconds at a speed of 1500 rpm and subsequently a small aliquot of the mixture was put on the pre-heated sample cell. For the preparation of the cup foams, the reactants were mixed for 3 seconds at 1500 rpm upon which the foam expansion started. The temperature development in the foam was measured using a type K thermocouple with a Lascar EL-USB-TC-LCD temperature data logger. The thermocouple was pre-positioned at the desired location prior to foaming - see for instance Figure 33 as an example. The cup foams were further analyzed after having cooled down to room temperature. For the post cure study the foams were transferred

to the pre-heated oven immediately after completion of the foam rise. Foams were taken out of the oven at preset time intervals and samples were cut from the foam for further analysis.



**Figure 33.** The dimensions of the cup foam and the positions of the thermocouple for the temperature measurements

## 4.2 Analysis methods

### High performance liquid chromatography (HPLC)

The HPLC analyses were performed using a self-assembled HPLC system. The system consisted of two Flom AI-12-13-S HPLC pumps, a Knauer dynamical mixing chamber, a Knauer degasser, a Knauer Smartline 3800 autosampler, a Schambeck SFD 12560/150 HPLC column oven and a Knauer K 2500 Single Wavelength UV detector. Two columns were used in series as stationary phase. Column 1 was a Waters Symmetry<sup>®</sup> C18 column with a dimension of 4.6 mm×150 mm and a particle size of 5 μm. Column 2 was a Macherey-Nagel NUCLEODUR<sup>®</sup> 300-5 C18 ec column with a dimension of 4.6 mm × 250 mm and a particle size of 5 μm. The column oven was set at 30 °C and the UV detector was set at 295nm. The HPLC system was run using a modified version of NTeqGPC Control P301 V6.0.01 software and the data evaluations were performed using the Chromatographica V1.0.25 software.

HPLC grade acetonitrile and water were used as solvents. The eluent gradient is shown in Table 33. Samples were prepared as 10mg/mL solutions in acetonitrile. 0.5wt% *p*-Xylene was pre-added to the acetonitrile as internal standard. Prior to

injection the samples were filtered using CHROMAFIL Xtra PTFE filters with a pore size of 0.2  $\mu\text{m}$ .

**Table 33.** Eluent gradient in HPLC analysis

<b>Time (s)</b>	<b>Eluent volume (Water/Acetonitrile) (mL)</b>
0	0.60/0.40
2	0.60/0.40
1200	0.30/0.70
2800	0.30/0.70
4500	0.10/0.90
6000	0.10/0.90

### **Liquid chromatography–mass spectrometry (LC-MS)**

LC-MS analyses were conducted using an Agilent HPLC 1200 Series coupled to an Agilent 6224 ESI-TOF mass spectrometer. The column used for HPLC was an Agilent Extend-C18 column with a dimension of 2.1 mm  $\times$  50 mm and a particle size of 1.8  $\mu\text{m}$ .

Acetonitrile and water, both doped with 0.1wt% formic acid, were used as solvents. The eluent gradient is shown in Table 34. Samples were prepared at concentrations of 2mg/mL in acetonitrile. All the samples were filtered prior to analysis using CHROMAFIL Xtra PTFE filters with a pore size of 0.2  $\mu\text{m}$ .

**Table 34.** Eluent gradient in LC-MS analysis

<b>Time (s)</b>	<b>Eluent volume (Water/Acetonitrile) (mL)</b>
0	0.18/0.12
1	0.18/0.12
1500	0.09/0.21
2400	0.09/0.21
2700	0.03/0.27
3300	0.03/0.27

#### **Electrospray ionization mass spectrometry (ESI-MS)**

ESI-MS spectra were obtained using an Agilent 6224 ESI-TOF mass spectrometer. Samples were prepared as 2.5mg/mL solutions in acetonitrile. Prior to testing the samples were filtered using CHROMAFIL Xtra PTFE filters with a pore size of 0.2  $\mu\text{m}$ .

#### **Nuclear Magnetic Resonance spectroscopy (NMR)**

NMR spectra were recorded with Bruker Avance I 400MHz or 500MHz using dimethyl sulfoxide- $d_6$  (DMSO- $d_6$ ) or chloroform- $d$  ( $\text{CDCl}_3$ ) as deuterated solvents and Tetramethylsilane (TMS) as internal standard for chemical shift calibration. MestReNova 10.0.1 software was used for data processing. Spectra baselines were corrected by using polynomial fitting with an order of 3 before integrations were applied.

#### **Attenuated total reflectance infrared spectroscopy (ATR-IR)**

Offline ATR-IR spectra were obtained using a Bruker VERTEX 70 with an A225/Q Platinum ATR accessory. Spectra were scanned 32 times from  $4500\text{ cm}^{-1}$  to  $400\text{ cm}^{-1}$  with a resolution of  $2\text{ cm}^{-1}$ .

Online ATR-IR spectra were obtained with a Bruker TENSOR 27 equipped with a

heatable ATR accessory. A scan was taken from  $4000\text{ cm}^{-1}$  to  $600\text{ cm}^{-1}$  with a resolution of  $2\text{ cm}^{-1}$ . The sample cell of the ATR accessory was pre-heated to the desired temperature. Then a small aliquot of the freshly prepared reactant mix was put onto the sample cell and the scan was started immediately. A scan was taken every 4 seconds and the total duration of the measurement amounted to 10 minutes.

The obtained spectra were processed using OPUS and Unscrambler 11.0 software and plotted with Origin 2019. Spectra were smoothed using Savitzky-Golay transformation with a polynomial order of 2 and 9 smoothing points. The baselines of the online FTIR spectra were corrected using the linear offset method in the Unscrambler 11.0 software and the baselines of the offline FTIR spectra were corrected using the function of rubber band correction in the OPUS software. The spectra were normalized using the aromatic C-H stretching vibration as described in previous chapters.

As offline and online spectra were recorded on different instruments using different methods, the data obtained were not always directly comparable.

### **Gel permeation chromatography (GPC)**

The molecular weight distribution was measured using a MZ-Gel Super-FG column with dimensions of  $8\text{mm} \times 300\text{mm}$  equipped with a RI/UV detector. Tetrahydrofuran was used as solvent. Sample was prepared in a concentration of ca.  $10\text{mg/mL}$  in tetrahydrofuran with toluene as internal standard. The sample was filtered using a CHROMAFIL Xtra PTFE filter with a pore size of  $0.2\ \mu\text{m}$  before injection. The molecular weight was calibrated against polystyrene.

### **Soxhlet extraction**

The Soxhlet extractions were conducted with a 250 mL extractor, a 500 mL round bottom flask and a condenser. Ca. 10g foam samples were ground using a mortar and the powder was transferred into cellulose thimbles for extraction. Dichloromethane was used as solvent and the samples were extracted for 24 hours. Thereafter the dichloromethane was removed using a rotary evaporator and the raw extracts were



vacuum treated for about 4 hours using an oil pump after which the extract weights were determined. The absolute amounts of bisphenol A diglycidyl ether in the extracts were determined using  $^1\text{H}$  NMR with phenanthrene as an internal standard.

#### **Dynamic mechanical analysis (DMA)**

DMA was carried out using a TA ARES-G2 instrument. Samples with dimensions of 60mm  $\times$  12mm  $\times$  2-6mm were cut from selected parts of the foam. As the rigid foam samples could not always be cut to the same thickness, the sample thickness was measured and taken into account in the calculations of the modulus. The clamp distance was 40 mm, the oscillation frequency was 1 Hz and the controlled deformation was 0.5%. The samples were heated in a step heating mode from - 80  $^\circ\text{C}$  to 200  $^\circ\text{C}$  with a temperature gradient of 5  $^\circ\text{C}$ . At each temperature interval, the values of  $G'$ ,  $G''$  and  $\tan \delta$  were recorded.

#### **Thermogravimetric analysis (TGA)**

Thermogravimetric analyses data were obtained using a NETZSCH STA 409C/CD instrument. The measurements were conducted under a nitrogen atmosphere using a gas flow rate of 50mL/min and a sample size of about 40 mg. The temperature was increased from 25  $^\circ\text{C}$  to 700  $^\circ\text{C}$  at a heating rate of 10  $^\circ\text{C}/\text{min}$ .

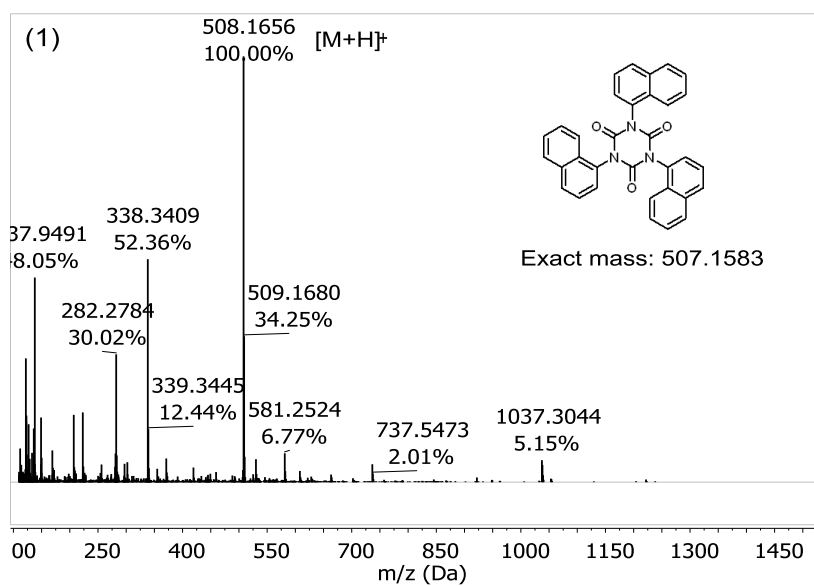
### **4.3 Monofunctional model reaction systems**

#### **4.3.1 Preparation and characterization of the reference substances used for product identification**

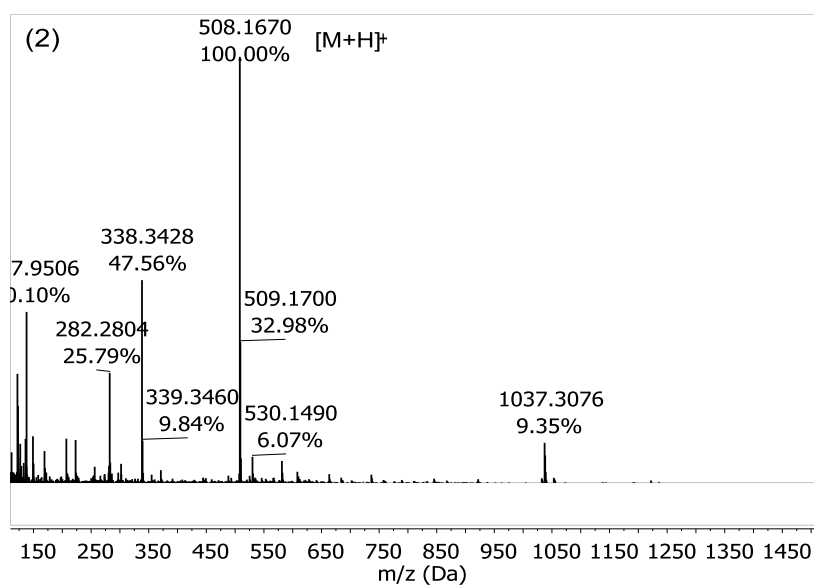
##### **Tris (1-naphthyl) Isocyanurates conformational isomers (referred to as *syn-* / *anti-isocyanurate*)**

Two conformational isomers: *syn-* and *anti-* tris (1-naphthyl) isocyanurates were separated from the reaction products present in the “Ep\_ROH\_NCO\_DAB” system. The separation was made possible by applying column chromatography using Kieselgel 60 as a stationary phase and dichloromethane as a solvent. The structures of

*syn*- and *anti*-tris (1-naphthyl) isocyanurate were determined by using  $^1\text{H}$  NMR,  $^{13}\text{C}$  NMR, ESI-MS and ATR-IR. The combination of the results from ESI-MS (+) and ATR-IR (Figure 34 and Figure 35) revealed that the two substances were tris (1-naphthyl) isocyanurate isomers. The exact mass of tris (1-naphthyl) isocyanurate is 507.1583. Base peaks of  $m/z=508.1656$  and  $508.1670$  were found in the ESI-MS (+) spectra for the *syn* and *anti* isomers, respectively (Figure 34). The base peaks correspond to an isocyanate trimer molecule charged with one proton ( $[\text{M}+\text{H}]^+$ ). ATR-IR shows the two substances both having absorbances at  $1710\text{cm}^{-1}$  and  $1394\text{cm}^{-1}$  which correspond to the isocyanurate C=O and C-N stretching vibrations, respectively. Therefore, the iminoxadiazinedione isomer can be excluded. The conformations of these two isomers were further distinguished by using NMR spectroscopy (Figure 36 and Figure 37). In the *syn*-tris (1-naphthyl) isocyanurate, the three naphthyl groups have the same chemical environment: the protons and carbons in the symmetrical positions show the same chemical shift in the  $^1\text{H}$  NMR and  $^{13}\text{C}$  NMR spectra (Figure 36 (a) and Figure 37(a)). However, in the *anti*-tris (1-naphthyl) isocyanurate, one naphthyl ring has a different chemical environment, hence proton *c7* in *anti*-tris (1-naphthyl) isocyanurate shows a different chemical shift to that of the protons *a7* and *b7* (Figure 36 (b)). In the  $^{13}\text{C}$  NMR, the signals of the *syn*-tris (1-naphthyl) isocyanurate are all singlets (Figure 37 (a)), whereas every signals of the *anti*-tris (1-naphthyl) isocyanurate are split into two adjacent singlets (Figure 37 (b)). The *anti*-tris (1-naphthyl) isocyanurate sample was submitted to single crystal X-ray crystallography analysis to determine its exact conformation. Unfortunately, the quality of the crystal was insufficient to obtain a detailed analysis, nevertheless, there was sufficient evidence suggesting that the substance was an isocyanurate and not an iminoxadiazinedione isomer.

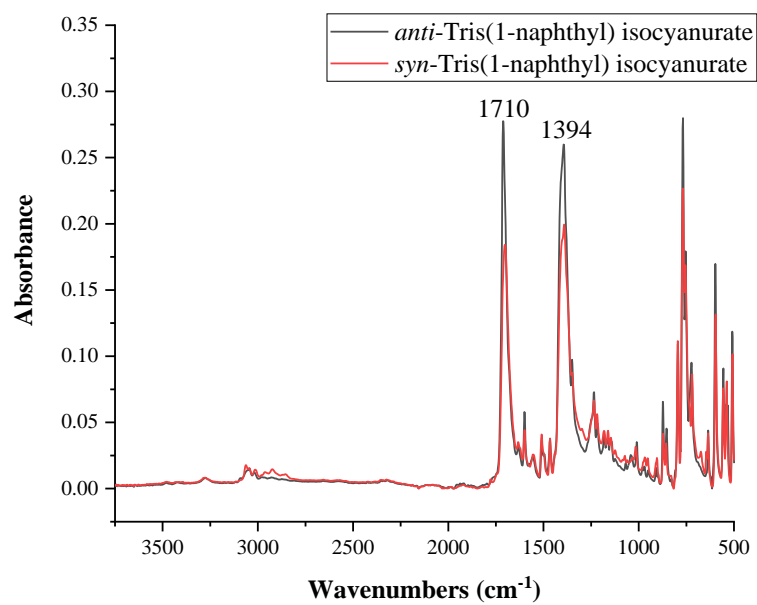


(a) ESI-MS (+): 508.1656[M+H]<sup>+</sup>



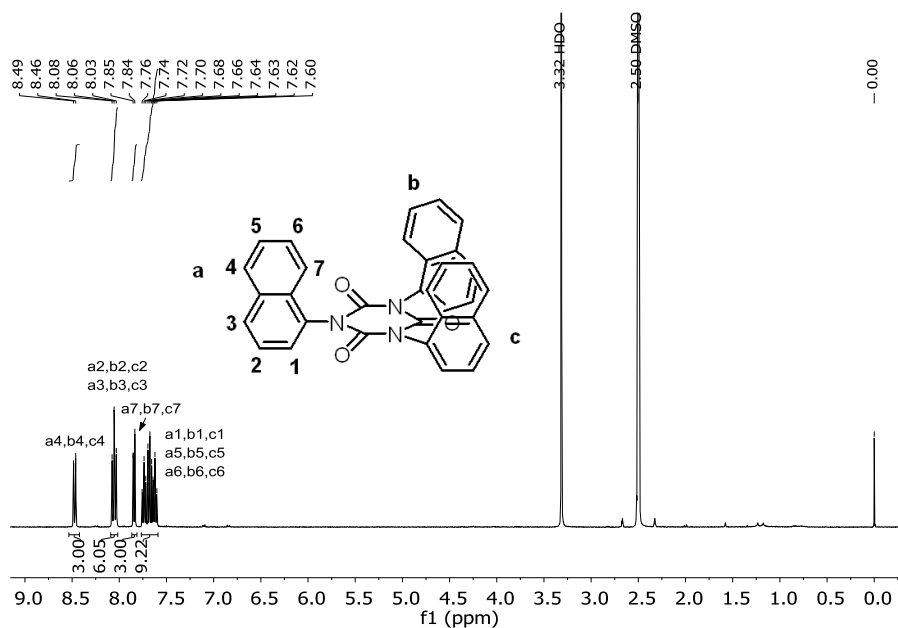
(b) ESI-MS (+): 508.1670[M+H]<sup>+</sup>

**Figure 34.** ESI-MS(+) spectra of (a) *syn*-tris (1-naphthyl) isocyanurate and (b) *anti*-tris (1-naphthyl) isocyanurate

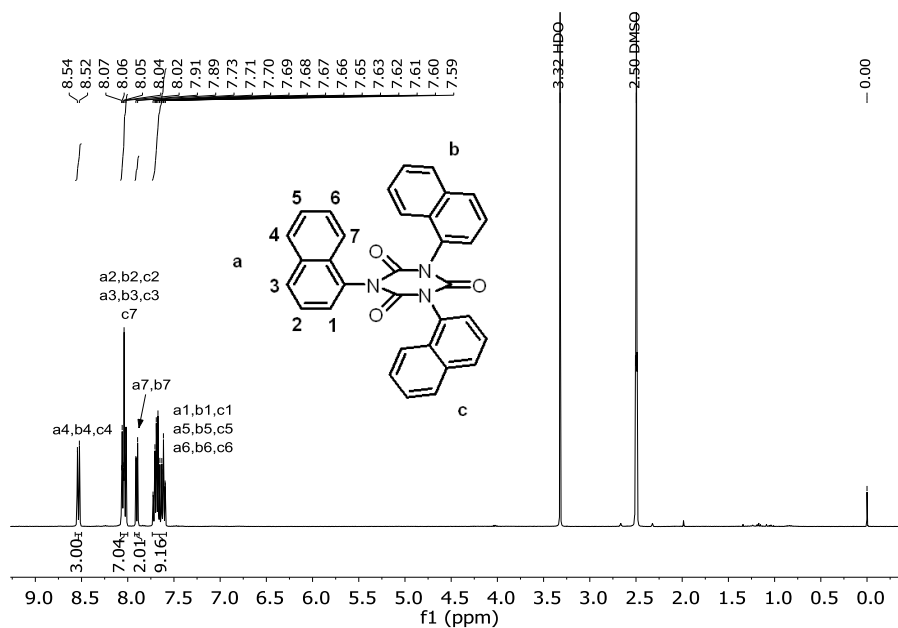


1710 cm<sup>-1</sup> (isocyanurate C=O stretching), 1394 cm<sup>-1</sup> (isocyanurate C-N stretching)

**Figure 35.** ATR-IR spectra of *syn*-tris (1-naphthyl) isocyanurate and *anti*-tris (1-naphthyl) isocyanurate

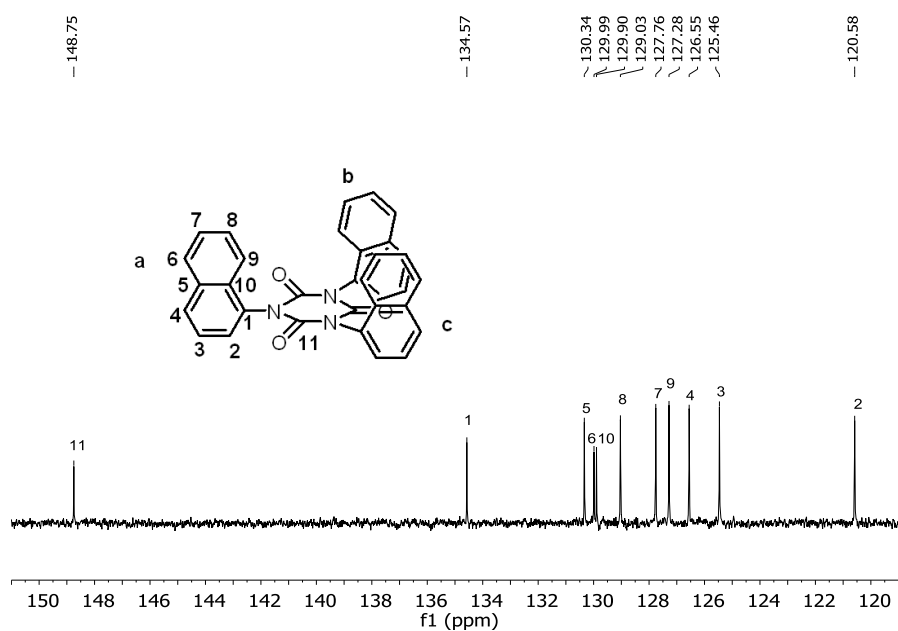


(a) *syn*-tris(1-naphthyl) isocyanurate,  $^1\text{H}$  NMR (400 MHz, DMSO- $d_6$ ,  $\delta$  ppm): 8.47 (d, 3H, Ar-H: a4, b4, c4), 8.03-8.08 (m, 6H, Ar-H: a2, b2, c2, a3, b3, c3), 7.84 (d, 3H, Ar-H: a7, b7, c7), 7.60-7.76 (m, 9H, Ar-H: a1, b1, c1, a5, b5, c5, a6, b6, c6)

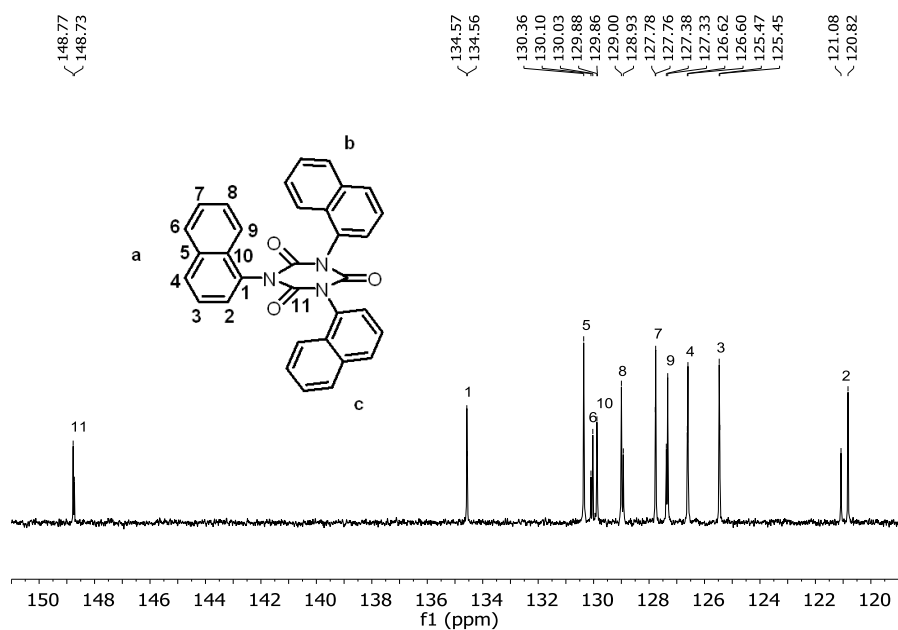


(b) *anti*-tris(1-naphthyl) isocyanurate,  $^1\text{H}$  NMR (400 MHz, DMSO- $d_6$ ,  $\delta$  ppm): 8.53 (d, 3H, Ar-H: a4, b4, c4), 8.02-8.07 (m, 7H, Ar-H: a2, b2, c2, a3, b3, c3, c7), 7.90 (d, 2H, Ar-H: a7, b7), 7.59-7.73 (m, 9H, Ar-H: a1, b1, c1, a5, b5, c5, a6, b6, c6)

**Figure 36.**  $^1\text{H}$  NMR spectra of (a) *syn*-tris (1-naphthyl) isocyanurate and (b) *anti*-tris (1-naphthyl) isocyanurate



(a) *syn*-tris (1-naphthyl) isocyanurate,  $^{13}\text{C}$  NMR (400 MHz,  $\text{CDCl}_3$ ,  $\delta$  ppm): 148.75, 134.57, 130.34, 129.99, 129.90, 129.03, 127.76, 127.28, 126.55, 125.46, 120.58

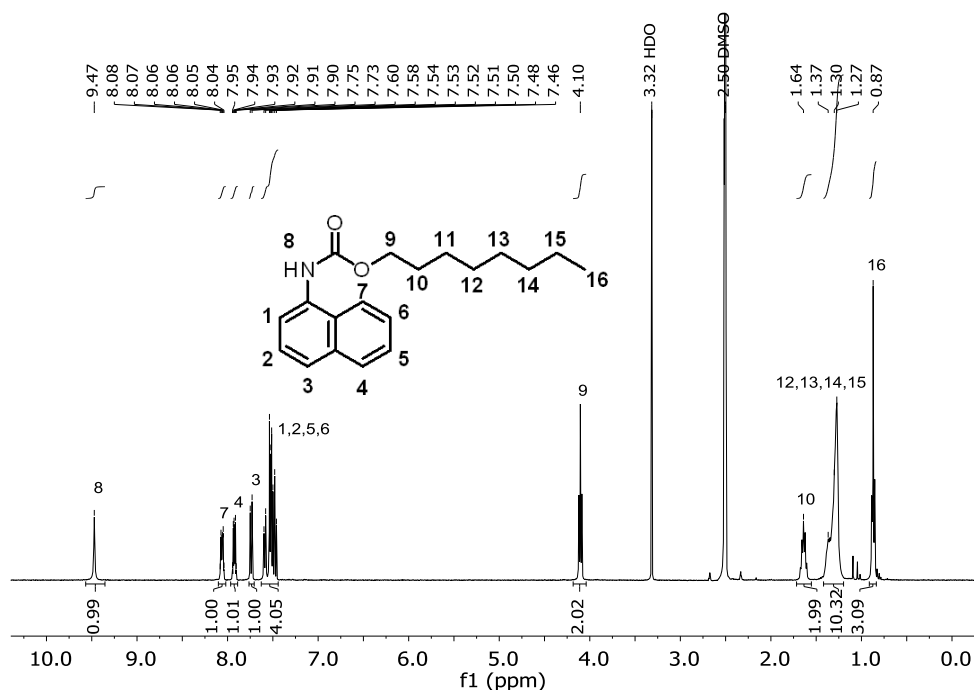


(b) *anti*-tris (1-naphthyl) isocyanurate,  $^{13}\text{C}$  NMR (400 MHz,  $\text{CDCl}_3$ ,  $\delta$  ppm): 148.77, 148.73, 134.57, 134.56, 130.36, 130.10, 130.03, 129.88, 129.86, 129.00, 128.93, 127.78, 127.76, 127.38, 127.33, 126.62, 126.60, 125.47, 125.45, 121.08, 120.82

**Figure 37.**  $^{13}\text{C}$  NMR spectra of (a) *syn*-tris (1-naphthyl) isocyanurate and (b) *anti*-tris (1-naphthyl) isocyanurate

### Octyl *N*-1-naphthalenylcarbamate (referred to as urethane)

The octyl *N*-1-naphthalenylcarbamate was separated from the reaction products of the “Ep\_ROH\_NCO\_DAB” system by column chromatography. Kieselgel 60 was used as a stationary phase. Ethyl acetate (EE) and petroleum ether (PE) 50-70 mixtures were used as solvent and an eluent gradient (EE: PE from 1:5 to 5:1, v:v) was applied. The structure of the octyl *N*-1-naphthalenylcarbamate was confirmed by  $^1\text{H}$  NMR.



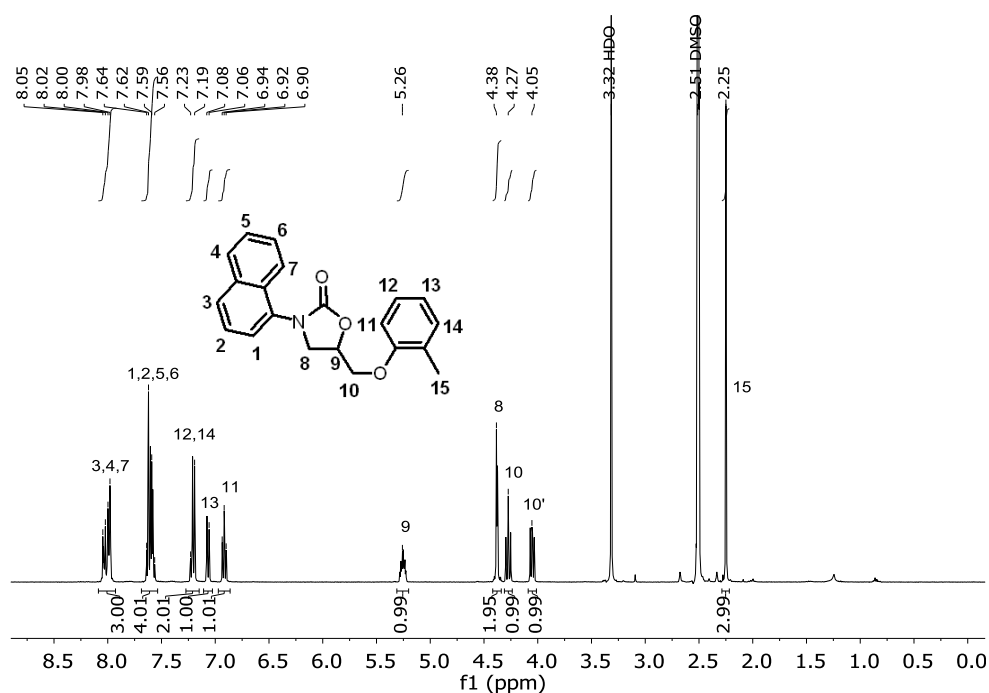
$^1\text{H}$  NMR (400 MHz, DMSO- $d_6$ ,  $\delta$  ppm): 9.47 (s, 1H, NH), 8.08- 8.04 (m, 1H, Ar-H), 7.95- 7.90 (m, 1H, Ar-H), 7.75-7.46 (m, 4H, Ar-H), 4.10 (t, 2H, CH<sub>2</sub>), 1.64 (m, 2H, CH<sub>2</sub>), 1.37-1.27 (m, 10H, CH<sub>2</sub>), 0.87 (t, 3H, CH<sub>3</sub>).

**Figure 38.**  $^1\text{H}$  NMR spectrum of Octyl *N*-1-naphthalenylcarbamate

### 5-[(2-Methylphenoxy)methyl]-3-(1-naphthalenyl)-2-oxazolidinone (referred to as oxazolidinone)

The 5-[(2-Methylphenoxy)methyl]-3-(1-naphthalenyl)-2-oxazolidinone was separated from the reaction products of the “Ep\_ROH\_NCO\_DAB” system by using the same method as that for octyl *N*-1-naphthalenylcarbamate. The structure of the

5-[(2-Methylphenoxy)methyl]-3-(1-naphthalenyl)-2-oxazolidinone was confirmed by  $^1\text{H}$  NMR.



$^1\text{H}$  NMR (400 MHz, DMSO- $d_6$ ,  $\delta$  ppm): 8.05-7.98 (m, 3H, Ar-H), 7.64-7.56 (m, 4H, Ar-H), 7.23-7.19 (m, 2H, Ar-H), 7.08-7.06 (d, 1H, Ar-H), 6.94-6.90 (m, 1H, Ar-H), 5.26 (m, 1H, CH), 4.38 (d, 2H,  $\text{CH}_2$ ), 4.27 (m, 1H,  $\text{CH}_2$ ), 4.05 (m, 1H,  $\text{CH}_2$ ), 2.25 (s, 3H,  $\text{CH}_3$ )

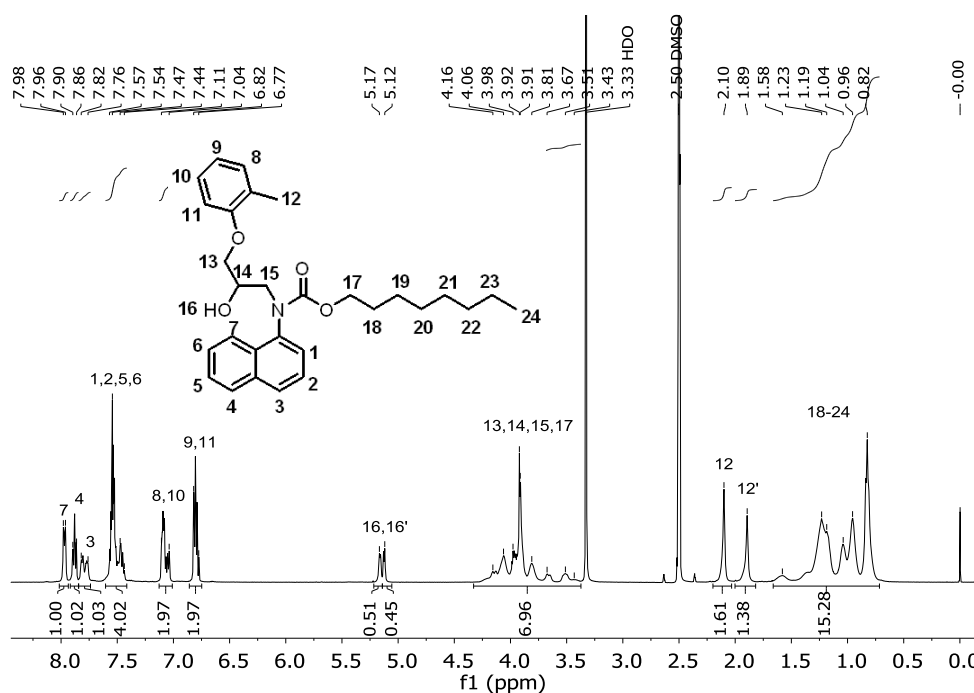
**Figure 39.**  $^1\text{H}$  NMR spectrum of 5-[(2-Methylphenoxy)methyl]-3-(1-naphthalenyl)-2-oxazolidinone

## Alcohol\_2

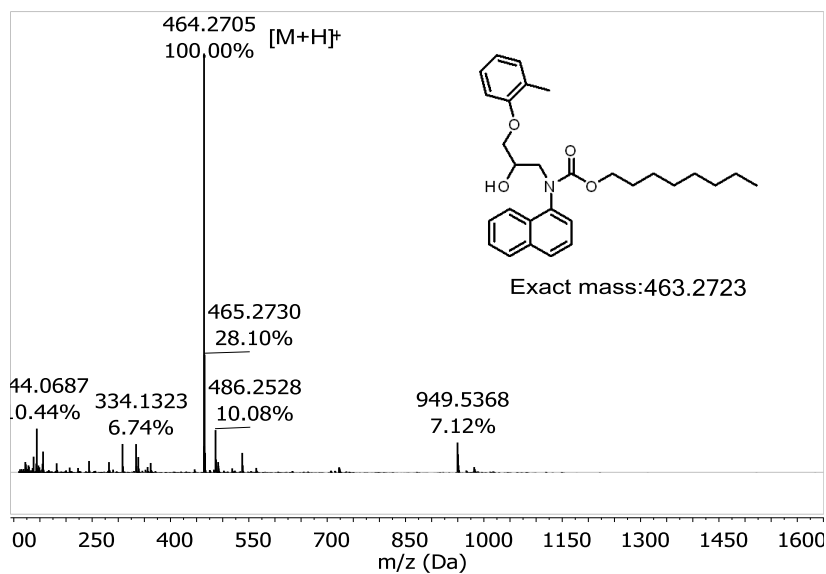
The alcohol\_2 was separated from the reaction products of the “Ep\_ROH\_NCO\_DAB” system by using the same method as that for octyl *N*-1-naphthalenylcarbamate. The structure of alcohol\_2 was determined by  $^1\text{H}$  NMR and ESI-MS (+). In the  $^1\text{H}$  NMR, the hydroxyl group showed up as two adjacent singlets (16 and 16’) with an integral ratio of 1:0.88. The same signal split (12 and 12’) was observed for the methyl group on the benzene ring with a similar integral ratio of 1:0.86. The signal split in the  $^1\text{H}$  NMR was considered to be attributed to the presence of two alcohol\_2 conformational



isomers. The fact that two alcohol\_2 conformational isomers exist is supposed to be caused by the sterical hindrance between the crowded naphthyl, 2-methyl phenoxy and hydroxyl groups. Regioselective isomers may also lead to differences in the chemical shift, but in the model epoxide-urethane reaction system discussed in section 3.1.1.3, this was shown not to be the case. In this model reaction, signals of 12, 12', 16 and 16' were observed in the  $^1\text{H}$  NMR during the reaction process, however, only 5-oxazolidinone was formed in the final product and no 4-oxazolidinone was detected. Therefore, the observed signal splits were attributed to the differences in conformation. As the molecular conformation is not the focus of this thesis, the alcohol\_2 isomers were treated as the entire amount of alcohol\_2 without any further differentiation.



(a)  $^1\text{H}$  NMR (400 MHz,  $\text{DMSO-d}_6$ ,  $\delta$  ppm): 7.98-7.96 (m, 1H, Ar-H), 7.90-7.86 (m, 1H, Ar-H), 7.82-7.76 (m, 1H, Ar-H), 7.57-7.44 (m, 4H, Ar-H), 7.11-7.04 (m, 2H, Ar-H), 6.82-6.77 (m, 2H, Ar-H), 5.17 (d, 0.51H, OH), 5.12 (d, 0.45H, OH), 4.16-3.43 (m, 7H, CH,  $\text{CH}_2$ ), 2.10 (s, 1.61H,  $\text{CH}_3$ ), 1.89 (s, 1.38H,  $\text{CH}_3$ ), 1.58- 0.82 (m, 15H,  $\text{CH}_2$ ,  $\text{CH}_3$ )

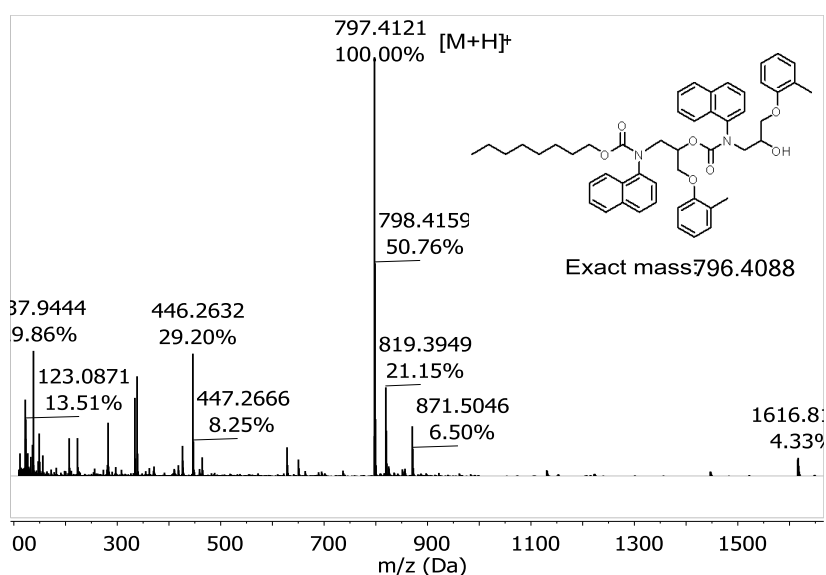


(b) ESI-MS (+): 464.2705 [M+H]<sup>+</sup>

**Figure 40.** (a) <sup>1</sup>H NMR spectrum and (b) ESI-MS (+) spectrum of Alcohol\_2

### Alcohol\_3

Alcohol\_3 was separated from the reaction products of the “Ep\_ROH\_NCO\_DAB” system by the same method as that for octyl *N*-1-naphthalenylcarbamate. The molecular composition was confirmed by the ESI-MS (+). The mass comparison was accurate to the first decimal place.

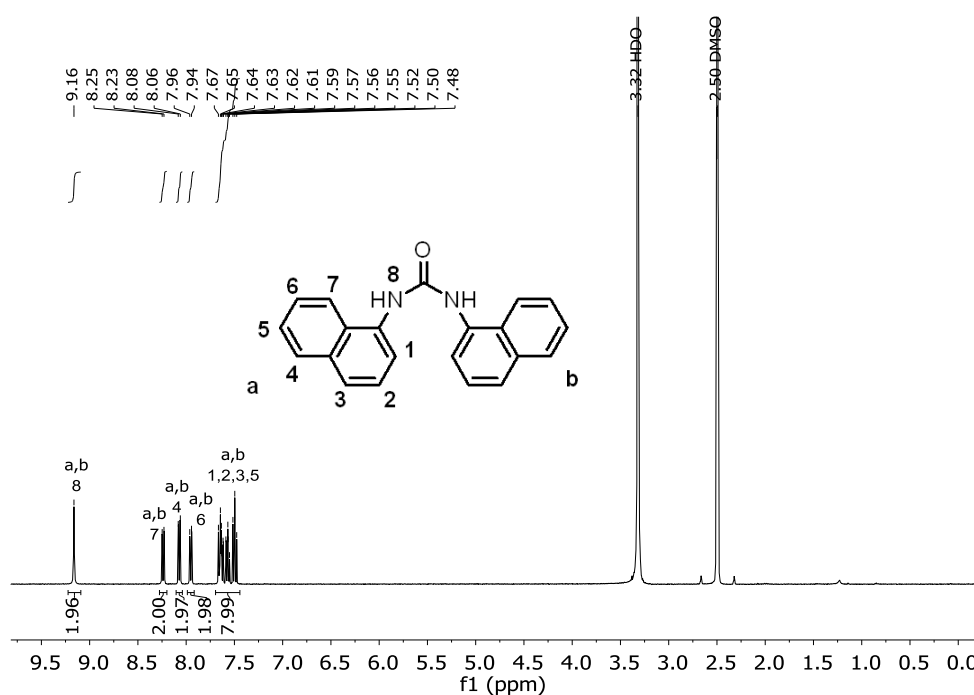


ESI-MS (+): 797.4121 [M+H]<sup>+</sup>

**Figure 41.** ESI-MS (+) spectrum of Alcohol\_3

## *N,N'*-Di-1-naphthylurea

A beaker was filled with 75mL of an acetone / water mixture (acetone: H<sub>2</sub>O = 9:1, v:v) and kept at room temperature. 1-Naphthyl isocyanate (1g, 5.9 mmol) was added dropwise to the acetone / water mixture while stirring. The reaction was allowed to further react for another 20 minutes after the addition had finished. Then the crude product was filtered off and rinsed with acetone. The obtained *N,N'*-di-1-naphthylurea was dried in a vacuum oven at 40 °C under a pressure of less than 10 mbar for 24 hours and its structure was confirmed by <sup>1</sup>H NMR.



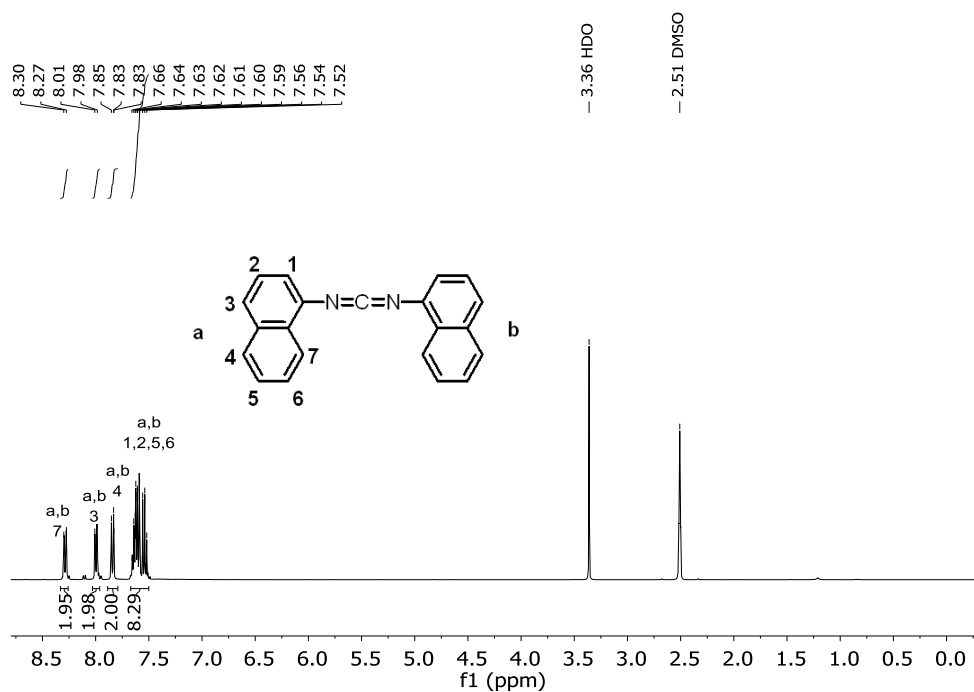
<sup>1</sup>H NMR (500 MHz, DMSO-d<sub>6</sub>, δ ppm): 9.16 (s, 2H, NH), 8.25-8.23 (m, 2H, Ar-H), 8.08-8.06 (m, 2H, Ar-H), 7.96-7.94 (m, 2H, Ar-H), 7.67-7.48 (m, 8H, Ar-H)

**Figure 42.** <sup>1</sup>H NMR spectrum of *N,N'*-Di-1-naphthylurea

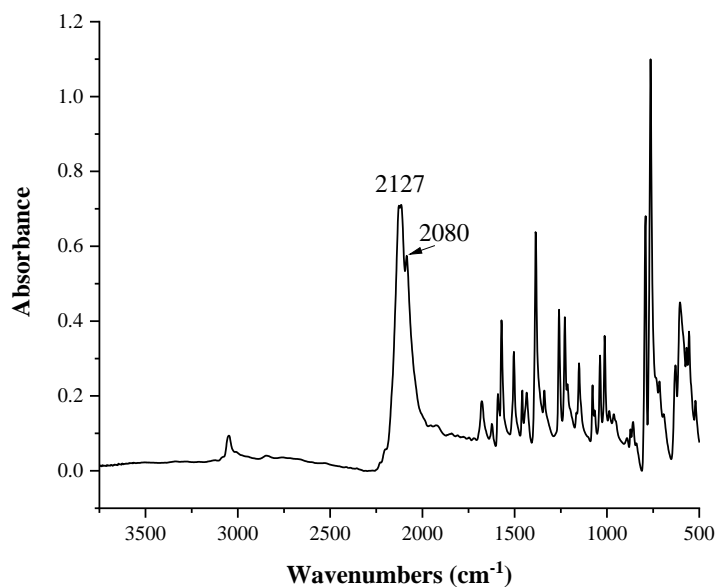
## *N,N'*-Di-1-naphthylcarbodiimide (referred to as carbodiimide)

5g 1-naphthyl isocyanate (30mmol) was mixed with 0.005g 3-methyl-1-phenyl-2-phospholene 1-oxide (0.025 mmol) and reacted at 120 °C for 4 hours under argon protection. The crude product was recrystallized from diethyl ether and the structure of the *N,N'*-di-1-naphthylcarbodiimide was confirmed by <sup>1</sup>H NMR and ATR-IR. The obtained carbodiimide was used for the synthesis of isourea,

guanidine and oxazolidinimine.



(a)  $^1\text{H}$  NMR (400 MHz,  $\text{DMSO-d}_6$ ,  $\delta$  ppm): 8.30-8.27 (m, 2H, Ar-H), 8.01-7.98 (m, 2H, Ar-H), 7.85-7.83 (m, 2H, Ar-H), 7.66-7.52 (m, 8H, Ar-H)

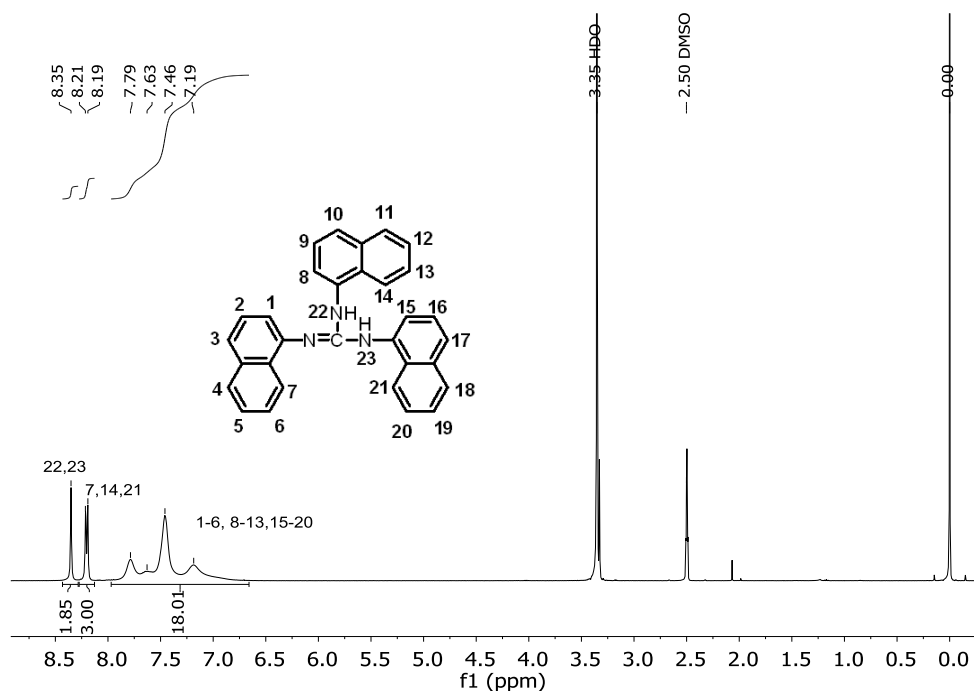


(b) ATR IR:  $2127\text{ cm}^{-1}$  and  $2080\text{ cm}^{-1}$  ( $\text{N}=\text{C}=\text{N}$  stretching)

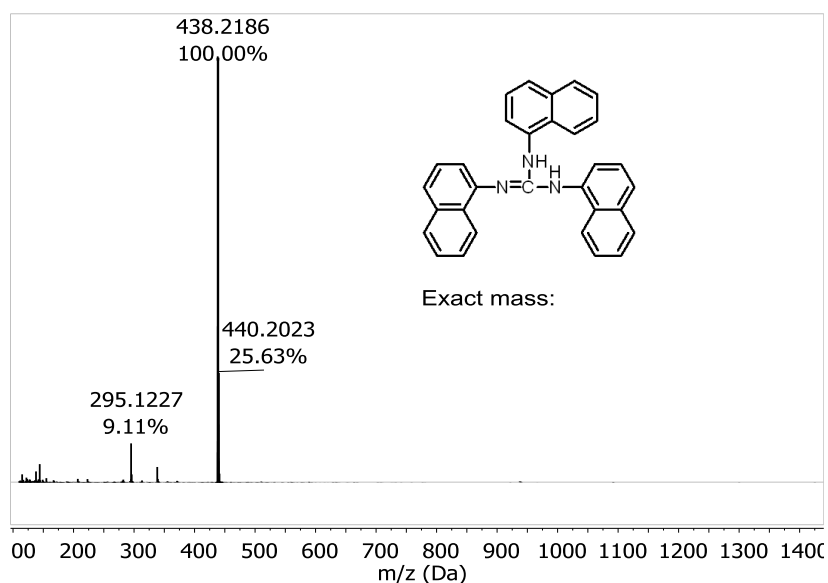
**Figure 43.** (a)  $^1\text{H}$  NMR spectrum and (b) ATR-IR spectrum of *N,N'*-Di-1-naphthylcarbodiimide

### *N, N', N''*-Tri-1-naphthalenylguanidine (referred to as guanidine)

0.06g 1-naphthyl amine (0.42 mmol) was mixed with 0.1235g *N, N'*-di-1-naphthylcarbodiimide (0.42 mmol) and reacted at 130 °C for 30 minutes under argon protection. The crude product was purified by recrystallization from acetonitrile. The structure of *N, N', N''*-tri-1-naphthalenylguanidine was confirmed by <sup>1</sup>H NMR and ESI-MS (+).



(a) <sup>1</sup>H NMR (400 MHz, DMSO-d<sub>6</sub>, δ ppm): 8.35 (s, 2H, NH), 8.21-8.19 (m, 3H, Ar-H), 7.79-7.19 (m, 18H, Ar-H)

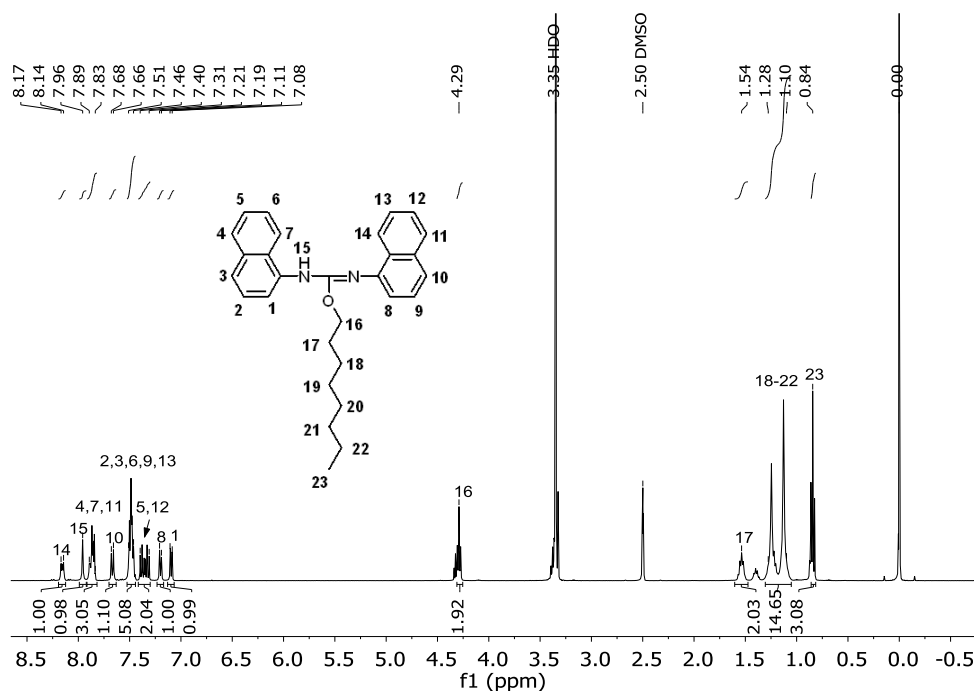


(b) ESI-MS (+): 438.2186 [M+H]<sup>+</sup>

**Figure 44.** (a) <sup>1</sup>H NMR spectrum and (b) ESI-MS (+) spectrum of *N,N'*-Di-1-naphthylcarbodiimide

#### **Octyl *N,N'*-dinaphthalenylcarbamidate (referred to as isourea)**

0.30g 1-octanol (2.31 mmol) was mixed with 0.65g *N,N'*-di-1-naphthylcarbodiimide (2.23 mmol) and reacted at 130 °C for 20 minutes under argon protection. 1-Octanol was added in slight excess to prevent further reaction between octyl *N,N'*-dinaphthalenylcarbamidate and *N,N'*-di-1-naphthylcarbodiimide. The structure of the octyl *N,N'*-dinaphthalenylcarbamidate was confirmed by <sup>1</sup>H NMR. In the <sup>1</sup>H NMR spectrum, the excess of unreacted 1-octanol can also be observed.

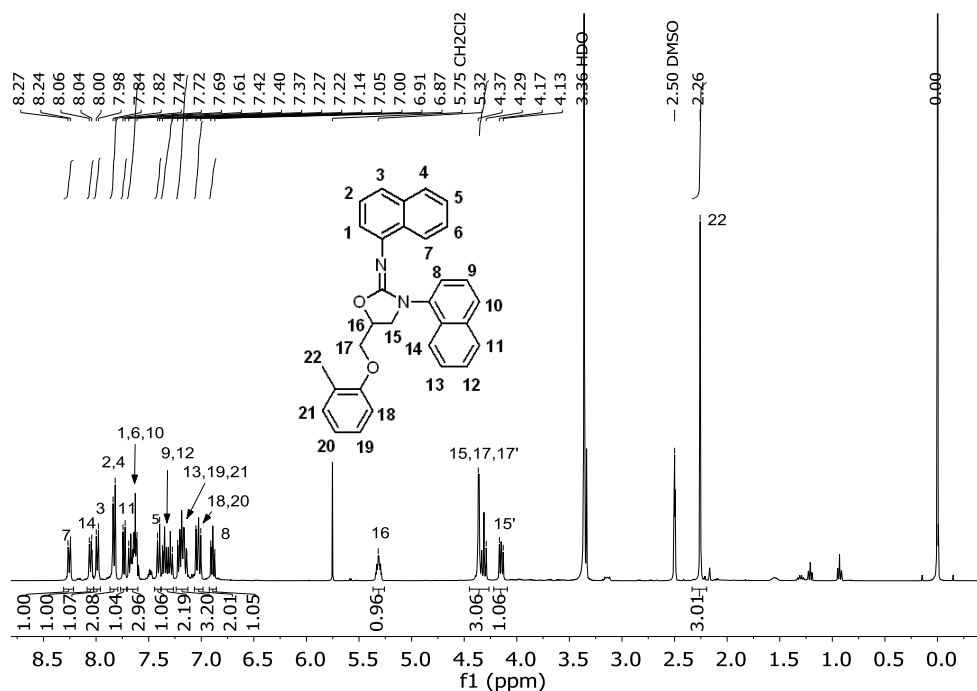


$^1\text{H}$  NMR (400 MHz,  $\text{DMSO-d}_6$ ,  $\delta$  ppm): 8.17-8.14 (m, 1H, Ar-H), 7.96 (s, 1H, NH), 7.89-7.83 (m, 3H, Ar-H), 7.68-7.66 (d, 1H, Ar-H), 7.51-7.46 (d, 1H, Ar-H), 7.40-7.31 (m, 2H, Ar-H), 7.21-7.19 (d, 1H, Ar-H), 7.11-7.08 (d, 1H, Ar-H), 4.29 (m, 2H,  $\text{CH}_2$ ), 1.54 (m, 2H,  $\text{CH}_2$ ), 1.28-1.10 (m, 10H,  $\text{CH}_2$ ), 0.84 (t, 3H,  $\text{CH}_3$ )

**Figure 45.**  $^1\text{H}$  NMR spectrum of *N,N'*-dinaphthalenylcarbamide

***N*-[5-[(2-Methylphenoxy) methyl]-3-naphthyl-2-oxazolidinylidene] naphthylamine (referred to as oxazolidinimine)**

0.116g glycidyl 2-methylphenyl ether (0.71 mmol), 0.208g *N,N'*-di-1-naphthylcarbodiimide (0.71 mmol) and 0.016g DABCO<sup>®</sup> T (0.11 mmol) were mixed and reacted at 160 °C for 10 minutes under argon protection. The structure of *N*-[5-[(2-Methylphenoxy) methyl]-3-naphthyl-2-oxazolidinylidene] naphthylamine was confirmed by  $^1\text{H}$  NMR.



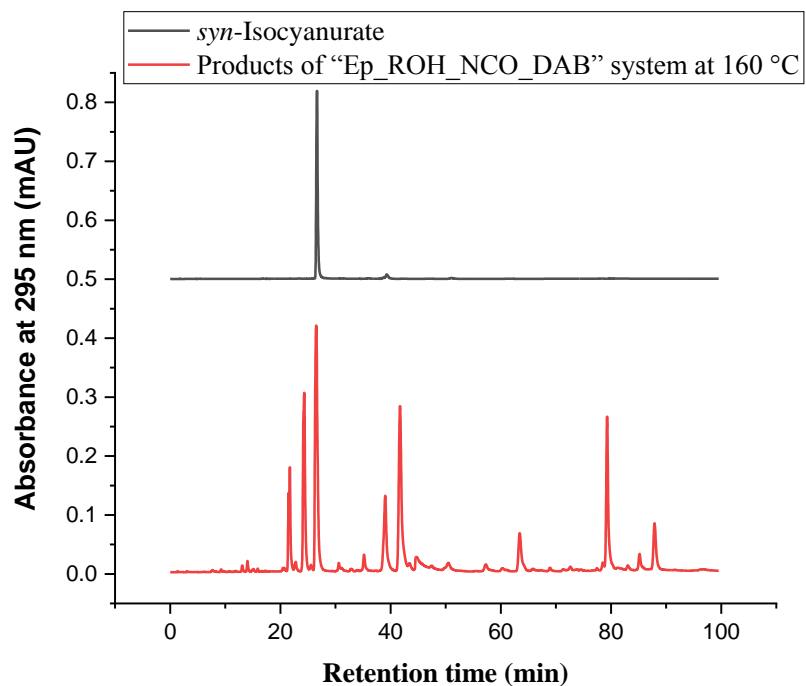
<sup>1</sup>H NMR (400 MHz, DMSO-d<sub>6</sub>, δ ppm): 8.27-8.24 (d, 1H, Ar-H), 8.06-8.04 (m, 1H, Ar-H), 8.00-7.98 (d, 1H, Ar-H), 7.84-7.82 (m, 2H, Ar-H), 7.74-7.72 (d, 1H, Ar-H), 7.69-7.61 (m, 3H, Ar-H), 7.42-7.40 (m, 1H, Ar-H), 7.37-7.27 (m, 2H, Ar-H), 7.22-7.14 (m, 3H, Ar-H), 7.05-7.00 (m, 2H, Ar-H), 6.91-6.87 (d, 1H, Ar-H), 5.32 (m, 1H, CH), 4.37-4.29 (m, 3H, CH<sub>2</sub>), 4.17-4.13 (dd, 1H, CH<sub>2</sub>), 2.26 (s, 3H, CH<sub>3</sub>)

**Figure 46.** <sup>1</sup>H NMR spectra of N-[5-[(2-Methylphenoxy)methyl]-3-naphthyl]-2-oxazolidinylidene naphthylamine

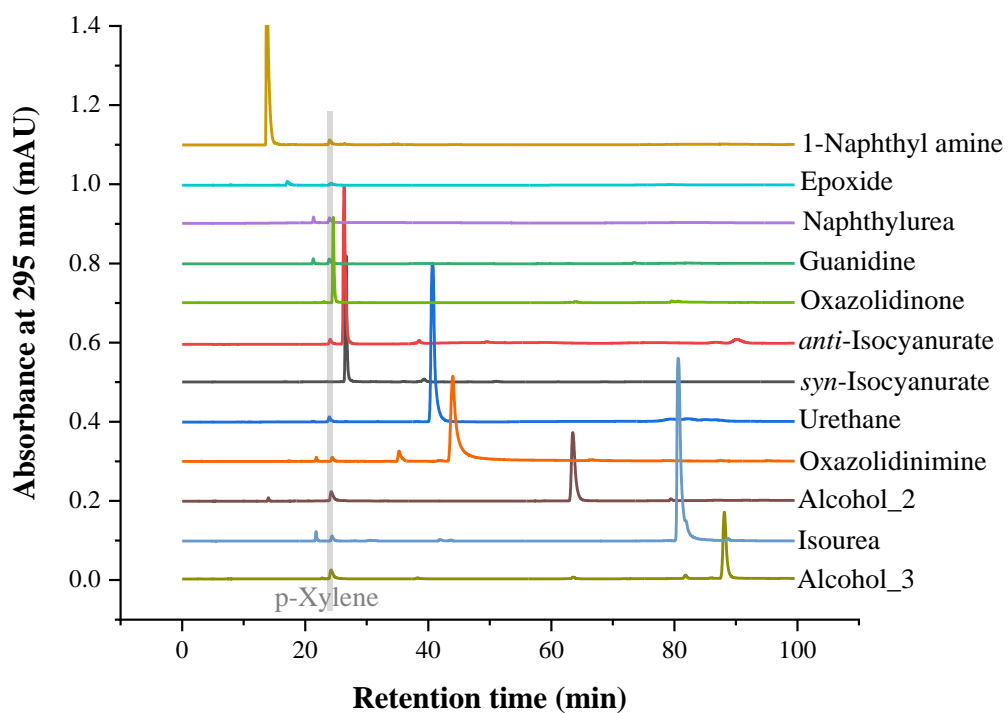
### 4.3.2 Product assignment in HPLC

The obtained reaction products as well as the reference substances were prepared as 10mg/mL solutions in acetonitrile with 0.5wt% *p*-xylene as internal standard. The samples were run under the same conditions as described in Section 4.2. The peaks in HPLC were assigned by comparing the retention times with those of the reference substances. The assignment of *anti*-tris (1-naphthyl) isocyanurate is shown in Figure 47 as an example. The retention time for each of the reference substances is summarized in Figure 48 and Table 35.





**Figure 47.** The assignment of *anti*-tris (1-naphthyl) isocyanurate in HPLC



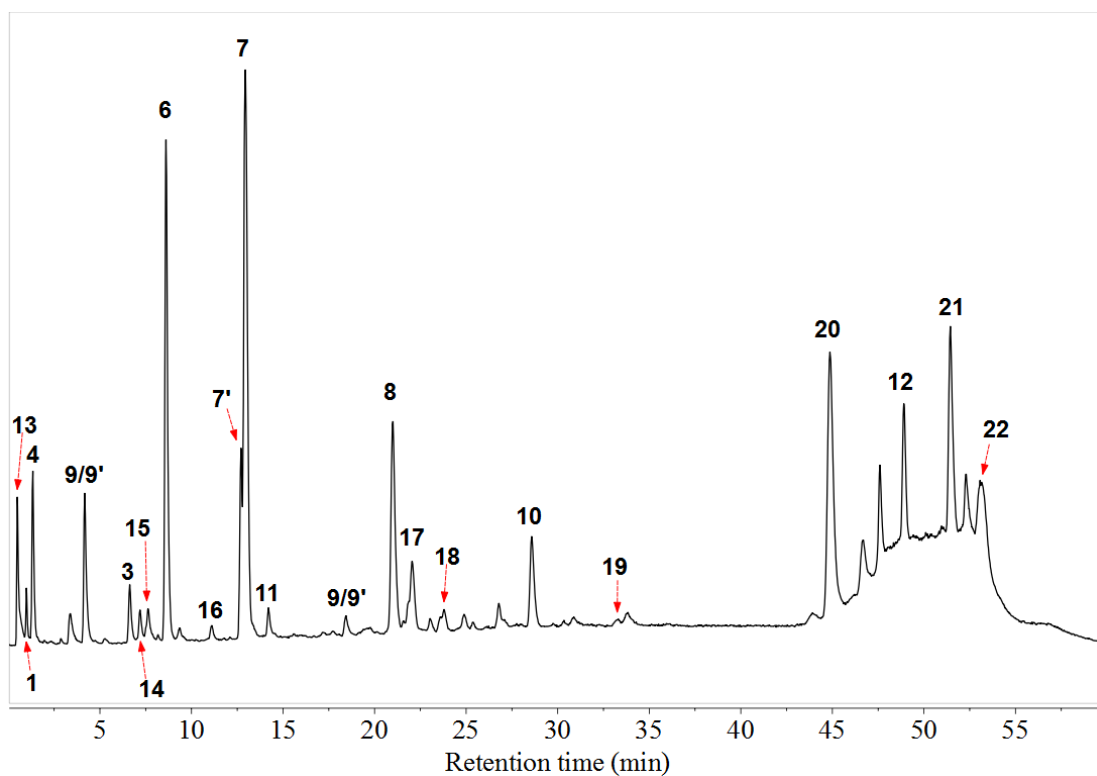
**Figure 48.** The retention times of the reference substances

**Table 35.** The retention times of the reference substances

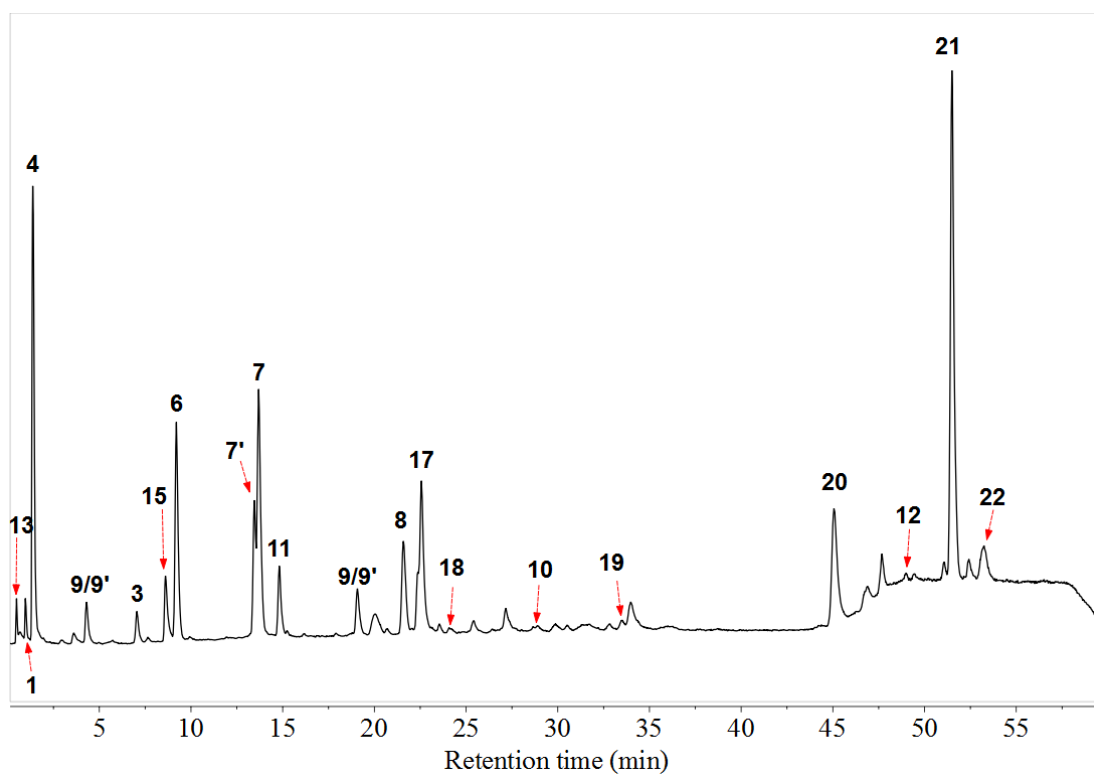
Reference substance	Retention time (min)
1-Naphthyl amine	13.8
Epoxide (unreacted)	17.1
<i>N,N'</i> -Di-1-naphthylurea	21.3
Guanidine	21.2
<i>p</i> -Xylene	24.0
Oxazolidinone	24.6
<i>anti</i> -Tris(1-naphthyl) isocyanurate / <i>syn</i> -Tris(1-naphthyl) isocyanurate	26.3
Urethane	40.7
Oxazolidinimine	44.1
Alcohol_2	63.5
Isourea	80.7
Alcohol_3	88.1

#### 4.3.3 Product assignment in LC-MS

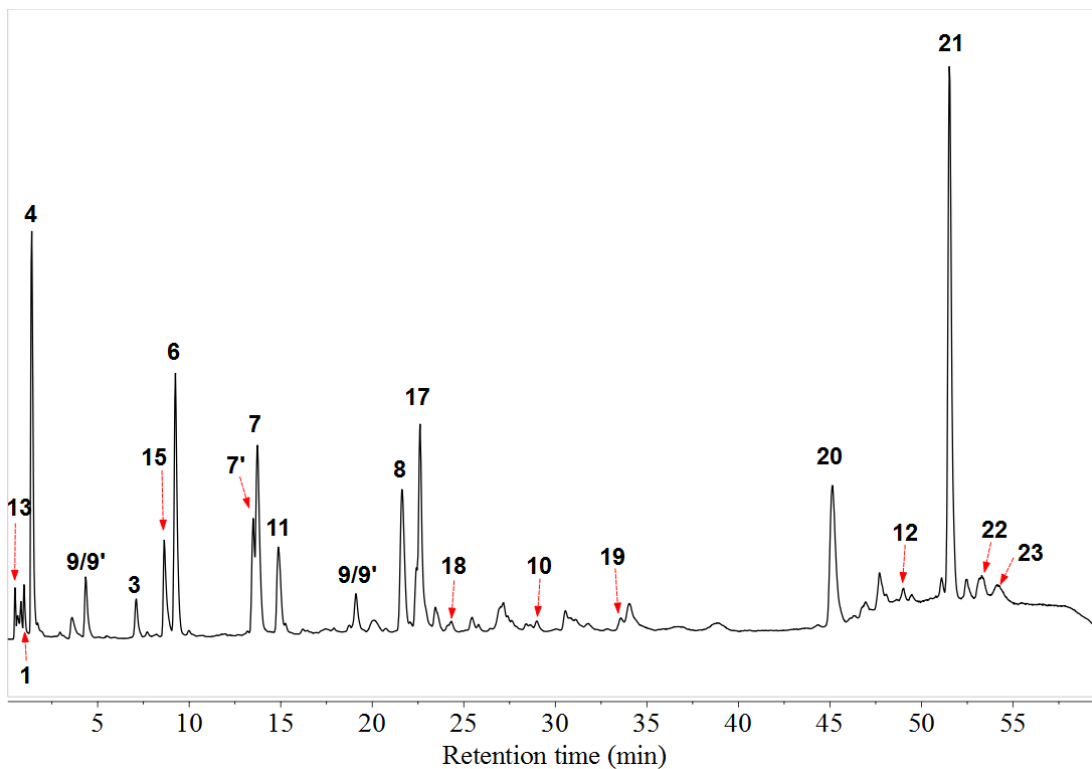
The LC chromatograms of the various reaction products obtained in the different reaction systems are shown in Figure 49. For each component detected in the LC chromatogram, the corresponding mass peak  $[M+H]^+$  in ESI-MS (+) was assigned and the results are given in Table 36. The peak label shares the same order with those in Table 4. The assignment was performed by comparing the  $m/z$  value of the found mass peak to the exact mass of the potential reaction products plus one proton. The assignment was accurate to at least the first decimal place, which was proven to be sufficient to distinguish between molecules with slight differences in the exact masses.



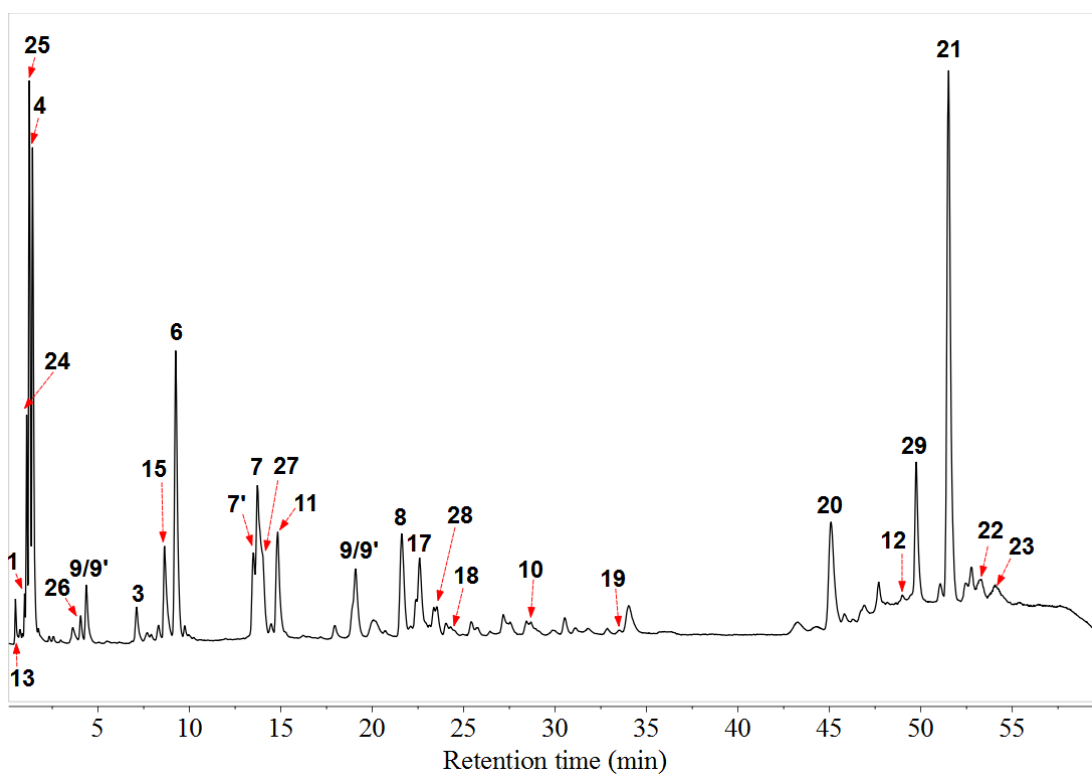
**Figure 49 (a).** LC chromatogram of the reaction products obtained in the “Ep\_ROH\_NCO\_DAB” system at 160 °C



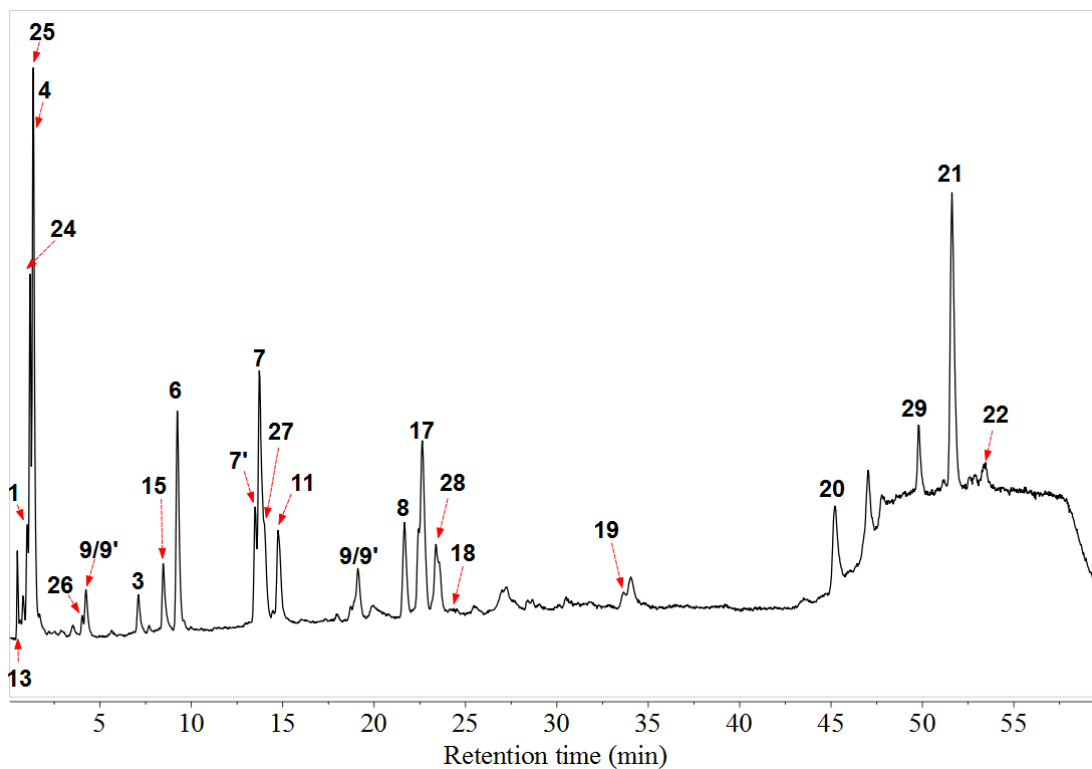
**Figure 49(b).** LC chromatogram of the reaction products obtained in the “Ep\_ROH\_NCO\_H<sub>2</sub>O\_DAB” system at 160 °C



**Figure 49 (c).** LC chromatogram of the reaction products obtained in the “Ep\_ROH\_NCO\_FA\_DAB” system at 160 °C

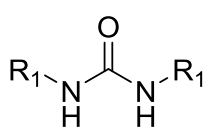


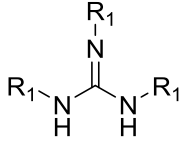
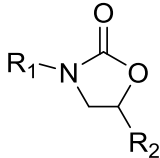
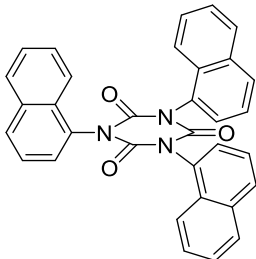
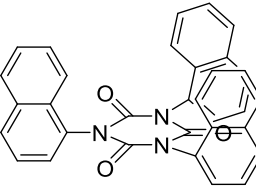
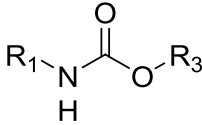
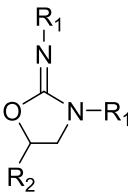
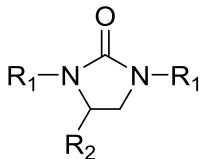
**Figure 49 (d).** LC chromatogram of the reaction products obtained in the “Ep\_ROH\_NCO\_RNH<sub>2</sub>\_DAB” system at 160 °C



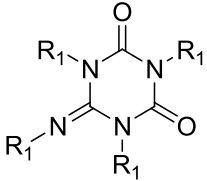
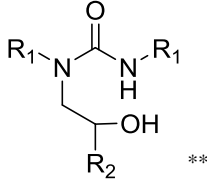
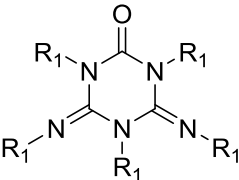
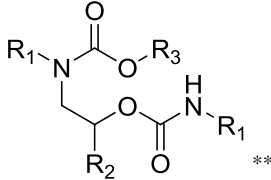
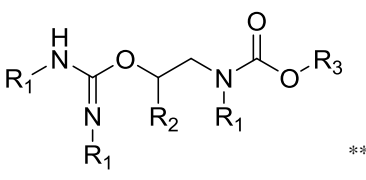
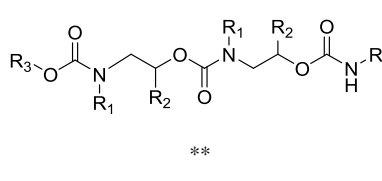
**Figure 49 (e).** LC chromatogram of the reaction products obtained in the “Model” system at 160 °C

**Table 36.** Product assignment of peaks in Figure 49

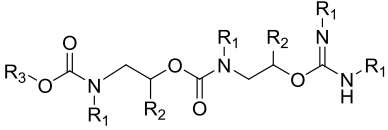
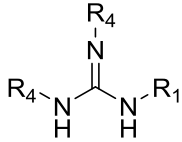
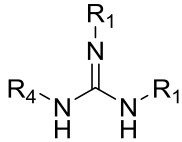
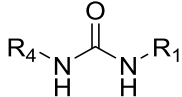
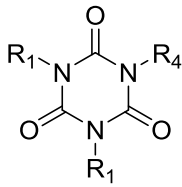
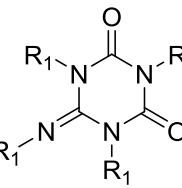
Peak	Chemical structure *	Exact mass	[M+H] <sup>+</sup> found in mass spectra (m/z)
1	$R_1-NH_2$	143.0735	144.0806
3		312.1263	313.1356

4		437.1892	438.2044
6		333.1365	334.1552
7		507.1583	508.1809
7'		507.1583	508.1717
8		299.1885	300.1982
9		458.1994	459.2135
9'		458.1994	459.2135

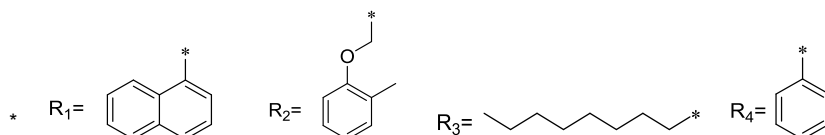
10		463.2723	464.2809
11		424.2515	425.2619
12		796.4088	797.4164
13		128.1313	129.1257
14		601.2729	602.2801
15		583.2624	584.2713
16		307.1572	308.1634

17		632.2212	633.2294
18		476.2100	477.2152
19		757.2842	758.2919
20		632.3250	633.3331
21		757.3880	758.3963
22		965.4615	966.4697



23	 <p style="text-align: center;">**</p>	1090.5245	1091.5026
24	 <p style="text-align: center;">**</p>	393.2205	394.2355
25		415.2048	416.2481
26		290.1419	291.1455
27		485.1739	486.1689
28		610.2367	611.2367

<b>29</b>		735.2998	736.4056
-----------	--	----------	----------

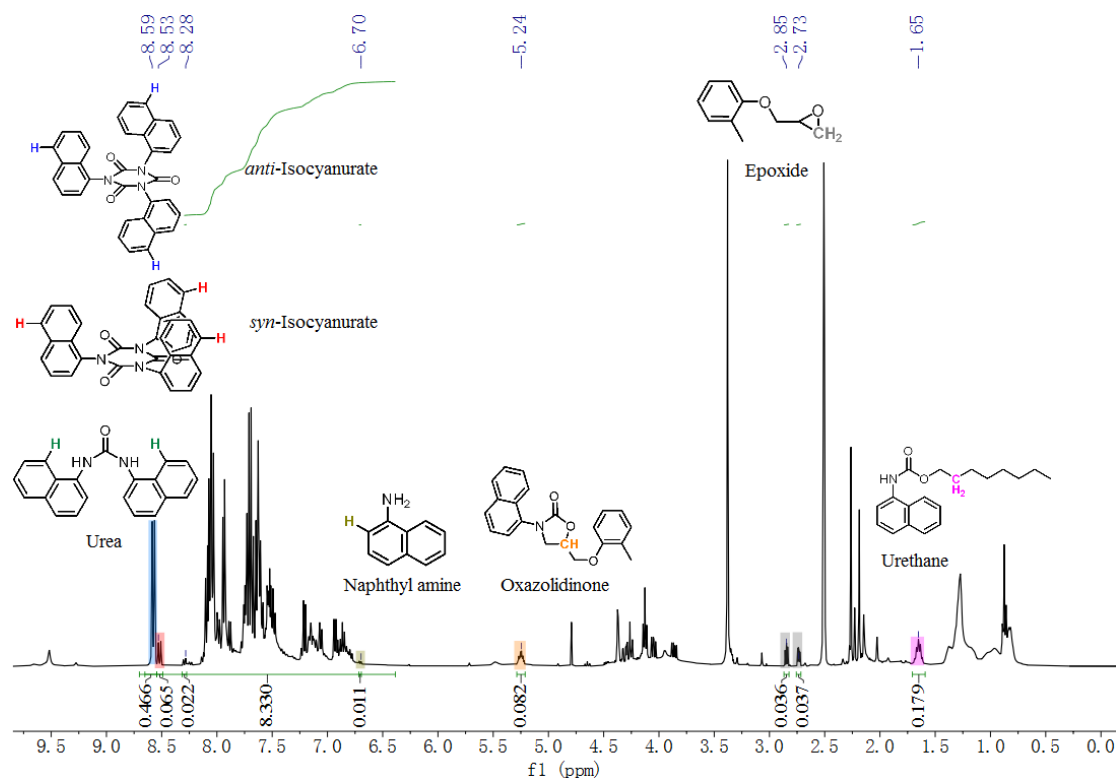


\*\* And / or regioisomers

#### 4.3.4 Product quantification by <sup>1</sup>H NMR

DMSO-d<sub>6</sub> was used as deuterated solvent. In some cases, dichloromethane was added first to dissolve or disperse the entire reaction product prior to the preparation of a sample for the NMR analysis. Then the dichloromethane was evaporated again before adding the deuterated solvent.

The non-overlapping characteristic chemical shifts in <sup>1</sup>H NMR were used to quantify the amount of each individual product in the reaction mixture. The chemical shifts used for the quantification of each component were as follows: *anti*-Isocyanurate: 8.58 ppm, *syn*-isocyanurate: 8.52 ppm, oxazolidinone: 5.24 ppm, urethane: 1.65 ppm, *N,N'*-di-naphthyl urea: 8.29 ppm, 1-naphthyl amine: 6.70 ppm, epoxide: 2.85 ppm, 2,6-dimethyl-aniline: 6.40 ppm, *N*-(2,6-dimethylphenyl)-*N'*-naphthyl urea: 2.28 ppm, Alcohol<sub>2</sub>: 5.12 ppm and 5.17 ppm, 1,1-diethyl-3-(naphthalen-1-yl)urea: 1.18. The peak area integrals were used for the quantification. Below the quantification of the products obtained in the “Ep\_ROH\_NCO\_DAB” system at 160 °C is shown as an example. The data obtained for the other reaction systems are listed in the Appendix.



**Figure 50.**  $^1\text{H}$  NMR spectrum of the reaction products obtained in the “Ep\_ROH\_NCO\_DAB” system at 160 °C, the characteristic chemical shift and peak area integrals used for the quantification of each individual product

The normalization was done on the basis of the total number of aromatic H atoms in the system. The equivalent amount of 1-naphthyl isocyanate that was added was set to 1. In the “Ep\_ROH\_NCO\_DAB” system, the reactants of glycidyl 2-methylphenyl ether, 1-octanol and 1-naphthyl isocyanate had an equivalent ratio of 1:0.5:3, respectively, therefore the total number of aromatic H atoms was set to 8.33 (glycidyl 2-methylphenyl ether has 4 aromatic H atoms, 1-naphthyl isocyanate has 7 aromatic H and 1-octanol has no aromatic H. The total number of aromatic H =  $4 \times 1/3 + 7 \times 1 = 8.33$ ). The product amounts were presented as the percentage of a reactant that had reacted to yield one of the reaction products. The general calculation is shown in Equation 3. As an example, the isocyanate conversion into *anti*-isocyanurate is represented by Equation 4. The conversions of isocyanate, epoxide and alcohol into each product based on the spectral information of Figure 50 are tabulated in Table 37.

Conversion of Reactant A into Product B

$$= \frac{\text{Equivalent}_{\text{Reactant A consumed to produce Product B}}}{\text{Equivalent}_{\text{Reactant A added in total}}} \times 100\% \quad \text{Equation 3}$$

Isocyanate conversion into anti – isocyanurate

$$= \frac{\text{Equivalent}_{\text{isocyanate consumed to produce anti-isocyanurate}}}{\text{Equivalent}_{\text{isocyanate added in total}}} \times 100\%$$

$$= \frac{0.466}{1} \times 100\% = 47\% \quad \text{Equation 4}$$

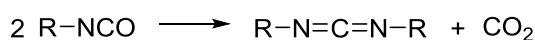
**Table 37.** Quantification of the products in Figure 50

Product	Isocyanate conversion into each product (%)	Epoxide conversion into each product (%)	Alcohol conversion into each product (%)
<i>anti</i> -Isocyanurate	47	-	-
<i>syn</i> -Isocyanurate	7	-	-
Oxazolidinone	8	25	-
Urethane	9	-	53
Urea	2	-	-
Naphthyl amine	1	-	-
Epoxide (unreacted)	-	11	-

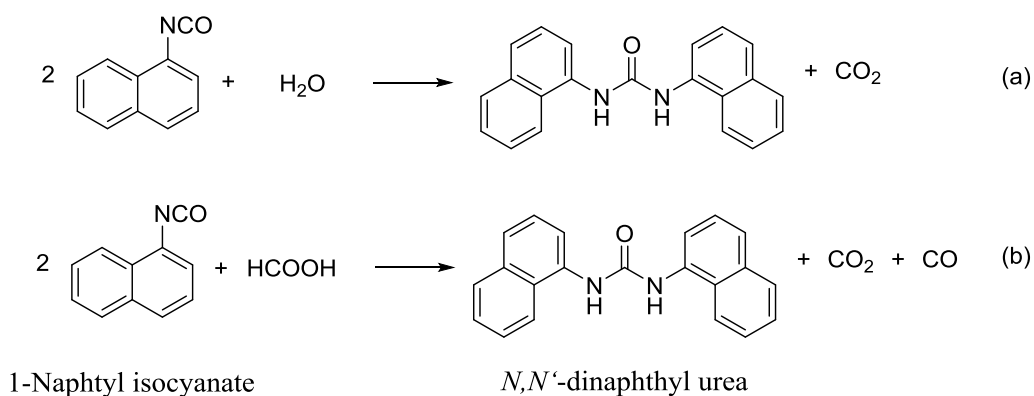
#### 4.3.5 Carbodiimide quantification by the gas evolution method

When 1 mole of carbodiimide is produced from isocyanate, 1 mole of CO<sub>2</sub> is released (see Scheme 16). Therefore, the amount of carbodiimide formed during the reaction can be calculated from the CO<sub>2</sub> evolution. In order to control the system temperature, the reactions were conducted with small amounts of reactant of about 2g. Thus, measuring the gas volume would be more accurate than measuring the gas weight. In

case there is water and/or formic acid present in the reaction system, then these will also generate gas (see Scheme. 17). When water and formic acid are added separately, the volume of CO<sub>2</sub> or CO formed by the water-isocyanate or formic acid-isocyanate reactions can be calculated from the urea amount in the final product. The urea amount in turn can be determined by <sup>1</sup>H NMR as described in Section 4.3.4 and the conversion of isocyanate into carbodiimide can then be calculated using Equation 5. The gas molar volume in the equation equals to 24.5 L/mol (25 °C, 1 atmosphere pressure).



**Scheme 16.** The formation of carbodiimide from isocyanate



**Scheme 17.** The reactions between isocyanate and (a) water (b) formic acid

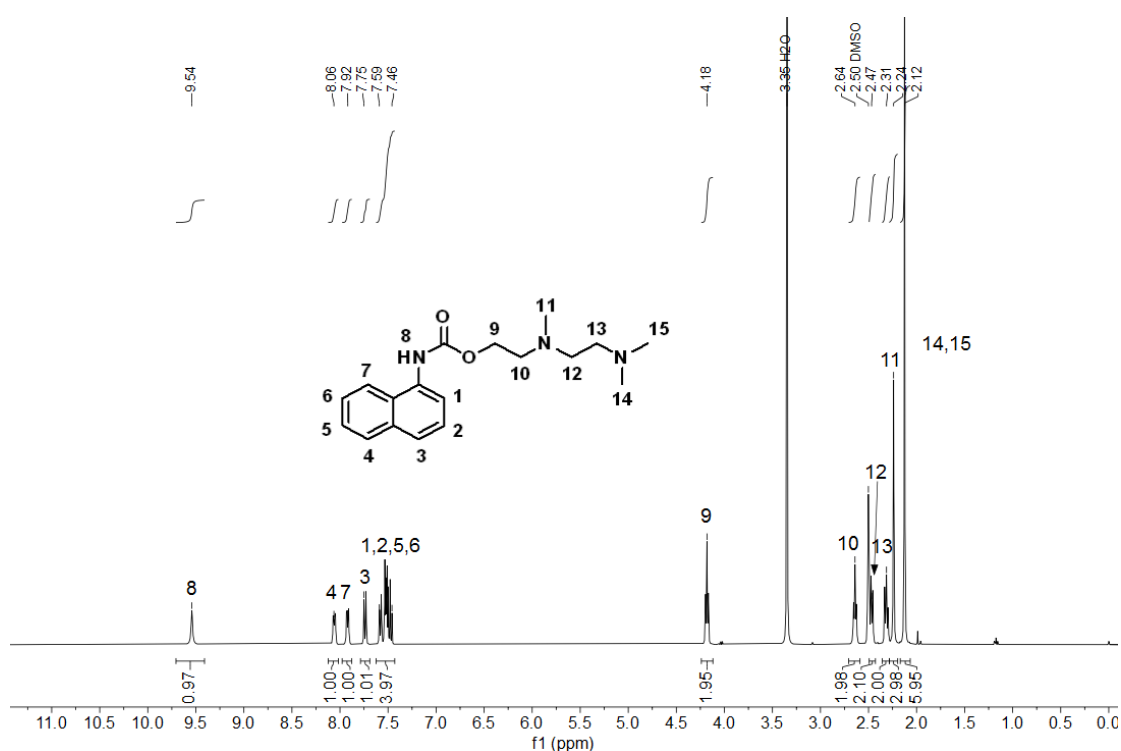
*Conversion of NCO into carbodiimide*

$$= \frac{(V_{gas\ total} - V_{gas\ non\ carbodiimide}) * 2}{Gas\ molar\ volume * Equivalent_{NCO\ added\ in\ total}} \quad \text{Equation 5}$$

#### 4.3.6 Preparation of DABCO<sup>®</sup> T-urethane

1.461g *N,N,N'*-trimethylaminoethyl ethanolamine (DABCO<sup>®</sup> T, 10 mmol) was dissolved in 15 mL dried acetone. 1.695g 1-Naphthyl isocyanate (10 mmol) was dissolved in 25 mL dried acetone. The *N,N,N'*-trimethylaminoethyl ethanolamine

acetone solution was dropped into the 1-naphthyl isocyanate acetone solution with a time duration of 2.5 hours under the stirring of a magnetic stirrer at room temperature. The mixture was stirred for another 0.5 hour when dripping was finished. Then the solvent was removed by rotary evaporator. The crude product was purified by column chromatography. Aluminum oxide was used as a stationary phase and ethyl acetate (EE) was used as solvent. The structure of the 2-((2-(dimethylamino)ethyl)(methyl)amino)ethylnaphthalen-1-ylcarbamate (DABCO<sup>®</sup>T-urethane) was confirmed by <sup>1</sup>H NMR.

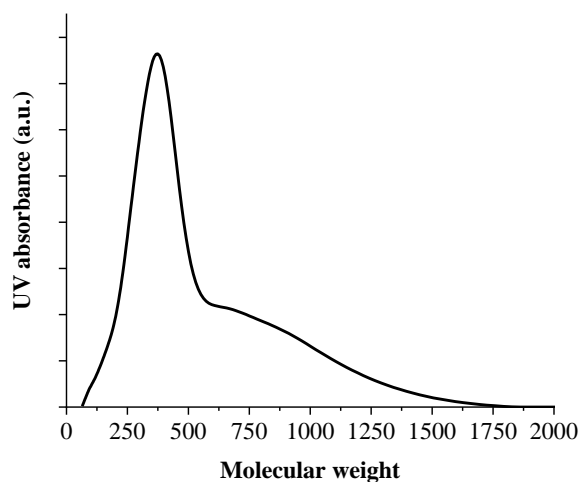


<sup>1</sup>H NMR 400 MHz, DMSO-d<sub>6</sub>, δ ppm): 9.54 (s, 1H, NH-H), 8.06 (m, 1H, Ar-H), 7.92 (m, 1H, Ar-H), 7.75 (d, 1H, Ar-H), 7.59-7.46 (m, 4H, Ar-H), 4.18 (t, 2H, CH<sub>2</sub>), 2.64 (t, 2H, CH<sub>2</sub>), 2.47 (t, 2H, CH<sub>2</sub>), 2.31 (t, 2H, CH<sub>2</sub>), 2.24 (s, 3H, CH<sub>3</sub>), 2.12 (s, 6H, CH<sub>3</sub>).

**Figure 51.** <sup>1</sup>H NMR spectra of 2-((2-(dimethylamino)ethyl)(methyl)amino)ethylnaphthalen-1-ylcarbamate

### 4.3.7 Molecular weight distribution

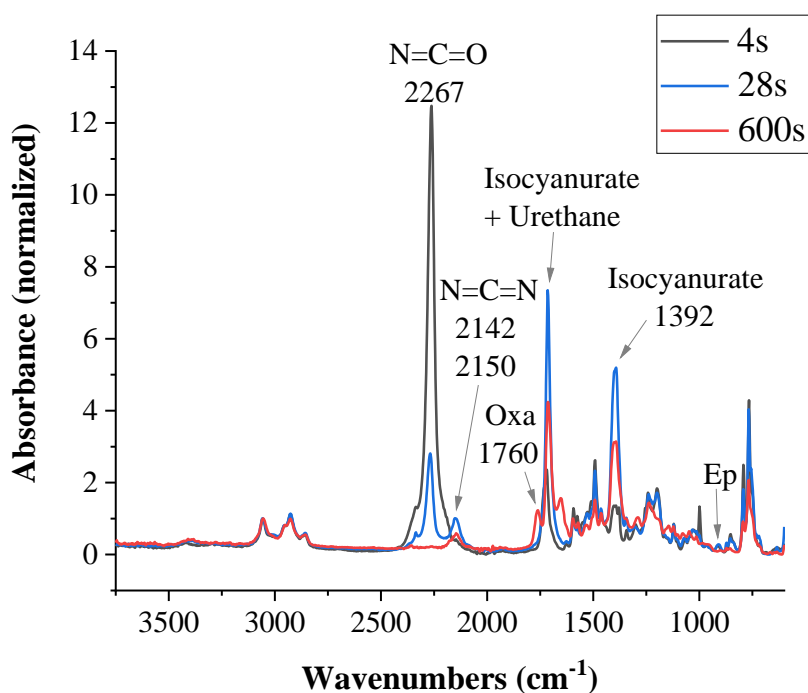
The product obtained from the “Ep\_ROH\_NCO\_DAB” system at 160 °C was submitted to GPC and the GPC trace is shown in Figure 52. The shape of the curve is indicative for a complex mixture of monomer and oligomer products. The tail end of the trace suggests the presence of oligomeric species with molecular masses between 1000 and 1700.



**Figure 52.** Molecular weight distribution of the reaction products from the “Ep\_ROH\_NCO\_DAB” system at 160 °C

### 4.3.8 Online FTIR spectroscopy

The online FTIR spectra were processed using the Unscrambler 11.0 software. The spectra were smoothed using the Savitzky-Golay method (Polynomial Order: 2, Smoothing Points: 9, Left Points: 4, Right Points: 4) and baselines were corrected by applying the “Offset and Linear Baseline Correction” function. The absorption intensities were normalized by using the aromatic C-H stretching at 3056  $\text{cm}^{-1}$ . The spectra recorded after 4s, 28s and 600s from the “Ep\_ROH\_NCO\_DAB” system that was isothermally reacted at 160 °C were plotted in Figure 53. In this figure the most important characteristic vibrations were labeled.



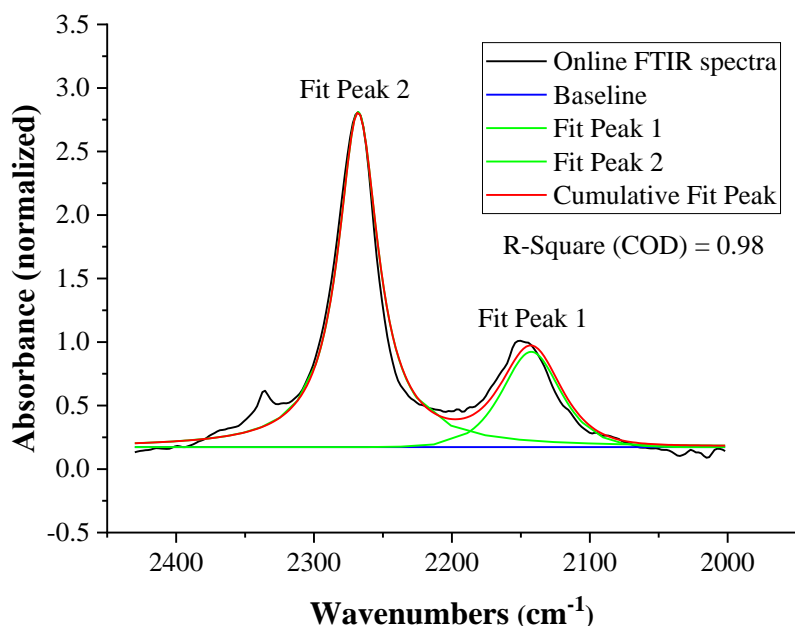
**Figure 53.** Online FTIR spectra recorded after 4s, 28s and 600s from the “Ep\_ROH\_NCO\_DAB” system at 160 °C

To resolve the overlap of the carbodiimide N=C=N stretching at 2142 and 2150  $\text{cm}^{-1}$  and the N=C=O stretching at 2267  $\text{cm}^{-1}$ , the Gaussian-Lorentzian Cross Function was used for peak fitting. The peak fitting of the above FTIR spectrum recorded at 28s is taken as an example. The peak properties of the fitting are shown in Table 38 and the fitting curves are presented in Figure 54.

**Table 38.** Peak properties of the fitting

Peak index	Peak Type	Center max ( $\text{cm}^{-1}$ )	Max Height	FWHM
1	Gaussian_LorenCross	2142.44	0.750049	49.4837
2	Gaussian_LorenCross	2267.99	2.63555	35.293





**Figure 54.** Peak fitting of the FTIR spectrum in Figure 52 recorded after 28 seconds

## 4.4 Foam systems

### 4.4.1 Determination of isocyanate conversion using FTIR

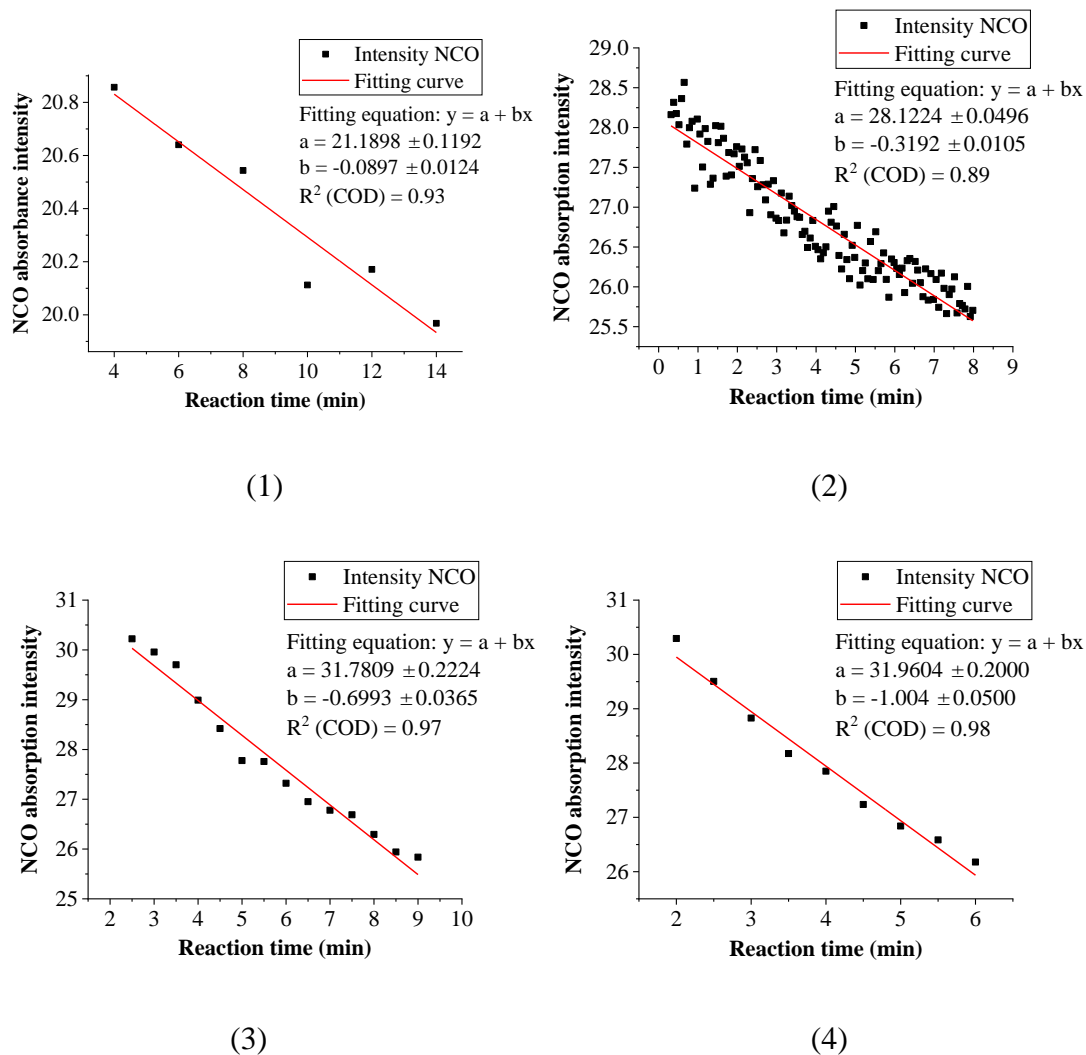
The isocyanate conversions in the foam systems were obtained using FTIR spectroscopy. Although  $\text{CO}_2$  and  $\text{CO}$  were released during the reaction, the theoretical mass change was less than 3% and therefore it can be ignored in the calibration. According to the Beer - Lambert law (Equation 6), the absorption ( $A$ ) of a species is proportional to the absorption coefficient ( $\epsilon$ ), the optical path length ( $\ell$ ) and the concentration of the species ( $c$ ). For the same species under the same measurement conditions,  $\epsilon$  is a constant. The difference in  $\ell$  among a series of tested samples can be compensated for by normalization of the spectra using an absorbance that does not change during the measurement. In doing so the concentration  $c$  is proportional to the absorption  $A$ . Based on this, the intensity of the isocyanate absorption at about  $2270 \text{ cm}^{-1}$  was used to calculate the NCO conversion as shown in Equation 7. The aromatic C-H stretching at  $3035 \text{ cm}^{-1}$  was used for the normalization of the spectra.

$$A = \varepsilon \times \ell \times c \quad \text{Equation 6}$$

$$NCO \text{ conversion} = \left(1 - \frac{c_{NCO \text{ residual}}}{c_{NCO \text{ initial}}}\right) \times 100 \% = \left(1 - \frac{I_{NCO \text{ residual}}}{I_{NCO \text{ initial}}}\right) \times 100 \%$$

$$\text{Equation 7}$$

$I_{NCO \text{ residual}}$  is the intensity of the isocyanate absorption in the tested sample and  $I_{NCO \text{ initial}}$  is the initial intensity of the isocyanate absorption before the reaction has started. As the reaction starts immediately once the Components A and B are mixed,  $I_{NCO \text{ initial}}$  can only be obtained by extrapolation to the starting time  $t=0$ . Based on the empirical kinetic law, the conversion rate of NCO ( $d[NCO]/dt$ ) is controlled by the reaction rate coefficient and the reactant concentrations. In the initial stage of the reaction when conversion is still low, the reaction rate coefficient and reactant concentrations can be assumed to be constant. Hence, in the initial stage, the reactant conversion should be linearly proportional to the reaction time. Based on this assumption,  $I_{NCO \text{ initial}}$  was determined by linear extrapolation to the starting time  $t=0$ . In order to slow down the conversion rate and to extend this linear region, the use of catalyst was omitted and the experiment was carried out at room temperature. The A-component *minus* catalyst was mixed with isocyanate in the usual manner. The time recording was started when starting mixing and the ATR IR cell was kept at room temperature. A small amount of the reaction mixture was put on the cell and spectra were recorded with at various time intervals. The obtained spectra were processed in the usual manner. Subsequently, the isocyanate intensities were plotted against reaction time and linear fittings were applied to the data points that were collected during the initial stages of the reaction. The value of  $I_{NCO \text{ initial}}$  was then obtained from the intercept of the linear fitting. The fitting results of the isothermal foam reaction system, cup foam system, “PUR/PIR” foam system and “Add. Ep” foam system are shown in Figure 55. The values of  $R^2$  were between 0.89 and 0.98, indicating relatively good fitting results.



**Figure 55.** Linear fittings to determine the values of  $I_{NCO \text{ initial}}$  in the different foam systems, (1) isothermal foam reactions, (2) cup foam system, (3) "PUR/PIR" system and (4) "Add. Ep" system

#### 4.4.2 Soxhlet extraction

The equipment for Soxhlet extractions consists of a 250 mL extractor, a 500 mL round bottom flask and a condenser. The tare weight of the 500 mL round bottom flask was determined prior to the experiment. About 10g sample material was ground to powder by using a mortar and put in a cellulose extraction thimble. Dichloromethane was used as solvent and the powder was extracted for 24 hours. Then dichloromethane was removed by rotary evaporation, the extract was vacuumed

using an oil pump for ca. 4 hours and subsequently the weight increase of the round bottom flask was determined. Phenanthrene was used as external standard to calculate the concentration of bisphenol A diglycidyl ether (BADGE) in the extract. Ca. 60-100mg extract and 20-30 mg phenanthrene were weighed accurately by using a 4 decimal place analytical balance and then dissolved in DMSO-d6 for <sup>1</sup>H NMR measurement. The area integrals of the chemical shifts at 4.26 ppm (1H, CH<sub>2</sub> in BADGE) and 8.84 ppm (2H, Ar-H in phenanthrene) were used for the calculation. The percentage of unreacted BADGE relative to the amount of BADGE added as reactant was calculated by using the Equation 8 and Equation 9. The theoretical mass of the foam was calculated by assuming that the water and formic acid had fully reacted.

$$m_{Unreacted\ BADGE} = \frac{m_{Ext}}{m_{Exts}} \times \frac{I_{BADGE}}{n_{BADGE}} \times \frac{n_{PHE}}{I_{PHE}} \times \frac{m_{PHEs}}{M_{PHE}} \times M_{BADGE} \quad \text{Equation 8}$$

$$Pct_{Unreated\ BADGE} = \frac{m_{Unreacted\ BADGE}}{m_{Foam\ sample}} \times \frac{m_{foam}}{m_{BADGE\ in\ recipe}} \times 100\% \quad \text{Equation 9}$$

where

$m_{Unreacted\ BADGE}$

– mass of the unreacted BADGE in the foam sample used for Soxhlet extraction

$m_{Ext}$  – mass of the extract after vacuum

$m_{Exts}$  – mass of extract used for NMR measurment

$m_{PHEs}$  – mass of phenanthrene used for NMR measurment

$I_{BADGE}$  – integral of the BADGE peak in NMR spectrum at 4.26 ppm

$I_{PHE}$  – integral of the phenanthrene peak in NMR spectrum at 8.84 ppm

$n_{BADGE}$  – number of protons for the BADGE signal at 4.26 ppm, equals to 1

$n_{PHE}$  – number of protons for the phenanthrene signal at 8.84, equals to 2

$M_{PHE}$  – molar mass of the phenanthrene

$M_{BADGE}$  – molar mass of the BADGE

$Pct_{Unreated\ BADGE}$

– percentage of unreacted BADGE relative to the total amount added as a reactant

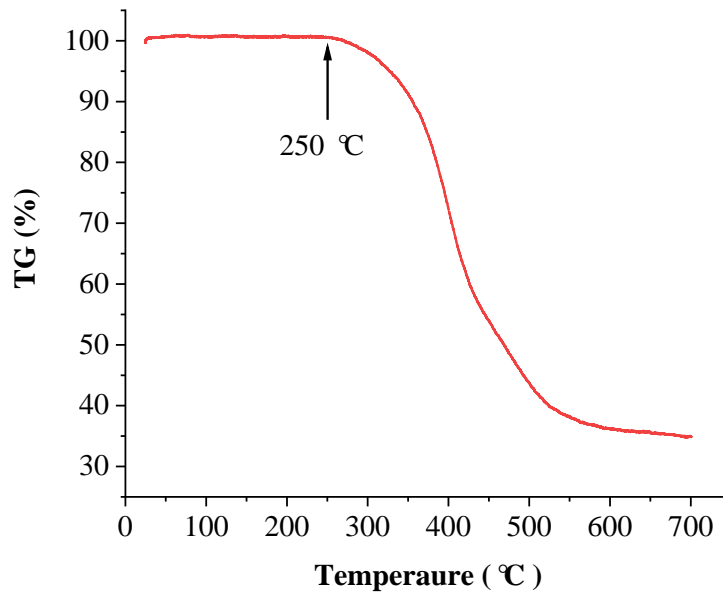
$m_{Foam\ sample}$  – mass of the foam sample for Sohxlet extraction

$m_{foam}$  – mass of the the cup foam

$m_{BADGE\ in\ recipe}$  – mass of the BADGE added in the recipe

#### 4.4.3 TGA measurements

The thermal stability of the polymer foam was determined using TGA. Samples were taken from the foam core and the measurement was carried out under N<sub>2</sub> atmosphere and a heating rate of 10 °C/min. The thermal degradation of the polymer started around 250 °C.



**Figure 56.** TGA spectra of samples from the foam core

## 5. Bibliography

- [1] G. W. Ball, G. A. Haggis, R. Hurd, J. F. Wood, *J. Cell. Plast.* **1968**, *4*, 248.
- [2] J. O. Akindoyo, M. D. H. Beg, S. Ghazali, M. R. Islam, N. Jeyaratnam, A. R. Yuvaraj, *RSC Adv.* **2016**, *6*, 114453.
- [3] H. E. Reymore, R. J. Lockwood, H. Ulrich, *J. Cell. Plast.* **1978**, *14*, 332.
- [4] H. Singh, A. K. Jain, *J. Appl. Polym. Sci.* **2009**, *111*, 1115.
- [5] E. Robertson, P. Waszeciak, M. Sherman, A. Conroy, *J. Cell. Plast.* **1980**, *16*, 279.
- [6] K. C. Frisch, *J. Cell. Plast.* **1965**, *1*, 321.
- [7] G.M.F. Jeffs, B. Mathys, I. D. Rosbotham, R. Frigo, *J. Cell. Plast.* **1991**, *27*, 13.
- [8] S. Cear, J. Feltzin, J. P. Baldino, *J. Cell. Plast.* **1977**, *13*, 21.
- [9] M. Modesti, A. Lorenzetti, *Eur. Polym. J.* **2001**, *37*, 949.
- [10] C. Dick, E. Dominguez-Rosado, B. Eling, J.J. Liggat, C.I. Lindsay, S.C. Martin, M.H. Mohammed, G. Seeley, C.E. Snape, *Polymer* **2001**, *42*, 913.
- [11] F. E. Golling, R. Pires, A. Hecking, J. Weikard, F. Richter, K. Danielmeier, D. Dijkstra, *Polym. Int.* **2019**, *68*, 848.
- [12] Q.-W. Lu, T. R. Hoye, C. W. Macosko, *J. Polym. Sci. A Polym. Chem.* **2002**, *40*, 2310.
- [13] M. F. Sonnenschein, *Polyurethanes: Science, technology, markets, and trends*, Wiley, Hoboken, New Jersey **2015**.
- [14] R. G. Arnold, J. A. Nelson, J. J. Verbanc, *Chem. Rev.* **1957**, *57*, 47.
- [15] Q. Xu, T. Hong, Z. Zhou, J. Gao, L. Xue, *Fire Mater.* **2018**, *42*, 119.
- [16] P. F. Schmit, G. M. Rambosek, *Polyisocyanurate preparation using double alkoxide catalysts*, US3736298A, **1973**.
- [17] T. Pelzer, B. Eling, H.-J. Thomas, G. A. Luinstra, *Eur. Polym. J.* **2018**, *107*, 1.

- [18] S. Dixon, B. Hundred, *Preparation of s-triazine -2,4,6(1H,3H,5H)-triones*, US2977360A, **1961**.
- [19] L. Nicholas, G. T. Gmitter, *J. Cell. Plast.* **1965**, *1*, 85.
- [20] I. S. Bechara, F. P. Carroll, R. L. Mascioli, *Hydroxyalkyl tertiary amine catalysts for isocyanate reactions*, US4026840A, **1977**.
- [21] J. Burkus, *Process of trimerizing organic isocyanates*, US2993870A, **1961**.
- [22] I. S. Bechara, R. L. Mascioli, *J. Cell. Plast.* **1979**, *15*, 321.
- [23] S. Dabi, A. Zilkha, *Eur. Polym. J.* **1981**, *17*, 35.
- [24] A. Al Nabulsi, D. Cozzula, T. Hagen, W. Leitner, T. E. Müller, *Polym. Chem.* **2018**, *9*, 4891.
- [25] H. A. Duong, M. J. Cross, J. Louie, *Org. Lett.* **2004**, *6*, 4679.
- [26] Z. Pustai, G. Vláš, A. Bodor, I. T. Horváth, H. J. Laas, R. Halpaap, F. U. Richter, *Angew. Chem. Int. Ed. Engl.* **2005**, *45*, 107.
- [27] M. Siebert, R. Sure, P. Deglmann, A. C. Closs, F. Lucas, O. Trapp, *J. Org. Chem.* **2020**, *85*, 8553.
- [28] H. E. Reymore, P. S. Carleton, R. A. Kolakowski, A.A.R. Sayigh, *J. Cell. Plast.* **1975**, *11*, 328.
- [29] W. Neumann, P. Fisher, *Angew. Chem. Int. Ed. Engl.* **1962**, *1*, 621.
- [30] K. Wagner, K. Findeisen, W. Schäfer, W. Dietrich, *Angew. Chem. Int. Ed. Engl.* **1981**, *20*, 819.
- [31] J. J. Monagle, *J. Org. Chem.* **1962**, *27*, 3851.
- [32] T. W. Campbell, J. J. Monagle, V. S. Foldi, *J. Am. Chem. Soc.* **1962**, *84*, 3673.
- [33] W. Neumann, *A process for the preparation of carbodiimides*, GB930036A, **1963**.
- [34] B. W. Tucker, H. Ulrich, *Catalysts for the preparation of bis-(2, 6-diethylphenyl)*

*carbodiimide*, US3345407A, **1967**.

- [35] M. Decostanzi, R. Auvergne, E. Darroman, B. Boutevin, S. Caillol, *Eur. Polym. J.* **2017**, *96*, 443.
- [36] M. Widemann, P. J. Driest, P. Orecchia, F. Naline, F. E. Golling, A. Hecking, C. Eggert, R. Pires, K. Danielmeier, F. U. Richter, *ACS Sustainable Chem. Eng.* **2018**, *6*, 9753.
- [37] W. J. Blank, Z. A. He, E. T. Hessell, *Prog. Org. Coat.* **1999**, *35*, 19.
- [38] F. W. Abbate, H. Ulrich, *J. Appl. Polym. Sci.* **1969**, *13*, 1929.
- [39] A. R. Leckart, H. V. Hansen, *Bismuth catalyst system for preparing polyurethane elastomers*, US4584362A, **1986**.
- [40] R. P. Houghton, A. W. Mulvaney, *J. Organomet. Chem.* **1996**, *518*, 21.
- [41] J. Burkus, *J. Org. Chem.* **1961**, *26*, 779.
- [42] R. van Maris, Y. Tamano, H. Yoshimura, K. M. Gay, *J. Cell. Plast.* **2005**, *41*, 305.
- [43] E. Delebecq, J.-P. Pascault, B. Boutevin, F. Ganachaud, *Chem. Rev.* **2013**, *113*, 80.
- [44] M. A. Semsarzadeh, A. H. Navarchian, *J. Appl. Polym. Sci.* **2003**, *90*, 963.
- [45] K. Schwetlick, R. Noack, *J. Chem. Soc., Perkin Trans. 2* **1995**, 395.
- [46] S.-W. Wong, K. C. Frisch, *J. Polym. Sci. A Polym. Chem.* **1986**, *24*, 2867.
- [47] S.-W. Wong, K. C. Frisch, *J. Polym. Sci. A Polym. Chem.* **1986**, *24*, 2877.
- [48] C. J. Lövenich, B. Raffel, *J. Cell. Plast.* **2006**, *42*, 289.
- [49] P. I. Kordomenos, J. E. Kresta, *Macromolecules* **1981**, *14*, 1434.
- [50] K. Ashida, K. C. Frisch, *J. Cell. Plast.* **1972**, *8*, 194.
- [51] K. S. Chian, S. Yi, *J. Appl. Polym. Sci.* **2001**, *82*, 879.
- [52] M. Flores, X. Fernández-Francos, J. M. Morancho, À. Serra, X. Ramis,



*Thermochim. Acta* **2012**, 543, 188.

- [53] D. Caille, J. P. Pascault, L. Tighzert, *Polym. Bull.* **1990**, 24, 23.
- [54] J. E. Herweh, W. J. Kauffman, *Tetrahedron Lett.* **1971**, 12, 809.
- [55] X. Wu, J. Mason, M. North, *Chemistry (Weinheim an der Bergstrasse, Germany)* **2017**, 23, 12937.
- [56] K. Chen, C. Tian, F. Cao, S. Liang, X. Jia, J. Wang, *J. Appl. Polym. Sci.* **2016**, 133, 43085.
- [57] H. J. Altmann, M. Clauss, S. König, E. Frick-Delaittre, C. Koopmans, A. Wolf, C. Guertler, S. Naumann, M. R. Buchmeiser, *Macromolecules* **2019**, 52, 487.
- [58] M. J. Marks, R. A. Plepys, *A process for preparing a polyoxazolidone*, WO1986006734A1, **1986**.
- [59] M. Uribe, K. A. Hodd, *Thermochim. Acta* **1984**, 77, 367.
- [60] M. Flores, X. Fernández-Francos, J. M. Morancho, À. Serra, X. Ramis, *J. Appl. Polym. Sci.* **2012**, 125, 2779.
- [61] M. J. Galante, R. J. J. Williams, *J. Appl. Polym. Sci.* **1995**, 55, 89.
- [62] E. H. M. Elageed, B. Chen, B. Wang, Y. Zhang, S. Wu, X. Liu, G. Gao, *Eur. J. Org. Chem.* **2016**, 2016, 3650.
- [63] J. Shang, Z. Li, C. Su, Y. Guo, Y. Deng, *RSC Adv.* **2015**, 5, 71765.
- [64] Y. Iwakura, S.-I. Izawa, *J. Org. Chem.* **1964**, 29, 379.
- [65] Y. Iwakura, S.-I. Izawa, F. Hayano, *J. Polym. Sci. A-1 Polym. Chem.* **1966**, 4, 751.
- [66] R. J. Young, P. A. Lovell, *Introduction to polymers*, CRC, Boca Raton, Fla. **2011**.
- [67] L. Wu, J. V. Gemert, R. E. Camargo, *Rheology Study in Polyurethane Rigid Foams*, Huntsman Corporation, Auburn Hills, MI, USA **2008**.

- [68] J. K. Gillham, *Polym. Eng. Sci.* **1986**, 26, 1429.
- [69] M. T. Aronhime, J. K. Gillham, in *Epoxy Resins and Composites III. Advances in Polymer Science*, Vol 78 (Eds: K. Dušek), Springer, Berlin, Heidelberg **1986**, p. 83.
- [70] M. T. Aronhime, J. K. Gillham, *J. Appl. Polym. Sci.* **1984**, 29, 2017.
- [71] J. B. Enns, J. K. Gillham, *J. Appl. Polym. Sci.* **1983**, 28, 2567.
- [72] X. Peng, J. K. Gillham, *J. Appl. Polym. Sci.* **1985**, 30, 4685.
- [73] M. Urbaniak, K. Grudzinski, *Polimery* **2007**, 52, 117.
- [74] S. Li, R. Vatanparast, E. Vuorimaa, H. Lemmetyinen, *J. Polym. Sci. B Polym. Phys.* **2000**, 38, 2213.
- [75] G. Wisanrakkit, J. K. Gillham, *J. Appl. Polym. Sci.* **1990**, 41, 2885.
- [76] J. Reignier, F. Méchin, A. Sarbu, *Polym. Test.* **2021**, 93, 106972.
- [77] M. Razmara, H. Saidpour, S. Arunachalam, in *International Conference on Fascinating Advancement in Mechanical Engineering (FAME 2008)*, Mepco Schlenk Engineering College, Sivakasi, **2008**, 11.
- [78] R. R. Romero, R. A. Grigsby, E. L. Rister, J. K. Pratt, D. Ridgway, *J. Cell. Plast.* **2005**, 41, 339.
- [79] P. Chaffanjon, R. A. Grigsby, E. L. Rister, R. L. Zimmerman, *J. Cell. Plast.* **2003**, 39, 187.
- [80] B. Raffel, C. J. Loevenich, *J. Cell. Plast.* **2006**, 42, 17.
- [81] S. Okuzono, H. Kisaka, Y. Tamano, D. W. Lowe, *J. Cell. Plast.* **1995**, 31, 277.
- [82] M. L. Listemann, A. C. Savoca, A. L. Wressell, *J. Cell. Plast.* **1992**, 28, 360.
- [83] D. K. Hoffman, *J. Cell. Plast.* **1984**, 20, 129.
- [84] L. Lunazzi, M. Mancinelli, A. Mazzanti, *J. Org. Chem.* **2012**, 77, 3373.
- [85] S. J. Peters, M. E. Kassabaum, M. K. Nocella, R. McDonald, *Eur. J. Org. Chem.*

**2015**, 2015, 6040.









[86] S. Okumoto, S. Yamabe, *J. Comput. Chem.* **2001**, 22, 316.









[87] V. Fiala, M. Lidařik, *Makromol. Chem.* **1972**, 154, 81.








[88] M. Dornbusch, U. Christ, R. Rasing, *Epoxy resins: Fundamentals and applications*, Vincentz Network, Hannover **2016**.


[89] D. Wegener, S. Reiter, H. Rasselberg, M. Schornstein, H.-D. Arntz, D. Br üning, *Foams of high thermal stability*, WO2012080185A1, **2012**.

## 6. Safety Data

Chemical	GHS Pictograms	Hazard Sentences	Precaution Sentences
glycidyl 2-methylphenyl ether		H315 - H317 - H341 - H411	P201 - P273 - P280 - P302 + P352 - P308 + P313
1-octanol		H319 - H412	P264 - P273 - P280 - P305 + P351 + P338 - P337 + P313 - P501
2,6-dimethylaniline		H302 + H312 + H332 - H315 - H335 - H351 - H411	P201 - P273 - P280 - P302 + P352 + P312 - P304 + P340 + P312 - P308 + P313
<i>N,N,N'</i> -trimethylaminoethyl ethanolamine		H315 - H319 - H335	P302 + P352 - P305 + P351 + P338
2-(2-(dimethylamino) ethoxy)- ethanol		H312 - H318	P280 - P305 + P351 + P338
6-dimethylamino-1-hexanol		H302 - H314- H412	P273- P280- P303 + P361 + P353 - P301 + P330 + P331- P304 + P340 + P310 - P305 + P351 + P338 + P310
2-dimethylaminoethanol		H226 - H302 + H312 - H314 - H331 - H335	P210 - P280 - P301 + P312 + P330 - P303 + P361 + P353 - P304 + P340 + P311 - P305 + P351 + P338 + P310
1-(bis(3-(dimethylamino)- propyl)amino)propan-2-ol		H302- H314- H372	P260 - P264 - P270 - P280 - P301 + P312 - P301 + P330 + P331- P303 + P361 + P353 - P304 + P340 - P305 + P351 + P338- P310 - P314 - P321 - P330 -

			P363- P405 - P501
<i>N,N,N',N'</i> -tetramethylethylene-diamine		H225 - H302 + H332 -H314	P210 - P280 - P301 + P330 + P331- P303 + P361 + P353- P304 + P340 + P312 - P305 + P351 + P338
tetraethylene glycol dimethyl ether		H360FD EUH019	P201- P308 + P313
triethylene glycol dimethyl ether		H319 - H360Df EUH019	P201 - P202 - P264 - P280 - P305 + P351 + P338 - P308 + P313
polyethylene glycol dimethyl ether	-	-	-
1-naphthyl isocyanate		H302 + H312 + H332 - H315 - H319 - H334 - H335	P280 - P301 + P312 + P330 - P302 + P352 + P312 - P305 + P351 + P338
1-naphthyl amine		H302 - H350 - H411	P201 - P202 - P264 - P273 - P301 + P312 - P308 + P313
formic acid		H226 - H302 - H314 - H331	P210 - P280 - P301 + P312 - P303 + P361 + P353 - P304 + P340 + P310 - P305 + P351 + P338
diethyl amine		H225 - H302 + H332 - H311 - H314 - H335 - H225 - H302 + H332 - H311 - H314 - H335	P210 - P280 - P210 - P280 - P301 + P312 - P303 + P361 + P353 - P304 + P340 + P310 - P305 + P351 + P338 - P301 + P312 - P303 + P361 + P353 - P304 + P340 + P310 - P305 + P351 + P338
3-methyl-1-phenyl-2-phospholene 1-oxide		H302 - H351 - H412	P201 - P273 - P301 + P312 + P330 - P308 + P313

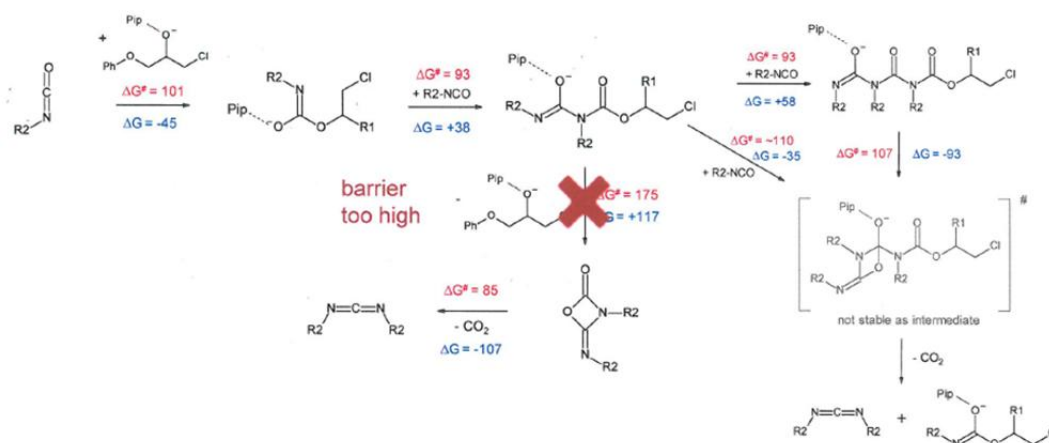
Lupranat® M 20 R		H315- H317- H319- H332- H334 -H335 - H351 - H373- EUH204	P280-P285-P302 + P352-P305 + P351 + P338-P403 + P233-P501-
polyethylene glycol 600	-	-	-
diethyl methyl benzene diamine		H302 -H312 -H319 -H373 -H410 -	P264 -P270 -P280 -P260 -P273 -P301+P312 -P330 -P302+P352 -P312 -P321 -P362+P364 -P305+P351+P338 -P337+P313 -P314 -P391 - P501
bisphenol A diglycidyl ether		H315 - H317 - H319	P261 - P264 - P272 - P280 - P302 + P352 - P305 + P351 + P338
Niax Silicone L-6900	-	-	-
dichloromethane		H315 - H319 - H336 - H351	P201 - P202 - P261 - P302 + P352 - P305 + P351 + P338 - P308 + P313
ethyl acetate		H225 - H319 - H336 - H225 - H319 - H336	P210 - P233 - P240 - P241 - P242 - P210 - P233 - P240 - P241 - P242 - P305 + P351 + P338 - P305 + P351 + P338
petroleum ether 50-70		H225 - H304 - H315 - H336 - H361f - H373 - H411	P201 - P210 - P273 - P301 + P310 - P303 + P361 + P353 - P331
acetonitrile		H225 - H302 + H312 - H319 - H331	P210 - P280 - P301 + P312 - P303 + P361 + P353 - P304 + P340 + P311 - P305 + P351 + P338

acetone		H225 - H319 - H336	P210 - P233 - P240 - P241 - P242 - P305 + P351 + P338
Kieselgel 60	-	-	-
Aluminum oxide	-	-	-

## 7. Appendix

### DFT calculation in support of the mechanism of carbodiimide formation

The mechanism of carbodiimide formation under the catalysis of piperidinium chloride was calculated with DFT by Rebecca Sure from BASF SE. The activation energy and the reaction energy of each reaction step are shown in Figure A-1.



**Figure A-1.** DFT calculation supporting the mechanism of carbodiimide formation  
(Rebecca Sure from BASF SE)

### Product quantification

“Ep\_ROH\_NCO\_DAB” system reacted at 80 °C

**Table A-1 (a).** Isocyanate conversion into different reaction products

	Product	Reaction 1	Reaction 2	Reaction 3	Reaction 4	Average	Experimental error
NCO conversion into	<i>anti</i> -Isocyanurate	52.0%	51.7%	54.7%	54.3%	53.2%	1.6%
	<i>syn</i> -Isocyanurate	25.0%	23.7%	23.0%	23.0%	23.7%	0.9%
	Oxazolidinone	0.3%	0.0%	0.7%	0.7%	0.4%	0.3%
	Urethane	12.8%	15.2%	15.5%	15.5%	14.8%	1.3%
	Urea	2.0%	4.0%	3.3%	3.3%	3.2%	0.8%
	Carbodiimide	-1.5% (0.0%)	(0.0%)	-3.9% (0.0%)	(0.0%)	-2.7% (0.0%)	1.7% (0.0%)
	Amine	0.3%	0.3%	1.0%	1.0%	0.7%	0.4%
	Others	7.5%	5.2%	1.8%	2.2%	4.2%	2.7%



**Table A-1 (b).** Epoxide conversion into different reaction products

	Product	Reaction 1	Reaction 2	Reaction 3	Reaction 4	Average	Experimental error
Ep conversion into	Oxazolidinone	1.0%	0.0%	2.0%	2.0%	1.3%	1.0%
	Unreacted epoxide	72.0%	88.0%	91.0%	91.0%	85.5%	9.1%
	Others	27.0%	12.0%	7.0%	7.0%	13.3%	9.5%

**Table A-1 (c).** Alcohol conversion into different reaction products

	Product	Reaction 1	Reaction 2	Reaction 3	Reaction 4	Average	Experimental error
ROH conversion into	Urethane	77.0%	91.0%	93.0%	93.0%	88.5%	7.7%
	Others	23.0%	9.0%	7.0%	7.0%	11.5%	7.7%

**“Ep\_ROH\_NCO\_DAB” system reacted at 130 °C**

**Table A-2 (a).** Isocyanate conversion into different reaction products

	Product	Reaction 1	Reaction 2	Reaction 3	Reaction 4	Reaction 5	Average	Experimental error
NCO conversion into	<i>anti</i> -Isocyanurate	51.3%	52.0%	52.7%	46.7%	47.2%	50.0%	2.8%
	<i>syn</i> -Isocyanurate	12.7%	20.0%	19.7%	12.0%	12.4%	15.4%	4.1%
	Oxazolidinone	5.7%	3.3%	3.3%	3.7%	3.7%	3.9%	1.0%
	Urethane	8.2%	11.2%	11.2%	9.5%	9.3%	9.8%	1.3%
	Urea	1.3%	0.7%	0.7%	2.9%	2.5%	1.6%	1.0%
	Carbodiimide	-0.1% (0.0%)	-0.6% (0.0%)	-0.6% (0.0%)	-2.7% (0.0%)	-2.1% (0.0%)	-1.2% (0.0%)	1.1% (0.0%)
	Amine	0.3%	0.7%	0.7%	1.2%	1.0%	0.8%	0.3%
	Others	20.5%	12.2%	11.8%	24.2%	23.9%	18.5%	6.1%

**Table A-2 (b).** Epoxide conversion into different reaction products

	Product	Reaction 1	Reaction 2	Reaction 3	Reaction 4	Reaction 5	Average	Experimental error
Ep conversion into	Oxazolidinone	17.0%	10.0%	10.0%	11.0%	11.2%	11.8%	2.9%
	Unreacted epoxide	6.0%	52.0%	52.0%	31.7%	31.4%	34.6%	19.0%
	Others	77.0%	38.0%	38.0%	57.3%	57.4%	53.5%	16.3%

**Table A-2 (c).** Alcohol conversion into different reaction products

	Product	Reaction 1	Reaction 2	Reaction 3	Reaction 4	Reaction 5	Average	Experimental error
ROH conversion into	Urethane	49.0%	67.0%	67.0%	56.7%	55.5%	59.0%	7.8%
	Others	51.0%	33.0%	33.0%	43.3%	44.5%	41.0%	7.8%

**“Ep\_ROH\_NCO\_DAB” system reacted at 160 °C**

**Table A-3 (a).** Isocyanate conversion into different reaction products

	Product	Reaction 1	Reaction 2	Reaction 3	Reaction 4	Average	Experimental error
NCO conversion into	<i>anti</i> -Isocyanurate	45.7%	43.3%	46.7%	46.3%	45.5%	1.5%
	<i>syn</i> -Isocyanurate	4.0%	8.0%	6.3%	5.7%	6.0%	1.7%
	Oxazolidinone	9.7%	8.3%	8.3%	8.0%	8.6%	0.7%
	Urethane	8.7%	8.8%	8.8%	8.5%	8.7%	0.2%
	Urea	2.7%	2.7%	2.0%	2.3%	2.4%	0.3%
	Carbodiimide	5.3%	5.3%	5.0%	1.9%	4.4%	1.6%
	Amine	0.7%	1.0%	0.7%	1.0%	0.8%	0.2%
	Others	23.4%	22.5%	22.2%	26.2%	23.6%	1.8%

**Table A-3 (b).** Epoxide conversion into different reaction products

	Product	Reaction 1	Reaction 2	Reaction 3	Reaction 4	Average	Experimental error
Ep conversion into	Oxazolidinone	29.0%	25.0%	25.0%	24.0%	25.8%	2.2%
	Unreacted epoxide	6.0%	4.0%	11.0%	4.0%	6.3%	3.3%
	Others	65.0%	71.0%	64.0%	72.0%	68.0%	4.1%

**Table A-3 (c).** Alcohol conversion into different reaction products

	Product	Reaction 1	Reaction 2	Reaction 3	Reaction 4	Average	Experimental error
ROH conversion into	Urethane	52.0%	53.0%	53.0%	51.0%	52.3%	1.0%
	Others	48.0%	47.0%	47.0%	49.0%	47.8%	1.0%

**“Model” system reacted at 80 °C**

**Table A-4 (a).** Isocyanate conversion into different reaction products

	Naphthyl Product	Reaction 1	Reaction 2	Average	Experimental error
NCO conversion into	<i>anti</i> -Isocyanurate	26.0%	25.7%	25.9%	0.1%
	<i>syn</i> -Isocyanurate	13.9%	13.4%	13.6%	0.2%
	Oxazolidinone	0.0%	0.0%	0.0%	0.0%
	Urethane	6.6%	6.6%	6.6%	0.0%
	Urea	33.1%	30.7%	31.9%	1.2%
	<i>N</i> -(2,6-dimethylphenyl)- <i>N'</i> -naphthyl urea	1.7%	2.4%	2.1%	0.4%
	Carbodiimide	0%	0%	0%	0%
	Amine	5.9%	9.7%	7.8%	1.9%
	Others	12.9%	11.4%	12.1%	0.7%

**Table A-4 (b).** Epoxide conversion into different reaction products

	Product	Reaction 1	Reaction 2	Average	Experimental error
Ep conversion into	Oxazolidinone	0.0%	0.0%	0.0%	0.0%
	Unreacted epoxide	95.0%	95.0%	95.0%	0.0%
	Others	5.0%	5.0%	5.0%	0.0%

**Table A-4 (c).** Alcohol conversion into different reaction products

	Product	Reaction 1	Reaction 2	Average	Experimental error
ROH conversion into	Urethane	92.0%	92.0%	92.0%	0.0%
	Others	8.0%	8.0%	8.0%	0.0%

**“Model” system reacted at 130 °C**

**Table A-5 (a).** Isocyanate conversion into different reaction products

	Naphthyl Product	Reaction 1	Reaction 2	Average	Experimental error
NCO conversion into	<i>anti</i> -Isocyanurate	27.1%	26.0%	27.1%	0.6%
	<i>syn</i> -Isocyanurate	11.1%	10.6%	11.1%	0.3%
	Oxazolidinone	1.4%	1.3%	1.4%	0.1%
	Urethane	5.0%	5.1%	5.0%	0.0%
	Urea	33.4%	33.9%	33.4%	0.2%
	<i>N</i> -(2,6-dimethylphenyl)- <i>N'</i> -naphthyl urea	0.5%	0.5%	0.5%	0.0%
	Carbodiimide	4.9%	6.4%	4.9%	0.8%
	Amine	1.1%	1.4%	1.1%	0.1%
	Others	15.3%	14.8%	15.3%	0.2%

**Table A-5 (b).** Epoxide conversion into different reaction products

	Product	Reaction 1	Reaction 2	Average	Experimental error
Ep conversion into	Oxazolidinone	10.0%	9.0%	10.0%	0.5%
	Unreacted epoxide	38.0%	40.0%	38.0%	1.0%
	Others	52.0%	51.0%	52.0%	0.5%

**Table A-5 (c).** Alcohol conversion into different reaction products

	Product	Reaction 1	Reaction 2	Average	Experimental error
ROH conversion into	Urethane	70.0%	71.0%	70.0%	0.5%
	Others	30.0%	29.0%	30.0%	0.5%

**“Model” system reacted at 160 °C**

**Table A-6 (a).** Isocyanate conversion into different reaction products

	Naphthyl Product	Reaction 1	Reaction 2	Average	Experimental error
NCO conversion into	<i>anti</i> -Isocyanurate	15.1%	10.6%	12.9%	2.3%
	<i>syn</i> -Isocyanurate	6.4%	4.7%	5.6%	0.9%
	Oxazolidinone	3.3%	4.7%	4.0%	0.7%
	Urethane	4.6%	4.2%	4.4%	0.2%
	Urea	36.1%	33.9%	35.0%	1.1%
	<i>N</i> -(2,6-dimethylphenyl)- <i>N'</i> -naphthyl urea	0.5%	0.4%	0.5%	0.0%
	Carbodiimide	28.6%		28.6%	-
	Amine	0.0%	0.0%	0.0%	0.0%
	Others	5.4%	12.9%	9.2%	3.8%

**Table A-6 (b).** Epoxide conversion into different reaction products

	Product	Reaction 1	Reaction 2	Average	Experimental error
Ep conversion into	Oxazolidinone	23.0%	33.0%	28.0%	5.0%
	Unreacted epoxide	4.0%	1.0%	2.5%	1.5%
	Others	73.0%	66.0%	69.5%	3.5%

**Table A-6 (c).** Alcohol conversion into different reaction products

	Product	Reaction 1	Reaction 2	Average	Experimental error
ROH conversion into	Urethane	64.0%	59.0%	61.5%	2.5%
	Others	36.0%	41.0%	38.5%	2.5%

## Acknowledgements

I would like to take this opportunity to thank the following people, who provided their generous guidance and support during my doctorate study.

My gratitude goes first to Prof. Dr. Gerrit A. Luinstra, who provided me with the opportunity to conduct my doctorate study in Hamburg and guided me during the doctorate period with his profound knowledge in chemistry as well as the meticulous academic attitude.

My appreciation also goes to Prof. Dr. Berend Eling, who is an expert in the polyurethane field. His guidance helped me bridge the knowledge gap between academia and industry. I wouldn't have come this far without his support. I also benefit a lot in research methodology and academic writing under his generous instruction.

Besides, I would like to thank BASF Polyurethanes GmbH and the Universität Hamburg for the financial support of my doctorate study.

In the next, I want to express my sincere thanks to Stefan Auffarth, who helped me with the organization and communication when doing the experiments in BASF Polyurethanes GmbH; Rebecca Sure from BASF SE, who provided the result of the DFT calculation; Michael Gröger, who conducted the GPC measurements; Uta Sazama, who did the TGA measurements; the DMA department in BASF Polyurethanes GmbH, the MS and NMR departments in Universität Hamburg for conducting the corresponding measurements; My thanks also go to the staffs in TMC: Dr. Felix Scheliga, Dr. Robert Meyer, Kathleen Pruntsch, Klaus Hilgendorf and Holger Stockhusen as well as my colleagues: Niklas Voigt who helped me when translating the Abstract into German, Fabian Ratzke, Linyu Mu, Jessica Redmann, Xiangyun Kong, Yannick Wencke, Tim Beermann and all the other colleagues in the group. At last, my grateful goes to my beloved family.

## **Declaration on Oath**

Hiermit erkläre ich an Eides statt, dass ich die vorliegende Dissertationsschrift selbst verfasst und keine anderen als die angegebenen Quellen und Hilfsmittel benutzt habe.

I hereby declare upon oath that I have written the present dissertation independently and have not used further resources and aids than those stated.

Hamburg,

Signature